UNIVERSIDADE FEDERAL DE VIÇOSA

Investigation of the Use of Shredded Tire Rubber in Gypsum Boards for Sound Absorption Purposes

Ramon Ribeiro Fontes
Doctor Scientiae

VIÇOSA - MINAS GERAIS
2026

RAMON RIBEIRO FONTES

Investigation of the Use of Shredded Tire Rubber in Gypsum Boards for Sound Absorption Purposes

Thesis submitted to the Civil Engineering Graduate Program of the Universidade Federal de Viçosa in partial fulfillment of the requirements for the degree of *Doctor Scientiae*.

Adviser: Jose M. Franco de Carvalho

Co-advisers: Tulio M. de S. Tiburcio
Leonardo G. Pedroti

VIÇOSA - MINAS GERAIS
2026

Ficha catalográfica elaborada pela Biblioteca Central da Universidade Federal de Viçosa - Campus Viçosa

T
F683i
2026

Fontes, Ramon Ribeiro, 1972-
Investigation of the use of shredded tire rubber in gypsum boards for sound absorption purposes / Ramon Ribeiro Fontes. – Viçosa, MG, 2026.
1 tese eletrônica (194 f.): il. (algumas color.).

Texto em inglês.
Orientador: José Maria Franco de Carvalho.
Tese (doutorado) - Universidade Federal de Viçosa, Departamento de Engenharia Civil, 2026.
Inclui bibliografia.
DOI: https://doi.org/10.47328/ufvbbt.2026.263
Modo de acesso: World Wide Web.

1. Isolamento acústico. 2. Gesso. 3. Borracha - Reaproveitamento. I. Carvalho, José Maria Franco de, 1979-. II. Universidade Federal de Viçosa. Departamento de Engenharia Civil. Programa de Pós-Graduação em Engenharia Civil. III. Título.

CDD 22. ed. 620.23

Bibliotecário(a) responsável: Bruna Silva CRB-6/2552

RAMON RIBEIRO FONTES

Investigation of the Use of Shredded Tire Rubber in Gypsum Boards for Sound Absorption Purposes

Thesis submitted to the Civil Engineering Graduate Program of the Universidade Federal de Viçosa in partial fulfillment of the requirements for the degree of *Doctor Scientiae*.

APPROVED: February 24, 2026.

Assent:

Ramon Ribeiro Fontes
Author

Jose Maria Franco de Carvalho
Adviser

I dedicate this work to my mother and my father.

ACKNOWLEDGMENTS

Initially, I thank God for granting me the opportunity, strength, and perseverance necessary to achieve the accomplishments attained throughout this journey.

To my mother, I express my deepest gratitude for her unconditional support, tireless prayers, constant affection, and for being a permanent source of encouragement in the realization of this shared dream.

To my wife, I am grateful for her understanding, patience, and support during the periods of absence. To my children, Gabriel and Júlia, I thank them for their understanding regarding the limitations imposed on our family life throughout these five years dedicated to my doctoral studies.

To my advisor, Prof. Dr. José Maria Franco de Carvalho, I extend my sincere gratitude for his academic guidance, the trust placed in my work, his continuous encouragement, and his valuable contributions throughout the development of this research.

To my co-advisors, Prof. Dr. Leonardo Gonçalves Pedroti, for his guidance in the laboratory, and Prof. PhD. Túlio Márcio de Salles Tibúrcio, for his contributions, academic rigor, and support during the development of this work, I offer my sincere thanks.

To the professors of the Department of Civil Engineering at the Federal University of Viçosa — Prof. Dr. Flávio Antônio Ferreira, Prof. Dr. Gustavo de Souza Veríssimo, and Prof. Dr. José Luiz Rangel Paes — I thank them for their academic contributions, the availability of laboratory facilities, and the quality of the courses taught.

To the distinguished members of the doctoral examination committee — Prof. Dr. Sabrina Barbosa (Architecture/UERJ), Prof. Dr. Ernani Simplício Machado (Architecture/UFJF), and Prof. Dr. Paulo Buchner (Mechanical Engineering/UFV) — I express my gratitude for their valuable suggestions, constructive criticism, and remarks that significantly contributed to the improvement of this work.

To my doctoral colleagues Jean Antônio Emerick, Roziani Gomes, Gustavo Lopes, and Ariel Miranda de Souza, I thank them for their support, collaboration, and assistance in laboratory activities and coursework.

I also thank the undergraduate research scholarship student in Civil Engineering, Jean Carlos Bernardes Dias, and the Chemistry technician, Nathália Matias Albuini, for their valuable collaboration and support in carrying out the laboratory tests.

I am grateful to the Federal University of Rio de Janeiro and the Federal University of Ouro Preto for conducting the laboratory tests. Finally, I express my gratitude to the Federal University of Viçosa for the infrastructure, institutional support, and academic environment that made this research possible.

This work has been sponsored by the following Brazilian research agencies: Coordination for the Improvement of Higher Education Personnel (CAPES; Financing code 001), Minas Gerais State Foundation for Research Aid (FAPEMIG) and National Council of Scientific and Technological Development (CNPq).

“No achievement is built alone. Family provides the roots, friends strengthen the journey, and teachers illuminate the path that transforms dreams into accomplishments.”

ABSTRACT

FONTES, Ramon Ribeiro, D.Sc., Universidade Federal de Viçosa, February, 2026. **Investigation of the Use of Shredded Tire Rubber in Gypsum Boards for Sound Absorption Purposes**. Adviser: Jose Maria Franco de Carvalho. Co-advisers: Tulio Marcio de Salles Tiburcio and Leonardo Goncalves Pedroti.

Noise pollution is one of the major contemporary environmental problems, with direct impacts on human health, well-being, and performance, especially in indoor environments such as homes, offices, and classrooms. In this context, this thesis investigates the development of gypsum boards incorporating crushed waste tire rubber, with a focus on acoustic conditioning and sound absorption, particularly at low frequencies. The research combines acoustic performance, mechanical feasibility, and environmental sustainability, proposing an innovative approach for acoustic boards or panels for vertical enclosure systems in the construction industry. The research was structured into three main stages: (1) a bibliometric and systematic review of the literature on the use of rubber waste in acoustic applications in the built and urban environments; (2) the experimental development of gypsum-based composites with different rubber contents, particle size distributions, and the addition of microfibers, evaluated through mechanical testing, microstructural analyses, physicochemical characterizations, and measurements of sound absorption coefficients using impedance tubes; and (3) the validation of acoustic performance under real conditions of use, through the application of the boards in classrooms, with measurements of the reverberation time parameter.

The use of waste tire rubber in gypsum panels and boards constitutes a technically and environmentally sustainable alternative, with potential application in acoustic treatment for dry construction systems, contributing to the mitigation of indoor noise and to the valorization of solid waste in the construction industry.

Keywords: gypsum panels; sound absorption; rubber waste

RESUMO

FONTES, Ramon Ribeiro, D.Sc., Universidade Federal de Viçosa, fevereiro de 2026. **Investigação do uso da borracha de pneus triturados em placas de gesso para fins de absorção sonora**. Orientador: Jose Maria Franco de Carvalho. Coorientadores: Tulio Marcio de Salles Tiburcio e Leonardo Goncalves Pedroti.

A poluição sonora é um dos principais problemas ambientais contemporâneos, com seus impactos diretos sobre a saúde, o bem-estar e o desempenho humano, especialmente em ambientes internos como residências, escritórios e salas de aula. Nesse contexto, esta tese investiga o desenvolvimento de placas de gesso incorporados com resíduos de borracha de pneus triturados, com foco no condicionamento acústico e na absorção sonora, particularmente em baixas frequências. A pesquisa alia desempenho acústico, viabilidade mecânica e sustentabilidade ambiental, propondo uma abordagem inovadora para placas acústicas ou painéis para sistemas de vedação vertical na construção civil.
A pesquisa foi estruturada em três etapas principais: 1- uma revisão bibliométrica e sistemática da literatura sobre o uso de resíduos de borracha em aplicações acústicas no ambiente construído e urbano, 2- o desenvolvimento experimental de compósitos de gesso com diferentes teores, granulometrias de borracha e adição de microfibras, avaliados por meio de ensaios mecânicos, análises microestruturais, caracterizações físico-químicas e medições de coeficientes de absorção sonora em tubos de impedância; 3- a validação do desempenho acústico em condições reais de uso, por meio da aplicação de placas sem salas de aula, com medições do parâmetro tempo de reverberação.
O uso de resíduos de pneus em painéis e placas de gesso configura uma alternativa técnica e ambientalmente sustentável, com potencial de aplicação no tratamento acústico em sistemas construtivos a seco, colaborando para a mitigação do ruído interno e para a valorização de resíduos sólidos na construção civil.

Palavras-chave: painéis de gesso; absorção sonora; resíduos de borracha

SUMÁRIO

1 GENERAL INTRODUCTION

1.1 Introduction

Noise pollution has become one of the main environmental problems faced by human society. Excessive exposure to noise, due to the rapid growth of cities and their transportation and industrial activities, has caused harm to both humans and animals (Tao *et al.*, 2021). According to Bistafa (2018), there are numerous problems related to noise, including hearing loss, stress, hypertension, sleep loss, reduced opportunities for rest, lack of concentration, and decreased productivity, all of which lead to a deterioration in quality of life. In the physical realm, noise-induced ailments include headaches, digestive dysfunction, hormonal disorders, and cardiovascular disturbances, among others (Souza; Almeida; Bragança, 2021). The perception of noise as a significant environmental pollutant intensified with urban growth and industrialization beginning in the 19th century (Mommertz, 2009). From the 20th century onward, however, noise came to be treated as a public health problem and a formal scientific field (Egan, 2007). As a result, from the 1960s onward, architectural acoustics standards have included conditions to restrict noise pollution in urban environments and building interiors, in order to protect occupants.

The problems caused by reverberation and unwanted noise can be reduced through the use of sound absorption and sound insulation panels. However, the greatest difficulty arises in mitigating noise at low frequencies — from 20 to 400 Hz — since sound absorption control is easier to achieve at mid and high frequencies (Sanchis *et al.*, 2022). The acoustic performance of buildings has, in several countries, become a requirement of laws and building codes, given its impact on human health (ProAcústica, 2022, p. 4). In Brazil, standard NBR 15575-1 (Associação Brasileira de Normas Técnicas – ABNT, 2013) defined — based on the admissible levels set out in NBR 10152 (ABNT, 2017) — the performance levels that building systems must meet in order to attenuate the transmission of noise generated both externally and internally in residential buildings (ProAcústica, 2013, p. 4). Within the construction industry, NBR 15575-4 (ABNT, 2013) addresses elements of residential buildings that bound the structure and its spaces vertically, such as façades and internal walls or partitions. As a constructive interface also responsible for acoustic insulation between dwelling units, it directly affects the occupants' quality of life.

Furthermore, clarity of communication — through speech intelligibility — comfort achieved by low noise levels, and sustained attention are fundamental factors in the

performance and productivity of office workers (Martins; Miranda, 2019). Speech intelligibility is influenced by room acoustics. Adding more sound absorption to a space will reduce reverberation, thereby improving speech intelligibility at short distances between source and receiver (Reinten *et al.*, 2017). For Bastos *et al.* (2021), the intelligibility of messages delivered by teachers in educational environments and students' learning are compromised by ambient noise levels and excessive reverberation, resulting in stress, fatigue, and difficulty concentrating.

The assessment of acoustic comfort in offices must take into account noise measurement, to be carried out through sound pressure level (SPL) measurements, reverberation time (RT), as well as quantification of background noise and speech intelligibility (Martins; Miranda, 2019). In noisy environments, or where background noise levels rise, people tend to speak louder to be understood, and consequently become more fatigued. This is explained by the Lombard effect, which describes the tendency of speakers to raise their voice level as background noise increases (Reinten *et al.*, 2017).

According to Mehrzad *et al.* (2022), economic development and population growth have brought serious environmental problems, such as noise pollution and global warming. Global warming in particular has become a severe environmental issue, driving climate change and greenhouse gas emissions. The same researcher further notes that the construction industry is responsible for more than 40% of global energy consumption, generating nearly 45% of such emissions. According to Basner and McGuire (2018), the WHO estimated that in the high-income countries of Western Europe — with a population of approximately 340 million people — at least one million healthy life years are lost every year due to environmental noise.

Therefore, the search for residual or low-environmental-impact materials suitable for use in construction — such as boards, panels, ceiling tiles, and vertical sealing systems with appreciable acoustic performance — is of significant interest to the construction industry. Accordingly, developing boards for internal gypsum partition panels incorporating ground tire rubber waste, with the aim of correcting acoustic problems such as reverberation and echo while also reducing noise transmission between rooms, is the central interest of this research.

1.2 Objectives

1.2.1 General objectives

To research and evaluate the performance and sustainable potential of gypsum matrices or composites incorporating ground tire rubber for acoustic treatment in the construction industry.

1.2.2 Specific objectives

The following specific objectives are listed:

- To determine which incorporation levels or limits of ground tire rubber particles in gypsum matrices will not compromise the mechanical performance of the boards or panels.
- To detect which incorporation levels of tire rubber particles and which particle sizes yield the best Noise Reduction Coefficient (NRC).
- To identify which particle sizes provide the best sound absorption performance specifically at low frequencies.
- To classify the influence of tire rubber particle size on sound absorption and damping.
- To demonstrate that ground tire rubber waste enhances sound absorption at low frequencies.
- To validate the laboratory test results of the research by comparing them with tests conducted under real-use conditions through acoustic board prototypes.

1.3 Justification

According to Bridi (2020, p. 173), the COVID-19 pandemic, which broke out in 2020, demanded disease-containment measures, among which social distancing was one of the primary means of curbing the spread of the virus. As a result of these measures, a challenge was posed to everyone: how to continue producing and working remotely. Remote work — commonly referred to as "home office" — was a solution adopted by many companies and institutions to reduce the spread of the virus caused by people commuting between home and the workplace. According to Silva (2004), it is important for employees to have an adequate space in which to carry out their work activities, with good acoustic insulation and ergonomics, thereby preventing occupational illnesses arising from their working conditions. As noted by

Bortolan *et al.* (2021), when higher education teachers who worked remotely during the pandemic were asked which requirements or attributes caused discomfort, 75% of respondents indicated that noise accounted for 47.6% of complaints, alongside other ergonomic factors such as furniture, equipment, temperature, and lighting.

The acoustic quality of a learning environment influences the learning process. When this condition is unfavorable, the learning environment becomes exhausting (Engel; Herrmann; Zannin, 2021). Other factors are also important for learning in educational settings. Speech perception, for instance, depends on the sound level at which content is delivered by the teacher, as well as the location and distance between speaker and listener, and the physical characteristics of the space — including room shape and the absence or presence of materials with lower or higher sound absorption coefficients (Sala; Rantala, 2016). The three most appropriate acoustic parameters or descriptors for characterizing the acoustic quality of classrooms are: speech intelligibility, measured through the STI (Speech Transmission Index); Definition D50; and Reverberation Time (RT), as set out in ANSI/ASA S12.60 (Acoustical Society of America – ASA, 2010). Short reverberation times are used to achieve better word intelligibility in spaces intended for speech (Barron, 2009). For Santos and Oiticica (2020), in dining and gastronomic environments, good acoustic quality depends on a balance between intelligibility and privacy. Due to this factor, excessive reverberation caused by insufficient use of absorptive materials leads occupants to raise their voice levels in order to overcome background noise and be understood. In the urban environment, motor vehicles are the primary source of noise, arising from engine sound, exhaust systems, horns, and tire friction against the road surface.

According to Serviço Social do Transporte e Serviço Nacional de Aprendizagem do Transporte – SEST SENAT (2017), the Brazilian automotive industry produces an average of 450,000 tonnes of discarded tires per year — equivalent to approximately 90 million tires from passenger vehicles alone. A waste tire takes, on average, around 600 years to decompose in nature. According to Jena, Nayak and Satapathy (2020), among all solid wastes generated by the advance of civilization, waste rubber tires have become a major environmental concern, as production is increasing at an accelerating rate driven by growing demand for automobiles. In China, according to Chen *et al.* (2021), more than 10 million tonnes of tires have been discarded over recent decades, causing serious environmental problems. Under CONAMA Resolution nº 258 (Brasil, 1999), tire manufacturers were designated as responsible for the final disposal of their products — meaning that for each new unit produced and placed on the market, a disposal destination must be assigned to one waste tire. According to Jena, Nayak and Satapathy (2020),

more than 1.5 billion tires are generated worldwide, causing environmental pollution; in the United States alone, 300 million unusable tires are produced. To prevent the environmental pollution arising from the disposal of these materials, one solution is their use in construction, which is already being encouraged by many countries around the world (Jena; Nayak; Satapathy, 2020). Material recovery is complicated by the fact that a new tire cannot be obtained from a recycled one. One adopted solution is the use of waste tires in other applications, such as acoustic insulation (Parres; Crespo-Amorós; Nadal-Gisbert, 2009). According to Fernández-Berridi *et al.* (2006), tire recycling or reprocessing is one of the preferable processes under the so-called waste management hierarchy, particularly from an environmental standpoint. The recovery and reuse of tires in various applications is an example of this, since the base polymer can be incorporated into new formulations, resulting in cost savings on raw materials and the preservation of natural resources and the environment. Rubber tire recycling consists of three components: energy recovery through heat, processing, and original-use application (Zhang *et al.*, 2009). Of the total volume generated, 40% is used as fuel, 26% is shredded into rubber crumb, 13% is disposed of in landfills, and only 5.5% is incorporated into the construction industry. According to Fernández-Berridi *et al.* (2006), using waste tires as a new source of raw material for various applications can be a partial solution to the major environmental problems generated by these products with regard to their disposal in waste deposits.

There is no question that the construction industry has a negative impact on the environment, owing to its high consumption of finite natural resources, high energy demand, high waste generation, and significant CO_2 emissions (Masuero, 2021). Currently, the construction industry generates megatonnes of waste in the form of Construction and Demolition Waste (CDW) from buildings at the end of their useful life cycle (End-of-Life — EOL) (European Commission, 2019). The construction industry is responsible for 40% of all waste generated worldwide. Given the difficulty of precisely quantifying the amount of waste produced and the percentage that is recovered, a large share of this waste is directed to landfills, exceeding the volume of domestic waste (Ya'cob *et al.*, 2013). Enormous quantities of construction and demolition waste have been generated worldwide. Considered the world's largest producer of construction and demolition waste (CDW) — with approximately 2.3 billion tonnes in 2019 — the United States, together with the European Union, produced around 600 and 834 million tonnes of CDW respectively in 2018 (Elshaboury *et al.*, 2022). For Rashad (2016), it has become necessary to incorporate waste materials — such as rubber — into construction products, in order to reduce landfill use and the depletion of virgin raw materials. The development of new technologies and innovative solutions through the reuse of waste

materials, new materials, and processes that incorporate them will bring new gains from a sustainability standpoint, thereby contributing to a reduction in environmental impact (Masuero, 2021).

In light of all this, the present research proposes to develop sustainable solutions for mitigating airborne noise through building elements composed of gypsum combined with eco-efficient materials. The development of new absorptive and eco-efficient materials will provide additional options for controlling sound reverberation time and, consequently, improve the intelligibility of the human voice in noisy environments. Likewise, new absorptive materials also contribute to noise reduction when associated with vertical sealing systems, as in the case of dry construction methods.

1.4 Originality

The results to be achieved in the experimental planning will contribute to the state of the art in vertical sealing systems, supporting both acoustic insulation and acoustic conditioning of the built environment. The panel to be developed may thus be incorporated into the existing structural technology of the dry construction system (Drywall), becoming an additional alternative for the mitigation or control of airborne noise.

Another factor that reinforces the originality of this research is the use of ground tire rubber waste in construction materials for acoustic treatment purposes. These green or eco-efficient materials reduce the environmental impact of the construction and demolition industry while also decreasing the consumption of gypsum.

With regard to NBR 15575-1 (ABNT, 2013), from a consumer rights perspective, housing with better acoustic performance contributes to the overall quality of residential performance and consequently influences the occupant's quality of life, increasing their satisfaction with the product.

Within the realm of green building certification systems — such as LEED (Leadership in Energy and Environmental Design) — this panel offers multiple contributions: under Materials and Resources, it reduces material use by partially replacing gypsum with rubber; under Innovation in Design, it contributes by employing sustainable strategies; and under Environmental Quality, it enhances the building's acoustic comfort. This eco-efficient vertical sealing system therefore helps improve the score required to obtain LEED certification and other quality certifications.

It is important to note that the literature review conducted for this research found that various waste materials have already been used in civil construction, including rice husks, sugarcane bagasse, fibers, cellulose, and numerous other products. However, their specific application in vertical sealing systems incorporating ground tire rubber waste, targeting performance specifically in the low-frequency range of the sound spectrum, has not yet been researched.

1.5 References

ACOUSTICAL SOCIETY OF AMERICA. ASA/ANSI S12.60/Part 1-2010 (R2024). **Performance criteria, design requirements, and guidelines for schools – part 1**: permanent schools. Melville, NY: ASA, 2010. Available in: https://img.antpedia.com/standard/files/pdfs_ora/20251028/1/ASA%20ANSI%20S12.60_Part%201-2010(R2024).pdf. Access in: 23 set. 2022.

ASSOCIAÇÃO BRASILEIRA DE NORMAS TÉCNICAS. **NBR 15575-1/2013**: Edificações habitacionais – desempenho parte 1: requisitos gerais. 4.ed. Rio de Janeiro: ABNT, 2013. Available in: https://ufsb.edu.br/propa/images/dinfra/coman/Legisla%C3%A7%C3%B5es/NBR15575-1.pdf. Access in: 24 nov. 2020.

ASSOCIAÇÃO BRASILEIRA DE NORMAS TÉCNICAS. **NBR 10152/2017 – Acústica**: Níveis de pressão sonora em ambientes internos a edificações. 2.ed. Rio de Janeiro: ABNT, 2017. Available in: https://normadedesempenho.com.br/wp-content/uploads/2022/10/NBR-10152.pdf. Access in: 14 mar. 2020.

BARRON, M. **Acoustics, auditorium design, architectural**. 2 ed. London: Spon Press, 2009. https://doi.org/10.4324/9780203874226

BASNER, M.; McGUIRE, S. WHO environmental noise guidelines for the European region: a systematic review on environmental noise and effects on sleep. **International Journal of Environmental Research and Public Health**, v. 15, n. 3, 519, 2018. https://doi.org/10.3390/ijerph15030519

BASTOS, L. P.; LIMA, L. C.; SANTOS, G. B.; MELO, G. V.; MESQUITA, A. L. A. Simulação com painéis de fibra de açaí para melhoria da inteligibilidade da fala em sala de aula. **Ambiente Construído**, v. 21, n. 4, p. 45-63, 2021. Available in: https://seer.ufrgs.br/ambienteconstruido/article/view/107123. Access in: 20 fev. 2023.

BISTAFA, S. R. **Acústica aplicada ao controle do ruído**. 2.ed. São Paulo: Blucher, 2018.

BORTOLAN, G. M. Z.; SANTOS, F. A. N. V.; DOMENECH, S. C.; FERREIRA, M. G. G. Análise da experiência do trabalho remoto em home office de professores do ensino superior. **Ergodesign & HCI**, v. 9, n. 2, p. 141-157, 2021. https://doi.org/10.22570/ergodesignhci.v9i2.1612

BRASIL. Ministério do Meio Ambiente. Conselho Nacional do Meio Ambiente. **Resolução CONAMA nº 258, de 26 de agosto de 1999**. Dispõe sobre a coleta e destinação final de pneus inservíveis. Available in: https://www.normasbrasil.com.br/norma/?id=96050. Access in: 21 out. 2024.

BRIDI, M. A. A pandemia Covid-19: crise e deterioração do mercado de trabalho no Brasil. **Estudos Avançados**, v. 34, n. 100, p. 141-165, 2020. https://www.doi.org/10.1590/s0103-4014.2020.34100.010

CHEN, B.; ZHENG, D.; XU, R.; LENG, S.; HAN, L.; ZHANG, Q.; ... ; CHENG, J. Disposal methods for used passenger car tires: One of the fastest growing solid wastes in China. **Green Energy and Environment**, v. 7, n. 6, p. 1298-1309, 2021. https://doi.org/10.1016/j.gee.2021.02.003

EGAN, M. D. **Architectural acoustics**. Plantation, FL: J. Ross Publishing, 2007.

ELSHABOURY, N.; AL-SAKKAF, A.; ABDELKADER, E. M.; ALFALAH, G. Construction and demolition waste management research: a science mapping analysis. **International Journal of Environmental Research and Public Health**, v. 19, n. 8, 4496, 2022. https://doi.org/10.3390/ijerph19084496

ENGEL, M. S.; HERRMANN, J. O.; ZANNIN, P. H. T. Conforto acústico ambiental no ambiente construído: medições e simulações do índice de transmissão da fala (STI), definição do som (D50) e tempo de reverberação (TR) em salas de aula universitárias. In: SIMPÓSIO BRASILEIRO ONLINE DE GESTÃO URBANA, 5, 2021, São Paulo. **Anais...** São Paulo: UNESP, 2021. Available in: https://www.researchgate.net/publication/353523202_Conforto_Acustico_Ambiental_no_Ambiente_Construido_Medicoes_e_Simulacoes_do_Indice_de_Transmissao_da_Fala_STI_Definicao_do_Som_D50_e_Tempo_de_Reverberacao_TR_em_Salas_de_Aula_Universitarias. Access in: 23 fev. 2023.

EUROPEAN COMMISSION. **The European green deal**: communication from the Commission to the European Parliament, the European Council, the Council, the European Economic and Social Committee and the Committee of the Regions. Brussels: European Commission, 2019. Available in: https://www.coleurope.eu/european-green-deal. Access in: 14 jan. 2024.

FERNÁNDEZ-BERRIDI, M. J.; GONZÁLEZ, N.; MUGICA, A.; BERNICOT, C. Pyrolysis-FTIR and TGA techniques as tools in the characterization of blends of natural rubber and SBR. **Thermochimica Acta**, v. 444, n. 1, p. 65-70, 2006. https://doi.org/10.1016/j.tca.2006.02.027

JENA, B. P.; NAYAK, B. B.; SATAPATHY, S. Physical & mechanical characterization of composites from waste tire rubber crumb. **Materials Today: Proceedings**, v. 26, n. 2, p. 1752-1756, 2020. https://doi.org/10.1016/j.matpr.2020.02.368

MARTINS, R. V.; MIRANDA, E. F. V. Conforto acústico de escritórios em ambiente industrial de usina hidrelétrica. **PARC Pesquisa em Arquitetura e Construção**, v. 10, e019029, 2019. http://dx.doi.org/10.20396/parc.v10i0.8653712

MASUERO, A. B. Desafio da construção civil: crescimento com sustentabilidade ambiental. **Matéria (Rio de Janeiro)**, v. 26, n. 4, 2021. https://doi.org/10.1590/S1517-707620210004.13123

MEHRZAD, S.; TABAN, E.; SOLTANI, P.; SAMAEI, S. E.; KHAVANIN, A. Sugarcane bagasse waste fibers as novel thermal insulation and sound-absorbing materials for application in sustainable buildings. **Building and Environment**, v. 211, 108753, 2022. https://doi.org/10.1016/j.buildenv.2022.108753

MOMMERTZ, E. **Acoustics and sound insulation**: principles, planning, examples. Base, Suíça: Birkhäuser, 2009.

PARRES, F.; CRESPO-AMORÓS, J. E.; NADAL-GISBERT, A. Mechanical properties analysis of plaster reinforced with fiber and microfiber obtained from shredded tires. **Construction and Building Materials**, v. 23, n. 10, p. 3182-3188, 2009. https://doi.org/10.1016/j.conbuildmat.2009.06.040

PROACÚSTICA. Associação Brasileira para a Qualidade Acústica. **Manual ProAcústica sobre a norma de desempenho ABNT NBR 15575:2021 Acústica**. 4.ed. São Paulo: ProAcústica, 2022. Available in: https://www.proacustica.org.br/manuais-proacustica/manual-proacustica-sobre-a-norma-de-desempenho-4edicao/. Access in: 30 jan. 2024.

RASHAD, A. M. A comprehensive overview about recycling rubber as fine aggregate replacement in traditional cementitious materials. **International Journal of Sustainable Built Environment**, v. 5, n. 1, p. 46-82, 2016. https://doi.org/10.1016/j.ijsbe.2015.11.003

REINTEN, J.; BRAAT-EGGEN, P. E.; HORNIKX, M.; KORT, H. S. M.; KOHLRAUSCH, A. The indoor sound environment and human task performance: a literature review on the role of room acoustics. **Building and Environment**, v. 123, p. 315-332, 2017. https://doi.org/10.1016/j.buildenv.2017.07.005

SALA, E.; RANTALA, L. Acoustics and activity noise in school classrooms in Finland. **Applied Acoustics**, v. 114, p. 252-259, 2016. https://doi.org/10.1016/j.apacoust.2016.08.009

SANCHIS, E. J.; ALCARAZ, J. S.; BELDA, I. M.; BORRELL, J. M. G. Sustainable multiple resonator sound absorbers made from fruit stones and air gap. **Alexandria Engineering Journal**, v. 61, n. 12, p. 10219-10231, 2022. https://doi.org/10.1016/j.aej.2022.03.063

SANTOS, K. M. M.; OITICICA, M. L. G. R. Qualidade acústica em ambientes gastronômicos. **Brazilian Applied Science Review**, v. 4, n. 3, p. 1040-1052, 2020. https://doi.org/10.34115/basrv4n3-023

SERVIÇO SOCIAL DO TRANSPORTE E SERVIÇO NACIONAL DE APRENDIZAGEM DO TRANSPORTE. **Campanha nacional do SEST SENAT faz alerta sobre a importância da reutilização e reciclagem do material**. 08 fev. 2017. Available in: https://www.sestsenat.org.br/noticia/cerca-de-450-mil-toneladas-de-pneus-sao-descartados-por-ano-no-brasil. Access in: 12 jul. 2022.

SILVA, R. T. **O teletrabalho e suas influências na qualidade de vida no trabalho**. 2004. 193f. Dissertação (Mestrado em Administração) – Universidade de São Paulo, São Paulo, 2004. https://doi.org/10.11606/D.12.2004.tde-01102008-003037

SOUZA, L. C. L.; ALMEIDA, M. G.; BRAGANÇA, L. **Bê-á-bá da acústica arquitetônica: ouvindo a arquitetura**. São Carlos: EdUFSCar, 2021.

TAO, Y.; REN, M.; ZHANG, H.; PEIJS, T. Recent progress in acoustic materials and noise control strategies – a review. **Applied Materials Today**, v. 24, 101141, 2021. https://doi.org/10.1016/j.apmt.2021.101141

YA'COB, A. S.; ZAWAWI, W. N. A. A.; ISA, M. H.; OTHMAN, I. Factors that affect sustainable construction waste management efforts at site. **WIT Transactions on Ecology and the Environment**, v. 179, p. 1169-1176, 2013. Available in: https://www.witpress.com/cart/openaccessdownload. Access in: 31 dez. 2021.

ZHANG, S. L.; XIN, Z. X.; ZHANG, Z.X.; KIM, J. K. Characterization of the properties of thermoplastic elastomers containing waste rubber tire powder. **Waste Management**, v. 29, n. 5, p. 1480-1485, 2009. https://doi.org/10.1016/j.wasman.2008.10.004

2 THEORETICAL FOUNDATION

2.1 Sound and noise

According to Bistafa (2018), sound is the sensation produced in the auditory system, whereas noise is an unwanted sound, generally associated with a negative connotation. According to Silva (2011), there are two important concepts related to the word sound: first, sound as a vibration or physical disturbance that propagates through a medium, and second, sound as the psychophysiological auditory sensation perceived by our ears. For Souza, Almeida and Bragança (2021), any sound that is undesirable for a given activity is considered noise, even in the case of music that interferes with the progress of an activity within a specific space, thereby impairing the function of the environment. According to Bistafa (2018), noise appears to have disturbed people since the time they began living in cities. As reported by Carvalho (2010), the definition of noise is highly subjective, since what is considered noise by some people may be interpreted as sound by others. Noise permeates human activities 24 hours a day and has been identified as one of the main causes of deterioration in people's quality of life (Bistafa, 2018). According to Bujoreanu *et al.* (2017), human acoustic comfort includes protection against noise and is closely related to the concept of sound absorption.

2.2 Negative impact of noise on human health and well-being

According to Bistafa (2018), noise deteriorates quality of life, causing health problems in addition to economically and financially impacting the lives of individuals and organizations. The author also reports estimates indicating that noise-induced hearing loss affects up to 10 million people in the United States. The World Health Organization (WHO, 2011) published a study whose results, coordinated by its European regional office, highlighted evidence regarding the effects of noise on health and presented estimates of the number of diseases resulting from it. This publication, supported by a Joint Research Centre report of the European Commission, recognizes that environmental noise is responsible for a significant burden of disease, and therefore noise pollution is considered the second largest environmental risk factor, ranking immediately after air pollution.

According to Bistafa (2018), the non-auditory effects of noise manifest themselves in cardiovascular function in the form of hypertension, variations in blood pressure, and changes in heart rate. Consequently, noise also causes respiratory disorders and alterations in an

individual's physical and mental health. This broad range of symptoms leads noise to be considered a generalized stress factor. According to Basner *et al.* (2014), noise fragments sleep, reducing its continuity as well as its total duration. As reported by Riedy *et al.* (2021), the results of a survey conducted by the National Sleep Foundation indicate that at least sixty percent of Americans consider having a quiet, dark, and cool bedroom to be an important factor for achieving a good night's sleep. Basner *et al.* (2014) further state that sleep disturbance is one of the most harmful non-auditory effects on a person's quality of life and health, impairing alertness and daytime performance. According to Rocca *et al.* (2022), acoustic comfort is an essential requirement in all indoor environments where people remain for prolonged periods.

2.3 Types of noise and forms of transmission

According to Carvalho (2010), noise can technically be defined as an intermittent/ random oscillation, classified into airborne noise and impact noise. For Souza, Almeida and Bragança (2021), noise may propagate in the form of airborne noise as well as through vibrations in solids and by impact. However, Valle (2009) defines the two forms of sound or noise transmission as airborne transmission, which propagates through any open passage, such as gaps in poorly closed doors and windows, and structural transmission, which is transmitted through the vibration of walls, slabs, and floors.

2.4 Acoustic treatment: insulation vs. conditioning

According to Silva (2011), acoustic treatment is a set of operations intended to attenuate the level of sound energy between the generating source and the listener or receiver. However, Valle (2009) states that for decades these two concepts have been confused, although each one influences the other; nevertheless, they are intended to provide different approaches or effects. Figure 2-1 presents a diagram of what occurs in the acoustic treatment of an environment, distinguishing the objectives of acoustic insulation and acoustic conditioning. In the acoustic insulation of an environment, the transmission of incident energy through a wall to an adjacent environment should not occur, thus promoting the reflection of incident sound energy back into the original environment. In acoustic conditioning, however, the sound energy incident on a wall or material should be dissipated through absorption or transmission, and should not be reflected back into the environment.

Figure 2-1 – Diagram illustrating the distinction in acoustic treatment between insulation and conditioning

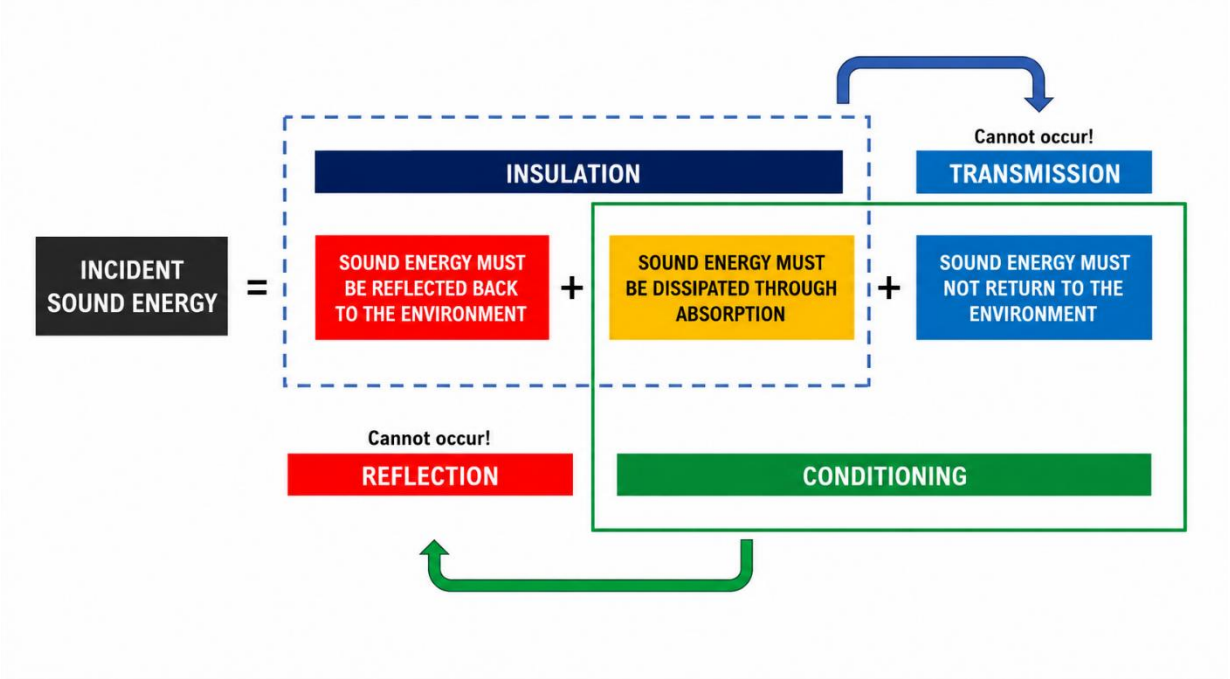

Source: The author (2022).

2.4.1 Acoustic insulation

According to Souza, Almeida and Bragança (2021), two terms are used when referring to noise reduction: insulation and isolation. Insulation refers to the treatment of airborne noise, whereas isolation is used for impact noise or vibration. On the other hand, Valle (2009) characterizes acoustic insulation as the condition in which noise is prevented from passing either from inside to outside or from outside to inside an environment. As explained by Bistafa (2018), sound insulation is measured through transmission loss (TL), which is used to prevent noise from being transmitted from one environment to an adjacent one. According to Silva (2011), acoustic insulation consists of architectural solutions whose objective is to reduce the level of noise generated in one environment from reaching a neighboring one, separated by a panel, partition wall, or barrier. The author also reports that this noise transmission occurs through direct passage via the wall, indirect passage through flanking paths or neighboring structures (slabs, columns, beams), or through openings such as windows, doors, ceiling voids, floor cavities, ducts, and similar elements. According to Bistafa (2018), an insulating structure is generally dense and reflective. For Silva (2011), sound insulation varies according to frequency, making it necessary to carry out measurements within the frequency ranges in which intervention is desired.

2.4.2 Acoustic conditioning

Acoustic conditioning is the acoustic treatment applied to a specific environment in which the objective is to create a pleasant sound environment by controlling echoes and reverberation (Valle, 2009, p. 163). According to Souza, Almeida and Bragança (2021), for a room to have good acoustics, it must provide good speech intelligibility, absence of external noise interfering with the sound of interest, proper sound diffusion and distribution, in addition to an adequate reverberation time. According to Campos (2012), the acoustic conditioning of an environment is achieved through two fundamental measures: the correction of the room's reverberation time based on internal acoustic absorption, and the improvement of sound distribution through the geometry of the room and its reflective surfaces.

2.5 Acoustic characteristics and properties of materials

According to Bujoreanu *et al.* (2018), the acoustic behavior of materials continues to be of great interest due to the many applications involving the need to attenuate or isolate sound in industrial and architectural components. As highlighted by Bistafa (2018), an absorbent material has a fibrous and porous structure through which sound waves can propagate and lose part of their sound energy. These materials are generally low in density and do not provide sound insulation properties. According to Souza, Almeida and Bragança (2021), the more porous a material is, the greater its absorption tends to be, which is usually indicated by the absorption coefficient, presenting variations according to the frequency of the incident sound. According to Bistafa (2018), the ability of a given material or structure to absorb or isolate noise is its main indicator of acoustic performance. However, Souza, Almeida and Bragança (2021) reports that a good insulating material is not always a good absorbing material, and vice versa. Although the functions of insulation and absorption are complementary, they require different characteristics or behaviors from materials when subjected to sound.

2.5.1 Classification of acoustic absorbing materials

The acoustic conditioning of reverberant environments involves the use of absorbing materials, according to Souza, Almeida and *Bragança* (2012, p. 129). The manner in which acoustic materials or elements absorb sound energy classifies them as porous or fibrous materials, vibrating panels or membranes, and resonators. However, Bistafa (2018) classifies

the materials used for sound absorption as porous (sponges or foams) or fibrous (rock wool and glass wool). These are lightweight materials that do not possess structural characteristics. Porous or fibrous materials are those that allow airflow into their interior, thereby providing good sound absorption, especially at high frequencies (above 2,000 Hz) (Tang; Yan, 2017).

According to Souza, Almeida and Bragança (2021), fibrous or porous materials are those that present a network of interconnected pores. According to Tang and Yan (2017), fibrous materials are economical and efficient in noise reduction, and their absorption coefficient is generally determined by porosity, thickness, and pore size. The acoustic absorption mechanism of fibrous materials can mainly be attributed to the viscous effect of air, which converts acoustic energy into thermal energy. According to Asdrubali, Schiavoni and Horoshenkov (2012), fibrous materials include various mineral wools, such as rock wool and glass wool. These materials are low-cost; however, mineral wools may pose health risks during handling, such as skin irritation and respiratory problems caused by inhalation (silicosis). As reported by Tang and Yan (2017), it is important to select the diameter, thickness, and porosity of the fibers in order to achieve optimal noise reduction efficiency.

According to Tao *et al.* (2021), porous materials are those containing interconnected pores that allow the passage of sound waves, which are dissipated mainly through frictional heating between vibrating air molecules and the pore surfaces. According to Carvalho (2010), the variation in the acoustic absorption of a material as a function of incident frequencies can be explained by its relationship with the shapes and dimensions of pores and fibers. Therefore, based on wavelength, it is understandable that these materials are more effective absorbers at high frequencies. Figure 2-2 illustrates the vibration behavior in the fibers of porous materials and the reflections occurring within the pores of a porous material.

Materials considered porous, such as polyurethane foams, have a high production cost, and their manufacturing process is regarded as highly aggressive to the environment due to the emission of toxic gases and high energy consumption (Asdrubali; Schiavoni; Horoshenkov, 2012).

According to Ermann (2015), a material is considered a good sound absorber when it presents one of the following properties or manufacturing conditions: porosity, a less smooth surface, lower weight, greater thickness provided that the material is porous, materials mounted over an air space, as well as those with fiber orientations that create several small interconnected air pockets. In addition, the author emphasizes that materials with absorption coefficients greater than 0.50 are generally considered sound-absorbing materials, whereas materials with absorption coefficients lower than 0.20 are generally considered sound-reflecting materials.

Figure 2-2 – Behavior of vibration in the fibers of porous material and reflections within the pores of a porous material

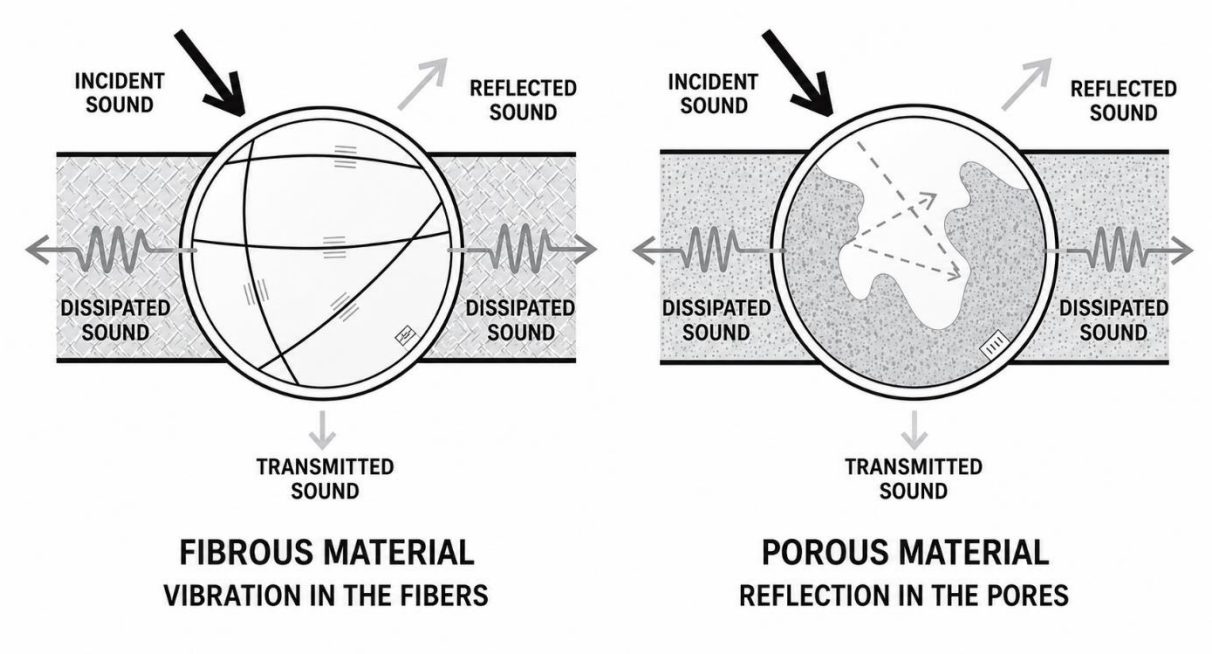

Source: Carvalho (2010).

2.6 Sound dissipation mechanisms

Sound dissipation is the fundamental process through which the organized mechanical energy of a sound wave is converted into disordered energy (heat) or removed from an acoustic system. This phenomenon occurs through several physical mechanisms that act both within the fluid itself (bulk losses) and at its boundaries (surface losses) (Garrett, 2020). The main sound dissipation mechanisms, shown in Figure 2-3, include mechanisms in homogeneous fluids, boundary mechanisms and absorbing materials, among other dissipation mechanisms. Mechanisms in homogeneous fluids are those processes that occur during wave propagation through the medium, regardless of the proximity of solid surfaces (Garrett, 2020).

One example is viscosity, which occurs when a sound wave travels through a fluid and the different velocities of neighboring particles generate internal friction. This “viscous drag” promotes the diffusion of particle momentum, resulting in energy losses through friction that are converted into heat (Long, 2006). Another process, called thermal conduction, occurs when the compressions and rarefactions of the sound wave create local temperature variations. Heat flows from compressed regions (hotter) to rarefied regions (cooler) in an attempt to equalize the temperature. Since this process is irreversible, part of the acoustic energy is lost to the

medium (Kuttruff, 2006). Another sound dissipation mechanism is molecular relaxation, also known as molecular absorption. This process occurs in polyatomic gases (such as air) when the wave energy is transferred from the translational motion of molecules to internal rotational and vibrational modes (Garrett, 2020). It is also defined as the time required for this energy to return to translational mode and reestablish thermal equilibrium. If this time is compatible with the wave period, significant dissipation occurs (Long, 2006). Bulk viscosity is another term used for a process that groups the loss effects associated with the hydrodynamic compression of the fluid, distinct from shear viscosity (Garrett, 2020).

However, in architectural acoustics, the so-called boundary mechanisms and absorbing materials refer to the interactions of sound with solid surfaces or porous materials, which constitute one of the most effective forms of dissipation in this field (Kleiner; Tichy, 2014). These mechanisms can be classified into three categories: thermoviscous boundary layers, friction in porous materials, and dissipation in resonators. According to Garrett (2020), thermoviscous boundary layers are defined as the thin layers formed near a rigid wall: the viscous boundary layer, where air velocity must decrease to zero, generating friction; and the thermal boundary layer, where the temperature fluctuations of the wave are dissipated through heat conduction with the wall. Another mechanism is friction in porous materials, which according to Mommertz (2009), occurs when the sound wave penetrates the pores of materials such as glass wool or open-cell foams containing interconnected pores. The oscillating air experiences momentum losses due to viscous friction with the fiber walls and flow resistance. Another process is dissipation in resonators, which according to Kleiner and Tichy (2014), occurs in devices such as Helmholtz resonators or vibrating panels that dissipate energy through air friction in the resonator “neck” or through internal damping of the panel material during bending.

There are also other dissipation mechanisms, such as hysteresis and internal damping, structural and chemical relaxation, sound radiation, and cavitation. According to Rindel (2017), hysteresis and internal damping are processes that occur in solids and elastomeric materials such as rubber, where energy is dissipated due to internal friction between molecules during cycles of deformation and elastic recovery. Structural and chemical relaxation, according to Garrett (2020), occurs in liquids such as seawater, where dissipation is increased by molecular rearrangement processes, known as molecular repacking, and by association-dissociation chemical reactions of salts such as boric acid and magnesium sulfate, triggered by the pressure variations of the wave. Sound radiation, although technically a transfer of energy rather than a conversion into heat, is treated in vibrating systems such as strings or plates as an energy loss

from the original system because the energy is spread into the surrounding medium (Garrett, 2020). Finally, cavitation, according to Kuttruff (2006), occurs in liquids under high pressure variations, where the rapid formation and collapse of vapor bubbles emit impulses that dissipate the original energy into a broad spectrum of noise.

Figure 2-3 – Sound dissipation mechanisms

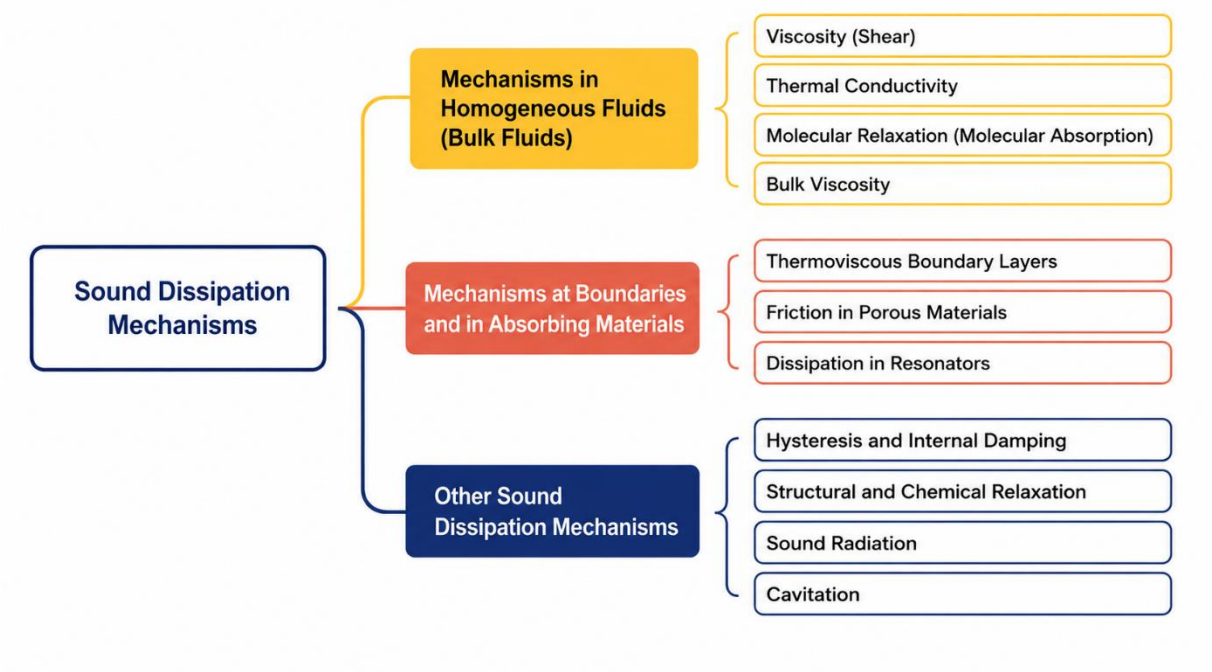

Source: The author (2025).

2.6.1 Sound

According to Bistafa (2018), sound can be defined as a variation in ambient pressure detectable by the auditory system.

2.6.2 Period

Period (T) is the time interval required for one cycle to be completed in the curve representing the variation of ambient pressure over time (Bistafa, 2018). According to Valle (2009), the period is the duration of one cycle.

2.6.3 Frequency

It is defined as the inverse of the period. According to Valle (2009), frequency is the number of cycles that occur each second and is also one of the most important characteristics of sound. Equation 2-1 presents the frequency formula (Bistafa, 2018).

Equation 2-1 – Frequency formula

$$f = 1 / T$$

2.6.4 Wavelength

Wavelength (λ) is defined as the distance from any sound pressure value required for one cycle to be completed in the sound pressure versus distance curve (Bistafa, 2018, p. 20). Wavelength can be obtained using Equation 2-2. Figure 2-4 presents the graphical representation of a sound wave, highlighting the wavelength (Bistafa, 2018).

Equation 2-2 – Wavelength formula

$$\lambda = C/f$$

Figure 2-4 – Graphical representation of a sound wave highlighting the wavelength

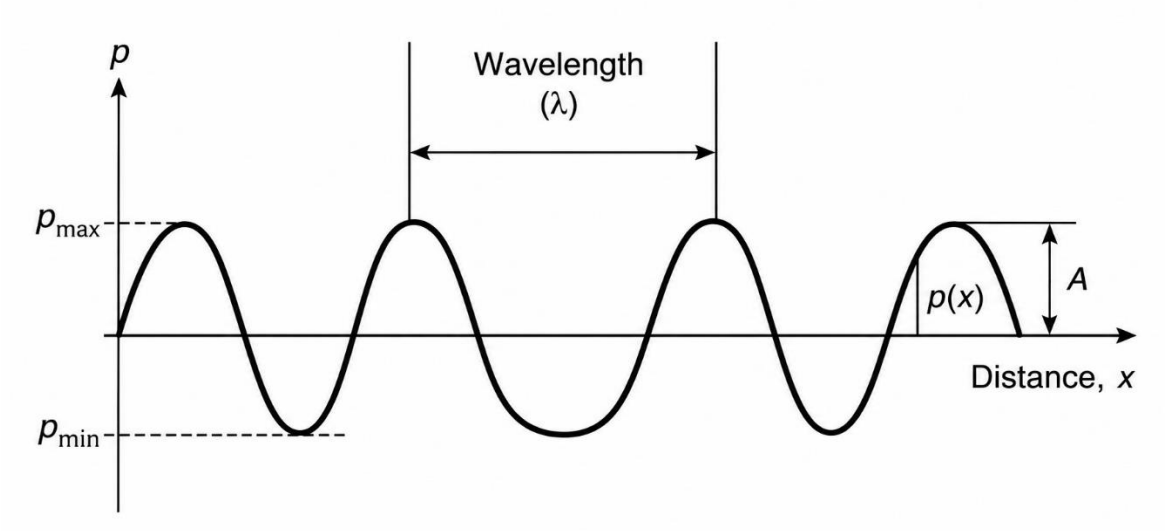

Source: Bistafa (2018).

2.7 The sound spectrum

According to Bistafa (2018), the sound spectrum provides the effective value of sound pressure for each frequency present in a sound. It is obtained through a mathematical operation called the Fourier Transform applied to the waveform. Figure 2-5 presents the graphical representation of the waveform of a noise signal and its sound spectrum.

Figure 2-5 – Graphical representation of the waveform of a noise signal (a) and its sound spectrum (b)

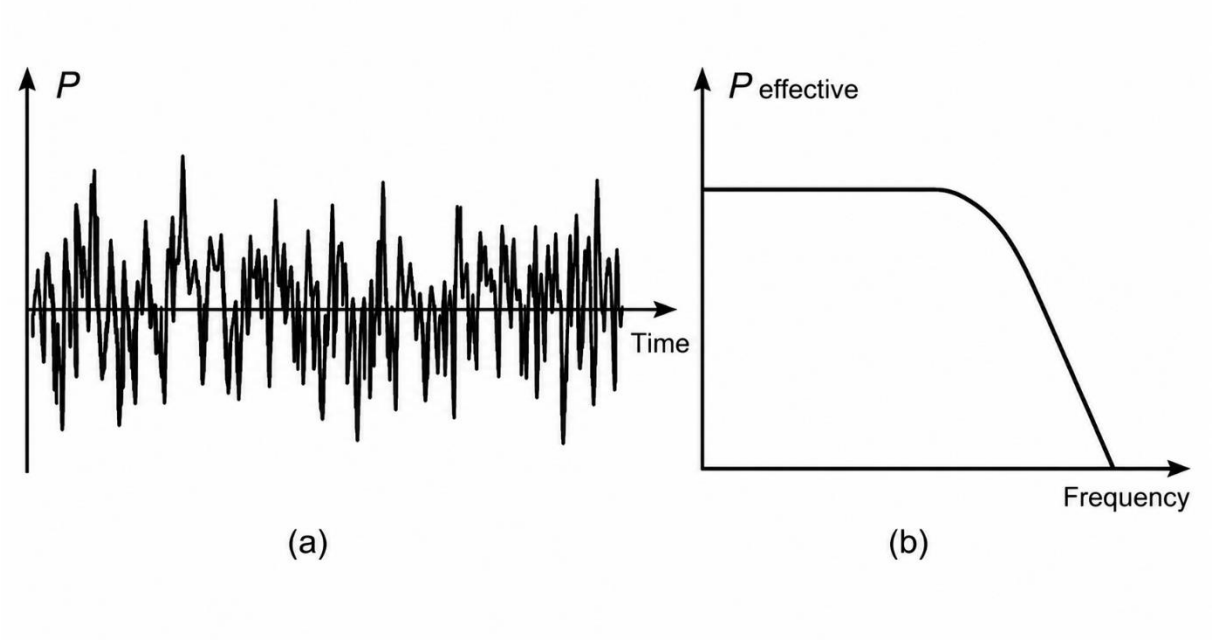

Source: Bistafa (2018).

2.8 Human hearing range

According to Bistafa (2018), the range of frequencies detected by the human ear varies from 20 Hz to 20,000 Hz, or 20 kHz. Sounds below 20 Hz are called infrasound, while those above 20 kHz are referred to as ultrasound. Figure 2-6 presents the audio spectrum divided and subdivided into frequency bands.

Figure 2-6 – The audio spectrum divided and subdivided into frequency bands

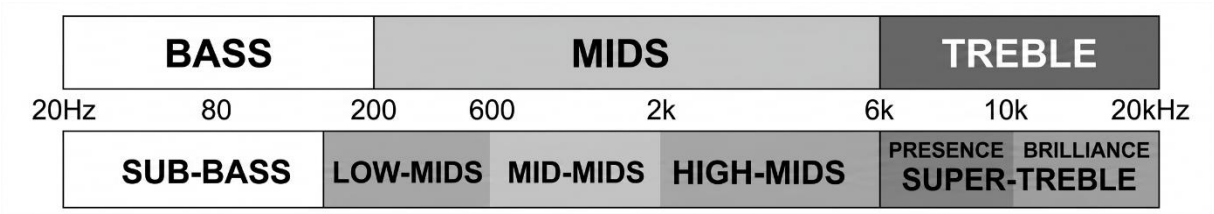

Source: Valle (2009).

2.9 Octave bands

Octave bands are groupings of frequency intervals used in acoustics to simplify the measurement and analysis of sound (Ermann, 2015). They divide the audible spectrum into practical sections based on the way the human ear perceives sound (Mehta; Johnson; Rocafort, 1998). An octave is defined as a frequency band in which the upper limit (fu) is exactly twice the lower limit (fL), represented by a 2:1 ratio (Mommertz, 2009). For example, the interval between 200 Hz and 400 Hz constitutes one octave (Mehta; Johnson; Rocafort, 1998).

The use of octave bands is due to the fact that human frequency perception is logarithmic (Everest; Pohlmann, 2021). The ear perceives musical intervals as ratios between frequencies rather than arithmetic differences; thus, the interval from 100 Hz to 200 Hz is perceived as having the same “size” as the interval from 1000 Hz to 2000 Hz, since both represent a 2:1 ratio (Mehta; Johnson; Rocafort, 1998). For purposes of international standardization (ISO/ANSI), the audible spectrum is commonly divided into 10 octave bands (31.5, 63, 125, 250, 500, 1000, 2000, 4000, 8000, and 16,000 Hz), identified by their center frequencies (Egan, 2007). Successive center frequencies are always double the preceding one (Ermann, 2015). In architectural acoustics, the eight octaves ranging from 63 Hz to 8000 Hz are the most commonly used (Mehta; Johnson; Rocafort, 1998).

Since the ratio is constantly 2:1, the bandwidth in Hertz increases as the frequency rises. For example, the 2000 Hz band encompasses many more physical frequencies (Hz) than the 250 Hz band (Ermann, 2015). Octave bands allow architects and engineers to describe the “color” or quality of a sound — whether it is rich in low or high frequencies—in a technical and organized manner. When a more detailed analysis is required, octaves may be subdivided into one-third octave bands, in which each octave is composed of three smaller bands, or even into divisions of 1/6 or 1/12 octave (Ermann, 2015).

2.10 Bel

Bel (symbol B, named in honor of Alexander Graham Bell) is a measure of the power level relative to a reference power and may assume both positive values (power greater than the reference) and negative values (power lower than the reference) (Bistafa, 2018, p. 30).

2.10.1 Decibel

In 1929, engineers at Bell Labs created the decibel (symbol dB) as a submultiple of the bel, such that 1 B is equivalent to 10 dB. It is widely used for comparing powers or quantities proportional to power (Bistafa, 2018, p. 30).

2.10.2 dB Scale

It is the logarithmic scale used to measure sound pressure level. A twofold increase in sound energy (for example, two identical jackhammers instead of one) causes the sound pressure level to increase by 3 dB. A tenfold increase in sound energy (10 jackhammers) causes the sound pressure level to increase by 10 dB, which is perceived as approximately twice as loud.

2.11 Weighting curve (A)

The (A) filter is a frequency weighting applied to sound pressure levels. It is used in sound pressure level meters (sound level meters) with the purpose of approximating the sensitivity perceived by the auditory system.

2.12 Sound pressure level

Sound pressure level is a logarithmic measure of the effective pressure of a sound relative to a reference value. It is measured in decibels (dB) above a reference level. The reference sound pressure in air is 20 μPa (2×10^{-5} Pa). This value is believed to correspond to the threshold of human hearing at a sound frequency of 1000 Hz.

2.13 L_{max}

It is the highest sound pressure level within a given period of time.

2.14 L_{eq}

It is the average sound pressure level within a given period of time. If the A filter is used for frequency weighting, the average level is referred to as LAeq. The A-weighted equivalent sound pressure level (LAeq) is probably the most widely used index because it correlates well with many psychophysiological effects of noise.

2.15 Sound absorption coefficient

According to Bistafa (2018), the absorption coefficient determined in a reverberation chamber is called the Sabine absorption coefficient (ãS). According to Bujoreanu *et al.* (2017), the sound absorption coefficient quantifies how much sound is absorbed by a material and transmitted through it. For Bujoreanu *et al.* (2018), the absorption coefficient (α) is defined as the ratio between the absorbed energy and the incident energy (Ei). It can also be defined as the ratio between all non-reflected energy (Er) and the incident energy. Equation 2-3 presents the formula for the sound absorption coefficient (α), where (Er) is the energy reflected by the material, (Ei) is the incident sound energy on the material, and 1 is a constant value.

Equation 2-2 – Formula for the sound absorption coefficient (α), where (Er) is the energy reflected by the material, (Ei) is the incident sound energy on the material, and 1 is a constant value (Bujoreanu *et al.*, 2018)

$$\alpha = 1 - \frac{E_r}{E_i}$$

According to Bistafa (2018), sound absorption (ãS) is mainly used to control the reverberation time of a given enclosure. According to Bujoreanu *et al.* (2018), the absorption coefficient can be measured in a reverberation room according to the ISO 354 standard (International Organization for Standardization – ISO, 2003a) or by using the standing wave tube technique presented in Part 1 of ISO 10534/1996 (ISO, 1996), as well as the transfer

function method described in Part 2 (ISO, 2023). As reported by Bistafa (2018), the absorption coefficient increases according to the increase in thickness and density of porous and fibrous materials. According to Pedroso, Brito and Silvestre (2017), the best way to compare the performance of acoustic insulation materials is through their sound absorption coefficient or through their effective behavior, known as the mass law. According to Valle (2009), some materials absorb certain frequencies better, while other materials absorb different frequencies. Thus, some materials will be more reflective and diffusive, being responsible for the amount of time sound reverberates within an environment. Three parameters are important and commonly analyzed in absorbing materials: airflow resistivity, porosity, and tortuosity (Buratti *et al.*, 2018).

2.16 Noise reduction coefficient (NRC)

According to Pedroso, Brito and Silvestre (2017), the NRC is defined as the arithmetic average of the sound absorption performance of a material based on four frequencies (250, 500, 1000, and 2000 Hz) in octave bands. It is used to provide general parameters for sound absorption within the frequency ranges of human speech, although it does not reflect the material's behavior throughout the entire audible frequency range. Equation 2-4 presents the formula for the Noise Reduction Coefficient (NRC).

Equation 2-3 – Formula for the NRC (Pedroso; Brito; Silvestre, 2017)

$$NRC = (\alpha 250 + \alpha 500 + \alpha 1000 + \alpha 2000) / 4$$

According to Bistafa (2018), the NRC is defined as a single number responsible for summarizing the sound absorption capacity of a material, being used in an initial analysis to compare the performance of two absorbing materials.

2.17 Sound transmission coefficient

According to Bistafa (2018), the parameter used to characterize the ability of a wall to isolate or transmit sound is its sound transmission coefficient (τ). The lower its value, the lower the transmitted sound intensity, and therefore, the more insulating the wall will be.

2.18 Sound transmission loss (TL)

According to Bistafa (2018), sound transmission loss is used to characterize the sound insulation of a wall and is a quantity derived from the sound transmission coefficient. Equation 2-5 presents the formula for sound transmission loss.

Equation 2-4 – Formula for sound transmission loss (Bistafa, 2018)

$$PT = 10\ Log\ (1/\tau)$$

According to Tao *et al.* (2021), transmission loss (TL) represents the decibel reduction in sound wave power when it passes through a material (panel-type sound absorbers), and it can be measured using an impedance tube in accordance with ASTM E1050-12 (Advancing Standards Transforming Markets – ASTM, 2012) and ISO 10534 (ISO, 1996).

2.19 Reverberation time (RT) and T60

According to Valle (2009), reverberation consists of countless sound reflections occurring throughout all areas of a closed or semi-enclosed environment, taking place at very short time intervals. Reverberation is measured in milliseconds and is referred to as Reverberation Time (RT). According to Gaspar *et al.* (2020), reverberation time is the acoustic parameter or descriptor initially used in the acoustic evaluation of an enclosed space. It quantifies the persistence of sound within a room after the interruption of the sound source and is crucial for the acoustic conditioning design of rooms (Procel Edifica, 2011).

Reverberation Time is measured in seconds and corresponds to the time required for the sound energy in an enclosed environment to decay to one-millionth of its original value (Everest; Pohlmann, 2021). In terms of sound pressure, this corresponds to a 60 dB reduction in the sound level of the environment, and this acoustic descriptor is called T60. T60 depends mainly on the volume of the space or room and the total sound absorption (Procel Edifica, 2011). The volume of a room is directly proportional to T60, and vice versa (Ermann, 2015). In rooms with larger volumes, sound travels greater distances between reflections, resulting in a slower decay (Ermann, 2015).

Figure 2-7 presents the reverberation time of a sound source decaying by 60 dB within a time interval of 1.9 seconds. In practice, the slope of the decay is measured between -5 dB

and -35 dB from the initial level and is referred to as T30 (a 30 dB decay after the initial decay of -5 dB).

Figure 2-7 – T60 reverberation time of a sound source decaying by 60 dB over a time interval of 1.9 seconds

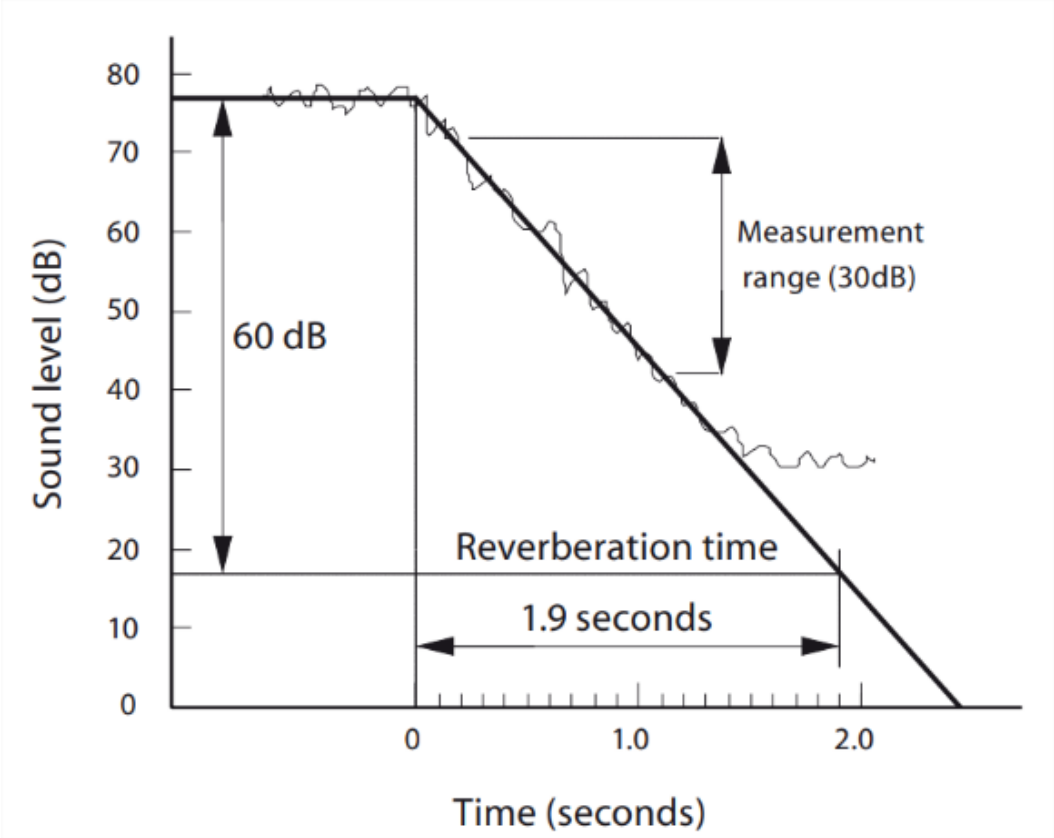

Source: Barron (2009).

This occurs, as explained by Valle (2009), because the amount of time sound reverberates within an environment depends on the finishing materials and the way the room is occupied. Since the acoustic absorption of materials varies according to frequency, the room's RT60 also varies with frequency. When referring to the reverberation time of an environment, it generally refers to the RT60 at mid frequencies and, by convention, is specified at 500 Hz.

In summary, T60 is the fundamental measure of room acoustics, determining whether sound will be perceived as "dry" (low T60) or "live" (high T60) (Kleiner; Tichy, 2014). The search for the ideal T60 is a compromise between the clarity desired for speech and the resonance desired for music (Appleton, 2007). In practice, it is often impossible to measure the full 60 dB decay due to the relationship between the source sound level and the background noise level of the environment (Ermann, 2015). T60 is by far the most important criterion for the acoustic quality of indoor environments (Mommertz, 2009). For this reason, T60 is

frequently extrapolated from measurements of decay over a smaller range, such as EDT, T20, and T30. The measurement begins 5 dB below the average steady-state level in order to disregard the influence of the direct sound and the first reflections (Procel Edifica, 2011).

2.19.1 Optimum Reverberation Time (OT)

According to NBR 12179 (Associação Brasileira de Normas Técnicas – ABNT, 1992), the Optimum Reverberation Time is the reverberation time considered ideal for a given enclosure and a specific activity, expressed in seconds. The ideal T60 value depends directly on the function of the environment. In spaces intended for spoken word, such as classrooms or conference rooms, the recommended T60 at mid frequencies—the range in which human hearing is most sensitive—should be short, generally ≤ 0.8 s, or even 0.4 s for maximum intelligibility (Pierce, 2019). This reverberation time ensures speech clarity and intelligibility, preventing syllables from overlapping and causing masking effects. The Brazilian standard NBR 12179 (ABNT, 1992) adopts Figure 2-8, which presents Optimum Reverberation Time values for various uses or sound expressions in spaces with volumes ranging from 30 to 30,000 m³ at the frequency of 500 Hz.

Figure 2-8 – Graph of the optimum reverberation time

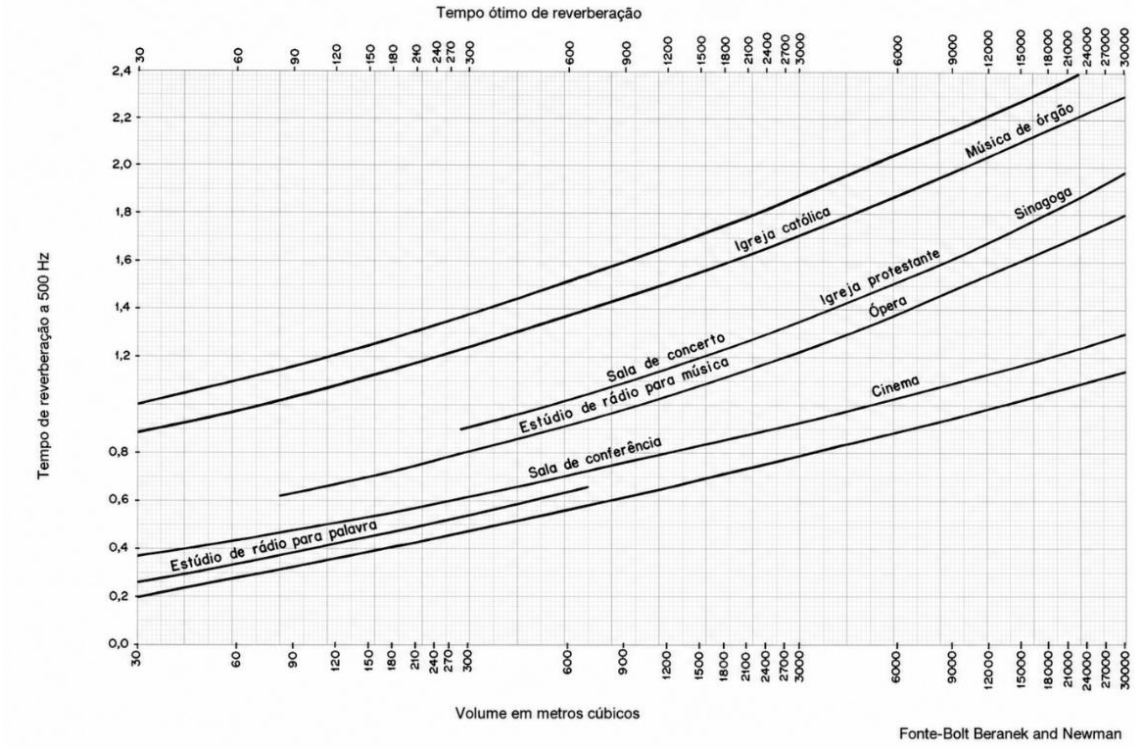

Source: NBR 12179 (ABNT, 1992).

2.19.2 Early reflections

According to Valle (2009), Early Reflections or primary reflections are those that occur in an enclosed environment before the sound becomes diffuse, spreading evenly throughout the entire space. Caused by reflective areas or surfaces located near the sound source, they may produce different phenomena due to time delay, such as sound cancellations, and may also impair intelligibility and generate echoes. Figure 2-9 presents a graph representing the direct sound, the first reflections, and the reverberation of sound decaying by 60 dB.

Figure 2-9 – Graph of reverberation time and early reflections

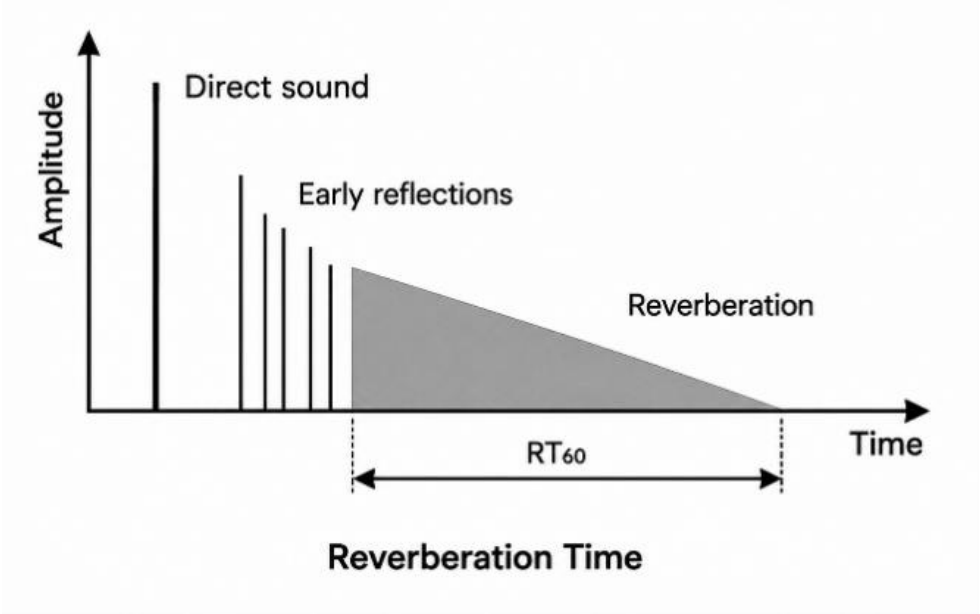

Source: Valle (2009, p. 94).

2.19.3 EDT10

The term or acoustic descriptor EDT refers to Early Decay Time (Ermann, 2015). This descriptor is a crucial acoustic metric frequently used to characterize reverberation in enclosed spaces and is directly related to how reverberation is subjectively perceived by the listener (Aletta; Kang, 2020). When the acoustic descriptor is accompanied by the number 10, associated with EDT (implicit in its definition), EDT10 refers to the amplitude of the sound pressure level (SPL) decay used to calculate this metric (Ermann, 2015). Its calculation is defined as the time, in seconds, required for the sound energy level (or sound pressure level) to decay by 10 dB from its initial steady-state value, with this time then multiplied by 6 (Ermann,

2015). This measurement highlights the importance of variations in the early sound reflections (Aletta; Kang, 2020).

The descriptor is a reverberation measure calculated from the initial portion of the room decay curve (Long, 2006). EDT is considered a superior indicator of reverberation in music, presenting a higher correlation with subjective evaluations of concert halls, for example, than other methods such as reverberation time (T60) (Ermann, 2015). EDT better evaluates the subjective impression of reverberation (Aletta; Kang, 2020), since the initial decay largely defines the subjective impression of the entire reverberation event (Everest; Pohlmann, 2021). EDT is one of several ways to characterize sound decay because it uses the decay time of the first 10 dB multiplied by 6 (Ermann, 2015). EDT is measured differently because it considers early reflections, making it a more sensitive parameter for room acoustic evaluation than T30 (Aletta; Kang, 2020).

Among the three descriptors, EDT (Early Decay Time) is the one that most closely resembles the subjective perception of the human ear regarding the reverberation of an environment (Ermann, 2015). The human ear is more sensitive to the initial portion of sound decay (the first 10 to 20 dB of reduction) while the sound is still occurring, such as during speech or a musical performance (Everest; Pohlmann, 2021). EDT measures precisely the first 10 dB of decay (extrapolated to 60 dB), capturing the sense of “liveliness” perceived by the listener at the moment notes or syllables end (Beranek, 2004). Unlike T20 and T30, which intentionally ignore the first 5 dB of decay in order to obtain a more stable and “global” measurement of the room, EDT is extremely sensitive to early reflections (Everest; Pohlmann, 2021). Since the auditory system integrates these early reflections with the direct sound (Haas Effect), they define the perception of intimacy and clarity that the brain processes as the “acoustics” of the place (Ziemer, 2020). While T30 reflects the global physical properties of the room volume, EDT reflects what the listener actually experiences at a specific position (Aletta; Kang, 2020). In summary, if the objective is to measure the sensation of reverberance perceived by the ear, EDT is the most accurate tool (Ermann, 2015).

2.19.4 T20

T20 is one of the methodologies used in room acoustics to measure and extrapolate the T60 reverberation time (Ermann, 2015). Reverberation time, by definition, is the time required for the sound energy level in a room to decrease by 60 dB after the sound source has been interrupted (Rindel, 2017). Since it is often impractical to measure the full 60 dB decay due to

limitations related to background noise level or sound source power (Ermann, 2015), T20 uses a smaller decay interval to estimate T60 (Rindel, 2017).

The calculation of T20 is defined as the time required for the sound pressure level to decay by 20 dB (Rindel, 2017). The evaluation range for T20 typically begins 5 dB below the average steady-state sound level in the room and ends 25 dB below this same initial level (that is, from -5 dB to -25 dB of decay) (Rindel, 2017). The time measured within this 20 dB range is then multiplied by three in order to extrapolate the total 60 dB decay value (Ermann, 2015). The Brazilian standard NBR ISO 3382-2 (ABNT, 2017a), which addresses the measurement of room acoustic parameters, uses the 20 dB evaluation range, and the resulting value is denoted as T20 (Rindel, 2017).

2.19.5 T30

Similarly, T30, like T20, uses the time required for sound to decay within an environment. T30 uses a 30 dB variation, generally from -5 dB to -35 dB relative to the peak of the direct sound, and doubles this time in order to extrapolate T60 (Kleiner; Tichy, 2014).

2.19.6 D50

D50 is a fundamental acoustic metric used to evaluate speech intelligibility within a space (Aletta; Kang, 2020). It is also referred to as the “definition” criterion (Kuttruff, 2016). D50 (Definition 50) is an acoustic descriptor that represents one of the earliest attempts to relate the ratio between early sound energy and total sound energy to intelligibility, based on the publication by Thiele (1953). According to Long (2006), useful energy is the sum of the direct sound and the reflected energy that reaches the listener within 50 milliseconds (50 ms) after the direct sound. The descriptor provides complementary information regarding the balance between early and late reflections within a space.

Reflections with delays shorter than approximately 50 ms are generally perceived as “useful reflections” or “early reflections”, which increase the apparent loudness of the direct sound and contribute to better speech comprehension. The practical limit of 50 ms corresponds to a path difference of 17 meters, since higher values may cause echoes (Procel Edifica, 2011). In environments intended for music, this limit for early reflections is often extended to 80 milliseconds or 100 milliseconds, depending on the type of composition and the author. The D50 index is calculated using Equation 2-6.

Equation 2-6 – Equation for calculating D50 (Pierce, 2019)

$$D50 = (energy\ in\ the\ first\ 50ms) \ / \ (total\ energy)$$

In the equation, g(t) is the impulse response, and the entire numerator represents the sound energy arriving within the first 50 milliseconds (ms) after the direct sound. It represents the energy of the direct sound and the early reflections that the auditory system typically integrates as "useful sound." The denominator represents the total arriving sound energy (the integral of the squared impulse response), including late reverberation.

Regarding the meaning of D50 in terms of the acoustic quality of speech clarity, average D50 values below 0.3 (or 30%), especially in the frequency bands up to 2 kHz, indicate poor speech transmission clarity. Low clarity is considered particularly concerning for effective speech transmission (Aletta; Kang, 2020).

2.19.7 C80

The C80 descriptor (also known as the Clarity Factor or Clarity Index), which uses an 80 ms limit for early reflections, is an objective acoustic parameter used to evaluate the clarity and transparency of music within an environment (Kuttruff, 2016). The concept of clarity, in subjective terms, refers to the sensation of hearing or perceiving the individual parts or instruments within a musical piece or speech (Aletta; Kang, 2020). Objectively, C80 quantifies the balance between early (useful) sound energy and late reverberant sound energy (Aletta; Kang, 2020).

The formal definition of C80 is the logarithmic ratio (in decibels) of the sound energy arriving within the first 80 milliseconds (ms) after the arrival of the direct sound, compared to the total sound energy arriving after these 80 ms (Kuttruff, 2016). According to Ziemer (2020), the calculation of C80 is expressed by Equation 2-7:

Equation 2-7 – Equation for calculating C80 (Ziemer, 2020)

$$C_{80} = \left(\frac{\int_0^{80ms} p^2(t)dt}{\int_{80ms}^{\infty} p^2(t)dt} \right) dB$$

In Equation 2-7, (p) corresponds to sound pressure, and (t) represents time. C80 is listed as a metric primarily related to musical clarity. Typical acceptable values for concert halls, for example, range from approximately -5 dB to +3 dB. Regarding musical quality, the average C80 values in the 500 Hz, 1 kHz, and 2 kHz bands ranged between -2.7 dB and -3.7 dB in highly successful concert halls, such as those in Boston and Vienna (Long, 2006). However, values below 4 dB at frequencies under 500 Hz are indicative of poor musical clarity (Aletta; Kang, 2020).

In the architectural context, in large, monumental structures such as cathedrals or mosques with immense volumes and few surfaces close to the receiver (such as suspended reflectors), late reflections tend to dominate, resulting in very low C80 values. Regarding spatial dependence, the value of C80 is highly dependent on the position of both the receiver and the sound source (Aletta; Kang, 2020). The 80 ms limit is chosen for C80, unlike D50 (Definition, which uses 50 ms), in order to characterize musical transparency, whereas D50 is often used to evaluate speech intelligibility (Kuttruff, 2016).

C80 is a parameter that is inverse or concurrent to reverberation. When its value is positive, this indicates that the energy of the early reflections (ER) dominates, suggesting high clarity or indicating clearer sound and generally better speech intelligibility. A negative value indicates that late sound or reverberation contains more energy (Ziemer, 2020). In environments where classical and musical clarity is a key factor, such as concert halls, C80 values typically range between -4 decibels (dB) and +1 dB for unoccupied rooms (Ermann, 2015).

2.20 Spoken word and sung word

The frequency range of human voices covers a significant portion of the audible spectrum (20 Hz to 20 kHz). The energy content of the voice varies drastically with frequency, depending on whether the voice is spoken or sung, and whether the analysis concerns the fundamental frequency or the harmonics (Kleiner; Tichy, 2014). Human speech generally contains energy in the range of approximately 100 Hz to 5 kHz (Mehta; Johnson; Rocafort, 1998). More specifically, human speech contains energy from about 125 Hz to 8000 Hz (Egan, 2007).

The frequency range for speech is typically divided into two regions. Approximately 75% of sound energy is concentrated in vowels, which are mainly associated with low frequencies (Egan, 2007). Most speech power is concentrated in frequencies below 1 kHz, with 80% of the power below 500 Hz (Everest; Pohlmann, 2021). Vowels contribute primarily to

the tone and distinctive quality of an individual voice (Mehta; Johnson; Rocafort, 1998). The peak region of maximum speech energy (power) is concentrated between 200 Hz and 600 Hz, corresponding to the mid frequencies (Everest; Pohlmann, 2021).

The relatively small amount of power at high frequencies is essential for speech intelligibility (Everest; Pohlmann, 2021). Consonants, which contain most of the information necessary for articulation and word distinction, occupy higher frequencies (Egan, 2007). Frequencies above 1 kHz, specifically in the range from 2 kHz to 4 kHz, are primarily responsible for intelligibility (information) and auditory sensitivity (Mehta; Johnson; Rocafort, 1998).

Regarding gender differences, the vibration frequency of the female voice is generally higher than that of the male voice because women's vocal cords are typically shorter and thinner (Egan, 2007). The peak of the male voice generally occurs around 400 Hz, while the peak of the female voice is close to 500 Hz (Mehta; Johnson; Rocafort, 1998). The efficiency of the human voice within the audible spectrum is generally analyzed from two perspectives: where the greatest energy (power) is concentrated and where the greatest intelligibility (information) is concentrated.

The consensus in the literature indicates that the voice is more efficient in terms of power at low and mid frequencies, but more efficient in terms of intelligibility at mid and high frequencies. Frequency analysis is crucial because the sensitivity of human hearing is highly dependent on frequency (Garrett, 2020).

2.21 Speech intelligibility and speech transmission Index (STI)

Speech Intelligibility (or Speech Intelligibility of Speech) is primarily defined as the ability of listeners to understand speech within an environment, such as during a toast at a party or a lecture in a classroom (Ermann, 2015). According to Santos (2020), speech intelligibility is defined by the percentage of phonemes understood and is therefore the fundamental acoustic characteristic of an environment, reflecting the degree of word comprehension within a space.

According to IEC 60268-16 (International Eletrotechnical Commission – IEC, 2020), speech is the primary means of communication between people. In the vast majority of situations, the speech signal is degraded along its transmission channel or throughout the path traveled by the signal between the speaker (sound source) and the listener (receiver). This degradation causes a reduction in speech intelligibility at the listener's position. Similarly, it

can be defined as the ability to understand the sound of words received by the listener (receiver) after traveling the path between the sound source (speaker) and the receiver.

Therefore, the Speech Transmission Index (STI) is a rapid measurement method used to assess speech intelligibility, with values ranging from 0 to 1. Values below 0.30, 0.45, and 0.60 are considered respectively bad, poor, and fair. However, values above 0.45, 0.60, and 0.75 are classified as fair, good, and excellent.

2.22 Classroom evaluation

The acoustic evaluation of a classroom (or lecture/teaching rooms) is crucial, since approximately 75% of the time spent in these environments is dedicated to oral communication (speech and listening) (Mommertz, 2009). The primary objective of acoustic design for classrooms is to ensure high speech intelligibility throughout the entire space while minimizing artifacts and background noise that may mask the teacher's voice (Egan, 2007).

For classrooms, the acoustic descriptors focus on speech clarity and background noise control, with Reverberation Time (RT) being the most important criterion (Mommertz, 2009). Table 2-1 presents the main descriptors used in the evaluation of the acoustics of rooms intended for spoken words.

The acoustic descriptors reveal that the evaluation of speech and music characterization and quality in an enclosed environment has much in common from the perspective of clarity and correct sound reproduction (Kleiner; Tichy, 2014). For environments optimized for speech, such as classrooms, the most crucial parameters are generally Reverberation Time (T60) and the Speech Transmission Index (STI) (Mommertz, 2009). Classrooms are considered small- to medium-volume spaces where speech intelligibility is crucial. To achieve this, they require short reverberation times. The recommended values for occupied classrooms typically range between 0.5 and 0.7 seconds (s) in the frequency bands from 250 Hz to 2000 Hz (Mommertz, 2009).

Table 2-1 – Main descriptors used in the acoustic evaluation of rooms intended for spoken word

Descriptor	Focus and function
Reverberation Time (RT or T60)	Describes the decay of sound over time and is the most important criterion for the acoustic quality of a classroom (Mommertz, 2009). An excessively long RT reduces speech intelligibility because successive syllables overlap and blend together (Egan, 2007).
Speech Transmission Index (STI or RASTI)	STI (Speech Transmission Index), or its faster version RASTI, is an objective metric used to quantify speech intelligibility (Mommertz, 2009). Low RASTI values are associated with reduced student performance in noisy school environments (Ermann, 2015).
Definition (D50)	A metric similar to STI, used to evaluate the suitability of an environment for speech. D50 indicates the ability of a room to provide precision in the articulation of vocal sounds (Mommertz, 2009).
Noise Criteria (NC / RC)	They are used to specify the maximum allowable levels of continuous background noise (typically from HVAC systems), ensuring that noise does not mask speech and does not cause distraction (Egan, 2007).
Signal-to-Noise Ratio (S/N)	Speech intelligibility is determined by the signal-to-noise approach. For good comprehension to occur, the speaker's signal must be sufficiently audible in relation to the background noise (for example, +10 to +15 dB above the noise level) (Ermann, 2015).

Source: The author (2025).

The field of architectural acoustics focuses on the mid- and high-frequency range because it plays a crucial role in promoting speech intelligibility, reflecting an evolutionary preference of the human ear for sounds in these frequencies (Ermann, 2015). If a classroom were evaluated using C80, the ideal condition would be for it to present positive values (or at least values above the -4 dB threshold) (Aletta; Kang, 2020), since this would indicate that the environment is acoustically dry (low reverberation) and promotes good separation between syllables and musical notes, which is the opposite of the "smearing" caused by excessive reverberation (Ermann, 2015).

To objectively evaluate the clarity of spoken word, the parameter corresponding to C80 is D50 (Definition), which uses a 50 ms limit (Beranek, 2004; Mommertz, 2009). The complexity of acoustic evaluation in classrooms may be compared to that of orchestras, where instead of evaluating melody and harmony, the analysis focuses on the clarity and separation of sounds (consonants and syllables) within a field of noise and reverberation. This analysis ensures that essential communication is not "drowned out" by the environment itself or by external interferences.

2.22.1 Pink noise

Pink noise is a type of aperiodic and stationary signal widely used in acoustic measurements because it possesses a specific spectral distribution (Garrett, 2020). The main characteristics of pink noise are defined by its power spectrum, namely Spectral Density and Energy per Octave. The spectral density of pink noise is inversely proportional to 1/f (where f is the frequency), resulting in a greater prevalence of low frequencies (by analogy to red light, which has low frequency) (Everest; Pohlmann, 2021).

Energy per octave is another characteristic of pink noise. It has equal energy per octave (or one-third octave band). The spectral level of pink noise is characterized by a downward slope of −3 dB/octave (Everest; Pohlmann, 2021). In acoustic applications, pink noise is generally preferred over white noise because its energy distribution more closely resembles the way the human ear subjectively perceives sound (Everest; Pohlmann, 2021). In acoustic reflection perception tests, the audibility threshold curves for pink noise are very similar to those of classical music, making it a reasonable substitute for music in such experiments (Everest; Pohlmann, 2021).

White noise is a type of aperiodic signal that possesses a continuous and constant spectrum, containing equal amounts of all frequencies within a frequency band of interest (Serafin *et al.*, 2022). By analogy with white light, which is assumed to be uniformly composed of all optical frequencies, white noise is characterized by a spectral density that is constant throughout the entire frequency range (Pierce, 2019). The waveform of white noise is rough and characterized by a flat spectrum (Serafin *et al.*, 2022).

White noise is used as an idealization of spectral density in which $p^2f(f)$ (sound pressure spectral density) remains constant over the frequency band of interest. This distinguishes it from pink noise, whose spectral density is proportional to 1/f, resulting in a greater prevalence of low frequencies (by analogy with red light, associated with low frequency) (Serafin *et al.*, 2022). White noise is defined by its spectral uniformity, meaning that it has the same energy at each frequency across the spectrum (Serafin *et al.*, 2022).

White noise may be understood as a type of fill light (white light) that uniformly illuminates all colors (frequencies) within an environment, ensuring that no “color” (frequency) stands out more than another. In contrast, pink noise would resemble a light source that favors warmer colors (low frequencies) (Serafin *et al.*, 2022).

2.22.2 White noise or pink noise

NBR ISO 3382-2 (ABNT, 2017a), which addresses the measurement of reverberation time (RT) in ordinary rooms, specifies the requirements for the excitation signal but does not directly quantify the difference in RT measurement results specifically caused by the use of white noise versus pink noise. However, the standard establishes criteria regarding the spectrum of the signal used in room excitation to ensure reliable measurements, which indirectly explains the role of pink noise (pink spectrum) (ABNT, 2017a).

For room excitation using the interrupted noise method, the signal fed into the sound source must be obtained from random broadband noise or pseudo-random electrical noise. However, the crucial spectral requirement is related to the analysis frequency. The spectrum must be reasonably flat within the octave band to be effectively measured. For octave-band measurements, the signal bandwidth must be greater than or equal to one octave. For one-third octave-band measurements, the signal bandwidth must be greater than or equal to one-third octave (ABNT, 2017a).

Pink spectrum (or pink noise) is typically used in room acoustics because it possesses equal energy per octave band or one-third octave band. If a white noise signal is used—which has constant energy per frequency and therefore decreasing energy in octave bands as frequency increases—the energy at high frequencies may be insufficient to excite the room adequately or may result in a reverberant sound level that is not flat across the analysis bands (ABNT, 2017a). Shaping the spectrum into a “pink spectrum” is a practical way to ensure that the sound spectrum within the room (the stationary reverberant sound field) is suitable for measurement within the required frequency ranges (at least 125 Hz to 4000 Hz in octave bands for engineering and precision methods).

Although the difference in results is not quantified in terms of measurement error, the choice of excitation signal is related to measurement reliability and the signal-to-noise ratio. The main implication of using pink noise is to ensure a sufficient level; that is, the omnidirectional source must produce a sound pressure level high enough to provide decay curves beginning at least 35 dB above the residual sound pressure level for T20 determination (or 45 dB for T30) in all frequency bands. Regarding the adequacy of the sound spectrum (whether random or pseudo-random), it must be reasonably flat within the octave or one-third octave band being measured, which is often facilitated by shaping the signal into a pink spectrum within the reverberant field.

Therefore, if either white noise or pink noise is used and both are capable of meeting the minimum dynamic range requirement and maintaining a reasonably flat spectrum within the frequency band of interest, the expected RT (reverberation time) result will be the same. Pink spectrum is simply the preferred engineering technique for achieving these ideal excitation conditions throughout the measurement spectrum (from 88 Hz to 5657 Hz) (ABNT, 2017a). Table 2-2 presents a comparison between white noise and pink noise.

Table 2-2 – Comparison between white noise and pink noise

Type of noise	**Spectral caracteristic**	**Common use**
White noise	Flat spectrum (uniform energy per frequency)	Electrical measurements
Pink noise	Spectral density $\propto 1/f$ (uniform energy per octave)	Acoustic measurements and substitute for music

Source: Everest and Pohlmann (2021).

2.22.3 Sweep signal

The sweep signal or swept-sine wave (also known as a chirp signal), is a type of deterministic signal used in acoustic measurements, especially to determine the Room Impulse Response (RIR), from which Reverberation Time (T60 or RT) is calculated (Kleiner; Tichy, 2014). This method, which uses the sweep signal, is an advanced acoustic measurement technique that has become an attractive and efficient alternative to traditional methods such as interrupted noise and Maximum Length Sequence (MLS) (Rindel, 2017).

The sweep is a sinusoidal signal with varying frequency (Kleiner; Tichy, 2014). In the context of room acoustics measurements, it generally covers the entire frequency range of interest in a single sweep (Rindel, 2017). Measurements may be performed using slow sweeps (in analog techniques) or fast sweep sine wave chirp signals in systems based on Fast Fourier Transform (FFT) (Kleiner; Tichy, 2014). In architectural acoustics studies, such as those conducted in cathedrals, a sine sweep signal may be emitted by an omnidirectional sound source (such as a dodecahedron loudspeaker), with the frequency increasing exponentially over time (for example, during 20 s, covering octave bands from 63 Hz to 16 kHz) (Aletta; Kang, 2020).

The sweep signal is used in reverberation time measurements and is essentially employed to obtain the Room Impulse Response (RIR). The RIR is considered the “acoustic

signature" of a space and contains all the information necessary to characterize the enclosure as an acoustic filter between the source and the receiver (Kleiner; Tichy, 2014). From the measured RIR, Reverberation Time is calculated using the Integrated Impulse Response Method (or Schroeder method), which involves the reverse-time integration of the squared impulse response.

The swept-sine method presents several significant advantages compared to other measurement techniques (Rindel, 2017). Four of these advantages are as follows:

First, the High Signal-to-Noise Ratio (SNR), since it is possible to inject a large amount of energy into the room over an extended period, which increases the SNR and efficiently suppresses background noise (Kleiner; Tichy, 2014).

Second, Immunity to Harmonic Distortion. The post-processing of the sweep signal can reject unwanted harmonics generated by the measurement system (such as loudspeakers and amplifiers), making the measurement more accurate and less dependent on system linearity (Everest; Pohlmann, 2021).

Third, the Lower Crest Factor. The swept-sine signal has a lower crest factor (peak-to-RMS ratio) than noise signals. This allows the use of higher excitation levels without overloading the loudspeaker (Rindel, 2017).

Finally, Robustness Against Temporal Variations. The swept-sine method is more robust against temporal variations (changes in the environment during measurement) (Rindel, 2017).

By using the integrated impulse response method with the sweep signal, a single sweep can cover the entire required frequency range (Rindel, 2017). Furthermore, because the signal is deterministic, the stochastic nature of traditional noise excitation is avoided, and measurement uncertainty due to analysis time can be neglected (Rindel, 2017).

2.23 NBR 3382-2 standard

The Brazilian Standard NBR ISO 3382-2 (ABNT, 2017a) addresses the measurement of room acoustic parameters, specifically reverberation time in ordinary rooms. It details the measurement procedures, including the required equipment, the number of measurement positions, and the methods used to evaluate and present the test data, such as the interrupted noise method and the integrated impulse response method.

The standard establishes three levels of measurement accuracy—survey, engineering, and precision—and defines how to calculate and report measurement uncertainty as well as the

degree of nonlinearity of sound level decay curves within an environment. The standard standardizes reverberation time measurements and the acoustic evaluation of rooms (ABNT, 2017a).

2.24 Cocktail party

According to Bronkhorst (2000), in establishments intended for gastronomy it is common for an effect known as the "cocktail party effect" to occur. This effect is defined as a person's ability to focus auditory attention on a specific sound stimulus while simultaneously filtering a series of other stimuli and/or noises present in the environment, referred to as background noise.

2.25 Vocal effort and the lombard effect

According to ISO 9921 (ISO, 2003b), vocal effort is classified according to speech level as follows: relaxed speech (up to 54 dB); normal raised speech (up to 60 dB); more raised speech (up to 66 dB); loud speech (up to 72 dB); and very loud speech (up to 78 dB). Table 2-3 presents the vocal effort of a male speaker, A-weighted, relating the speech level (dB re 20 μPa) measured at 1 m in front of the mouth.

Table 2-3 – Vocal effort of a male speaker, A-weighted, relating speech level (dB re 20 μPa) measured at 1 m in front of the mouth

Vocal effort	**$L_{S,A,\ 1m\ dB}$**
Very loud	78
Loud	72
Raised	66
Normal	60
Relaxed	54

Source: Translation and adaptation of Table A.1 from ISO 9921 (ISO, 2003b).

According to Rindel, Christensen and Gade (2012), based on this relationship, there is an involuntary tendency for people to increase their vocal effort as the environmental noise level (background noise) increases. This relationship is known as the Lombard Effect, which

manifests around 45 dB of background noise, corresponding to a vocal effort of approximately 55 dB in order to achieve intelligibility within the environment.

According to Rindel (2010), there is a relationship between speech level and the ambient noise level. This phenomenon, referred to as the "Lombard Slope," demonstrates that immediately after the onset of the Lombard Effect, people's speech level increases by 0.5 dB for every additional 1 dB increase in ambient noise, in order to maintain intelligibility in conversations.

2.26 Mass law

According to Carvalho (2010), in the absence of acoustic insulation indices, the Mass Law is adopted, as illustrated in the following graph, where the direct proportionality between the insulation level and the frequency of a sound can be observed. Figure 2-10 shows that the higher the frequency (the higher-pitched the sound), the greater the insulation indices will be.

Figure 2-10 – Graph of the relationship between frequency and sound insulation

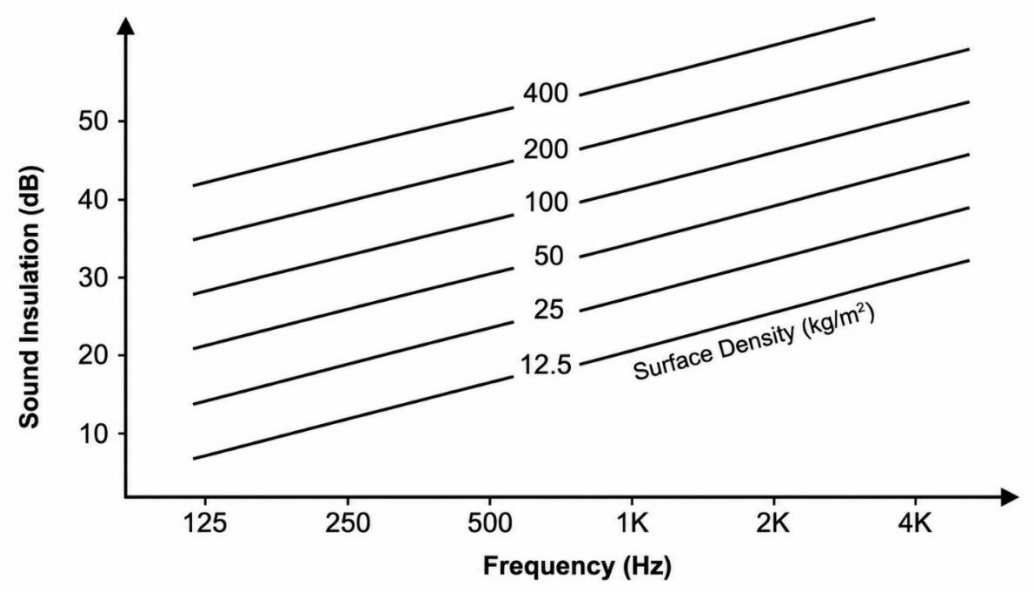

Source: Carvalho (2010).

According to Souza, Almeida and Bragança (2021), low-frequency sounds are more difficult to isolate than high-frequency sounds. Thus, the sound of a tuba may be transmitted between environments more easily than the sound of a violin with the same intensity. According to Bistafa (2018), whenever a change occurs in the medium through which sound propagates,

there will be a reduction in the sound intensity transmitted to the following medium; in this case, two propagation medium changes occur: air-wall and wall-air.

As highlighted by Souza, Almeida and Bragança (2021), the insulation capacity of a wall decreases at the frequencies for which its construction material is capable of undergoing resonance. Figure 2-11 illustrates how the angle of incidence of the sound wave may promote the coincidence between the wavelength of the incident sound and the wavelength associated with the flexibility of the wall material.

Figure 2-11 – Coincidence effect

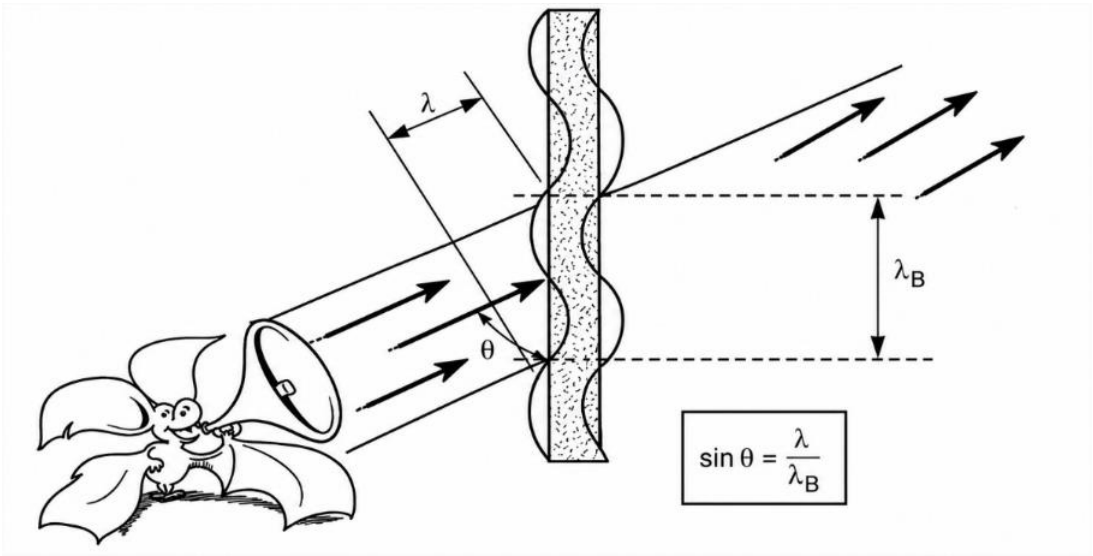

Fonte: Souza, Almeida and Bragança (2021).

2.26.1 Mass-spring-mass effect

According to Souza, Almeida and Bragança (2021), an important aspect of the acoustic insulation capacity of a material system is constructing it in such a way as to create empty cavities within it or to fill these cavities with absorbing material. This phenomenon is known as the mass–spring–mass effect. The greater the separation between the panels (masses) of the construction system, the greater the insulation at low frequencies. Another important factor is that the greater the mass of the spring, the greater its insulation capacity. Figure 2-12 illustrates how insulation increases with the mass of the spring.

Figure 2-12 – Mass-spring-mass effect in a construction system

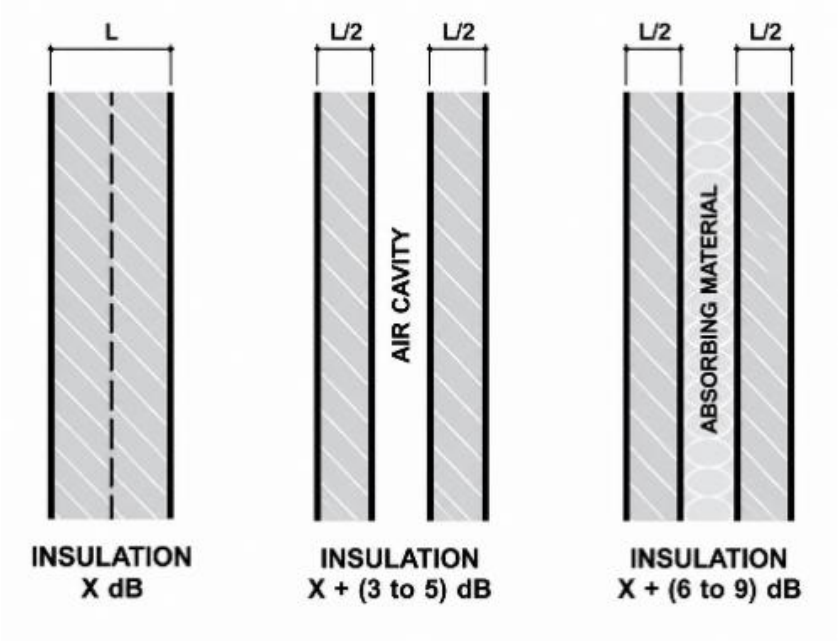

Source: Carvalho (2010).

2.27 Acoustic comfort in the built environment – NBR 10152

The standard establishes the technical procedures to be adopted in the execution of sound pressure level measurements in indoor building environments, as well as the reference values for evaluating results according to the intended use of the space (ABNT, 2017b). According to Basner and McGuire (2018), most people perceive a sound level of 30 dB as quiet and non-annoying up to 50 dB. However, from approximately 65 dB onward, noise becomes disturbing for conversation and activities requiring concentration.

In Table 2, the reference values for indoor environments within a building are presented according to their intended uses. According to ABNT (2017b), for acoustic evaluation purposes, an environment is considered suitable for use when its representative sound pressure levels are equal to or lower than the reference values presented in Table 2-4 of the standard, allowing a tolerance of up to 5 dB for RLAeq and RLASmax and up to 5 for RLNC.

The behavior of a product during its use can be defined as performance. In Brazil, the NBR 15575-1 (ABNT, 2013) standard aims to evaluate building quality according to user requirements related to Safety, Habitability, and Sustainability. It is based on three performance categories: minimum, intermediate, and superior. The standard evaluates the performance of roofing systems, installations, equipment and plumbing systems, flooring systems, internal and external vertical sealing systems, as well as general requirements.

Table 2-4 – Reference values for indoor building environments according to their intended uses

Intended use	Reference values		
	RLA_{eq} (dB)	RLA_{Smax} (dB)	RL_{NC}
Airports, bus and railway stations			
Check-in areas, ticket offices	45	50	40
Boarding areas and circulation areas	50	55	45
Shopping centers			
Circulation areas	50	55	45
Stores	45	50	40
Food courts	50	55	45
Parking garages	55	60	50
Clinics and hospitals			
Wards	35	40	30
Operating rooms	35	40	30
Consulting rooms	35	40	30

Source: Table 4 adapted from ABNT (2017b).

From the acoustic perspective, with the objective of protecting user health, the standard adopts the requirements of NBR 10152 (ABNT, 2017b) as a reference. This standard establishes noise levels compatible with acoustic comfort in various environments.

2.28 Natural and synthetic rubber

Humanity first came into contact with greases and resinous materials in Antiquity. Egyptians and Romans used these materials to glue documents, seal containers, stamp objects, among other applications. In the sixteenth century, the Portuguese and Spanish came into contact with latex extracted from a native tree of the Americas, the rubber tree. After the coagulation and drying of the latex, the product exhibited properties that were previously unknown. In Europe, it was initially used to erase pencil marks (Canevarolo Jr., 2006).

Its origin comes from the tree *Hevea brasiliensis* (commonly known as the rubber tree), which is commercially cultivated (Massey, 2019, p. 325). Natural rubber is an elastomer. Other rubbers are classified as synthetic and are, in most cases, obtained from petroleum derivatives. There are several types of rubber available on the market according to NBR 11597 (ABNT, 1997b). Table 2-5 presents some examples.

Table 2-5 – Most common types of rubber available on the market

Brazilian standards	
GEB	Brazilian Dark Granulated
CEB	Brazilian Dark Crepe
GCB	Brazilian Light Granulated
CCB	Brazilian Ligh Crepe
Internacional standards	
RSS-1	Ribbed Smoked Sheet
SAR	Standard African Rubber
SIR	Standard Indonesian Rubber
SMR	Standard Malaysian Rubber
SSR	Standard Singapore Rubber
SVR	Standard Vietnam Rubber
TSR	Technically Specified Rubber
TTR	Thailand Technically Specified Rubber

Source: Grison, Becker and Sartori (2010).

The liquid extracted from the rubber tree, called latex, is a natural hydrocarbon polymer. Latex is produced by several tropical plants; however, the vast majority of global production originates from the extraction of the rubber tree (*Hevea brasiliensis*). Natural rubber presents some difficulties in use due to its properties; for example, at low temperatures it becomes hard and brittle, while at high temperatures it becomes soft and sticky. Because of these behaviors, rubber must undergo a process called vulcanization, which consists of its hardening. This process was discovered in 1839 by Charles Goodyear (Fogaça, 2022). The name vulcanization was given in honor of Vulcan, the Roman god of fire and the underworld (Canevarolo Jr., 2006).

The temperature range that natural rubber can withstand is from -20°C to +70°C. The vulcanization process occurs at approximately 145°C. Any temperature above this value causes the material to decompose, forming a sticky residue. One way to prevent this phenomenon is by adding 20 parts of polybutadiene, which enables processing at temperatures up to 150°C without problems (Grison; Becker; Sartori, 2010).

Vulcanization gives rubber the property of resilience, which is the ability of the material to return the mechanical energy it receives, in addition to providing high elasticity. These properties allow the material to be used in the manufacture of various products, such as automobile tires. Compared to synthetic rubber, natural rubber is capable of reaching an elongation up to 900% greater than its initial dimension. Its best properties are achieved when it contains the lowest amount of additives. Therefore, the greater the number of products added to it, the lower its resilience, flexibility, strength, and elasticity. However, because rubber degrades easily under heat and light exposure, additives containing antiozonant and antioxidant

protective agents are incorporated to ensure a longer service life (Grison; Becker; Sartori, 2010, p. 24).

The natural rubber polymer extracted from latex is an addition polymer, also known as polyisoprene, formed by the addition of 1,4-isoprene monomers (methyl-1,3-diene) (Fogaça, 2022). Synthetic rubbers, on the other hand, are diene polymers. Natural rubber is a high-molecular-weight amorphous polymeric material. Depending on the application, its formulation may vary, since its different types are composed of distinct polymers. These polymers are divided into three classes: synthetic fibers, plastics, and rubbers. Their molecules are chemically bonded.

The SBR elastomer (Styrene-Butadiene Rubber elastomer) is a synthetic product very similar to natural rubber. It is less elastic, but more homogeneous. It undergoes a vulcanization process at temperatures ranging from 120°C to 170°C, receiving sulfur dosages of approximately 2.0 phr and accelerator dosages from 1.5 to 2.0 phr. Its physicomechanical properties are achieved through the incorporation of reinforcing fillers known as carbon black and precipitated silica. SBR is the rubber most commonly used in the manufacture of tires and many other products, making it the most consumed rubber in the world (Grison; Becker; Sartori, 2010, p. 24).

According to Fernández-Berridi *et al.* (2006), a piece of tire rubber basically consists of a mixture of two or more polymers, carbon black, inorganic compounds (such as calcium carbonate and silica), and a large number of organic substances used as plasticizers, antioxidants, lubricants, vulcanization agents, among others, dissolved within the polymeric matrix.

2.29 Waste materials

The construction sector is of great importance for the development of a country. However, this activity consumes a significant amount of environmental resources. It is estimated that, internationally, the sector is responsible for consuming between 40% and 75% of natural resources. In Brazil, the percentage is approximately 25% of the total waste generated (Mattes, 2019).

Agribusiness is another activity responsible for generating waste. For example, sugarcane bagasse and ash resulting from the burning of rice husks generate large volumes of material that require sustainable applications. According to Campos (2012), a study that incorporated sugarcane bagasse together with oat fibers for the development of acoustic

materials demonstrated that these materials presented good acoustic performance, thereby offering a new destination for the waste material.

In the state of Rio Grande do Sul, Brazil, approximately 35,000 tons of rice husk ash are generated annually. In a study conducted by Santos (2020) to investigate acoustic performance in impact noise insulation for floor screeds, rice husk ash was used in combination with tire rubber powder. Another example is slag from the steel industry, a residue originating from the production of ferrosilicon manganese alloys, which is used in the manufacture of rock wool, a material employed in acoustic treatment applications. According to Carvalho (2019), the incorporation of industrial waste into cementitious matrices is a strategy with significant potential for mitigating environmental impacts.

2.30 References

ADVANCING STANDARDS TRANSFORMING MARKETS. **ASTM E1050-12**: standard test method for impedance and absorption of acoustical materials using a tube, two microphones and a digital frequency analysis system. West Conshohocken, PA: ASTM, 2012. Available in: https://webstore.ansi.org/standards/astm/astme105012. Access in: 15 jun. 2024.

ALETTA, F.; KANG, J. Historical acoustics: relationships between people and sound over time. **Acoustics**, v. 2, n. 1, p. 128-130, 2020. https://doi.org/10.3390/acoustics2010009

APPLETON, I. **Buildings for the performing arts**: a design and development guide. 2.ed. Burlington, MA: Routledge, 2007.

ASDRUBALI, F.; SCHIAVONI, S.; HOROSHENKOV, K. V. A review of sustainable materials for acoustic applications. **Building Acoustics**, v. 19, n. 4, p. 283-312, 2012. https://doi.org/10.1260/1351-010X.19.4.283

ASSOCIAÇÃO BRASILEIRA DE NORMAS TÉCNICAS. **NBR 12179/1992**: tratamento acústico em recintos fechados. Rio de Janeiro: ABNT, 1992. Available in: https://www.normas.com.br/visualizar/abnt-nbr-nm/5286/abnt-nbr12179-tratamento-acustico-em-recintos-fechados-procedimento. Access in: 16 jun. 2024.

ASSOCIAÇÃO BRASILEIRA DE NORMAS TÉCNICAS. **NBR 11597/1997**: Borracha natural - requisitos e métodos de ensaio. Rio de Janeiro: ABNT, 1997. Available in: https://www.target.com.br/produtos/normas-tecnicas/34299/nbr11597-borracha-natural-requisitos-e-metodos-de-ensaio. Access in: 15 out. 2024.

ASSOCIAÇÃO BRASILEIRA DE NORMAS TÉCNICAS. **NBR 15575-1/2013**: Edificações habitacionais – desempenho parte 1: requisitos gerais. 4.ed. Rio de Janeiro: ABNT, 2013. Available in: https://ufsb.edu.br/propa/images/dinfra/coman/Legisla%C3%A7%C3%B5es/NBR15575-1.pdf. Access in: 24 nov. 2020.

ASSOCIAÇÃO BRASILEIRA DE NORMAS TÉCNICAS. **NBR ISO 3382-2/2017**: acústica - medição de parâmetros de acústica de salas. Parte 2: Tempo de reverberação em salas comuns. Rio de Janeiro: ABNT, 2017a. Available in: https://www.normas.com.br/visualizar/abnt-nbr-nm/11982/abnt-nbriso3382-2-acustica-medicao-de-parametros-de-acustica-de-salas-parte-2-tempo-de-reverberacao-em-salas-comuns. Access in: 15 jun. 2024.

ASSOCIAÇÃO BRASILEIRA DE NORMAS TÉCNICAS. **NBR 10152/2017 – Acústica**: Níveis de pressão sonora em ambientes internos a edificações. 2.ed. Rio de Janeiro: ABNT, 2017b. Available in: https://normadedesempenho.com.br/wp-content/uploads/2022/10/NBR-10152.pdf. Access in: 14 mar. 2018.

BARRON, M. **Acoustics, auditorium design, architectural**. 2 ed. London: Spon Press, 2009. https://doi.org/10.4324/9780203874226

BASNER, M.; McGUIRE, S. WHO environmental noise guidelines for the European region: a systematic review on environmental noise and effects on sleep. **International Journal of Environmental Research and Public Health**, v. 15, n. 3, 519, 2018. https://doi.org/10.3390/ijerph15030519

BASNER, M.; BABISCH, W.; DAVID, A.; BRINK, M.; CLARK, C.; JANSSEN, S.; STANSFELD, S. Auditory and non-auditory effects of noise on health. **The Lancet**, v. 383, n. 9925, p. 1325-1332, 2014. Available in: https://www.thelancet.com/journals/lancet/article/PIIS0140-6736(13)61613-X/abstract. Access in: 15 fev. 2023.

BERANEK, L. **Concert halls and opera houses**: music, acoustics, and architecture. 2.ed. New York, NY: Springer, 2004.

BISTAFA, S. R. **Acústica aplicada ao controle do ruído**. 2.ed. São Paulo: Blucher, 2018.

BRONKHORST, A. W. The cocktail party phenomenon: a review of research on speech intelligibility in multiple-talker conditions. **Acta Acustica United with Acustica**, v. 86, n. 1, p. 117-128, 2000. Available in: https://pascal-francis.inist.fr/vibad/index.php?action=getRecordDetail&idt=5720732. Access in: 16 ago. 2024.

BUJOREANU, C.; NEDEFF, F.; BENCHEA, M.; AGOP, M. Experimental and theoretical considerations on sound absorption performance of waste materials including the effect of backing plates. **Applied Acoustics**, v. 119, p. 88-93, 2017. Disponível em : https://www.sciencedirect.com/science/article/abs/pii/S0003682X1630603X. Access in: 30 jun. 2023.

BUJOREANU, C.; IRIMICIUC, S.; BENCHEA, M.; NEDEFF, F.; AGOP, M. A fractal approach of the sound absorption behaviour of materials. Theoretical and experimental aspects. **International Journal of Non-Linear Mechanics**, v. 103, p. 128-137, 2018. https://doi.org/10.1016/j.ijnonlinmec.2018.05.005

BURATTI, C.; BELLONI, E.; LASCARO, E.; MERLI, F.; RICCIARDI, P. Rice husk panels for building applications: thermal, acoustic and environmental characterization and comparison with other innovative recycled waste materials. **Construction and Building Materials**, v. 171, p. 338-349, 2018. https://doi.org/10.1016/j.conbuildmat.2018.03.089

CAMPOS, R. V. M. **Painéis para tratamento acústico utilizando fibras naturais**. 2012. 112f. Dissertação (Mestrado em Engenharia Urbana) – Universidade Estadual de Maringá, Maringá, 2012.

CANEVAROLO JR., S. V. **Ciência dos polímeros**: um texto básico para tecnólogos e engenheiros. 2.ed. São Paulo: ArtLiber, 2006.

CARVALHO, R. P. **Acústica arquitetônica**. 2.ed. Brasília: Arch-Tec, 2010.

CARVALHO, J. M. F. **Obtention of eco-efficient cement-based composites using industrial waste**. 2019. 230f. Tese (Doutorado em Engenharia Civil) – Universidade Federal de Ouro Preto, Ouro Preto, 2019. Available in: http://www.locus.ufv.br/handle/123456789/24812. Access in: 21 ago. 2024.

EGAN, M. D. **Architectural acoustics**. Plantation, FL: J. Ross Publishing, 2007.

ERMANN, M. **Architectural acoustics illustrated**. New Jersey: NJ: Wiley, 2015.

EVEREST, F. A.; POHLMANN, K. C. **Master handbook of acoustics**. 7.ed. New York: McGraw Hill, 2021.

FERNÁNDEZ-BERRIDI, M. J.; GONZÁLEZ, N.; MUGICA, A.; BERNICOT, C. Pyrolysis-FTIR and TGA techniques as tools in the characterization of blends of natural rubber and SBR. **Thermochimica Acta**, v. 444, n. 1, p. 65-70, 2006. https://doi.org/10.1016/j.tca.2006.02.027

FOGAÇA, J. **Borracha natural e borracha sintética**. 20 jun. 2022. Available in: https://brasilescola.uol.com.br/quimica/borracha-natural-sintetica.htm. Access in: 22 mai. 2024.

GARRETT, S. L. **Understanding acoustics**. Cham: Springer International Publishing, 2020.

GASPAR, A.; PEREIRA, A.; GODINHO, L.; AMADO MENDES, P.; MATEUS, D. **Desempenho acústico de um painel reconfigurável para um auditório multiusos**. In: CONGRESO IBÉRICO DE ACÚSTICA, 11, 2020, Coimbra, Portugal. **Anais...** Coimbra, Portugal: SPA, 2020. Available in: https://documentacion.sea-acustica.es/publicaciones/Faro20/ID57.pdf. Access in: 7 mai. 2024.

GRISON, E. C.; BECKER, E. J.; SARTORI, A. F. **Borrachas e seus aditivos**: componentes, influências e segredos. Porto Alegre: Letra & Vida, 2010.

INTERNATIONAL ELETROTECHNICAL COMMISSION. **IEC 60268-16:2020**: sound system equipment – Part 16: Objective rating of speech intelligibility by speech transmission index. Geneva, Suíça: IEC, 2020. Available in: https://www.vde-verlag.de/iec-normen/249172/iec-60268-16-2020.html.. Access in: 20 fev. 2024.

INTERNATIONAL ORGANIZATION FOR STANDARDIZATION. **ISO 10534-1:1996**: Acoustics – Determination of sound absorption coefficient and impedance in impedance tubes. Part 1: Method using standing wave ratio. Genebra, Suíça: ISO, 1996. Available in: https://www.iso.org/standard/18603.html. Access in: 20 abr. 2023.

INTERNATIONAL ORGANIZATION FOR STANDARDIZATION. **ISO 354-2003**: Acoustics – Measurement of sound absorption in a reverberation room. Genebra, Suíça: ISO, 2003a. Available in: https://www.iso.org/standard/34545.html#:~:text=ISO%20354%3A2003%20specifies%20a%20method%20of%20measuring%20the,persons%20or%20space%20absorbers%2C%20in%20a%20reverberation%20room. Access in: 20 abr. 2023.

INTERNATIONAL ORGANIZATION FOR STANDARDIZATION. **ISO 9921-2003**: Ergonomics – Assessment of speech communication. Genebra, Suíça: ISO, 2003b. Available in: https://www.iso.org/standard/33589.html. Access in: 20 abr. 2023.

INTERNATIONAL ORGANIZATION FOR STANDARDIZATION. **ISO 10534-2:2023**: Acoustics – Determination of acoustic properties in impedance in tubes. Part 2: Two-microphone technique for normal sound absorption coefficient and normal surface impedance. 2.ed. Genebra, Suíça: ISO, 2023. Available in: https://www.iso.org/standard/81294.html. Access in: 20 abr. 2025.

KLEINER, M.; TICHY, J. **Acoustics of small rooms**. London: CRC Press, 2014. https://doi.org/10.1201/b16866

KUTTRUFF, H. **Acoustics**: an introduction. London: CRC Press, 2006. https://doi.org/10.1201/9780367807696

KUTTRUFF, H. **Room acoustics**. 6.ed. Boca Raton: CRC Press, 2016. https://doi.org/10.1201/9781315372150

LONG, M. **Architectural a coustics**. Burlington, MA: Elsevier Academic Press, 2006.

MASSEY, L. K. Thermoset elastomers or rubbers: overview. In: McKEEN, L. W. **The effects of UV light and weather on plastics and elastomers**. 4.ed. Elsevier, 2019. p. 325-326. https://www.doi.org/10.1016/C2018-0-00612-X

MATTES, W. **A construção civil e o desenvolvimento sustentável**. 9 mar. 2019. Available in: https://vivagreen.com.br/greenarq/construcao-civil-e-o-desenvolvimento-sustentavel/. Access in: 25 jul. 2022.

MEHTA, M. L.; JOHNSON, J.; ROCAFORT, J. **Architectural acoustics**: principles and design. London, UK: Pearson, 1998.

MOMMERTZ, E. **Acoustics and sound insulation**: principles, planning, examples. Basel, Suíça: Birkhäuser, 2009.

PAZ, G. S.; SANTOS, J. L. P. Uso da casca de arroz e pó de pneu no isolamento do ruído de impacto. In: SIMPÓSIO BRASILEIRO DE METROLOGIA EM ACÚSTICA E VIBRAÇÕES, 2, 2002, Rio de Janeiro. Rio de Janeiro: SOBRAC, 2002.

PEDROSO, M.; BRITO, J.; SILVESTRE, J. D. Characterization of eco-efficient acoustic insulation materials (traditional and innovative). **Construction and Building Materials**, v. 140, p. 221-228, 2017. https://doi.org/10.1016/j.conbuildmat.2017.02.132

PIERCE, A. D. **Acoustics**: an introduction to its physical principles and applications. 3. ed. Cham: Springer International Publishing, 2019.

PROCEL EDIFICA. **Acústica arquitetônica**. Rio de Janeiro: PROCEL, 2011. Available in: https://toaz.info/doc-view-4. Access in: 4 nov. 2025.

RIEDY, S. M.; SMITH, M. G.; ROCHA, S.; BASNER, M. Noise as a sleep aid: a systematic review. **Sleep Medicine Reviews**, v. 55, 101385, 2021. https://doi.org/10.1016/j.smrv.2020.101385

RINDEL, J. H. Verbal communication and noise in eating establishments. **Applied Acoustics**, v. 71, n. 12, p. 1156-1161, 2010. https://doi.org/10.1016/j.apacoust.2010.07.005

RINDEL, J. H. **Sound insulation in buildings**. Boca Raton, FL: CRC Press, 2017. https://doi.org/10.1201/9781351228206

RINDEL, J. H.; CHRISTENSEN, C. L.; GADE, A. C. Dynamic sound source for simulating the Lombard effect in room acoustic modeling software. In: INTER-NOISE AND NOISE-CON CONGRESS AND CONFERENCE, 2012, **Proceedings…** New York, NY: InterNoise, 2012. p. 954-966. Available in: https://ince.publisher.ingentaconnect.com/content/ince/incecp/2012/00002012/00000011/art00095/#. Access in: 5 set. 2024.

ROCCA, M.; DI PUCCIO, F.; FORTE, P.; LECCESE, F. Acoustic comfort requirements and classifications: buildings vs. yachts. **Ocean Engineering**, v. 255, 111374, 2022. https://doi.org/10.1016/j.oceaneng.2022.111374

SANTOS, K. M. M.; OITICICA, M. L. G. R. Qualidade acústica em ambientes gastronômicos. **Brazilian Applied Science Review**, v. 4, n. 3, p. 1040-1052, 2020. https://doi.org/10.34115/basrv4n3-023

SERAFIN, S.; BUXTON, B.; GAVER, B.; BLY, S. **Auditory interfaces**. London: Focal Press, 2022. https://doi.org/10.4324/9781003260202

SILVA, P. **Acústica arquitetônica & condicionamento de ar**. 6.ed. Belo Horizonte: EDTAL - Empresa Termo Acústica Ltda, 2011.

SOUZA, L. C. L.; ALMEIDA, M. G.; BRAGANÇA, L. **Bê-á-bá da acústica arquitetônica: ouvindo a arquitetura**. São Carlos: EdUFSCar, 2021.

TANG, X.; YAN, X. Acoustic energy absorption properties of fibrous materials: a review. **Composites Part A: Applied Science and Manufacturing**, v. 101, p. 360-380, 2017. https://doi.org/10.1016/j.compositesa.2017.07.002

TAO, Y.; REN, M.; ZHANG, H.; PEIJS, T. Recent progress in acoustic materials and noise control strategies – a review. **Applied Materials Today**, v. 24, 101141, 2021. https://doi.org/10.1016/j.apmt.2021.101141

VALLE, S. **Manual prático de acústica**. 3.ed. Rio de Janeiro: Música e Tecnologia, 2009.

WORLD HEALTH ORGANIZATION. **Burden of disease from environmental noise – quantification of healthy life years lost in Europe**. Copenhagen, Dinamarca: WHO, 2011. Available in: https://www.who.int/publications/i/item/9789289002295. Access in: 5 set. 2024.

ZIEMER, T. **Psychoacoustic music sound field synthesis**: creating spaciousness for composition, performance, acoustics and perception. 7.ed. Cham: Springer, 2020.

3 REVIEW OF THE USE OF WASTE TIRE RUBBER FOR SOUND ABSORPTION AND THERMAL INSULATION IN BUILT AND URBAN ENVIRONMENTS1

Ramon Ribeiro Fontes [1], José Maria Franco de Carvalho [1], Túlio Márcio de Salles Tibúrcio [2], Leonardo Gonçalves Pedroti [1], Ariel Miranda de Souza [1]*
[1] *Department of Architecture and Urbanism, Federal University of Viçosa, Viçosa, 36570-900, Brazil.*
[2] *Department of Civil Engineering, Federal University of Vicosa, Vicosa, 36570-900, Brazil.*
*Corresponding author: E-mail ariel.souza@ufv.br, telephone +55 32 98831 8035

Graphical Abstract

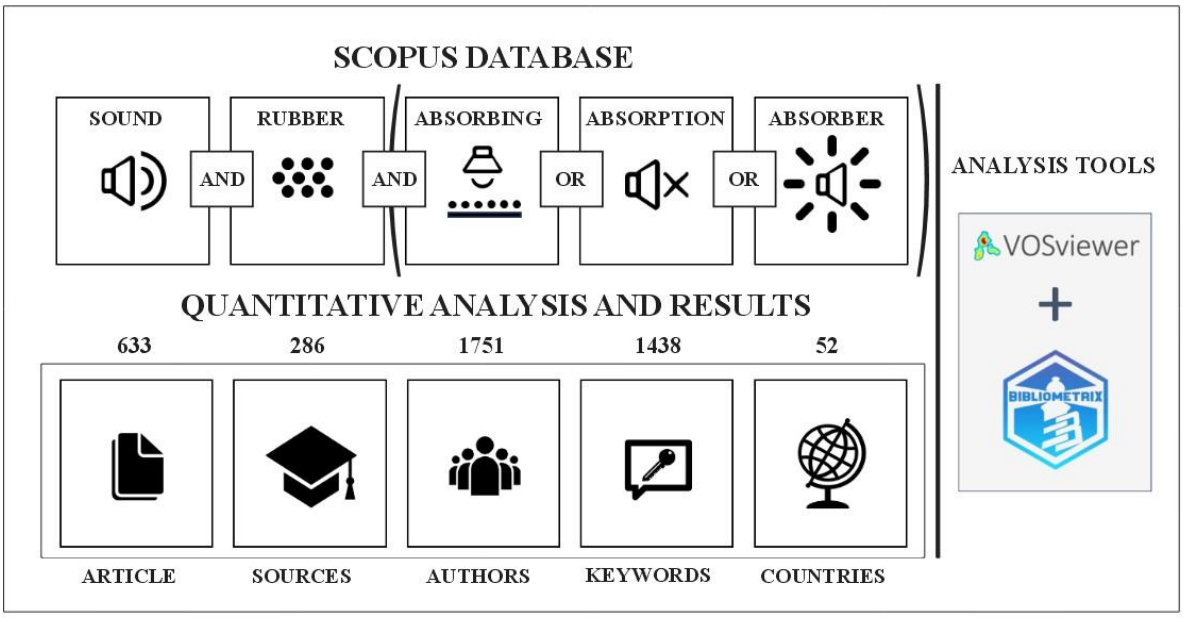

Abstract: This study presents a comprehensive systematic review and bibliometric analysis of the use of waste tire rubber (WTR) in acoustic and vibroacoustic applications, with emphasis on sound absorption, vibration damping, and associated thermal effects. By synthesizing publications from 1941 to 2026, the analysis reveals a clear paradigm shift in the last decade, in which WTR evolved from a passive filler into a functional material engineered for multi-scale noise mitigation. The reviewed literature demonstrates that fine rubber particles promote enhanced sound energy dissipation through increased porosity, tortuosity, and acoustic impedance matching, whereas coarser rubber inclusions are more effective for vibration damping and impact noise control due to their viscoelastic behavior. The study further highlights the inherent trade-offs between improved acoustic–thermal performance and mechanical strength reduction, emphasizing the need for optimized material design tailored to specific frequency ranges and loading conditions. Despite the growing body of research, significant gaps remain, particularly regarding the lack of standardized acoustic characterization methods, limited long-term durability assessments, and insufficient coupling between experimental studies and predictive modeling. Emerging research themes identified in recent years include rubber-based acoustic metamaterials, underwater sound absorption systems, hybrid porous–viscoelastic composites, and tunable structures designed for low-frequency noise control, indicating a shift toward application-driven and mechanism-oriented material design.
Keywords: Acoustics, sound absorption, waste, metamaterials, sustainability.

[1] Article submitted to the Journal of Sound and Vibration on February 8, 2026.

3.1 Introduction

Noise pollution has become one of the primary environmental challenges faced by human society. Excessive exposure to noise, driven by the rapid growth of cities and their transportation and industrial activities, has caused harm to both humans and animals (Tao *et al.*, 2021). According to Bistafa (2018), various issues are associated with noise, including hearing loss, stress, hypertension, sleep disturbances, reduced rest opportunities, lack of concentration, and decreased productivity, all leading to a deterioration in quality of life. In the physical realm, noise-induced hearing losses, headaches, hormonal and cardiovascular disorders, and digestive dysfunctions, among others, have been identified (Souza; Almeida; Bragança, 2012).

Basner and McGuire (2018) state that the World Health Organization (WHO) estimated that, in high-income countries of Western Europe, with a population of approximately 340 million, at least 1 million healthy life years are lost annually due to environmental noise. These issues emerged in the 1960s, prompting the development of architectural acoustics standards to regulate and address conditions that restrict or decrease noise pollution, aiming to protect urban users and building interiors.

Mehrzad *et al*. (2022) highlight that economic development and population growth have led to significant environmental problems, including not only noise pollution but also global warming, manifested through climate change caused by greenhouse gas emissions.

Rubber from tires is considered a non-biodegradable waste, releasing chemicals into the soil and water and emitting CO_2 during incineration, thereby altering the planet's ecosystem. When accumulated and discarded in junkyards, these tires release methane into the atmosphere, contributing to climate change. End-of-life tires (ELT) have an estimated recovery rate of about 90% in the United States and Europe, with nearly 4 million tires destined for landfills, potentially reaching 5 million by 2030 (Vanjare, 2023).

According to Dong *et al*. (2021), considering the life cycle phases of tires (Life Cycle Assessment – LCA), including production, transportation, use, and end-of-life, the usage phase has the most significant environmental impact, producing approximately 550 kg CO_2 eq. to 840 kg CO_2 eq. per tire. It is estimated that nearly 1 billion tons of end-of-life tires (ELT), without adequate treatment processes, are discarded in landfills or even directly as waste each year, with only a small percentage being recycled (Liu *et al.*, 2020).

Automobile tires, responsible for vehicle movement and serving as the primary point of interaction with the road, are crucial for their operation (Associação Nacional da Indústria de

Pneumáticos – ANIP, 2018). New technologies to reduce noise pollution are being developed in tire design, ranging from tread patterns to materials that can help decrease noise levels (Society of Automotive Engineers of Japan – SAEJ, 2020). These requirements stem from strengthened regulations addressing noise produced by tire–road interaction, established by the Working Party on Noise (GRB) of the World Forum for Harmonization of Vehicle Regulations (UNECE/WP.29) (SAEJ, 2020).

Mehrzad *et al*. (2022) note that the construction industry accounts for over 40% of global energy consumption, generating almost 45% of global greenhouse gas emissions. The construction sector's pursuit of residual or low environmental impact materials for construction elements aims to mitigate its own impact on nature. Therefore, shredded tire rubber waste, when used in the construction industry, reduces landfill usage and virgin raw material consumption, becoming a sustainable alternative for construction materials (Rashad, 2016).

According to Callister and Rethwisch (2016), tire rubber is composed of polymers, large molecules formed by repeating structural units called monomers. Polymers, especially styrene-butadiene rubber (SBR), confer desirable characteristics such as high elasticity, resistance to swelling in organic solvents, and the ability to slow crack propagation through the material. The exact chemical composition of a tire can vary depending on the tire type and its specific application (Rodgers, 2020).

This article aims to review various applications of rubber for sound absorption purposes. Beyond a conventional narrative review, this study provides a comprehensive bibliometric and systematic assessment of the evolution of waste tire rubber as an acoustic and thermal functional material. This review serves as an important resource by consolidating dispersed evidence on how rubber has transitioned from a simple filler to an engineered component for noise mitigation across multiple scales and applications in urban and built environments. By identifying dominant research themes, emerging topics, and performance trade-offs, this work highlights knowledge gaps and future research pathways, while the bibliometric analysis contributes by quantitatively evaluating the scientific impact and research directions of studies that have utilized rubber in the development of acoustic composites.

3.2 Methodology

This review gathered the most relevant publications from peer-reviewed journals using the Scopus database, which provides comprehensive bibliometric coverage across science, engineering, and related fields. According to Martín-Martín *et al*. (2018) and Meho (2019),

Scopus-indexed bibliometric data offer broad and reliable coverage of journals relevant to this research field; therefore, a clear and transparent protocol was adopted to identify and select studies addressing rubber applications for sound absorption.

The collection of these articles was conducted up to February 2026. The keywords used in the bibliometric review were “sound AND rubber AND (absorbent OR absorption OR absorber)”, which returned a total of 633 documents as of February 2026. The selected articles were grouped into a CSV file and analyzed using VOSviewer, version 1.6.20, and PAJEK software. Out of these 633 documents, the top 10 most cited articles since 1941 were analyzed. Subsequently, from this dataset, 52 articles from the last five years were selected, and among these, the top 10 most cited were further examined.

Regarding the inclusion and exclusion criteria, articles that focused on rubber, especially rubber derived from shredded or end-of-life tires, or natural rubber, were considered. As exclusion criteria, articles whose main focus was not the acoustic performance of rubber were eliminated. However, this review also briefly discusses the consequences of rubber incorporation on other material properties of the composites. The research methodology can be visualized through the mind map in Figure 3-1.

Figure 3-1 – Research methodology

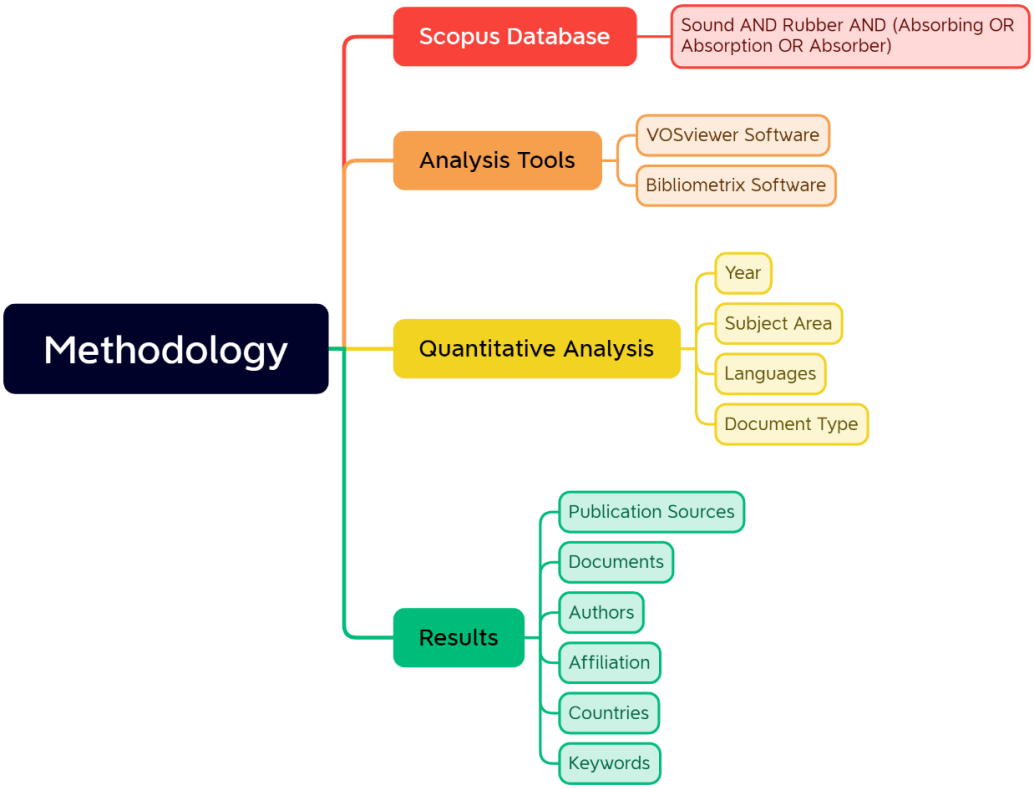

3.3 Analysis of the results

3.3.1 Quantitative analysis

Figure 3-2 illustrates the number of articles published per year. From the inception of the field in 1941 until 2005, the number of publications remained below ten documents annually. Notable exceptions occurred in 1989 and 1997, with seven and four publications, respectively. This trend provides an overview of the historical development and early scientific interest in rubber-based acoustic applications.

Figure 3-2 – Number of documents published per year from 1941 to 2025

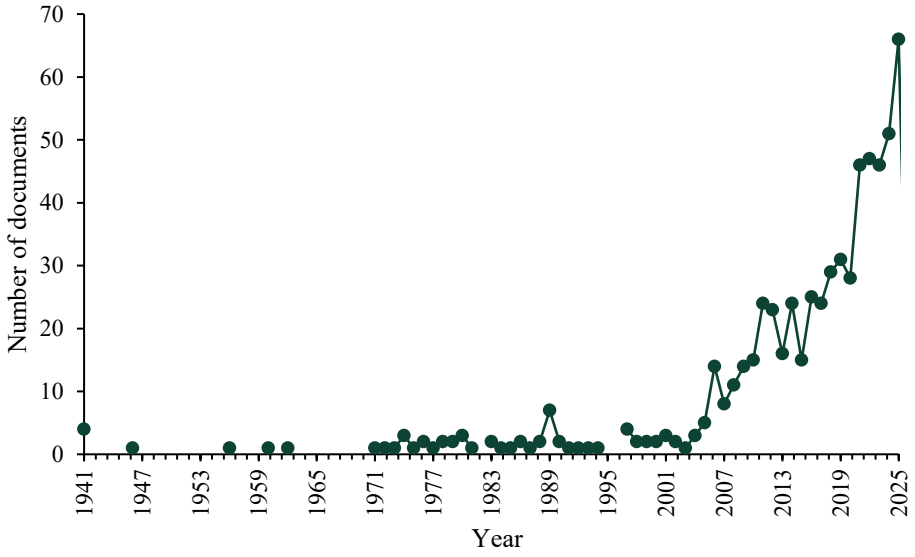

The first studies on rubber-related acoustic applications were published in 1941, comprising four articles by the same authors, Kosten and Zwikker (1941). One of these studies focused on the theoretical aspects of sound absorption by compressible walls with non-porous surface layers, while the remaining three investigated sound absorption measurements of porous rubber wall coverings. These early works examined cellular and sponge rubber, demonstrating their effectiveness as sound-absorbing materials. In 1980, the most cited and influential article addressed filled rubber materials for echo absorption in water-filled tanks (Corsaro; Klunder; Jarzynski, 1980), indicating applications in the acoustic visualization of simulated biomedical targets. In the same year, Snowdon (1979) published a highly cited study on vibration isolation, discussing the static and dynamic properties of rubber-like materials suitable for anti-vibration mounts.

The publication peaks observed in 1989 and 1997 were marked by highly influential contributions. In 1989, Dlubac *et al*. (1989), published a seminal study focusing on the requirements for developing sound and vibration absorbers, emphasizing the importance of understanding sound energy dissipation mechanisms and dynamic modulus measurements in viscoelastic materials. In 1997, Takahashi's (1997) presented a widely cited study on the "seat dip effect" (SDE), which examined the excessive attenuation of low-frequency sound waves passing over audience seating in auditoriums. Rubber foam was used as a surface covering to analyze the influence of sound absorption on SDE characteristics.

Over the last two decades, significant publication peaks occurred in 2006, 2011, 2019, 2021, and 2025, with 2025 showing the highest research output, totaling 181 documents. In 2006, Ivansson (2006) published a highly cited study on sound absorption by viscoelastic coatings with periodically distributed air-filled cavities, exploring the use of thin rubber layers for anechoic underwater coatings, particularly in submarine applications. In the same year, Asdrubali (2006) presented a comprehensive survey on the acoustic properties of sustainable materials for noise control, highlighting rubber as an environmentally friendly solution.

In 2011, Fatima and Mohanty (2011) published a highly cited study investigating the acoustic and flammability properties of biodegradable jute fiber composites bonded with rubber latex, demonstrating their suitability for acoustic insulation and flame retardancy. Additionally, Sánchez-Dehesa *et al*. (2010) conducted a systematic investigation of acoustic barriers based on sonic crystals made from recycled materials, including rubber crumbs, achieving effective sound attenuation.

In 2019, Sharma *et al*. (2019) investigated sound absorption in rubber coatings containing periodic voids and rigid inclusions. In parallel, Najib *et al.* (2011) examined the correlation between acoustic and dynamic mechanical properties of natural rubber foams, highlighting the influence of cell size, relative density, cross-linking density, and cell density on sound absorption performance.

A substantial increase in research output was observed in 2021, with 46 publications. Smirnova *et al*. (2021) reported on composite sound absorbers incorporating recycled tire crumbs, emphasizing the potential of rubber as a sustainable acoustic material. Duan *et al*. (2021) developed a tunable acoustic metamaterial based on a hexagonal honeycomb Helmholtz resonator with rubber coating, achieving enhanced sound absorption. In the same year, Grammelis *et al*. (2021) reviewed a wide range of recycled tire rubber applications, including asphalt mixtures, cementitious matrices, and sound-absorbing materials.

In 2022, a total of 47 articles were published. Pongsopha *et al*. (2022) investigated the effects of end-of-life tire rubber particles on lightweight aggregate concrete, reporting improved thermal and acoustic insulation compared to conventional lightweight concrete. Xu *et al*. (2022) studied porous asphalt mixtures incorporating rubberized binders, demonstrating enhanced wear resistance, crack resistance, durability, and noise reduction.

In 2023, with 46 publications, Eyssa, Afif and Moustafa (2023) explored ethylene-propylene-diene rubber (EPDM) nanocomposite foams reinforced with functionalized multi-walled carbon nanotubes for acoustic applications, highlighting their potential for acoustic panels and airborne sound insulation. Zeng *et al*. (2023) developed high-damping rubber composites based on nitrile butadiene rubber (NBR) and chloroprene rubber (CR) with various fillers, achieving effective sound insulation across a broad frequency range. Finally, Dong *et al*. (2023) proposed a solid–porous underwater metaconverter composed of a rubber layer and an optimized elastic metasurface for broadband underwater sound absorption and isolation.

Overall, the temporal evolution of research on rubber-based acoustic applications reveals a progressive diversification of materials, scales, and functionalities, with increasing emphasis on sustainability, advanced material design, and effective noise mitigation strategies. The incorporation of recycled tire rubber into asphalt mixtures, cementitious composites, foams, and metamaterial systems has emerged as a dominant trend in recent years. Table 3-1 summarizes the most influential studies and their main findings.

3.3.2 Publication sources

The VOSviewer software was used to process the data for the bibliometric review. The selected "type of analysis" was "bibliographic coupling", with the "unit of analysis" defined as "sources", and the minimum number of documents per source set to one, resulting in a total of 286 sources, as illustrated in Figure 3-3. Table 3-2 presents the top ten journals in the field. In the VOSviewer maps, graphical elements represent the relationships among the analyzed entities, in which node size reflects their relative relevance or frequency, while the links indicate the strength of connections based on shared bibliographic information (Van Eck; Waltman, 2022).

Table 3-1 – Main articles and finds on the subject, from 1941 to 2026

continues

Reference	Subjects	Main finds
Kosten and Zwikker (1941)	Sound absorption	Theory for compressible walls and measurements of sound absorption by porous rubber layers; Cellular and sponge rubber effective absorbers.
Corsaro, Klunder and Jarzynski (1980)	Rubber materials for sound absorption	Use of filled rubber materials for sound absorption in water-filled tanks; Applications for acoustic visualization of biomedical targets.
Snowdon (1980)	Vibration isolation	Use and characterization of anti-vibration assemblies; Static and dynamic properties of rubber-like materials for anti-vibration assemblies.
Dlubac *et al.* (1989)	Sound and vibration absorption	Use of viscoelastic materials for sound and vibration absorption; Importance of obtaining complex dynamic moduli for accurate measurement.
Takahashi (1997)	Acoustic design in performance halls	Analysis of the "seat dip effect" and impact of rubber foam on sound absorption.
Ivansson (2006)	Anechoic coatings	Thin rubber layers with air-filled cavities for anechoic underwater coatings; Rubber as an efficient anechoic coating on submarines.
Asdrubali (2006)	Sustainable acoustic materials	Rubber highlighted as a sustainable material for noise control in composites made from recycled tire granules.
Fatima and Mohanty (2011)	Biodegradable acoustic materials	Natural jute fiber and rubber latex as fire-resistant, noise-reducing materials.
Najib *et al.* (2011)	Foam properties for sound absorption	Effect of expansion temperature on foam properties influencing absorption capacity.
Sánchez-Dehesa *et al.* (2010)	Acoustic barriers	Rubber powder and periodic distribution of dispersers for acoustic barriers.
Benkreira, Khan and Horoshenkov (2011)	Sustainable acoustic insulation	Use of waste materials like tire and carpet fragments for acoustic barriers and impact sound insulation.
Ivansson (2006)	Anechoic coatings	Thin rubber layers with air-filled cavities for anechoic underwater coatings; Rubber as an efficient anechoic coating on submarines.
Fatima and Mohanty (2011)	Biodegradable acoustic materials	Natural jute fiber and rubber latex as fire-resistant, noise-reducing materials.

Table 3-1 – Main articles and finds on the subject, from 1941 to 2026

continuation

Reference	Subjects	Main finds
Najib *et al.* (2011)	Foam properties for sound absorption	Effect of expansion temperature on foam properties influencing absorption capacity.
Sánchez-Dehesa *et al.* (2010)	Acoustic barriers	Rubber powder and periodic distribution of dispersers for acoustic barriers.
Benkreira, Khan and Horoshenkov (2011)	Sustainable acoustic insulation	Use of waste materials like tire and carpet fragments for acoustic barriers and impact sound insulation.
Sharma *et al.* (2019a)	Rubber coatings for sound absorption	Rubber coatings with cavities impact acoustic performance; Finite element model analysis.
Bhingare, Prakash and Jatti (2019)	Sustainable sound-absorbing materials	Exploration of natural and waste materials for sound absorption; Rubber mentioned as a potential material.
Sharma *et al.* (2019b)	Viscoelastic matrix for sound resonances	Rubber-like viscoelastic matrix for sub-wavelength resonances in maritime applications.
Xiao *et al.* (2019)	Rubberized asphalt pavement	Damping characteristics and high elasticity of rubber particles for noise reduction.
Wang *et al.* (2019)	Rubber in asphalt mixtures	Rubber as an efficient modifier for sustainable and environmentally friendly asphalt composites.
Smirnova *et al.* (2021)	Tire rubber in sound-absorbing composites	Use of crushed tire rubber in gypsum-cement-pozzolana-based composites for improved sound absorption.
Duan *et al.* (2021)	Tunable acoustic metamaterial	Rubber in Helmholtz resonator for tunable acoustic metamaterial with perfect absorption.
Grammelis *et al.* (2021)	Tire rubber applications	Multiple applications of tire rubber in construction materials for enhanced durability, strength, and insulation.
Dissanayake *et al.* (2021)	Recycling textile waste with rubber	Cotton and polyester waste with natural rubber for acoustic insulation comparable to commercial panels.
Bala and Gupta (2021)	Shredded tire rubber in concrete	Assessment of properties related to thermal resistance, sound absorption, and vibration damping in rubberized concrete.
Chalangaran *et al.* (2021)	Rubber particles in concrete	Fine rubber particles enhance sound transmission loss in concrete, showcasing excellent insulation capabilities at high frequencies.

Table 3-1 – Main articles and finds on the subject, from 1941 to 2026

conclusion

Reference	Subjects	Main finds
Dong *et al.* (2022)	Metasurfaces for sound absorption	Rubber in reflective metasurfaces with multiple elastic mode conversions for broad-band underwater sound absorption.
Pongsopha *et al.* (2022)	End-of-life tire rubber in concrete	Rubberized lightweight aggregate concrete (RLWAC) with superior thermal and acoustic insulation properties compared to conventional lightweight aggregate concrete (LWAC).
Xu *et al.* (2022)	Porous asphalt mixtures	Rubberized asphalt demonstrated superior wear resistance, crack resistance, and noise reduction in traffic.
Eyssa, Afifi and Moustafa (2023)	Epdm rubber nanocomposites	Use of ethylene-propylene-diene rubber (EPDM) from tire rubber in nanocomposites for acoustic panels and airborne sound insulation.
Zeng *et al.* (2023)	High-damping rubber composites	Development of high-damping rubber composites for sound insulation across a wide range of frequencies using nitrile butadiene rubber (NBR) and chloroprene rubber (CR) as base materials.
Dong *et al.* (2023)	Underwater metaconverter	Rubber in a solid-porous underwater metaconverter for broadband sound absorption and isolation functionalities.

Figure 3-3 – Publication sources and their connections

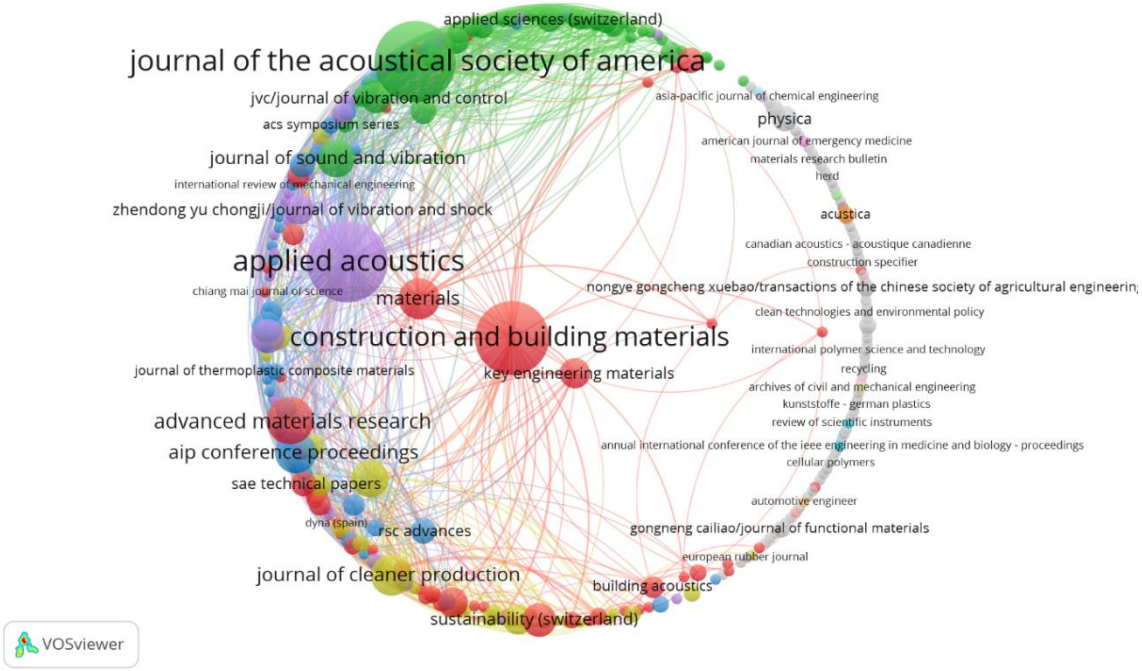

According to Table 3-2, the leading journals published a maximum of 23 articles on the topic, indicating that acoustic materials remain a relatively underexplored research area within scientific journals. The journals with the highest number of publications are primarily focused on acoustics and construction materials, suggesting that these outlets are the most sought after for disseminating research in this field and highlighting the interdisciplinary nature of the topic.

Table 3-2 – Top 10 document sources

Rank	Source	Publisher	Documents	Citations
1	Applied Acoustics	Elsevier	23	1264
2	Journal of the Acoustical Society of America	AIP	23	1044
3	Construction and Building Materials	Elsevier	20	1200
4	Advanced Materials Research	Trans Tech Publications Ltd	10	26
5	Journal of Cleaner Production	Elsevier	8	691
6	Materials	MDPI	8	1191
7	AIP Conference Proceedings	AIP	8	18
8	Journal of Sound and Vibration	Elsevier	7	306
9	Journal of Building Engineering	Elsevier	7	236
10	Sustainability (Switzerland)	MDPI	6	77

Nevertheless, a growing interest in the acoustic performance of sustainable materials can be observed, as evidenced by publications in journals such as *Journal of Cleaner Production* and *Sustainability*. Furthermore, open-access journals published by MDPI, including *Materials* and *Sustainability*, emerge as viable publication venues, presenting a high number of citations despite a lower volume of published articles. The table also highlights the prominence of Elsevier journals, which account for the highest citation counts, reflecting their strong scientific impact in the field.

3.3.3 Documents

The bibliographic coupling of the documents considered a minimum citation threshold of one, resulting in 485 documents out of the initial 633, as shown in Figure 3-4. Table 3-3 presents the ten most influential documents in the field.

Figure 3-4 – Result of the bibliographic coupling analysis

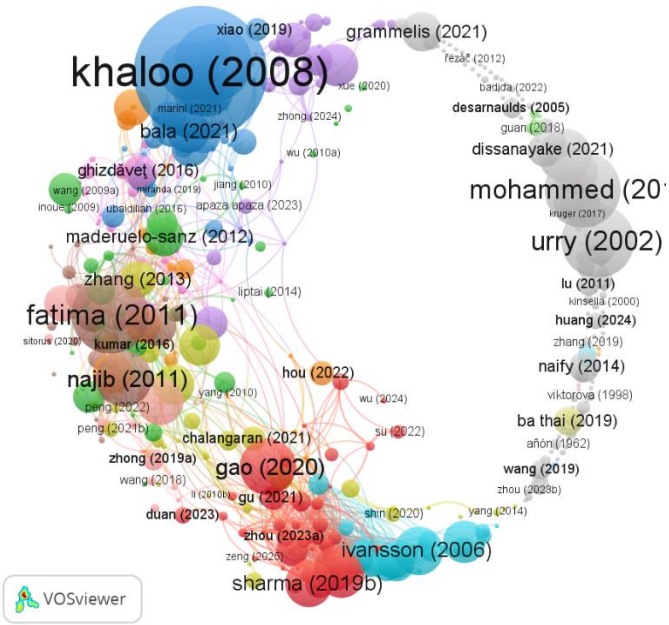

Figure 3-4 and Table 3-3 indicate that the most influential documents in the field are strongly associated with the early adoption of rubber in construction materials and its subsequent extension to acoustic and vibroacoustic applications. Highly cited works such as Khaloo, Dehestani and Rahmatabadi (2008), Sukontasukkul (2009), and Mohammed *et al.* (2012) form the core of the network and are primarily linked to the mechanical and physical

effects of tire rubber incorporation in cementitious composites, which later motivated investigations into sound absorption and insulation performance. Parallel to this construction-oriented cluster, foundational studies on elastomeric and viscoelastic behavior, such as Urry *et al.* (2002), provide the mechanical basis for understanding vibration damping mechanisms in rubber-based materials. Gao and Lu (2020) and Würsig, Greene Jr. and Jefferson (2000) reveal an expansion of the research scope toward underwater acoustics, low-frequency sound absorption, and noise mitigation in marine environments. The coupling structure highlights the progressive transition from macroscopic construction applications to mechanism-driven acoustic designs, including foams, porous structures, and acoustic metamaterials.

Table 3-3 – Documents and corresponding total link strength

Rank	Reference	Focus of study	Overview	Citations
1	Khaloo, Dehestani and Rahmatabadi (2008)	Mechanical properties of concrete with tire rubber	Lower density, reduced workability, decreased strength, and modulus of elasticity. Reduction in brittle behavior, crack width, and concrete propagation velocity.	709
2	Sukontasukkul (2009)	Application of rubber crumbs in precast concrete	Improved thermal properties, lower density, and better heat resistance. Increased sound absorption coefficient. Contribution to energy efficiency in construction.	294
3	Fatima and Mohanty (2011)	Acoustic and flammability properties of jute composites	Jute composite with rubber latex showed high sound transmission class. Good flame retardancy and low smoke density. Potential for acoustic treatment in construction.	290
4	Mohammed *et al.* (2012)	Use of granulated rubber in concrete blocks	Better compression strength, electrical and thermal resistance. Improved sound absorption at different frequencies. Potential for construction with enhanced thermal and acoustic properties.	279
5	Urry *et al.* (2002)	Mechanical and viscoelastic behavior of elastomeric proteins	Elastin: a representative ideal protein elastomer	264
6	Rashad (2016)	Recycling of rubber waste in cementitious materials	A comprehensive overview about recycling rubber as fine aggregate replacement in traditional cementitious materials	189
7	Gao and Lu (2020)	Underwater acoustic metamaterials for low-frequency sound absorption	An underwater metamaterial for broadband acoustic absorption at low frequency	172
8	Najib *et al.* (2011)	Correlation between acoustic and dynamic mechanical properties of rubber foams	Effect of foaming temperature on acoustic efficiency. Lower foaming temperature resulted in higher sound absorption. Higher temperature suitable for sound insulation.	169
9	Holmes, Browne and Montague (2014)	Application of crushed rubber in concrete panels	Decreased workability and compressive strength with increased rubber content. Increased sound absorption for higher rubber volumes. Sound insulation comparable to conventional concrete panels.	166
10	Würsig, Greene Jr. and Jefferson (2000)	Mitigation of underwater noise for marine mammals	Use of air bubble curtain to inhibit underwater noise. Successful in reducing sound levels, but did not eliminate all behavioral responses to loud noise.	159

3.3.4 Authors

The VOSviewer software was employed for data processing. The "type of analysis" was selected as "co-authorship", with the "unit of analysis" being "authors", and the minimum number of documents for an author was set at 2, resulting in 336 out of 1751 authors as illustrated in Figure 3-5. Table 3-4 displays the top 10 authors in the field. Information regarding bibliometric indices, total number of publications, citation counts, and authorship data for each author was extracted from the SCOPUS database and is reported in Table 3-5.

Figure 3-5 – Network visualization of the most published authors

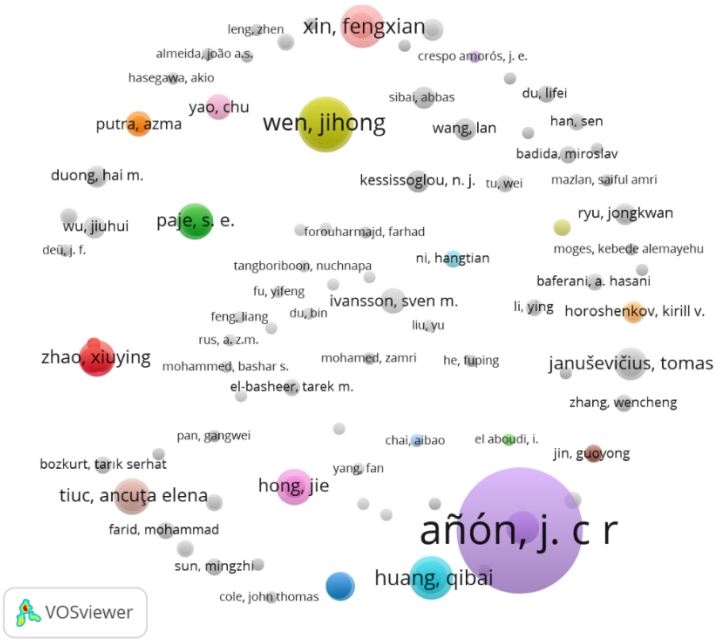

Table 3-6 – Most published authors

Rank	Author	Articles	Citations	Country	Affiliation
1	Wen, Jihong	14	370	China	National University of Defense Technology China
2	Yang, Haibin	12	291	China	National University of Defense Technology China
3	Zhao, Honggang	10	358	China	National University of Defense Technology China
4	Xin, Fengxian	10	259	China	Xi'an Jiaotong University
5	Huang, Qibai	10	88	China	Huazhong University of Science and Technology
6	Zhong, Jie	9	186	China	National University of Defense Technology China
7	Paje, Santiago Expósito	8	210	Spain	Universidad de Castilla-La Mancha
8	Zhao, Xiuying	8	130	China	Beijing University of Chemical Technology
9	Tiuc, Ancuta Elena	8	56	Romania	Universitatea Tehnica din Cluj-Napoca
10	Hong, Jie	8	46	China	Beihang University

Table 3-7 – Most relevant authors indices

Rank	Author	Index			Documents	Citations	Citation by article	First author	Co-author	Year of publication
		h	g	m						
1	Wen, Jihong	61	112	3.05	326	12742	39.09	1	195	2004
2	Yang, Haibin	19	34	1.73	43	1177	27.37	3	44	2013
3	Zhao, Honggang	35	64	1.75	93	4209	45.26	7	55	2004
4	Xin, Fengxian	41	66	2.56	144	4390	30.49	14	82	2008
5	Huang, Qibai	21	39	0.68	202	1561	7.73	0	29	1993
6	Zhong, Jie	12	27	1.20	27	850	31.48	5	40	2014
7	Paje, Santiago Expósito	25	38	0.93	68	1497	22.01	0	69	1997
8	Zhao, Xiuying	36	61	2.12	166	3734	22.49	10	28	2007
9	Tiuc, Ancuta Elena	11	25	0.92	42	626	14.90	11	57	2012
10	Hong, Jie	32	63	1.33	330	3991	12.09	44	235	2000

The co-authorship analysis reveals a strong concentration of scientific production among researchers affiliated with Chinese institutions, with particular emphasis on the *National University of Defense Technology China*, which includes several of the most productive authors in the field. Among the ten authors with the highest number of publications, the majority are from China, reflecting the consolidation of well-structured and highly productive research groups.

In addition to the high number of publications, authors such as Wen, Jihong, Zhao, Honggang, and Xin, Fengxian also present high impact indicators, as evidenced by citation counts and the *h* and *g* bibliometric indices, highlighting their scientific relevance within the field.

The results further indicate that scientific output is predominantly characterized by co-authorship, suggesting a strongly collaborative and interdisciplinary research field in which researchers operate within institutional and international networks. This interdisciplinarity and the establishment of partnerships strengthen authors' academic profiles by enhancing scientific recognition, increasing research visibility and dissemination, and consequently raising the likelihood of citations (Souza *et al.*, 2025).

The presence of European authors, such as Paje, Santiago Expósito and Tiuc, Ancuta Elena, although less concentrated, reinforces the global character of the research. Overall, the findings indicate that the advancement of the field has been driven by consolidated research groups, with a high level of scientific collaboration and sustained contributions over time.

3.3.5 Countries

Bibliographic coupling by country was based on occurrences limited to 1, resulting in the inclusion of 52 countries. Table 3-6 displays the top 10 collaborative countries in this field, and Figure 3-6 represents the network of countries.

Table 3-8 – Countries and corresponding total link strength

Rank	Country	Documents	Citations	Total link strength
1	China	226	3649	1203
2	USA	42	1144	311
3	Malaysia	33	751	564
4	India	27	654	295
5	Iran	23	1085	293
6	Spain	22	686	300
7	South Korea	20	111	80
8	Russian Federation	20	106	175
9	United Kingdom	16	541	275
10	Italy	16	308	277

Figure 3-6 – Network visualization of countries

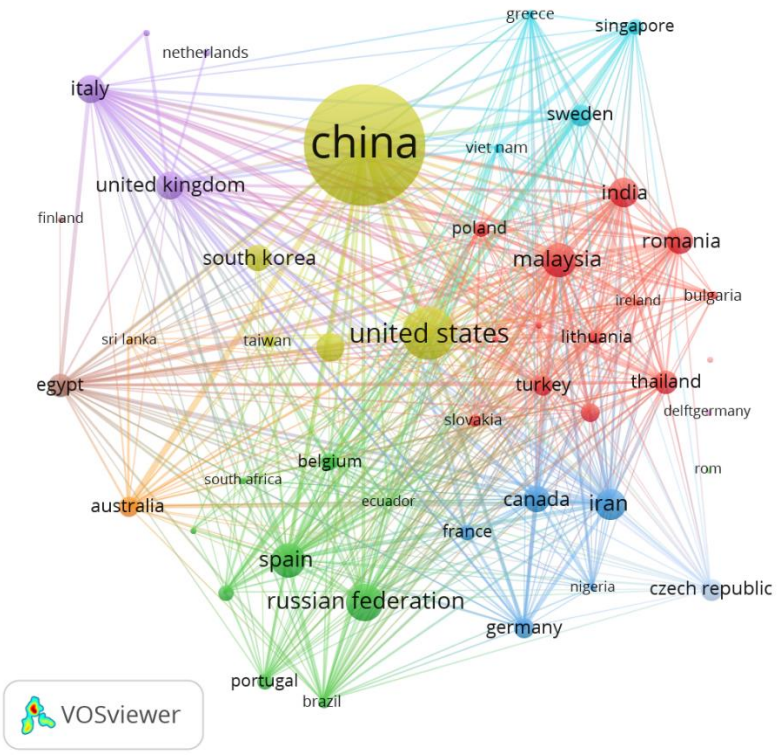

According to the country-based bibliographic coupling analysis, Table 3-6 reveals a distinction between developed and developing countries within the analyzed research field. Developing countries and emerging economies, such as China, India, Malaysia, Iran, and the Russian Federation, account for a substantial share of publications and exhibit high total link strength values, indicating intense scientific activity and strong international connectivity. In contrast, developed countries, including the United States, the United Kingdom, Spain, Italy,

and South Korea, although presenting a lower volume of publications, maintain relevant levels of citations and collaborative participation, playing a complementary role in the scientific and methodological consolidation of the field.

China stands out as the main hub of international collaboration, establishing connections with approximately 40 of the 52 countries identified in the analysis. This extensive collaborative network significantly contributes to knowledge advancement, enhances the international visibility of research, strengthens scientific ties among different regions, and increases the likelihood of research impact and citation.

3.3.6 Keywords

To conduct the analysis in the VOSviewer software, similar keywords were merged, considering variations in spelling, dashes, plurals, superscript, and subscript, as well as their counts. For the keyword analysis, "type of analysis" was set as "Co-occurrence," and the "unit of analysis" was chosen as "Author Keywords." The minimum number of occurrences for a keyword was restricted to 2, resulting in 251 outcomes from 1438 keywords. Table 3-7 presents the top 10 author keywords in the field.

Table 3-9 – Keyword occurrence and corresponding total link strength

Rank	Keyword	Occurrence	Total link strength
1	Sound absorption	87	29
2	Sound absorption coefficient	43	18
3	Crumb rubber	24	28
4	Rubber	23	33
5	Noise	18	24
6	Noise reduction	17	28
7	Acoustic properties	17	26
8	Underwater sound absorption	15	24
9	Mechanical properties	14	18
10	Impedance tube	13	7

Table 3-7 reveals that most studies are primarily linked to acoustic performance, with a strong emphasis on the internal dissipation of sound energy, as evidenced by the high occurrence of the keywords “sound absorption” and “sound absorption coefficient”. The frequent use of impedance tube highlights the predominance of standardized laboratory-scale

experimental methods in the field. Moreover, the fact that “crumb rubber” appears more frequently than the generic term rubber indicates an increasing concern with sustainability and circular economy principles, emphasizing the use of recycled tire rubber as a functional acoustic material rather than merely a conventional viscoelastic component. The co-occurrence of “acoustic properties” and “mechanical properties” reflects the well-documented trade-off between improved sound absorption and reduced mechanical performance, which explains why most applications are directed toward non-structural elements. Finally, the presence of keywords related to “noise reduction” and “underwater sound absorption” demonstrates both the applied nature of the research and the expansion of rubber-based acoustic solutions into advanced and specialized fields.

For cluster analysis, the "unit of analysis" was set as "All keywords". The minimum number of occurrences for a keyword was limited to 5, resulting in 330 outcomes from 4575 keywords. Figure 3-7 illustrates the keywords for each cluster, with a total of 6 clusters.

Figure 3-7 – Network visualization of keyword occurrence

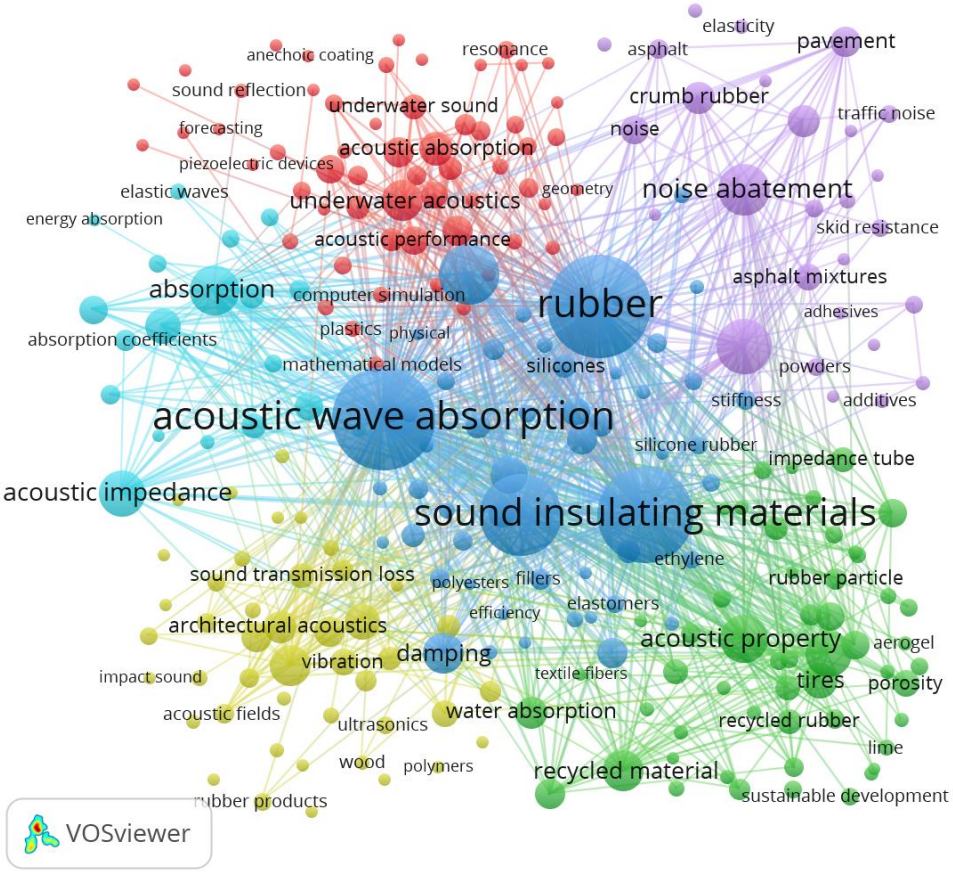

The dark blue cluster, which is the largest and most central cluster in the network, groups high-frequency keywords such as acoustic wave absorption, sound insulating materials, silicones, silicone rubber, elastomers, polyesters, fillers, damping, efficiency, ethylene, and stiffness. This cluster represents the core material–performance framework of the field, where acoustic behavior is directly linked to material composition and mechanical response. The coexistence of polymeric materials, fillers, and damping-related terms indicates that sound absorption is commonly investigated as a multifunctional property arising from viscoelasticity, composite design, and energy dissipation mechanisms.

The light blue cluster is more strongly associated with fundamental absorption descriptors and wave phenomena, including absorption, absorption coefficient, acoustic impedance, elastic waves, and energy absorption. This cluster reflects a more physics-oriented perspective, focusing on the quantification and interpretation of sound–material interactions. Compared to the dark blue cluster, which emphasizes material systems, the light blue cluster concentrates on acoustic parameters and wave propagation concepts that underpin experimental measurements and theoretical models.

The purple cluster connects keywords related to asphalt and transportation applications, such as pavement, traffic noise, crumb rubber, asphalt mixtures, elasticity, and noise abatement. This cluster highlights a strongly application-driven research stream, where waste tire rubber is incorporated into asphalt layers to reduce traffic-induced noise. The prominence of elasticity-related terms indicates that surface compliance and viscoelastic damping are key mechanisms for noise mitigation in pavement systems.

The green cluster groups keywords associated with recycled materials and sustainability, including recycled rubber, tires, porosity, acoustic property, recycled material, and sustainable development. This cluster emphasizes the role of waste tire rubber as a circular-economy material, with particular attention to how porosity and microstructural features influence acoustic performance. The strong linkage between sustainability and acoustic properties reflects the growing interest in environmentally responsible noise control solutions.

The yellow cluster encompasses terms related to architectural acoustics and vibration control, such as architectural acoustics, damping, vibration, sound transmission loss, and ultrasonics. This cluster represents building-scale applications, where rubber-based materials are used to mitigate structure-borne and airborne noise, improving indoor acoustic comfort through combined absorption and vibration attenuation mechanisms.

The red cluster is associated with highly specialized acoustic applications in underwater environments, grouping keywords such as underwater acoustics, underwater sound, anechoic

coating, resonance, and geometry. This research stream is primarily driven by naval and defense-related applications, where controlling sound reflection and absorption is critical for stealth, detection avoidance, and signal management. In this context, rubber-based materials are widely investigated as anechoic coatings and acoustic metamaterials due to their viscoelastic behavior and tunable impedance, which enable efficient absorption over targeted frequency ranges. Although these studies are not directly related to conventional building applications, they explain the strong scientific interest in underwater sound absorption and demonstrate how advanced acoustic concepts are being developed and validated in extreme environments.

The results of the trending topics evaluation are depicted in Figure 3-8. The analysis of emerging trend topics reveals a recent shift toward advanced acoustic concepts and engineered solutions. Keywords such as acoustic metamaterials, topology optimization, and structural design indicate a growing interest in designing rubber-based materials with tailored geometries to enhance sound absorption, particularly at low frequencies. At the same time, the increased relevance of underwater sound and underwater acoustics reflects the expansion of waste tire rubber applications into naval and defense-related environments, where impedance matching and energy dissipation under extreme conditions are critical.

Figure 3-8 – Results of the trending topics analysis

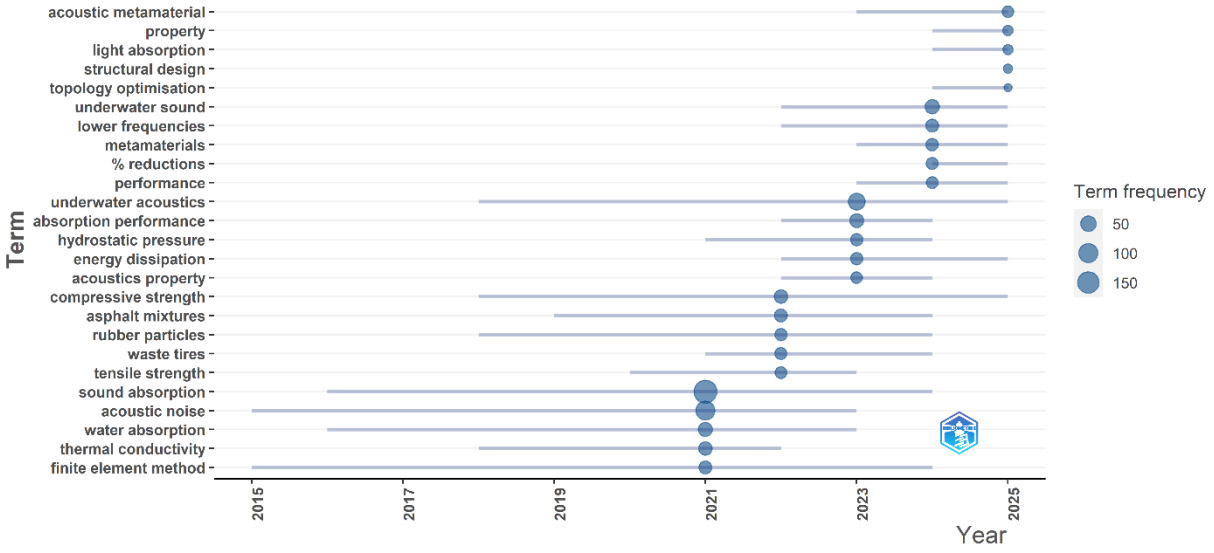

Source: Author (2025).

3.4 Systematic analysis of the recent literature on the utilization of rubber waste for acoustic purposes

After the bibliometric analysis, subject-area filters were applied to the retrieved documents, restricting the dataset to the following fields: Engineering, Materials Science, Physics and Astronomy, Environmental Science, Energy, Chemical Engineering, Chemistry, Computer Science, Mathematics, Biochemistry, Genetics and Molecular Biology, and Earth and Planetary Sciences. In addition, the Document Type filter was applied, including Articles, Conference Papers, Reviews, Book Chapters, Notes, and Conference Reviews. Subsequently, a keyword-based screening was performed, focusing on terms related to acoustics, material properties and characteristics, sustainability, the construction industry, and potential applications of rubber.

After these automatic filtering steps, a manual screening stage was conducted, in which the titles and abstracts of the remaining documents were carefully reviewed to assess their relevance to the scope of this study. As a result of this combined automated and manual filtering process, a final dataset of 52 relevant articles was selected. From this set, the most cited publications from the last five years were identified and are presented in Table 3-8.

Table 3-10 – Most cited articles filtered for the systematic analysis

S/n	Author	Title	Citations
1	Anu Bala, Supratic Gupta (2021)	Thermal resistivity, sound absorption and vibration damping of concrete composite doped with waste tire Rubber: A review	109
2	Panagiotis Grammelis, Georgios Mavrias, Nikolaos Margaritis, Petros Dallas e Dimitrios Rakopoulos (2021)	A review on management of end of life tires (Elts) and alternative uses of textile fibers	98
3	Quoc Ba Thai, Ren Ooi Chong, Phuc T.T. Nguyen, Duyen K. Le, Phung K. Le, Nhan Phan-Thien e Hai M. Duong (2020).	Recycling of waste tire fibers into advanced aerogels for thermal insulation and sound absorption applications.	79
4	Nirmala H. Bhingare, S. Prakash e Vijaykumar S. Jatti. (2019)	A review on natural and waste material composite as acoustic material	77
5	Lei Xu, Hangtian Ni, Yi Zhang, Daquan Sun e Yunpeng Zheng (2022)	Porous asphalt mixture use asphalt rubber binders: Preparation and noise reduction evaluation	65
6	Quoc Ba Thai, Toh Ee Siang, Duyen Khac Le, Wassim Akram Shah e Hai M. Duong (2019)	Advanced fabrication and multi-properties of rubber aerogels from car tire waste	61
7	Phattharachai Pongsopha, Piti Sukontasukkul, Hexin Zhang e Suchart Limkatanyu (2022)	Thermal and acoustic properties of sustainable structural lightweight aggregate rubberized concrete	56
8	Xinwu Xu, Huixiang Wang, Yan Sun, Jingquan Han e Runzhou Huang (2018)	Sound absorbing properties of perforated composite panels of recycled rubber, fiberboard sawdust, and high density polyethylene	51
9	Quoc Ba Thai, Khoa Le-Cao, Phuc T.T. Nguyen, Phung K. Le, Nhan Phan-Thien e Hai M. Duong (2021)	Fabrication and optimization of multifunctional nanoporous aerogels using recycled textile fibers from car tire wastes for oil-spill cleaning, heat insulating and sound absorbing applications	34
10	Mapoloko Mpho Phiri, Motshabi Alinah Sibeko, Mohau Justice Phiri e Shanganyane Percy Hlangothi (2019)	Effect of free foaming and pre-curing on the thermal, morphological and physical properties of reclaimed tyre rubber foam composites	27

In the mind map of Figure 3-9 on evaluations and research content regarding the incorporation of end-of-life tire rubber particles into various matrixes, we can observe how it has been utilized for acoustic comfort purposes.

Figure 3-9 – Mind map summarizing the composites raised in this study

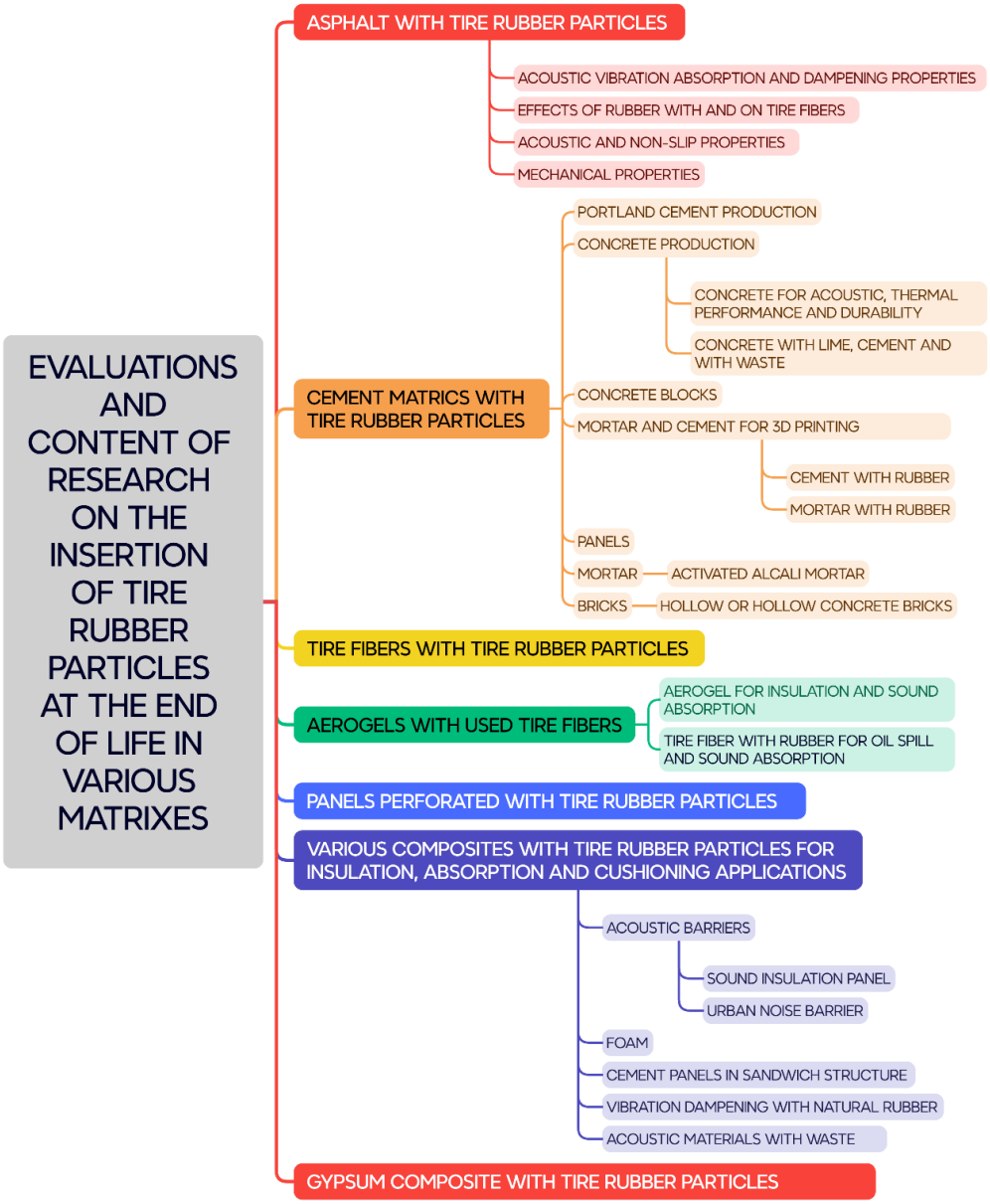

Source: Author (2025).

3.4.1 Asphalt with tire rubber particles

According to Mikhailenko *et al*. (2021) and Poulikakos *et al*. (2022), the addition of tire rubber can enhance sound absorption and contribute to the reduction of road traffic noise. Vázquez, Terán and Paje (2020) identified several factors that influence noise levels, including the dynamic stiffness of pavements and construction parameters such as maximum aggregate size, binder content, air void content, and density. Xu *et al*. (2022) reported that rubberized

asphalt exhibits improved properties, enhancing damping and reducing vibration and noise generated by tire-pavement friction, thereby contributing to traffic noise mitigation.

Lyu *et al*. (2021) suggested that, in porous elastic asphalts, an optimized mixture of polyurethane and rubber can balance mechanical and acoustic performance, achieving both structural strength and sound absorption. Marini and Lanotte (2021) reported that rubberized asphalt incorporating a specific content of crumb rubber modifier (CRM)–modified bitumen promotes interconnected air voids, leading to improved noise reduction performance.

Apaza *et al*. (2023) found that an asphalt mixture containing 1.50% rubber achieved a peak sound absorption coefficient of 0.71 within the frequency range of 570 to 650 Hz. Donavan and Janello (2021) investigated the use of rubber in asphalt for an asphalt rubber friction course (ARFC) overlay applied to existing Portland cement concrete (PCC) pavement. The ARFC, with a thickness of 25.4 mm, was implemented to reduce highway traffic noise, achieving an average reduction of 9.1 dBA. Wu *et al*. (2023) reported that tire rubber–modified asphalt improves the tire–pavement system due to the damping properties and sound absorption capability of rubber, thereby contributing to traffic noise reduction.

Overall, the reviewed studies demonstrate that rubberized asphalt represents a mature and application-oriented approach to traffic noise mitigation, with acoustic performance governed not only by rubber content but also by mixture design parameters influencing porosity, viscoelastic damping, and tire–pavement interaction. The literature indicates that optimized mix designs enable targeted tuning of pavement acoustic behavior, particularly within frequency ranges relevant to road traffic noise, while maintaining mechanical durability. These findings are primarily associated with the purple cluster identified in the bibliometric analysis, which groups studies focused on asphalt materials and pavement-related noise control strategies.

3.4.2 Cement-based composites

Studies have investigated the incorporation of shredded tire rubber into concrete and cement-based mixtures to enhance acoustic and thermal performance, among other properties. These investigations have primarily focused on improving sound absorption as a strategy to reduce noise in building applications.

According to Pongsopha *et al*. (2022), rubberized lightweight aggregate concrete (RLWAC) exhibits superior thermal and acoustic insulation properties compared to lightweight aggregate concrete (LWAC). The sound absorption coefficient increased with higher rubber

content, as the incorporation of recycled rubber generated additional voids within the concrete matrix. These voids enhance sound absorption by promoting friction between air molecules and pore surfaces, thereby converting acoustic energy into thermal energy.

Mhaya *et al*. (2022) reported that the highest sound absorption coefficient was achieved at the maximum rubber aggregate content, resulting in an improved noise reduction coefficient (NRC) due to increased air content. The study also demonstrated that both the size and type of rubber particles significantly influence acoustic performance, with coarse rubber aggregates showing greater sound insulation potential due to their enhanced ability to absorb and damp higher energy levels.

Sanyal, Mohanty and Sarkar (2023) observed that concrete incorporating crushed rubber residue exhibited higher sound absorption coefficients at low, ambient, and elevated temperatures compared to conventional concrete. Similarly, Asantey, Kalloush and Lotfy (2019) reported that crushed tire rubber provides durability and vibration absorption when used as aggregate in roads and sidewalks, contributing to improved concrete insulation properties.

Svoboda *et al*. (2021) found that cement composites containing recycled rubber demonstrated higher sound absorption capacity than those produced with natural aggregates. Lumnitzer *et al*. (2018) showed that sandwich panels composed of rubber layers and cement paste achieved excellent noise absorption performance, with coefficients exceeding 0.9 at 315 Hz and values above 0.4 for frequencies greater than 200 Hz, highlighting their potential for airborne noise insulation.

Atef *et al*. (2022) investigated Portland cement pastes incorporating different proportions of end-of-life tire rubber particles to evaluate sound absorption coefficient (SAC) and noise reduction coefficient (NRC). Increasing the rubber replacement ratio led to a reduction in void content in the cured pastes and a significant enhancement in sound absorption capacity. The NRC improved for rubber replacement levels of 5%, 15%, and 25% of ordinary Portland cement (OPC) compared to control samples.

Sambucci *et al*. (2022) reported that concrete blocks containing crushed rubber residues achieved improved noise reduction at medium and high frequencies. Blocks produced with cement mixed with tire rubber aggregates featuring fractal hollow design (FHD) geometry exhibited the highest sound absorption coefficient, reaching approximately 0.72 at 1000 Hz. In contrast, Haron *et al*. (2018) observed that concrete blocks incorporating tire rubber were particularly effective at absorbing low-frequency sound, making them suitable for traffic noise mitigation, especially at lower vehicle speeds.

Intaboot and Kanbua (2022) confirmed the sound absorption capability of concrete blocks incorporating tire rubber particles, reporting absorption coefficients ranging from 0.35 across frequencies between 125 Hz and 4000 Hz, with a peak value of 0.45 at 1000 Hz for samples containing 40% rubber by weight.

Sambucci *et al*. (2020) investigated cement-based mixtures for additive manufacturing in which mineral aggregates were replaced by recycled tire rubber particles, including rubber powder (RP) and rubber granules (RG). The authors reported reduced vibration propagation and enhanced sound insulation, attributed to the improved acoustic damping behavior of rubber, particularly at medium and high frequencies.

According to Sambucci and Valente (2021), the use of end-of-life tire rubber as a granular material in 3D-printed cement mortar improved sound attenuation performance. Enhanced acoustic isolation and sound absorption were attributed to the microstructural characteristics of the cementitious matrix, particularly within the frequency range of 2000 to 4000 Hz.

In a study on alkali-activated mortars incorporating recycled polyvinyl chloride (PVC) and rubber aggregates, El-Seidy *et al*. (2022) observed a 64.5% increase in the sound reduction index compared to the control mixture. The viscoelastic nature of polymer aggregates enabled effective dissipation of acoustic energy, contributing to both vibrational and acoustic damping.

Santos *et al*. (2019) examined the influence of rubber particles derived from discarded tires, in spherical and fibrous forms, on the sound absorption coefficient of rubberized mortars. The highest absorption values were observed for mixtures containing 30% spherical rubber and 7.5% fibrous rubber within the frequency range of 850 Hz to 2000 Hz. The results demonstrated that rubber particle morphology plays a critical role in acoustic performance. Spherical particles, due to their geometry and finer size, exhibited higher water absorption and produced lighter mortars, whereas fibrous rubber particles contributed less to weight reduction and acoustic enhancement.

Overall, the reviewed studies indicate that the incorporation of tire rubber into cement-based composites enhances sound absorption and vibration attenuation, mainly due to increased porosity, viscoelastic energy dissipation, and particle morphology effects. Acoustic performance is strongly governed by mixture design parameters, particularly rubber content and aggregate size, while trade-offs with mechanical strength remain a recurring limitation. These findings are mainly associated with the blue cluster identified in the bibliometric analysis, which links acoustic performance to mechanical behavior and material design considerations in rubber-modified composites.

3.4.3 Tire fibers with tire rubber particles

According to Ružickij *et al*. (2020), although tire fibers exhibit good sound absorption performance and represent a sustainable alternative to mineral wool, their availability remains limited, highlighting the need for further investigation into their effectiveness. In line with Ružickij *et al.* (2022), studies on sound absorption provided by end-of-life tire fibers showed that fibers containing lower amounts of residual rubber particles achieved higher sound absorption coefficients compared to fibers with greater impurity levels or higher quantities of rubber residues. This observation is further supported by Robert *et al*. (2022), who reported that the presence of rubber residues within tire fibers reduces their sound absorption capacity, particularly at lower frequencies. These findings emphasize the importance of effectively removing residual rubber particles to maximize the acoustic performance of tire-derived fibers.

Tire fibers exhibit effective sound absorption when residual rubber content is minimized, as impurities hinder pore accessibility and reduce absorption efficiency, particularly at low frequencies. This behavior is mainly associated with the light-blue cluster of the bibliometric analysis, which groups studies focused on sound absorption mechanisms in porous and fibrous materials.

3.4.4 Aerogels with tire rubber fibers

In the study by Thai *et al*. (2019), tire-derived fibers exhibited insulation performance approximately 10% higher than that of a commercial foam absorber, which presented a noise reduction coefficient (NRC) of 0.39. However, the acquisition of these fibers posed challenges, as it required specialized technical equipment and was associated with low recyclability.

Thai *et al*. (2020) reported that only fibers originally used in tire manufacturing achieved excellent sound absorption and thermal insulation performance. These fibers also demonstrated robust mechanical behavior, withstanding significant elastic deformation without fracture. For materials with equal thickness, rubber-based aerogels exhibited sound absorption performance approximately 3.5 times higher than silica/PET aerogels and outperformed conventional materials such as wool and cork. Notably, these aerogels were composed exclusively of fibers, without rubber residues.

According to Thai *et al*. (2021), although these aerogels exhibit high sound absorption capacity, they are relatively fragile, which limits their practical applications. In addition, their

production involves complex manufacturing routes and specialized techniques, increasing both cost and processing complexity.

Rubber fiber–based aerogels exhibit exceptional sound absorption and thermal insulation performance, driven by their highly porous structure and elastic fiber network. However, limitations related to mechanical fragility, manufacturing complexity, and scalability remain critical challenges. These findings are mainly associated with the light-blue cluster of the bibliometric analysis, which emphasizes sound absorption efficiency, energy dissipation, and impedance-related mechanisms in advanced porous materials.

3.4.5 Panels perforated containing tire rubber residues

In the study by Xu *et al*. (2018), perforated composite panels produced from mixtures of rubber waste, wood fiber sawdust, and high-density polyethylene exhibited high sound absorption coefficients, particularly at low frequencies. The hole diameter did not significantly influence absorption at higher frequencies; however, higher perforation rates led to increased sound absorption coefficients, substantially affecting the acoustic insulation performance of the panels. This behavior was attributed to the favorable acoustic impedance characteristics of natural and synthetic polymers, including residual rubber.

Astrauskas, Grubliauskas and Januševičius (2024) investigated perforated panels composed of layered rubber granules and plastic materials and reported sound transmission losses of approximately 12 dB in the frequency range of 250 to 1000 Hz and up to 20 dB between 1 and 4 kHz. In their configuration, a rubber-based layer was used to support an additional perforated plastic panel, forming a multilayer system. The combination of materials enhanced both sound absorption and acoustic insulation performance. The authors further observed that increasing the thickness of the rubber layer and the perforation angle of the plastic panel led to higher sound transmission loss.

Perforated panels incorporating tire rubber residues demonstrate effective sound absorption and insulation, particularly at low and mid frequencies, due to improved acoustic impedance matching and multilayer effects. Acoustic performance is strongly influenced by perforation rate, panel geometry, and rubber layer thickness. These results are mainly associated with the light-blue cluster of the bibliometric analysis, which groups studies focused on absorption efficiency and impedance-controlled acoustic behavior.

3.4.6 Various composites with tire rubber particles for insulation, absorption and cushioning applications

According to Haworth *et al*. (2018), the incorporation of recycled rubber into high-density polyethylene (HDPE) compounds resulted in improved sound absorption performance. Enhanced acoustic behavior was achieved by adding recycled rubber particles to both HDPE composites and HDPE–fiberglass composites, with an optimal acoustic damping observed at a rubber content of 20%. Multilayer composite structures incorporating gradients of rubber concentration through their thickness further improved sound absorption efficiency.

Chandran, Raj and Lakshmanan (2018) investigated the sound and vibration damping behavior of natural rubber compounds mixed with particles derived from used tires. Smaller rubber particles exhibited superior sound absorption, whereas larger particles were more effective for vibration reduction. The addition of silica improved the dispersion of rubber particles within the matrix, enhancing sound absorption by promoting porous-like behavior.

Badida *et al*. (2018) evaluated recycled tire rubber as an acoustic material obtained from end-of-life vehicles and reported sound absorption coefficients exceeding 0.50 in the frequency ranges of 500–800 Hz and above 1600 Hz. The sound reduction index remained above 12 dB across 100–6300 Hz, reaching a maximum value of 28.33 dB at 6300 Hz.

Phiri *et al*. (2019) developed recycled tire rubber foam composites as alternatives to virgin rubber and analyzed the effects of free foaming and pre-curing on their thermal, morphological, and physical properties. Tire rubber significantly influenced hardness, density, thermal stability, and dimensional stability of the foam composites.

Leelawanachai, Dedruktip and Tangboriboon (2020) examined natural rubber composites reinforced with alumina whisker fibers for insulation applications, reporting low thermal conductivity and effective sound absorption.

El Messiry and Ayman (2022) studied panels composed of textile fibers (cotton, wool, and Kapok) combined with tire rubber granules bonded with polyvinyl acetate (PVA). These panels exhibited significant sound transmission loss, particularly at high frequencies, with Kapok fiber-based panels showing the highest STL due to their low density and favorable interaction with sound waves.

According to Laxmi *et al*. (2023), composites incorporating crushed tire rubber with cement and fly ash demonstrated favorable acoustic performance and adequate mechanical strength for noise barrier applications. The highest sound absorption coefficients were observed

in the ranges of 500–1600 Hz and 3150–4000 Hz, with a peak value of 0.6 at 1600 Hz, corresponding to frequencies typical of traffic noise.

These studies demonstrate that hybrid composites incorporating tire rubber can be effectively tailored for sound absorption, insulation, and vibration damping through particle size control, multilayer design, and matrix selection. This body of work aligns mainly with the green cluster of the bibliometric analysis, which groups multifunctional composites designed for combined acoustic, thermal, and cushioning performance.

3.4.7 Gypsum-based composites with tire rubber

Studies have investigated gypsum-based composites incorporating rubber particles, reporting promising improvements in thermal, radiation, and acoustic insulation performance. However, these benefits are often accompanied by reductions in mechanical strength and workability (Korkut *et al.,* 2013; López-Zaldívar *et al.,* 2017; Pinto *et al.,* 2020).

Lozano-Díez *et al.* (2021) demonstrated that the incorporation of carbon fibers into gypsum–rubber composites increased tensile strength, reduced brittleness, and improved toughness and durability. These results indicate that such materials are suitable for prefabricated building elements, such as panels or boards.

Vilniškis and Januševičius (2023) showed that multilayer sandwich panels composed of plasterboard outer layers and a porous core made of devulcanized rubber granules recycled from end-of-life tires achieved high sound transmission loss, particularly with 25 mm thick rubber layers. The study also highlighted that higher-density plasterboards further enhanced the overall acoustic insulation performance.

Fiala *et al*. (2023) evaluated the acoustic performance of tire-fluff boards and sandwich gypsum/tire-fluff panels, confirming their effectiveness in improving noise reduction.

These studies indicate that gypsum–rubber composites are particularly effective in layered and sandwich configurations, where acoustic insulation gains can be achieved while partially mitigating mechanical limitations. This research trend is associated with the blue cluster, which emphasizes lightweight building panels and hybrid gypsum-based systems for sound insulation applications.

3.5 Concluding remarks and perspectives

This review consolidates the evolution of waste tire rubber (WTR) applications for acoustic purposes from 1941 to 2026, revealing a pronounced growth in research activity over the last decade. The results confirm WTR as a mature and sustainable solution for noise mitigation, with performance strongly governed by particle size and application context. Across asphalt, cementitious composites, and aerogels, smaller rubber particles consistently favor sound absorption through enhanced porosity, while larger particles are more effective for vibration damping and impact noise control.

The reviewed studies show that WTR-based composites exhibit frequency-dependent acoustic behavior, with rubberized asphalt performing mainly in the mid-frequency range (≈570–650 Hz) and cementitious systems showing higher absorption at medium and high frequencies (≈1000–4000 Hz), which are highly relevant for traffic noise. While WTR incorporation generally leads to reductions in strength and stiffness, it consistently improves ductility, fatigue resistance, and crack control. From a thermal perspective, WTR enhances high-temperature stability in asphalt and improves resistance to freeze–thaw cycles, although often at the expense of workability.

The main research gaps identified include improving interfacial bonding between rubber and mineral matrices, particularly in gypsum-based systems, and optimizing the processing of tire fibers to eliminate residual rubber that limits acoustic efficiency. Emerging research trends point toward architected materials, acoustic metamaterials, and 3D-printed cementitious composites incorporating WTR, enabling targeted sound absorption and tunable frequency responses. Given the persistent mechanical limitations, current evidence supports the application of WTR-based materials primarily in non-structural elements, where acoustic and thermal performance are the dominant design criteria.

These relationships between acoustic benefits, mechanical trade-offs, material typologies, and application domains are summarized in Figure 3-10, which presents a mind map synthesizing the positive and negative effects of incorporating crushed tire rubber into different composite systems, serving as a guideline for future research and material selection.

Figure 3-10 – Mind map summarizing the positive and negative effects of crushed tire rubber in different composite systems

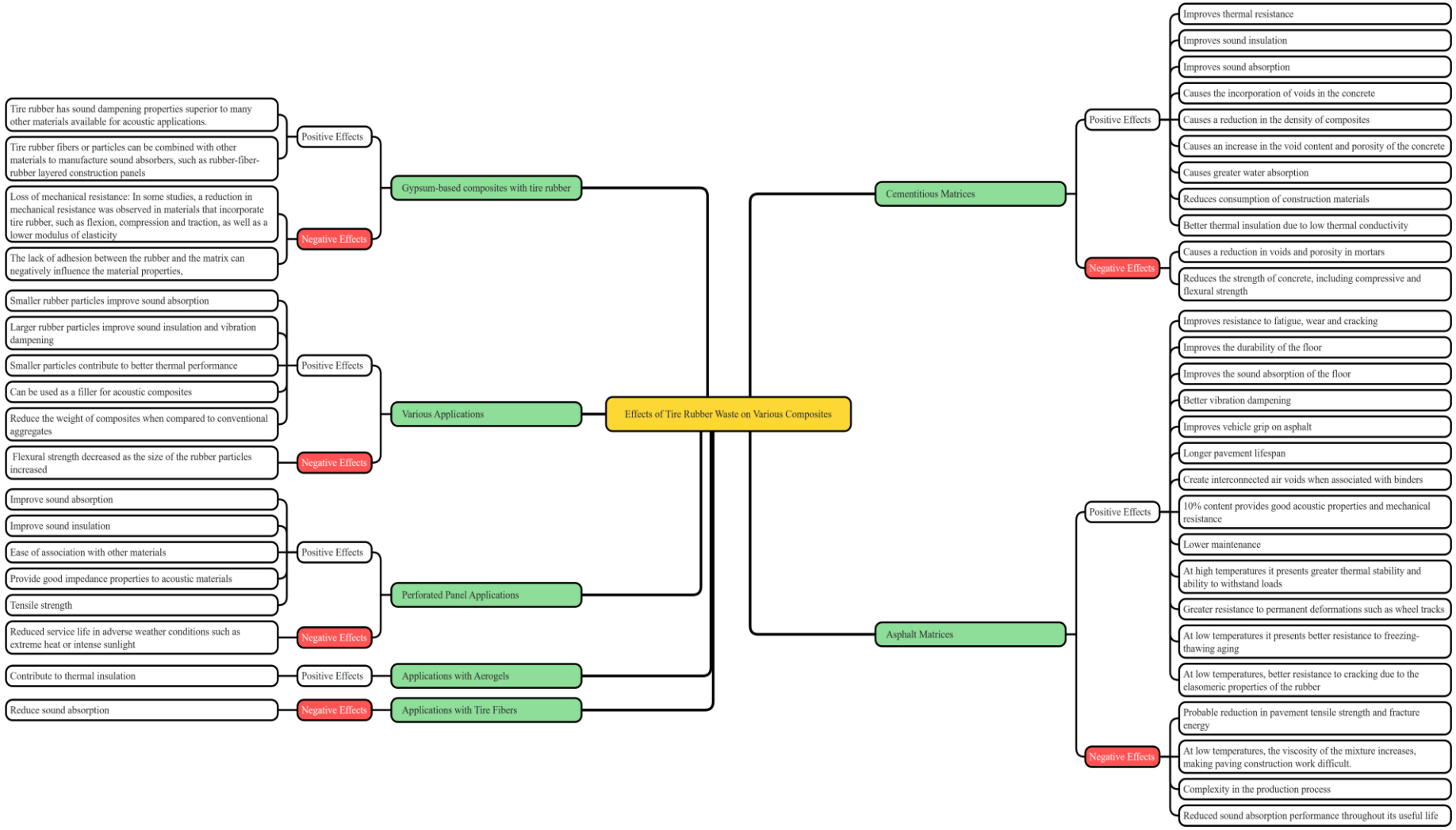

3.6 Acknowledgements

The authors express their gratitude to the National Council for Scientific and Technological Development (CNPq), the Coordination for the Improvement of Higher Education Personnel (CAPES), and the Minas Gerais Research Funding Foundation (FAPEMIG) for their ongoing support through research fellowships and institutional programs. Special thanks are also extended to the Research Group SICon-CNPq/UFV and the partner groups within the Minas Gerais Research, Scientific, Technological, and Innovation Network (Rede Mineira de Desenvolvimento Científico, Tecnológico e de Inovação) for providing the infrastructure, technical assistance, and academic environment essential to the development of this work.

3.7 Declaration of generative AI and AI-assisted technologies in the writing process

During the preparation of this work, the authors utilized generative AI and AI-assisted technologies to improve grammar, stylistic flow, and overall readability. Following this process, the authors critically reviewed and edited the generated content to ensure technical accuracy and assume full responsibility for the final integrity and originality of the publication.

3.8 References

APAZA, F. R. A.; VÁZQUEZ, V. F.; PAJE, S. E.; SAIZ, L.; GULISANO, F.; GALLEGO, J. The potential effect of crumb rubber on the maximum sound absorption performance of asphalt mixtures. **Construction and Building Materials**, v. 389, 131789, 2023. https://doi.org/10.1016/j.conbuildmat.2023.131789

ASANTEY, S.; KALLOUSH, A.; LOTFY, A. **Recycled materials in concrete applications - Benefits from waste Free Ontario act**. In: CSCE ANNUAL CONFERENCE - CANADIAN SOCIETY FOR CIVIL ENGINEERING, 2019, Montreal. Available in: https://legacy.csce.ca/elf/apps/CONFERENCEVIEWER/conferences/2019/pdfs/PaperPDFVersion_17_0219101714.pdf. Access in: 23 set. 2025.

ASDRUBALI, F. **Survey on the acoustical properties of new sustainable materials for noise control**. In: EURONOISE 2006 – EUROPEAN CONFERENCE ON NOISE CONTROL, 6., 2006. Available in: https://iris.uniroma3.it/handle/11590/180961. Access in: 30 jul. 2025.

ASSOCIAÇÃO NACIONAL DA INDÚSTRIA DE PNEUMÁTICOS. **Quase 200 anos de tecnologia**. 2018. Available at: https://www.anip.org.br/historia-e-fabricacao/. Accessed on: 12 Nov. 2023.

ASTRAUSKAS, T.; GRUBLIAUSKAS, R.; JANUŠEVIČIUS, T. Optimization of sound-absorbing and insulating structures with 3D printed recycled plastic and tyre rubber using the TOPSIS approach. **JVC/Journal of Vibration and Control**, v. 30, n. 7-8, p. 1772-1782, 2024. https://doi.org/10.1177/10775463231171218

ATEF, M.; BASSIONI, G.; AZAB, N. ; ABDELLATIF, M. H. On the acoustical performance of eco-friendly cementitious composite with recycled fine rubber particles. **Construction and Building Materials**, v. 325, 126830, 2022. https://doi.org/10.1016/j.conbuildmat.2022.126830

BADIDA, M.; SOBOTOVA, L.; BADIDOVA, A.; MORAVEC, M.; MIKULOVA, A. Research of chosen acoustics descriptors of developed materials from old automobile recycled materials. **Recycling**, v. 3, n. 2, 29, 2018. https://doi.org/10.3390/recycling3020029

BALA, A.; GUPTA, S. Thermal resistivity, sound absorption and vibration damping of concrete composite doped with waste tire Rubber: A review. **Construction and Building Materials**, v. 299, 123939, 2021. https://doi.org/10.1016/j.conbuildmat.2021.123939

BASNER, M.; McGUIRE, S. WHO environmental noise guidelines for the European region: A systematic review on environmental noise and effects on sleep. **International Journal of Environmental Research and Public Health**, v. 15, n. 3, 519, 2018. https://doi.org/10.3390/ijerph15030519

BENKREIRA, H.; KHAN, A.; HOROSHENKOV, K. V. Sustainable acoustic and thermal insulation materials from elastomeric waste residues. **Chemical Engineering Science**, v. 66, n. 18, p. 4157-4171, 2011. https://doi.org/10.1016/j.ces.2011.05.047

BHINGARE, N. H.; PRAKASH, S.; JATTI, V. S. A review on natural and waste material composite as acoustic material. **Polymer Testing**, v. 80, 2019. https://doi.org/10.1016/j.polymertesting.2019.106142

BISTAFA, S. **Acústica aplicada ao controle do ruído**. 2.ed. São Paulo: Blucher, 2018.

CALLISTER, W. D.; RETHWISCH, D. G. **Ciência e engenharia de materiais**: uma introdução. 9.ed. Rio de Janeiro: LTC, 2016.

CHALANGARAN, N.; FARZAMPOUR, A.; PASLAR, N.; FATEMI, H. Experimental investigation of sound transmission loss in concrete containing recycled rubber crumbs. **Advances in Concrete Construction**, v. 11, n. 6, p. 447-454, 2021. https://doi.org/10.12989/acc.2021.11.6.447

CHANDRAN, V.; RAJ, T. M.; LAKSHMANAN, T. Sound and vibration behavior assessment of different sizes of waste tyre rubber in natural rubber composites for damping applications. **Chiang Mai Journal of Science**, v. 45, n. 1, 515-527, 2018. Available in: https://epg.science.cmu.ac.th/ejournal/journal-detail.php?id=8768. Access in: 30 ago. 2025.

CORSARO, R. D.; KLUNDER, J. D.; JARZYNSKI, J. Filled rubber materials system: Application to echo absorption in waterfilled tanks. **Journal of the Acoustical Society of America**, v. 68, n. 2, p. 655-664, 1980. https://doi.org/10.1121/1.384724

DISSANAYAKE, D. G. K.; WEERASINGHE, D. U.; THEBUWANAGE, L. M.; BANDARA, U. A. A. N. An environmentally friendly sound insulation material from post-industrial textile waste and natural rubber. **Journal of Building Engineering**, v. 33, 101606, 2021. https://doi.org/10.1016/j.jobe.2020.101606

DLUBAC, J. J.; LEE, G. F.; DEIGAN, R. J.; LEE, J. D. Comparison of the complex dynamic modulus as measured by three apparatus. **Polymeric Materials Science and Engineering**, v. 60, p. 579-583, 1989. https://doi.org/10.1021/BK-1990-0424.CH003

DONAVAN, P. R.; JANELLO, C. J. Results of the 10-year Arizona quiet pavement pilot program. **Transportation Research Record**, v. 2675, n. 9, p. 1040-1048, 2021. https://doi.org/10.1177/03611981211005460

DONG, Y.; ZHAO, Y.; HOSSAIN, U.; HE, Y.; LIU, P. Life cycle assessment of vehicle tires: A systematic review. **Cleaner Environmental Systems**, v. 2, 100033, 2021. https://doi.org/10.1016/j.cesys.2021.100033

DONG, H.-W.; ZHAO, S.-D.; OUDICH, M.; SHEN, C.; ZHANG, C.; CHENG, L.; …; FANG, D. Reflective metasurfaces with multiple elastic mode conversions for broadband underwater sound absorption. **Physical Review Applied**, v. 17, n. 4, 044013, 2022. https://doi.org/10.1103/PhysRevApplied.17.044013

DONG, H.-W.; ZHAO, S.-D.; XIANG, P.; WANG, B.; ZHANG, C.; CHENG, L.; ...; FANG, D. Porous-solid metaconverters for broadband underwater sound absorption and insulation. **Physical Review Applied**, v. 19, n. 4, 044074, 2023. https://doi.org/10.1103/PhysRevApplied.19.044074

DUAN, M.; YU, C.; XIN, F.; LU, T. J. Tunable underwater acoustic metamaterials via quasi-Helmholtz resonance: From low-frequency to ultra-broadband. **Applied Physics Letters**, v. 118, n. 7, 071904, 2021. https://doi.org/10.1063/5.0028135

EL MESSIRY, M.; AYMAN, Y. Investigation of sound transmission loss of natural fiber/rubber crumbs composite panels. **Journal of Industrial Textiles**, v. 51, n. 3, p. 5347S-5369S, 2022. https://doi.org/10.1177/15280837211039574

EL-SEIDY, E.; SAMBUCCI, M.; CHOUGAN, M.; AL-KHEETAN, M. J.; BIBLIOTECA, I.; VALENTE, M.; GHAFFAR, S. H. Mechanical and physical characteristics of alkali-activated mortars incorporated with recycled polyvinyl chloride and rubber aggregates. **Journal of Building Engineering**, v. 60, 105043, 2022. https://doi.org/10.1016/j.jobe.2022.105043

EYSSA, H. M.; AFIFI, M.; MOUSTAFA, H. Improvement of the acoustic and mechanical properties of sponge ethylene propylene diene rubber/carbon nanotube composites crosslinked by subsequent sulfur and electron beam irradiation. **Polymer International**, v. 72, n. 1, p. 87-98, 2023. https://doi.org/10.1002/pi.6449

FATIMA, S.; MOHANTY, A. R. Acoustical and fire-retardant properties of jute composite materials. **Applied Acoustics**, v. 72, n. 2-3, p. 108-114, 2011. https://doi.org/10.1016/j.apacoust.2010.10.005

FIALA, L.; KONRÁD, P.; HOTĚK, P.; ČERNÝ, R. Determination of acoustic performance of tire-fluff and gypsum/tire-fluff boards by measurements in acoustic chambers. **AIP Conference Proceedings**, 2918, 020017, 2023. https://doi.org/10.1063/5.0170849

GAO, N.; LU, K. An underwater metamaterial for broadband acoustic absorption at low frequency. **Applied Acoustics**, v. 169, 107500, 2020. https://doi.org/10.1016/j.apacoust.2020.107500

GRAMMELIS, P.; MARGARITIS, N.; DALLAS, P.; RAKOPOULOS, D.; MAVRIAS, G. A review on management of end-of-life tires (Elts) and alternative uses of textile fibers. **Energies**, v. 14, n. 3, 571, 2021. https://doi.org/10.3390/en14030571

HARON, Z.; JUSLI, E.; NOR, H. M.; JAYA, R. P.; YAACOB, H.; YAHYA, K.; …, YAHYA, M. N. Prediction of sound absorption coefficient for double layer rubberised concrete blocks. **International Journal of Engineering and Technology (UAE)**, v. 7, n. 2.29, p. 704-710, 2018. https://doi.org/10.14419/ijet.v7i2.29.14002

HAWORTH, B.; CHADWICK, D.; CHEN, L.; ANG, Y. Thermoplastic composite beam structures from mixtures of recycled HDPE and rubber crumb for acoustic energy absorption. **Journal of Thermoplastic Composite Materials**, v. 31, n. 1, p. 119-142, 2018. https://doi.org/10.1177/0892705716681836

HOLMES, N.; BROWNE, A.; MONTAGUE, C. Acoustic properties of concrete panels with crumb rubber as a fine aggregate replacement. **Construction and Building Materials**, v. 73, p. 195-204, 2014. https://doi.org/10.1016/j.conbuildmat.2014.09.107

INTABOOT, N.; KANBUA, P. Investigation of concrete blocks mixed with recycled crumb rubber: A case study in Thailand. **Engineering and Applied Science Research**, v. 49, n. 3, p. 413-424, 2022. Available in: https://ph01.tci-thaijo.org/index.php/easr/article/view/246614. Access in: 6 jun. 2025.

IVANSSON, S. M. Sound absorption by viscoelastic coatings with periodically distributed cavities. **Journal of the Acoustical Society of America**, v. 119, n. 6, p. 3558-3567, 2006. https://doi.org/10.1121/1.2190165

KHALOO, A. R.; DEHESTANI, M.; RAHMATABADI, P. Mechanical properties of concrete containing a high volume of tire-rubber particles. **Waste Management**, v. 28, n. 12, p. 2472-2482, 2008. https://doi.org/10.1016/j.wasman.2008.01.015

KORKUT, T.; UMAÇ, Z. I.; AYGÜN, B.; KARABULUT, A.; YAPICI, S.; ŞAHIN, R. Neutron equivalent dose rate measurements of gypsum-waste tire rubber layered structures. **International Journal of Polymer Analysis and Characterization**, v. 18, n. 6, p. 423-429, 2013. https://doi.org/10.1080/1023666X.2013.814025

KOSTEN, C. W.; ZWIKKER, C. Theory of the absorption of sound by compressible walls with a non-porous surface-layer. **Physica**, v. 8, n. 2, p. 251-272, 1941. https://doi.org/10.1016/S0031-8914(41)90047-2

LAXMI, V.; THAKRE, C.; BISARYA, A.; VIJAY, R. An innovative approach for the development of sound absorbing material using industrial wastes. **Construction and Building Materials**, v. 369, 130523, 2023. https://doi.org/10.1016/j.conbuildmat.2023.130523

LEELAWANACHAI, W.; DEDRUKTIP, N.; TANGBORIBOON, N. Energy-absorption ability of embedding whisker alumina fiber into natural rubber composite for insulation applications. **Materials Science Forum**, v. 987, p. 47-52, 2020. https://doi.org/10.4028/www.scientific.net/MSF.987.47?urlappend=%3Futm_source%3Dresearchgate.net%26utm_medium%3Darticle

LIU, L.; CAI, G.; ZHANG, J.; LIU, X.; LIU, K. Evaluation of engineering properties and environmental effect of recycled waste tire-sand/soil in geotechnical engineering: A compressive review. **Renewable and Sustainable Energy Reviews**, v. 126, 109831, 2020. https://doi.org/10.1016/j.rser.2020.109831

LÓPEZ-ZALDÍVAR, O.; LOZANO-DÍEZ, R.; HERRERO-DEL-CURA, S.; MAYOR-LOBO, P.; HERNÁNDEZ-OLIVARES, F. Effects of water absorption on the microstructure of plaster with end-of-life tire rubber mortars. **Construction and Building Materials**, v. 150, p. 558-567, 2017. https://doi.org/10.1016/j.conbuildmat.2017.06.014

LOZANO-DÍEZ, R. V.; LÓPEZ-ZALDÍVAR, O.; HERRERO-DEL-CURA, S.; MAYOR-LOBO, P. L.; HERNÁNDEZ-OLIVARES, F. Mechanical behavior of plaster composites based on rubber particles from end-of-life tires reinforced with carbon fibers. **Materials**, v. 14, n. 14, 3979, 2021. https://doi.org/10.3390/ma14143979

LUMNITZER, E.; HRICOVÁ, B.; BEDNÁROVÁ, L.; PACANA, A. Development of materials obtained from recycled cars and their subsequent use in noise reduction. **Progress in Rubber, Plastics and Recycling Technology**, v. 34, n. 4, p. 221-229, 2018. https://doi.org/10.1177/1477760618798412

LYU, L.; DONG, Y.; ZHAO, D.; WEN, Y.; LI, R.; REN, X.; PEI, J. Mechanical and acoustic properties composition design and effects analysis of poroelastic road surface. **Journal of Materials in Civil Engineering**, v. 33, n. 10, 2021. https://doi.org/10.1061/(ASCE)MT.1943-5533.0003904

MARINI, S.; LANOTTE, M. Waste rubber from end-of-life tires in 'lean' asphalt mixtures — a laboratory and field investigation in the arid climate region. **Polymers**, v. 13, n. 21, 2021. https://doi.org/10.3390/polym13213802

MARTÍN-MARTÍN, A.; ORDUNA-MALEA, E.; THELWALL, M.; LÓPEZ-CÓZAR, E. D. Google Scholar, Web of Science, and Scopus: A systematic comparison of citations in 252 subject categories. **Journal of Informetrics**, v. 12, n. 4, p. 1160-1177, 2018. https://doi.org/10.1016/j.joi.2018.09.002

MEHO, L. I. Using Scopus's CiteScore for assessing the quality of computer science conferences. **Journal of Informetrics**, v. 13, n. 1, p. 419-433, 2019. https://doi.org/10.1016/j.joi.2019.02.006

MEHRZAD, S.; TABAN, E.; SOLTANI, P.; SAMAEI, S. E.; KHAVANIN, A. Sugarcane bagasse waste fibers as novel thermal insulation and sound-absorbing materials for application in sustainable buildings. **Building and Environment**, v. 211, 108753, 2022. https://doi.org/10.1016/j.buildenv.2022.108753

MHAYA, A. M.; SHAHIDAN, S.; ZUKI, S. S. M.; HUSEIEN, G. F.; AZMI, M. A. M.; ISMAIL, M.; MIRZA, J. Durability and acoustic performance of rubberized concrete containing POFA as cement replacement. **Sustainability**, v. 14, n. 23, 15510, 2022. https://doi.org/10.3390/su142315510

MIKHAILENKO, P.; PIAO, Z.; KAKAR, M. R.; ATHARI, S.; BUENO, M.; POULIKAKOS, L. D. Effect of waste PET and CR as sand replacement on the durability and effect of waste PET and CR as sand replacement on the durability and acoustical properties of semi dense asphalt (SDA) mixtures. **Sustainable Materials and Technologies**, v. 29, e00295, 2021. https://doi.org/10.1016/j.susmat.2021.e00295

MOHAMMED, B. S.; HOSSAIN, K. M. A.; SWEE, J. T. E.; WONG, G.; ABDULLAHI, M. Properties of crumb rubber hollow concrete block. **Journal of Cleaner Production**, v. 23, n. 1, p. 57-67, 2012. https://doi.org/10.1016/j.jclepro.2011.10.035

NAJIB, N. N.; ARIFF, Z. M.; BAKAR, A. A.; SIPAUT, C. S. Correlation between the acoustic and dynamic mechanical properties of natural rubber foam: Effect of foaming temperature. **Materials & Design**, v. 32, n. 2, p. 505-511, 2011. https://doi.org/10.1016/j.matdes.2010.08.030

PHIRI, M. M.; SIBEKO, M. A.; PHIRI, M. J.; HLANGOTHI, S. P. Effect of free foaming and pre-curing on the thermal, morphological and physical properties of reclaimed tyre rubber foam composites. **Journal of Cleaner Production**, v. 218, p. 665-672, 2019. https://doi.org/10.1016/j.jclepro.2019.02.051

PINTO, N.; FIORITI, C.; AKASAKI, J.; ACUNHA, T.; OKIMOTO, F. Performance of plaster composites incorporating rubber tire particles. **Revista Ingeniería de Construcción**, v. 35, n. 2, 2020. http://dx.doi.org/10.4067/S0718-50732020000200216

PONGSOPHA, P.; SUKONTASUKKUL, P.; ZHANG, H.; LIMKATANYU, S. Thermal and acoustic properties of sustainable structural lightweight aggregate rubberized concrete. **Results in Engineering**, v. 13, 100333, 2022. https://doi.org/10.1016/j.rineng.2022.100333

POULIKAKOS, L. D.; ATHARI, S.; MIKHAILENKO, P.; KAKAR, M.; BUENO, M.; PIAO, Z.; ...; HEUTSCHI, K. Effect of waste materials on acoustical properties of semi-dense asphalt mixtures. **Transportation Research Part D: Transport and Environment**, v. 102, 103154, 2022. https://doi.org/10.1016/j.trd.2021.103154

RASHAD, A. M. A comprehensive overview about recycling rubber as fine aggregate replacement in traditional cementitious materials. **International Journal of Sustainable Built Environment**, v. 5, n. 1, p. 46-82, 2016. https://doi.org/10.1016/j.ijsbe.2015.11.003

ROBERT, R.; SAULIUS, V.; TOMAS, J.; RAIMONDAS, G. The reuse method of waste tyre textile fibers for sound absorption applications. In: 2022 INTERNATIONAL CONFERENCE AND UTILITY EXHIBITION ON ENERGY, ENVIRONMENT AND CLIMATE CHANGE (ICUE), 2022, Pattaya, Thailand. **Proceedings...** Pattaya, Thailand: IEEE, 2022. https://www.doi.org/10.1109/ICUE55325.2022.10113515

RODGERS, B. **Tire engineering**. Boca Raton: CRC Press, 2020. https://doi.org/10.1201/9781003022961

RUŽICKIJ, R.; ASTRAUSKAS, T.; VALTERE, S.; GRUBLIAUSKAS, R. Sound absorption properties evaluation and analysis of recycled tyre textile fibre waste. **Environmental and Climate Technologies**, v. 24, n. 3, p. 318-328, 2020. https://doi.org/10.2478/rtuect-2020-0106

RUŽICKIJ, R.; SAULIUS, V.; TOMAS, J.; RAIMONDAS, G. The reuse method of waste tyre textile fibers for sound absorption applications. In: 2022 INTERNATIONAL CONFERENCE AND UTILITY EXHIBITION ON ENERGY, ENVIRONMENT AND CLIMATE CHANGE (ICUE) , 2022, Pattaya, Thailand. **Proceedings...** Pattaya, Thailand: IEEE, 2022. https://doi.org/10.1109/ICUE55325.2022.10113515

SAMBUCCI, M.; VALENTE, M. Acoustic behavior of 3d-printable cement mortars functionalized with recycled tire rubber aggregates. In: INTERNATIONAL CONGRESS ON SOUND AND VIBRATION, 27, 2021, Gliwice, Poland. **Proceedings…** Gliwice, Poland: Silesian University Press, 2021. Available in: https://iris.uniroma1.it/handle/11573/1577621?mode=complete. Access in: 12 jul. 2025.

SAMBUCCI, M.; VALENTE, M.; SIBAI, A.; MARINI, D.; QUITADAMO, A.; MUSACCHI, E. Rubber-cement composites for additive manufacturing: physical, mechanical and thermo-acoustic characterization. In: BOS, F.; LUCAS, S.; WOLFS, R.; SALET, T. (Eds.). **Second RILEM International Conference on Concrete and Digital Fabrication**. Cham.: Sringer, 2020. p. 113-124. https://doi.org/10.1007/978-3-030-49916-7_12

SAMBUCCI, M.; SIBAI, A.; FATTORE, L.; MARTUFI, R.; LUCIBELLO, S.; VALENTE, M. Finite element multi-physics analysis and experimental testing for hollow brick solutions with lightweight and eco-sustainable cement mix. **Journal of Composites Science**, v. 6, n. 4, 107, 2022. https://doi.org/10.3390/jcs6040107

SÁNCHEZ-DEHESA, J.; GARCIA-CHOCANO, V. M.; TORRENT, D.; CERVERA, F.; CABRERA, S. Noise control by sonic crystal barriers made of recycled materials. **Journal of the Acoustical Society of America**, v. 129, n. 3, p. 1173-1183, 2010. https://doi.org/10.1121/1.3508427

SANTOS, J. M. C.; GACHET-BARBOSA, L. A.; RODRIGUES, S.; ANGELIN, A. F.; MIRANDA JR., E. J. P. Influence of spheroid and fiber-like waste-tire rubbers on the sound absorption coefficient of rubberized mortars. **Materials Science Forum**, v. 958, p. 63-68, 2019. https://doi.org/10.4028/www.scientific.net/MSF.958.63

SANYAL, A. P.; MOHANTY, S.; SARKAR, A. Application of recycled aggregates generated from waste materials towards improvement in acoustical and thermal conductivity of concrete. **Materials Today: Proceedings**, 2023. https://doi.org/10.1016/j.matpr.2023.04.079

SHARMA, G. S.; SKVORTSOV, A.; MacGILLIVRAY, I.; KESSISSOGLOU, N. Sound absorption by rubber coatings with periodic voids and hard inclusions. **Applied Acoustics**, v. 143, p. 200-210, 2019a. https://doi.org/10.1016/j.apacoust.2018.09.003

SHARMA, G. S.; SKVORTSOV, A.; MacGILLIVRAY, I.; KESSISSOGLOU, N. Acoustic performance of periodic steel cylinders embedded in a viscoelastic medium. **Journal of Sound and Vibration**, v. 443, p. 652-665, 2019b. https://doi.org/10.1016/j.jsv.2018.12.013

SMIRNOVA, O. M.; NAVASCUÉS, I. M. P.; MIKHAILEVSKI, V. R. ; KOLOSOV, O. I. ; SKOOLOTA, N. S. Sound-absorbing composites with rubber crumb from used tires. **Applied Sciences**, v. 11, n. 16, 7347, 2021. https://doi.org/10.3390/app11167347

SNOWDON, J. C. Vibration isolation: use and characterization. **The Journal of the Acoustical Society of America**, v. 66, p. 1245-1274, 1979. https://doi.org/10.1121/1.383546

SOCIETY OF AUTOMOTIVE ENGINEERS OF JAPAN. **Tires**. SAEJ, 2020.

SOUZA, L. C. L.; ALMEIDA, M. G.; BRAGANÇA, L. **Bê-á-bá da acústica arquitetônica**: ouvindo a Arquitetura. 4. ed. São Carlos: EdUFSCar, 2012.

SOUZA, A. M.; CARVALHO, J. M. F.; SILVA, G. M.; PEDROTI, L. G.; SILVA, G. J. B.; PEIXOTO, R. A. F. Mapping the research landscape of calcined clay and LC3: A bibliometric perspective on emerging challenges and opportunities. **Applied Clay Science**, v. 277, 107952, 2025. https://doi.org/10.1016/j.clay.2025.107952

SUKONTASUKKUL, P. Use of crumb rubber to improve thermal and sound properties of pre-cast concrete panel. **Construction and Building Materials**, v. 23, n. 2, p. 1084-1092, 2009. https://doi.org/10.1016/j.conbuildmat.2008.05.021

SVOBODA, J.; DVORSKÝ, T.; VÁCLAVIK, V.; CHARVÁT, J.; MÁČALOVÁ, K.; HEVIÁNKOVÁ, S.; JANUROVÁ, E. Sound-absorbing and thermal-insulating properties of cement composite based on recycled rubber from waste tires. **Applied Sciences**, v. 11, n. 6, 2725, 2021. https://doi.org/10.3390/app11062725

TAKAHASHI, D. Seat dip effect: The phenomena and the mechanism. **Journal of the Acoustical Society of America**, v. 102, n. 3, p. 1326-1334, 1997. https://doi.org/10.1121/1.420052

TAO, Y.; REN, M.; ZHANG, H.; PEIJS, T. Recent progress in acoustic materials and noise control strategies – A review. **Applied Materials Today**, v. 24, 101141, 2021. https://doi.org/10.1016/j.apmt.2021.101141

THAI, Q. B.; SIANG, T. E.; LE, D. K.; SHAH, W. A.; PHAN-THIEN, N.; DUONG, H. M. Advanced fabrication and multi-properties of rubber aerogels from car tire waste. **Colloids and Surfaces A: Physicochemical and Engineering Aspects**, v. 577, p. 702-708, 2019. https://doi.org/10.1016/j.colsurfa.2019.06.029

THAI, Q. B.; CHONG, R. O.; NGUYEN, P. T. T.; LE, D. K.; LE, P. K.; PHAN-THIEN, N.; DUONG, H. M. Recycling of waste tire fibers into advanced aerogels for thermal insulation and sound absorption applications. **Journal of Environmental Chemical Engineering**, v. 8, n. 5, 104279, 2020. https://doi.org/10.1016/j.jece.2020.104279

THAI, Q. B.; LE-CAO, K.; NGUYEN, P. T. T.; LE, P. K.; PHAN-THIEN, N.; DUONG, H. M. Fabrication and optimization of multifunctional nanoporous aerogels using recycled textile fibers from car tire wastes for oil-spill cleaning, heat-insulating and sound absorbing applications. **Colloids and Surfaces A: Physicochemical and Engineering Aspects**, v. 628, 2021. https://doi.org/10.1016/j.colsurfa.2021.127363

URRY, D. W.; HUGEL, T.; SEITZ, M.; GAUB, H. E.; SHEIBA, L.; DEA, J.; XU, J.; PARKER, T. Elastin: a representative ideal protein elastomer. **Philosophical Transactions of the Royal Society B: Biological Sciences**, v. 357, n. 1418, p. 169-184, 2002. https://doi.org/10.1098/rstb.2001.1023

VAN ECK, N. J.; WALTMAN, L. **VOSviewer Manual**: Manual for VOSviewer version 1.6.20. Univeristeit Leiden, 2022. Available in: https://www.vosviewer.com/documentation/Manual_VOSviewer_1.6.20.pdf. Access in: 20 jun. 2025.

VANJARE, S. **End-of-Life Tire (ELT) management market**: top treatment technologies. 2023. Available at: https://inkwoodresearch.com/end-of-life-tire-management-market-insights/. Accessed: 12 nov. 2023.

VÁZQUEZ, V. F.; TERÁN, F.; PAJE, S. E. Dynamic stiffness of road pavements: Construction characteristics-based model and influence on tire/road noise. **Science of the Total Environment**, v. 736, 139597, 2020. https://doi.org/10.1016/j.scitotenv.2020.139597

VILNIŠKIS, T.; JANUŠEVIČIUS, T. Experimental research and transfer matrix method for analysis of transmission loss in multilayer constructions with devulcanized waste rubber. **Sustainability**, v. 15, n. 17, 12774, 2023. https://doi.org/10.3390/su151712774

WANG, W.; CHENG, Y.; CHEN, H.; TAN, G.; LV, Z.; BAI, Y. Study on the performances of waste crumb rubber modified asphalt mixture with eco-friendly diatomite and basalt fiber. **Sustainability**, v. 11, 5282, 2019. https://www.doi.org/10.3390/su11195282

WU, H.; SHEN, A.; CUI, H.; DAI, X.; LI, Y.; WANG, J. Effect of crumb rubber particles on antisliding and noise-reduction performance of asphalt pavement. **Journal of Materials in Civil Engineering**, v. 35, n. 6, 2023. https://doi.org/10.1061/JMCEE7.MTENG-14723

WÜRSIG, B.; GREENE JR., C. R.; JEFFERSON, T. A. Development of an air bubble curtain to reduce underwater noise of percussive piling. **Marine Environmental Research**, v. 49, n. 1, p. 79-93, 2000. https://doi.org/10.1016/S0141-1136(99)00050-1

XIAO, F.-P.; WANG, T.; WANG, J-Y.; SU, N.-Y..; HOU, X.-D.; CHEN, J.; LIU, J. Mechanism and research development of noise reduction technology of rubberized asphalt pavement. **China Journal of Highway and Transport**, v. 32, n. 4, p. 73-91, 2019. https://doi.org/10.19721/j.cnki.1001-7372.2019.04.005

XU, X.; WANG, H.; SUN, Y.; HAN, J.; HUANG, R. Sound absorbing properties of perforated composite panels of recycled rubber, fiberboard sawdust, and high density polyethylene. **Journal of Cleaner Production**, v. 187, p. 215-221, 2018. https://doi.org/10.1016/j.jclepro.2018.03.174

XU, L.; NI, H.; ZHANG, Y.; SUN, D.; ZHENG, Y.; HU, M. Porous asphalt mixture use asphalt rubber binders: Preparation and noise reduction evaluation. **Journal of Cleaner Production**, v. 376, 2022. https://doi.org/10.1016/j.jclepro.2022.134119

ZENG, X.; LI, G.; ZHU, J.; SAIN, M.; JIAN, R. NBR/CR-based high-damping rubber composites containing multiscale structures for tailoring sound insulation. **Macromolecular Materials and Engineering**, v. 308, n. 2, 2022. https://doi.org/10.1002/mame.202200464

4 ACOUSTIC AND MECHANICAL OPTIMIZATION OF ARCHITECTURAL GYPSUM PANELS THROUGH THE INTEGRATION OF RECYCLED TIRE RUBBER AGGREGATES AND MICROFIBERS

Abstract: This research investigates the development of sustainable gypsum composites reinforced with polypropylene microfibers and recycled tire rubber aggregates to enhance acoustic performance. Physicochemical characterization via SEM, FTIR, XRD, and Loss on Ignition (LOI) revealed that the rubber waste consists of a stable SBR and Natural Rubber blend reinforced with carbon black and inorganic fillers. A critical "encapsulation effect" was identified, where the gypsum paste seals the rubber's surface pores, hindering sound wave penetration and limiting airborne sound absorption at low frequencies. Mechanical properties, specifically flexural and compressive strengths, decreased with higher rubber content due to fragile Interfacial Transition Zones (ITZ) and the density mismatch between the hydrophobic rubber and hydrophilic matrix. The optimal technical balance was achieved by mixture 2400B20F06 (2.4 mm particles and 20% rubber content), which reached a compressive strength of 1.91 MPa and a peak sound absorption coefficient of 0.73 at 1250 Hz. Results indicate that while internal rubber inclusion is effective for vibration damping, airborne absorption is maximized in the 800–1250 Hz range.
Keywords: Gypsum composites, Recycled tire rubber, Acoustic insulation, Encapsulation effect, Sustainable materials.

4.1 Introduction

In Brazil, approximately 450,000 tons of tires—equivalent to 90 million units—are discarded annually, with each unit taking up to 600 years to decompose (Serviço Social do Transporte/Serviço Nacional de Aprendizagem do Transporte – SEST/SENAT, 2017). Driven by rising automobile demand, this waste has become a critical global concern, with China alone disposing of over 10 million tons in recent decades (Chen *et al.*, 2021). With more than 1.5 billion tires generated annually worldwide, developing sustainable reuse strategies is now an urgent environmental priority (Jena; Nayak; Satapathy, 2020).

The civil construction industry exerts a significant environmental impact primarily due to high consumption of non-renewable resources, elevated energy demand, and substantial CO^2 emissions (Masuero, 2021). A strategic alternative to mitigate the impacts of tire disposal is their application in building materials—a practice increasingly encouraged worldwide (Jena; Nayak; Satapathy, 2020). Among available solutions, the use of rubber for acoustic insulation is particularly notable (Parres; Crespo-Amorós; Nadal-Gisbert, 2009). However, while integrating waste into construction materials is an essential strategy to reduce landfill disposal (Rashad, 2016), only about 5.5% of recycled rubber is currently incorporated into the sector

(Zhang *et al.*, 2009). Developing new technologies that facilitate waste reuse within the production chain is therefore vital for achieving broader sustainability gains (Masuero, 2021).

The literature contains several studies investigating the reuse and applicability of various wastes in gypsum-based composites. These include the incorporation of rubber waste from tire retreading (Pinto, 2017), the use of rubber to enhance thermal performance (Meddah; Laoubi; Bederina, 2020), and the utilization of cocoa agro-industrial waste (Veloso *et al.*, 2021). In the context of partition systems, drywall is a frequent choice for environments requiring high acoustic performance, often incorporating additives like expanded polystyrene and fibers (Gypsum S/A, 2021).

This work investigates the development of gypsum composites reinforced with polypropylene microfibers and recycled rubber aggregates, utilizing a statistical experimental design to optimize their properties. The novelty of this approach lies in the integrated analysis of rubber morphology and surface chemistry, correlating the "encapsulation effect" identified via microscopy with sound absorption limitations. Additionally, the study proposes an innovative transition from an internal inclusion model to surface-mounted coating in functional prototypes, establishing technical guidelines for the industrial viability of sustainable, acoustically efficient gypsum boards.

4.2 Material and method

4.2.1 Material

The primary materials utilized in this study consist of commercial gypsum, recycled tire rubber aggregates, and polypropylene microfibers. The rubber waste, originally available in particle sizes up to 100mm, was processed to pass through a 2.36 mm sieve following NBR NM 248. Prior to mixture production, the crushed rubber was oven-dried at 105 +/- 5 degrees Celsius, homogenized, and separated into specific granulometric fractions: 2400, 1200, 600, 300, and 150 micrometers. The reinforcement phase was composed of 12 mm polypropylene microfibers provided by Maccaferri.

Characterization of the precursors and the resulting composites was conducted through a multi-laboratory protocol involving UFV, UFOP, and COPPE/UFRJ. The physical profile was established via laser granulometry, while the specific gravity was determined using kerosene immersion to prevent rubber particle flotation, yielding values of 1.18 g/cm^3 for rubber and 2.61 g/cm^3 for gypsum.

To investigate the internal structure and chemical interactions, the study employed Scanning Electron Microscopy (SEM) for particle morphology and Fourier-Transform Infrared Spectroscopy (FTIR) for identifying chemical bonds. SEM imaging focused on identifying surface defects, roughness, and porosity in the rubber waste that could influence the interfacial transition zone.

The composites developed in this study consist of a gypsum matrix reinforced with varying contents of polypropylene microfibers and recycled tire rubber aggregates. The production followed a Central Composite Design (CCD), resulting in 15 distinct mixtures with rubber particle sizes ranging from 150 to 2400 micrometers, residue contents from 0% to 40%, and fiber concentrations from 0 to 1200 g/m^3. These combinations were processed maintaining a constant water-to-gypsum ratio of 0.60 to evaluate how the interaction between the fibrous reinforcement and the elastomeric waste influences the mechanical properties, structural integrity, and sound absorption capacity of the final material.

4.2.2 Production of specimens and casting procedures

The specimens were produced based on experimental design combinations. Gypsum paste preparation followed NBR 12128 (Associação Brasileira de Normas Técnicas – ABNT, 2019): the gypsum powder was sprinkled over water for 1 minute, left to rest for another minute, and then manually homogenized for 1 minute to obtain a lump-free paste. The water-to-gypsum ratio was maintained constant at 0.60 for all mixtures. The rubber particles used were those retained on 2.40, 1.20, 0.60, 0.30, and 0.15 mm sieves, with polypropylene fiber contents ranging from 0 to 1200 g/m^3 (Table 4-1).

Cylindrical specimens ∅50x100 mm) were cast for physical properties; prismatic specimens (40 x 40 x 160 mm) for mechanical strength; and cylindrical discs (∅43x12,5 mm) for acoustic characterization. The acoustic molds were designed using SketchUp and fabricated via 3D printing (Prusa Mini+) using PETG filament to ensure the required flat and homogeneous surface according to ISO 10534-2 (International Organization for Standardization – ISO, 2023).

Table 4-1 – Experimental design for gypsum-rubber mixtures

Mixture ID	Rubber particle size range (µm)	Rubber content (% by mass of gypsum)	Fiber content (g/m^3)
B00F06	-	0	600
300B10F03	300	10	300
300B10F09	300	10	900
1200B10F03	1200	10	300
1200B10F09	1200	10	900
150B20F06	150	20	600
600B20F00	600	20	0
600B20F06	600	20	600
600B20F12	600	20	1200
2400B20F06	2400	20	600
300B30F03	300	30	300
300B30F09	300	30	900
1200B30F03	1200	30	300
1200B30F09	1200	30	900
600B40F06	600	40	600

4.2.3 Mechanical characterization

Mechanical characterization was performed through flexural and compressive strength tests conducted on prismatic specimens. These procedures followed the standardized guidelines of NBR 13207 (ABNT, 2017a) for gypsum, along with NBR 5739 (ABNT, 2018) for compression and NBR 7222 (ABNT, 2011) for tension in bending. To ensure stable results in the hardened state, all tests were executed after the completion of the required curing and drying periods. The comprehensive experimental sequence, ranging from the production to the evaluation of the gypsum-rubber-fiber composites, is illustrated in Figure 4-1.

Figure 4-1 – Preparation and mechanical testing of gypsum-rubber-fiber composite specimens: (a) prismatic and cylindrical molds used for casting; (b) demolded cylindrical and prismatic specimens after curing; (c) flexural strength test setup; (d) prismatic specime

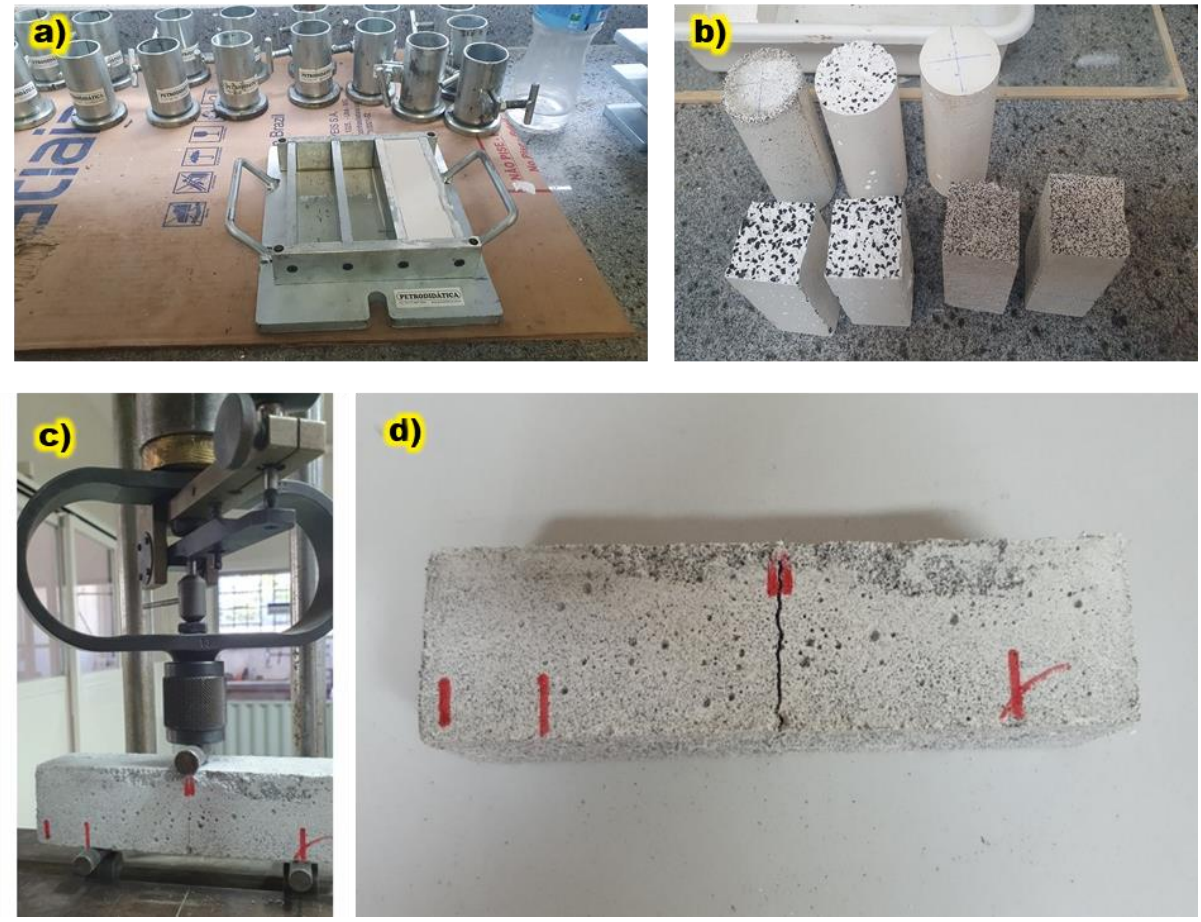

4.2.4 Ultrasonic Pulse Velocity (UPV) testing

According to Pinto and Akasaki (2016), Ultrasonic Pulse Velocity (UPV) is a non-destructive method used to correlate wave propagation speed with the material's internal properties, such as density and the presence of micro-cracks. In this study, the UPV was measured to evaluate the internal compactness and the damping effect of the rubber particles within the gypsum matrix. The elastomeric particles significantly dampen acoustic energy and delay wave propagation compared to a pure gypsum matrix.

For each composite, four cylindrical specimens were tested at 7 days of age. Measurements were performed using a Proceq Pundit Lab device with longitudinal P-waves at a frequency of 54 kHz, following the guidelines of ASTM C597 (Advancing Standards

Transforming Markets – ASTM, 2022) (Figure 4-2). This characterization provides a direct correlation with the composite's internal density and acoustic damping potential.

Figure 4-2 – Ultrasonic Pulse Velocity (UPV) setup: (a) Proceq Pundit Lab equipment; (b) UPV test being performed on a cylindrical gypsum-rubber specimen

4.2.5 Experimental design and statistical analysis

The experimental campaign was structured using a Central Composite Design (CCD) to evaluate the influence of composition parameters on the gypsum-rubber composite's performance and to determine optimal values. The variables investigated included the rubber aggregate particle size (ranging from 150 to 2400 mm), rubber content (0% to 40% by mass of gypsum), and fiber content (0 to 1200 g/m^3).

Statistical significance was assessed using p-values, and a desirability function approach was employed to evaluate the treatments' effects on the technological properties of the composites. Response Surface Methodology (RSM) was used to statistically model the relationship between the process variables and the primary response outputs.

For each experimental point defined in the design (Table 4-1), two replicates were performed, with the results reported as the average of three individual measurements per determination. This design ensured a comprehensive mapping of the interactions between rubber granulometry and reinforcement of fiber content within the gypsum matrix.

4.2.4 Acoustic characterization

The acoustic characterization of the composites was conducted through the determination of the sound absorption coefficient (a) using a four-microphone impedance tube at the Acoustics and Vibration Laboratory (LAVI – COPPE/UFRJ) Figure 4-3. This experimental setup was designed in accordance with the technical requirements established by ASTM E1050 (ASTM, 2019) and ISO 10534-2 (ISO, 2023). The measurement system comprised a white noise generator with a 20 kHz range, a power amplifier, 1/4" microphones, and a National Instruments 9234 acquisition board, all controlled via a dedicated LabVIEW 2017 interface.

Figure 4-3 – Impedance tube system used for sound absorption coefficient determination

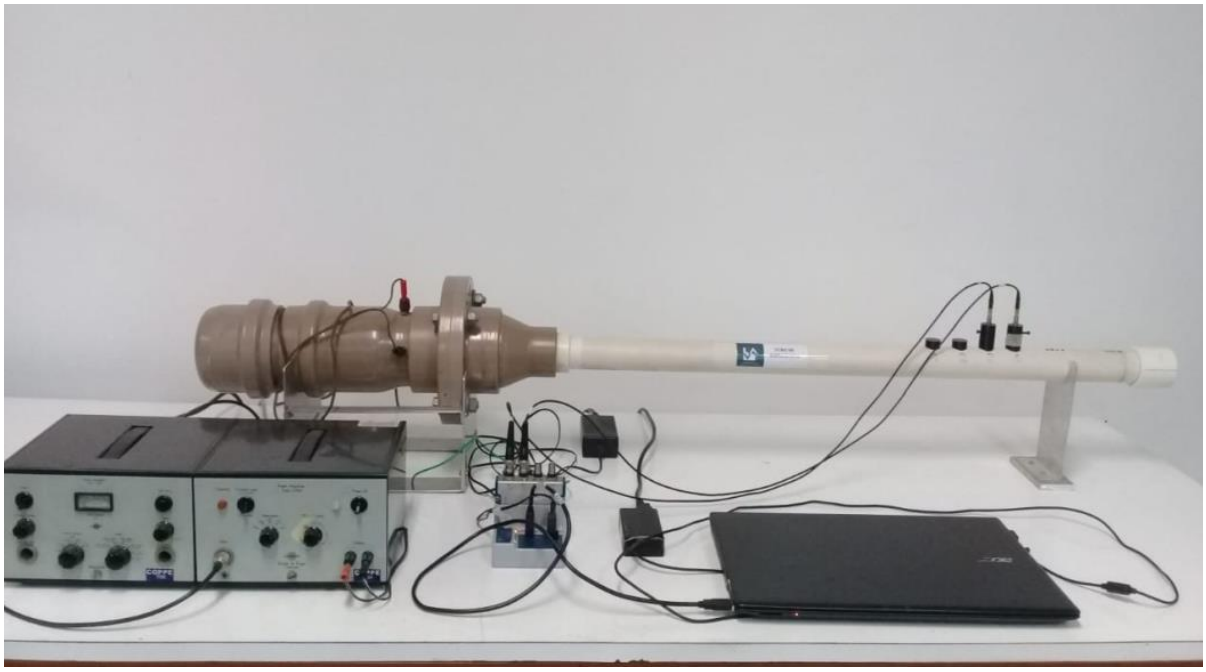

The acoustic evaluation of the 15 experimental mixtures was conducted across a broad frequency spectrum, covering the 100 Hz to 3400 Hz range. For each specific mixture, two

specimens were tested to account for material variability, with three distinct measurements performed per specimen utilizing microphone pairs 1-2, 2-3, and 3-4.

The preparation of these specimens involved the use of 3D-printed molds to ensure surface homogeneity, a controlled curing period, and final finishing before characterization, as illustrated in Figure 4-4. The final absorption coefficient (a) for each 1/3 octave frequency band, ranging from 100 to 3150 Hz, was calculated as the average of these six individual measurements.

Figure 4-4 – Fabrication and preparation of acoustic specimens: (a) 3D-printed molds designed for impedance tube compatibility; (b) acoustic specimens during the curing process; (c) final specimens after demolding, showcasing surface homogeneity; (d) set of specim

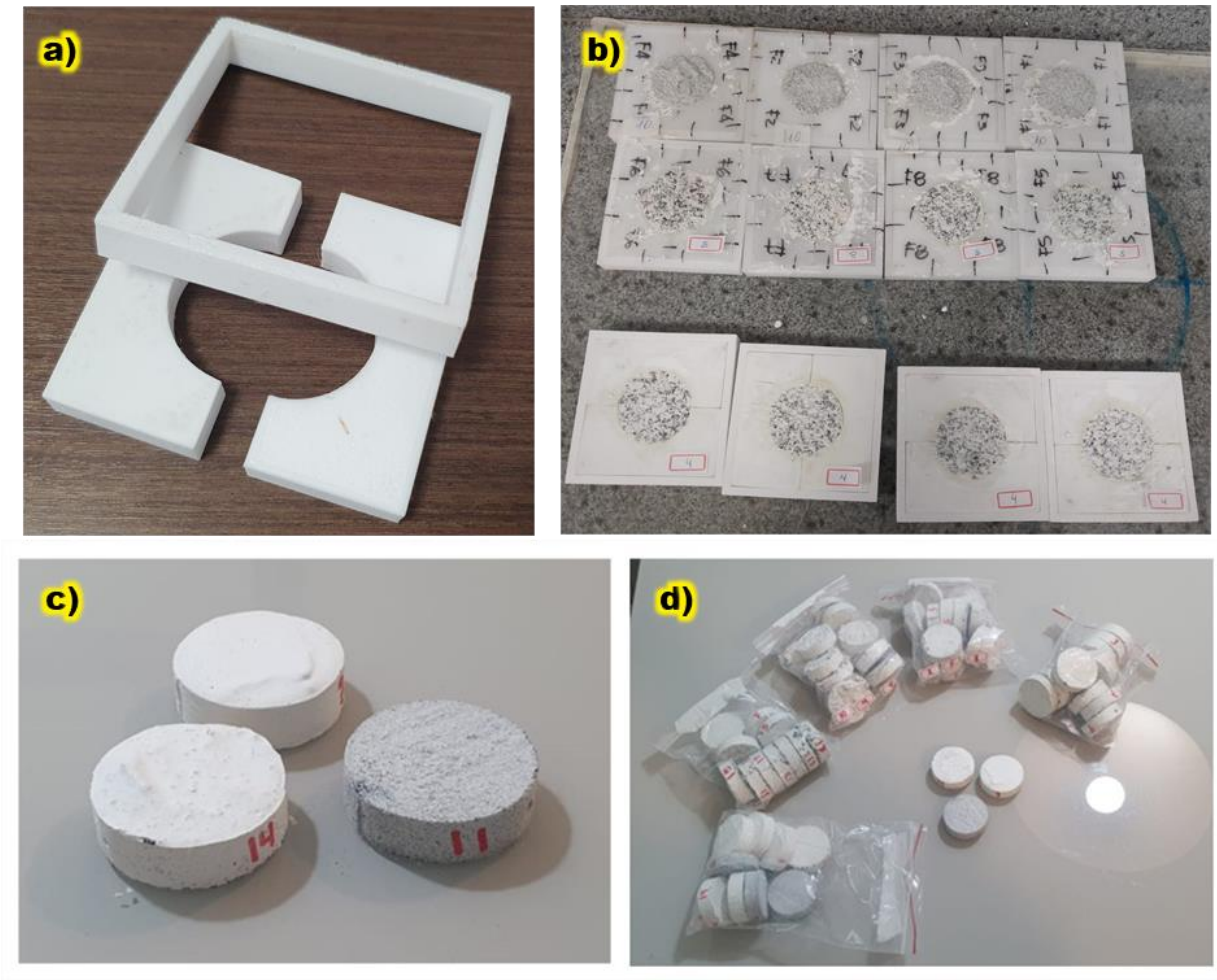

4.3 Results and discussion

4.3.1 Surface and morphological analysis of crushed rubber aggregates

The morphological characterization of the rubber waste was performed using a LEO 1430VP Scanning Electron Microscope (SEM) equipped with Energy Dispersive X-ray Spectroscopy (EDS) at the Nucleus of Microscopy and Microanalysis (NMM/UFV).

The analysis provided detailed information regarding the particle morphology (Figure 4-5). Particles passing through and retained on the 0.15 mm, 0.30 mm, and 0.60 mm sieves were examined. The crushed tire rubber crumbs exhibit an irregular aspect, varying from spherical to prismatic and elongated shapes. Small pores, surface roughness, and clefts or tears resulting from the crushing process are evident across the samples.

High-magnification micrographs (3000x and 5000x) revealed significant surface porosity and roughness. At lower magnifications (500x and 1000x), a negligible amount of tire fibers was identified among the rubber particles. SEM imaging further identified specific surface defects, such as cracks and chips, particularly in the coarser fractions (0.60 mm).

The irregular shapes and significant surface roughness identified via SEM are critical factors in the mechanical and acoustic behavior of the final composite. While high surface roughness typically aids mechanical interlocking, the presence of surface defects like clefts, cracks, and chips—especially in the 0.60 mm coarser fractions—acts as points of stress concentration that contribute to the decline in compressive and flexural strength observed in the results.

Furthermore, the "small pores" and "surface porosity" observed at 5000x magnification represent the potential acoustic pathways for sound dissipation. However, as noted in the acoustic results, these microscopic pores were likely sealed by the gypsum paste during the mixing process—the "encapsulation effect". This physical blockage prevents sound waves from entering the rubber's internal structure to convert acoustic energy into heat, explaining why internal rubber inclusion favored vibration damping over airborne sound absorption. The identification of negligible tire fibers also ensures that the reinforcement effects discussed later are primarily attributable to the added polypropylene microfibers rather than residual waste components.

Figure 4-5 – SEM micrographs of crushed tire rubber particles: (a) particles retained on 0.30 mm sieve (30x); (b) particles retained on 0.60 mm sieve (30x); (c) surface porosity of particles passing through 0.15 mm sieve (5000x); (d), (e) and f) surface porosity of particles; (g) Chips resulting from cutting during shredding; (h) Roughness.

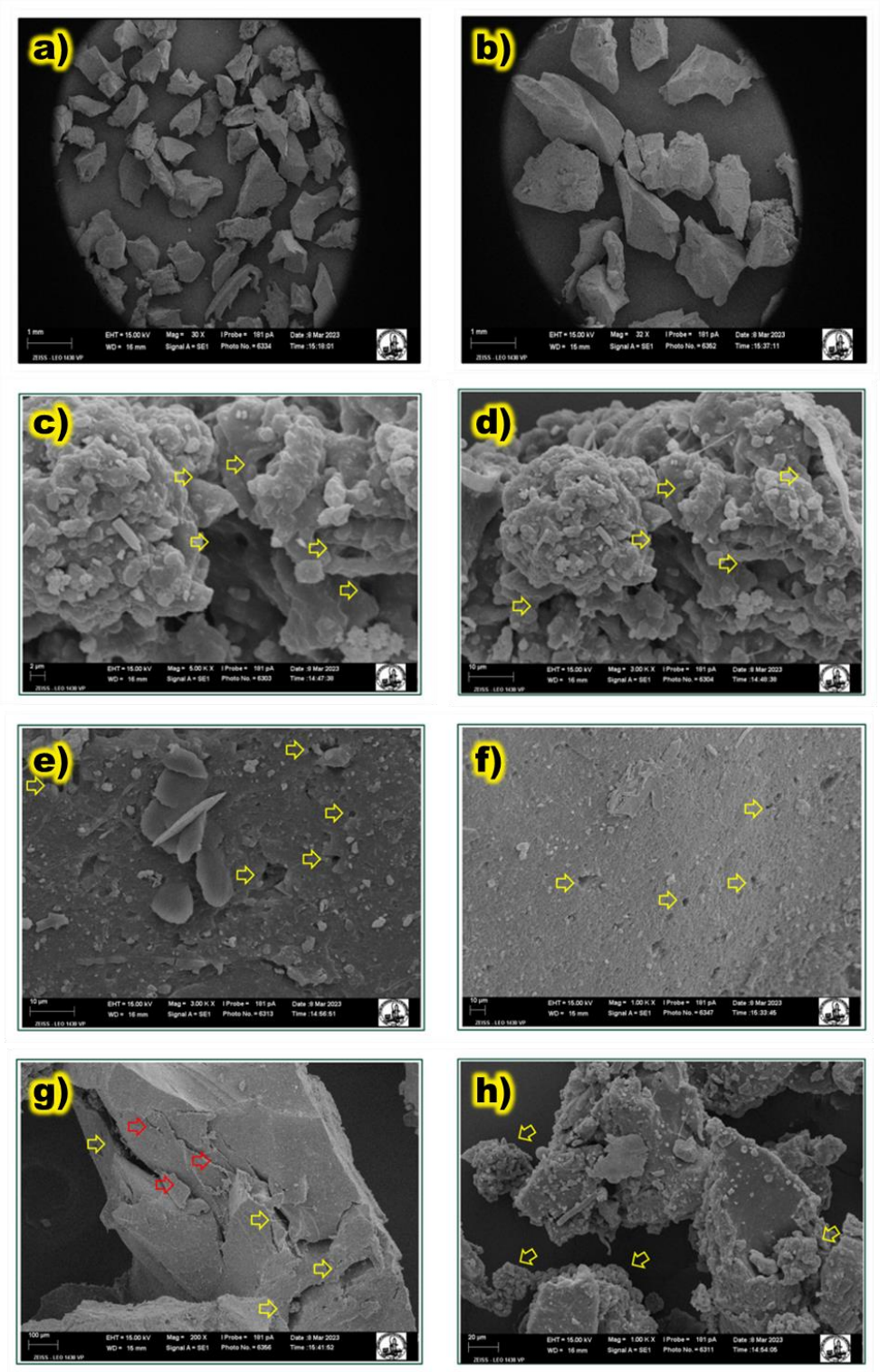

High-magnification micrographs (3000x and 5000x) revealed significant surface porosity and roughness. At lower magnifications (500x and 1000x), a negligible amount of tire fibers was identified among the rubber particles. SEM imaging further identified specific surface defects, such as cracks and chips, particularly in the coarser fractions (0.60 mm).

The irregular shapes and significant surface roughness identified via SEM are critical factors in the mechanical and acoustic behavior of the final composite. While high surface roughness typically aids mechanical interlocking, the presence of surface defects like clefts, cracks, and chips—especially in the 0.60 mm coarser fractions—acts as points of stress concentration that contribute to the decline in compressive and flexural strength observed in the results.

Furthermore, the "small pores" and "surface porosity" observed at 5000x magnification represent the potential acoustic pathways for sound dissipation. However, as noted in the acoustic results, these microscopic pores were likely sealed by the gypsum paste during the mixing process—the "encapsulation effect". This physical blockage prevents sound waves from entering the rubber's internal structure to convert acoustic energy into heat, explaining why internal rubber inclusion favored vibration damping over airborne sound absorption. The identification of negligible tire fibers also ensures that the reinforcement effects discussed later are primarily attributable to the added polypropylene microfibers rather than residual waste components.

4.3.2 Chemical characterization by Fourier Transform Infrared Spectroscopy (FTIR)

Chemical characterization by FTIR identified the chemical bonds of the rubber used in this research. Analysis was performed by the Ative Research Group at the Civil Construction Laboratory (UFOP) using a Thermo Scientific Nicolet iS5 spectrometer equipped with an iD1 transmission module (32 scans, 4 cm^{-1} resolution, Mid-Infrared region - MIR, 400 to 4000 cm^{-1}). The resulting FTIR spectrum of the crushed tire rubber is presented in Figure 4-6.

The FTIR spectrum of the crushed tire rubber reveals a complex composition (Table 4-2), dominated by an unsaturated rubber blend, primarily consisting of Styrene-Butadiene Rubber (SBR) and Natural Rubber (NR), which serves as the main polymeric base. The analysis further identifies various oxygenated additives typical of tire formulations, such as plasticizers, oils, and resins containing ester or ether groups, as evidenced by the absorption bands located between 1300 and 1000 cm^{-1}. Additionally, the presence of aromatics related to the SBR and styrene components is confirmed by specific spectral signals at 778 and 692 cm^{-1}.

Figure 4-6 – FTIR spectrum of crushed tire rubber particles

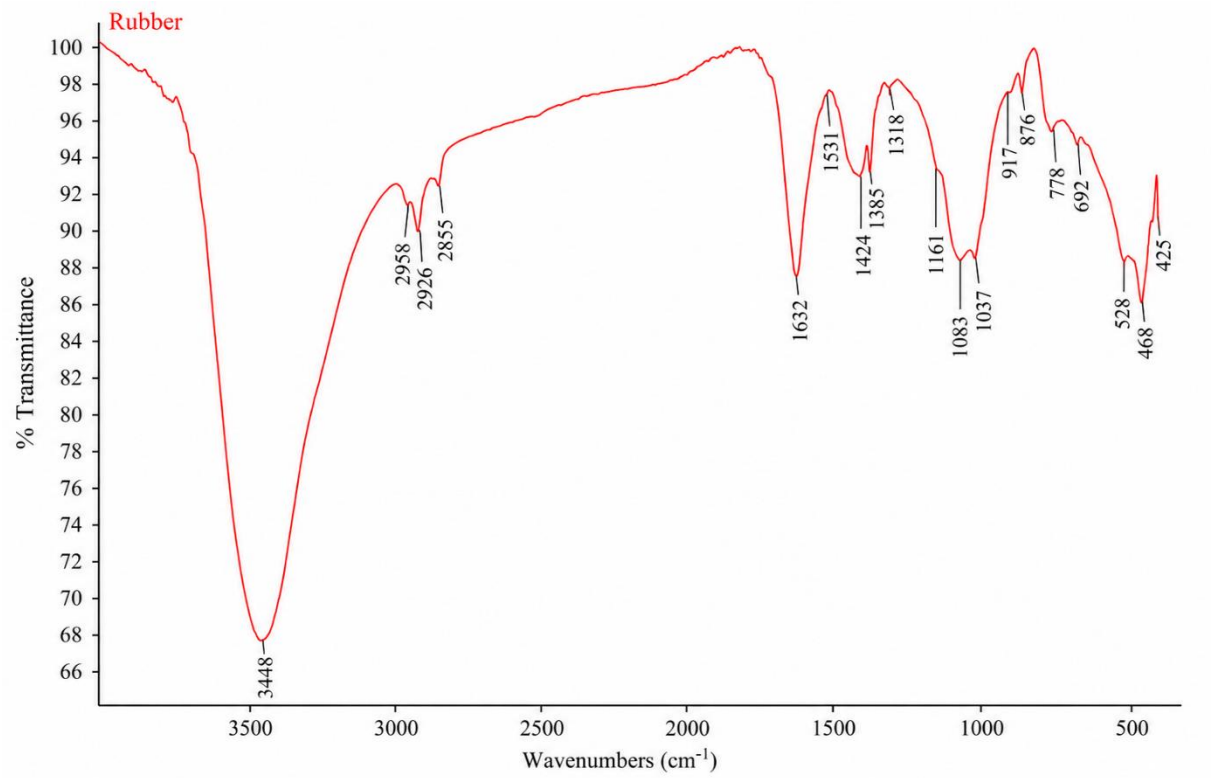

Table 4-2 – Functional groups and absorption peaks

Wavenumber (cm^{-1})	Appearance	Functional group	Compound class	Probable substance	Comments
3448	Strong, Broad	O-H Stretching	Alcohol	Resins	O-H stretching region, indicating alcohols or phenols.
3448	Medium	N-H Stretching	Aliphatic Primary Amine	-	-
2958	Medium	C-H Stretching	Alkane	Carbon Black	Aliphatic C-H stretching region, suggesting saturated hydrocarbons.
2958	Strong, Broad	N-H Stretching	Amine Salt	-	-
2926	Medium	C-H Stretching	Alkane	Carbon Black	Aliphatic C-H stretching region.
2926	Strong, Broad	N-H Stretching	Amine Salt	-	-
2855	Strong, Broad	N-H Stretching	Amine Salt	Anti-aging agents	Aliphatic C-H stretching region.
2855	Medium	C-H Stretching	Alkane	-	-
1632	-	C=O Stretching	Conjugated Aldehydes	-	-
1632	Medium	C=C Stretching	Conjugated Alkenes	-	Peak in the C=C vibration region in alkenes.
1632	Medium	C=C Stretching	Cyclic Alkenes	-	-
1531	Strong	N-O Stretching	Nitro Compound	Anti-aging agents	Peak in the C=C stretching region of aromatic rings.
1424	Medium	O-H Bending	Carboxylic Acid	Nylon	Associated with CH2 angular bending.
1385	Medium	O-H Bending	Phenol	-	Present in C-N bonds.
1318	Strong	C-N Stretching	Aromatic Amine	Vulcanized Rubber	Related to C-H bonds in R2-C=H alkenes.
1318	Strong	S=O Stretching	Sulfone	Carbon Black	-
1161	Strong	C-O Stretching	Tertiary Alcohol	-	Angular bending in C-H bonds.
1083	Strong	C-O Stretching	Primary Alcohol	-	Associated with C-O stretching.
1037	Strong	S=O Stretching	Sulfoxide	-	Aliphatic C-H stretching region.
1037	Strong	S=O Stretching	Sulfone	-	-
917	-	-	-	-	Peak in the C-C stretching region.
876	-	Buta-1,3-diene	Synthetic Rubber	Buna S / Natural Rubber	-
876	-	C=C Bending	Vinylidene Alkene	Natural Rubber	Related to hydrogen bonds.
778	Strong	C-Cl Stretching	Halogenated Compounds	Butyl Rubber	Associated with C-H bonds in substituents.
692	-	-	-	-	Vibration in C-Cl bonds.
528	-	-	-	-	Vibration in S-H bonds.
468	-	-	-	-	Associated with C-S bonds.
425	-	-	-	-	Related to C-Br bonds.

Further investigation into the lower wavenumber regions, specifically between 528 and 425 cm^{-1}, suggests potential halogenated contributions. These signals may indicate traces of halogenated rubbers, such as flame retardants, or PVC residues from additives and blends like PVC, BIIR, or BIMS.

In summary, the characterization confirms the presence of natural rubber, butyl rubber, carbon black, polyester, resins, and vulcanized rubber, alongside anti-aging agents and other minor chemical products. This chemical profile represents a typical recycled tire mixture and remains consistent with standard industrial tire formulations.

This chemical composition provides a molecular explanation for the poor mechanical performance seen in the high-volume rubber mixtures. The lack of reactive polar groups means the rubber particles do not chemically bond with the hydrophilic gypsum paste. Instead, the particles act as inert physical inclusions, where the presence of substances like vulcanized rubber (1318 cm^{-1}) and halogenated compounds (778 cm^{-1}) ensures a stable but non-cohesive interface with the matrix.

4.3.3 Thermal characterization – Loss on Ignition (LOI)

The Loss on Ignition (LOI) test was performed on the rubber particles to evaluate mass loss and degradation when exposed to high temperatures. The procedure followed ISO 247-1 (ISO, 2018), which specifies methods for determining ash content in raw, vulcanized, and compounded rubber. Particles retained on a 0.60 mm sieve were subjected to two methods: Method A at 550°C and Method B at 950°C.

The experimental data indicate that the rubber waste underwent significant mass reduction when subjected to high-temperature oxidative conditions. In Method A (550°C), the incomplete combustion observed in the lower layers suggests that the material possesses high thermal inertia and a dense packing factor, which hindered oxygen diffusion and heat transfer. This behavior is typical of vulcanized rubber compounds containing high concentrations of carbon black and inorganic fillers, which require higher temperatures or longer residence times for full oxidation.

Under the more aggressive conditions of Method B (950°C), total degradation of the organic fraction was achieved. The resulting byproducts, representing the residual ash content, showed no traces of the original black color, indicating the complete oxidation of the carbonaceous matrix. The final mass of the byproducts for all samples (M1 through M4)

remained remarkably consistent, with an average ash content representing approximately 95% of the initial mass in this specific test setup.

The diverse coloration of the ashes—comprising shades of green, white, blue, and gray—confirms the presence of various inorganic additives and metallic oxides (Figure 4-7). These findings suggest the presence of zinc oxide (ZnO), calcium carbonates, and other mineral fillers commonly used in tire manufacturing to improve mechanical properties and durability. The stability of the byproduct mass across different particle sizes (0.15 mm and 0.60 mm) indicates that the inorganic filler distribution is homogeneous throughout the waste material, regardless of the grinding scale.

Figure 4-7 – Byproducts of crushed tire rubber after Loss on Ignition (LOI) testing: (a) crucible containing sample M1; (b) crucible containing sample M2; (c) crucible containing sample M3; (d) crucible containing sample M4; (e) detailed view of M2 byproduct highl

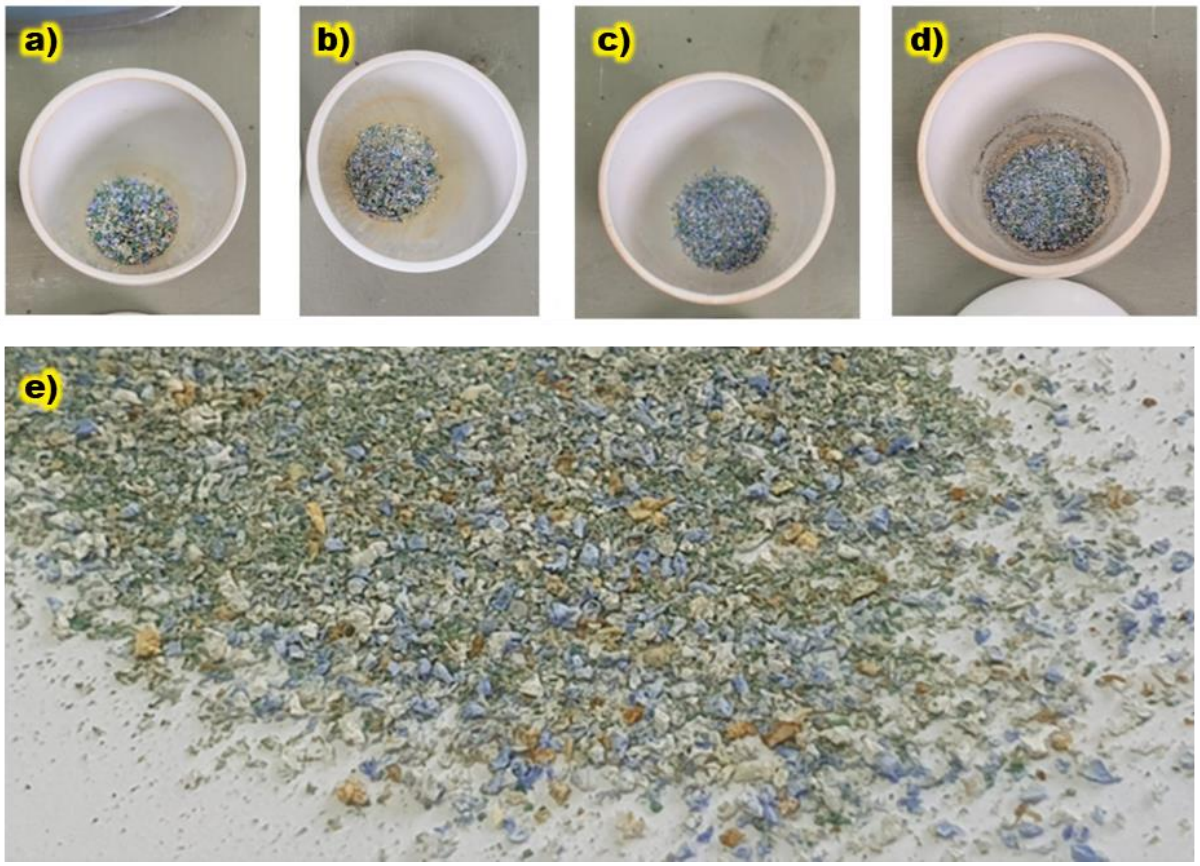

The high thermal inertia and incomplete combustion at 550°C confirm the presence of a stable, cross-linked polymeric structure reinforced with carbon black. This carbonaceous matrix, identified as a blend of SBR and Natural Rubber in the FTIR analysis, contributes to

the overall stability of the aggregates but also reinforces their chemical inertness during the gypsum hydration process. The significant organic degradation observed at 950°C isolates the inorganic fraction, revealing a consistent distribution of fillers that do not vary with the grinding scale.

The diverse coloration of the residual ash confirms the inclusion of various inorganic additives, such as zinc oxide and calcium carbonate, which are traditionally used in tire manufacturing to enhance durability. In the context of the developed composites, these mineral fillers and the carbon black matrix explain the significant density mismatch previously noted between the rubber (1.18 g/cm³) and the gypsum (2.61 g/cm³). Furthermore, while these inorganic components are homogeneous throughout the waste, their presence on the surface of the aggregates—as seen in the SEM micrographs—likely contributes to the low chemical affinity between the hydrophobic rubber and the hydrophilic gypsum, ultimately leading to the "encapsulation effect" and reduced mechanical adhesion discussed in the acoustic and strength results.

4.3.4 Mineralogical characterization (XRD)

X-ray Diffraction (XRD) was employed to determine the crystalline structure and identify inorganic fillers or additives within the rubber waste. The analysis was conducted at the Physics Department (DPF/UFV) using a D8 Discover diffractometer with Cu-Ka radiation (l = 1.5418 Å). Scanning was performed in the 2q range from 3° to 70°, with an increment of 0.05° and a scan speed of 1.00 step/second.

The XRD pattern (Figure 4-8) confirms that the crushed tire rubber is predominantly an amorphous material. This is characterized by the absence of sharp, well-defined diffraction peaks, replaced instead by a broad "halo" typical of disordered polymeric structures. In vulcanized rubber, the long polymer chains are cross-linked but remain randomly arranged, preventing the formation of a long-range crystalline lattice. This amorphous nature is intrinsically linked to the material's elastomeric properties, allowing for molecular mobility and elastic recovery under mechanical stress. Any minor reflections observed within the amorphous background are attributed to the presence of inorganic crystalline fillers.

Figure 4-8 – X-ray diffraction (XRD) pattern of crushed tire rubber

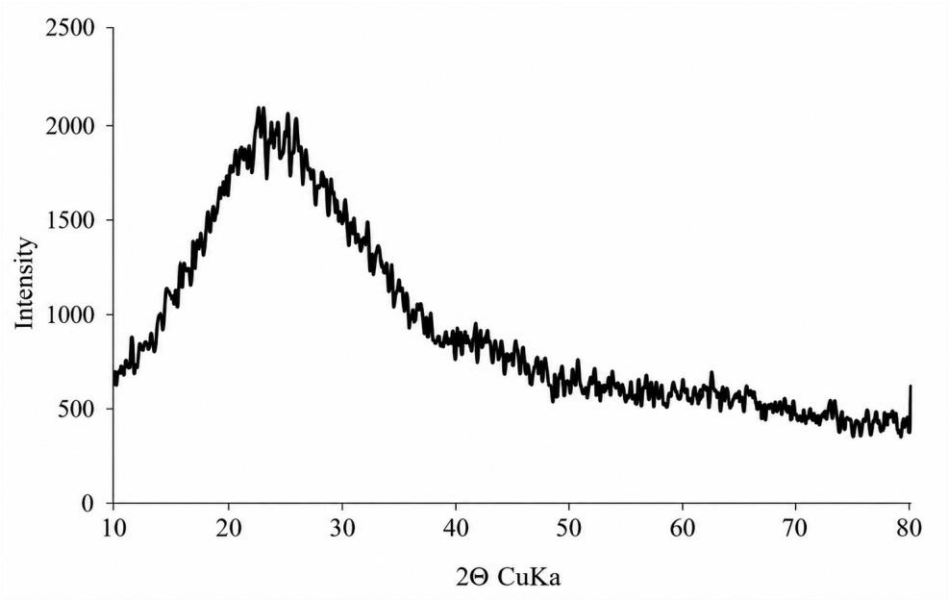

The predominantly amorphous nature of the rubber aggregates, evidenced by the broad diffraction halo centered between 2q = 20° and 25°, provides a structural explanation for the "damping effect" observed in the Ultrasonic Pulse Velocity (UPV) results. Unlike the highly crystalline and rigid structure of the gypsum matrix, the disordered polymeric chains of the rubber waste act as energy dissipators. This disordered arrangement facilitates micro-deformations when the composite is subjected to sound waves, effectively converting acoustic energy into low-grade heat through internal friction.

Furthermore, the minor reflections identified within the amorphous background correspond to the inorganic crystalline additives—such as zinc oxide and calcium carbonate—previously detected in the FTIR and Loss on Ignition (LOI) analyses. While these crystalline fillers improve the individual durability and mechanical properties of the tire rubber itself, their lack of chemical affinity with the mineral gypsum matrix contributes to the formation of fragile Interfacial Transition Zones (ITZ). This amorphous-crystalline mismatch between the elastomeric reinforcement and the rigid matrix is a primary driver for the mechanical strength reduction observed as the rubber-to-total-solids ratio increases.

4.3.5 Physical characterization: density and particle size distribution

Specific gravity was determined following NBR 16605 (ABNT, 2017b). For both the crushed tire rubber and the gypsum, water was replaced by kerosene as the immersion fluid. This substitution was necessary because rubber has a lower density than water, which would

cause particle flotation and invalidate the displacement measurements in the Chapman flask. The tests yielded specific gravity values of 1.18 g/cm³ for the rubber waste and 2.61 g/cm³ for the gypsum. Additionally, the loose unit mass was measured according to NBR NM 45 (ABNT, 2006).

The physical data reveal a significant density mismatch between the reinforcement (rubber) and the matrix (gypsum), with the gypsum being approximately 2.2 times denser than the waste. This difference suggests that, for the same mass, the rubber will occupy a substantially larger volume, which directly influences the density and thermal-acoustic properties of the final composite.

The particle size distribution was characterized through the sieving of a 500 g rubber sample, following NBR NM 248 (ABNT, 2003) and NBR NM ISO 3310-1 (ABNT, 2010). Although commercial rubber waste is available in sizes ranging from 0.60 mm to 100.00 mm, this study focused on particles passing through the 2.36 mm sieve. The experimental results indicated that 53.56% of the mass was retained on the 1.18 mm sieve, while 33.53% was retained on the 0.60 mm sieve. Smaller fractions included 10.09% on the 0.30 mm sieve and only 0.49% on the 0.15 mm sieve, with less than 1% of the material passing through the finest mesh (Figure 4-9).

Figure 4-9 – Particle size distribution curve of the crushed tire rubber waste

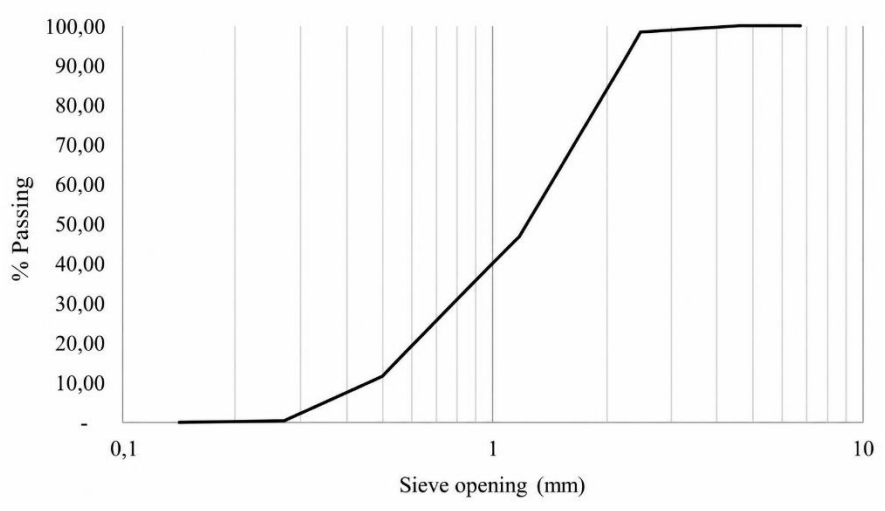

The high concentration of particles in the 0.60 mm to 1.18 mm range classifies the waste as a fine-to-medium aggregate. From a manufacturing standpoint, this distribution is optimal; the absence of coarse particles (above 2.40 mm) ensures that the boards can be cut or fastened without causing significant edge spalling or surface irregularities. Furthermore, the low

percentage of ultra-fine particles (below 0.15 mm) is beneficial, as excessive fines could compromise the mechanical strength of the hardened matrix.

4.3.6 Mechanical performance of gypsum-rubber composites

The mechanical characterization results for the developed composites, including flexural and compressive strengths, are summarized in Table 4-3. The reference mixture (B00F06), containing only fiber reinforcement without rubber aggregate, exhibited the highest performance, with a flexural strength of 2.06 MPa and compressive strength of 4.10 MPa. As the rubber content increased from 10% to 40%, a clear trend of reduction in mechanical properties was observed across all particle sizes.

The replacement of the rigid gypsum matrix with elastomeric rubber particles introduces significant points of stress concentration, directly accounting for the decline in mechanical performance. As noted by Pinto (2017) and Ferrández *et al.* (2025), this weakening effect is primarily attributed to the poor interfacial bonding between the hydrophobic rubber surfaces and the hydrophilic gypsum paste, leading to the formation of fragile Interfacial Transition Zones (ITZ).

Table 4-3 – Mechanical tests result of gypsum-rubber-fiber composites

Mixture ID	**Flexural strength [MPa]**	**Compressive strength [MPa]**
B00F06	2.06	4.10
300B10F03	1.48	2.41
300B10F09	1.40	3.00
1200B10F03	1.24	2.55
1200B10F09	1.20	3.06
150B20F06	1.20	2.15
600B20F00	1.04	2.17
600B20F06	1.00	2.25
600B20F12	1.21	2.09
2400B20F06	0.88	1.91
300B30F03	0.98	1.53
300B30F09	0.90	1.49
1200B30F03	0.64	1.60
1200B30F09	0.76	1.74
600B40F06	0.52	1.22

For instance, mixture 600B40F06, with the highest rubber content (40%), exhibited the lowest performance (0.52 MPa for flexure and 1.22 MPa for compression). According to Lozano-Díez *et al.* (2021), the low stiffness of the rubber compared to the mineral matrix, combined with its tendency to entrap air during mixing, results in increased overall porosity and the presence of micropores. Consequently, the combination of high porosity and weak interfacial adhesion prevents efficient stress transfer, significantly reducing both compressive and flexural strength as the rubber replacement level increases, a phenomenon also supported by Serna *et al.* (2012).

However, the influence of fiber content and rubber granulometry reveals a more complex interaction. While rubber reduces strength, the 12 mm polypropylene fibers mitigate the brittle nature of the matrix. The transition from 300 mm to 1200 mm in rubber size for the same rubber/fiber ratio (e.g., comparing 300B10F03 and 1200B10F03) suggests that coarser particles might lead to a more significant drop in flexural strength compared to finer aggregates. This is likely due to the larger ITZ areas created around coarser particles, which serve as preferential paths for crack propagation.

Based on the experimental data, mixture 300B10F09 (10% fine rubber at 300 mm and 900 g/m^3 of fibers) stands out with the best overall mechanical performance (3.00 MPa compression; 1.40 MPa flexure). The justification lies in the use of smaller diameter particles, which — as observed by Ferrández *et al.* (2025) — reduce ITZ thickness and minimize internal voids, while the high fiber content compensates for the tensile loss through a crack-bridging mechanism.

In an optimization scenario focused on acoustic insulation, mixture 600B20F12 (20% rubber at 600 mm and 1200 g/m^3 of fibers) emerges with the greatest technical balance. Despite having twice the waste load, it maintains a flexural strength of 1.21 MPa, exceeding the minimum requirement of 1.0 MPa for non-structural components. This is justified by the maximum fiber reinforcement "stitching" the matrix, ensuring residual ductility.

Finally, the analysis indicates that coarser particle sizes (600 mm to 1200 mm) become advantageous for high-volume incorporation (above 20%), as seen in 1200B30F09. In these cases, larger particles reduce the total hydrophobic surface area, preserving better matrix cohesion than a high dispersion of fine particles, provided the fiber reinforcement remains above 900 g/m^3.

4.3.7 Ultrasonic Pulse Velocity (UPV) results

The Ultrasonic Pulse Velocity (UPV) was measured to evaluate the internal compactness and the damping effect of the rubber particles within the gypsum matrix. The results for the 15 experimental mixtures are summarized in Table 4-4.

Table 4-4 – Results of Ultrasonic Pulse Velocity (UPV) testing

Mixture ID	Ultrasonic Pulse Velocity [m/s]
B00F06	2311
300B10F03	2470
300B10F09	2251
1200B10F03	2321
1200B10F09	2550
150B20F06	2190
600B20F00	2062
600B20F06	1521
600B20F12	2235
2400B20F06	2257
300B30F03	1709
300B30F09	1774
1200B30F03	1933
1200B30F09	1866
600B40F06	1551

The UPV values ranged from 1521 m/s to 2550 m/s, demonstrating a clear dependence on the composite's composition. In general, the inclusion of rubber particles leads to a reduction in velocity compared to the pure gypsum matrix, as elastomeric materials significantly dampen acoustic energy and delay wave propagation. This behavior is consistent with the findings of Pinto and Akasaki (2016), who highlighted that rubber's lower density and acoustic impedance interrupt the fast propagation typical of the dense, crystalline gypsum structure.

The influence of particle size is also evident. Fine granulometry (300 mm), due to its higher surface area and more extensive dispersion within the matrix, creates a larger number of interfaces that scatter the ultrasonic pulse, often resulting in lower velocities than those seen in mixtures with coarser aggregates (1200 mm) at the same replacement levels. For instance, comparing 1200B10F09 (2550 m/s) with 300B10F09 (2251 m/s) suggests that coarser particles may allow for more continuous "bridges" of gypsum matrix, facilitating faster wave travel.

Furthermore, the fiber content plays a secondary but relevant role. The slight decrease in UPV observed with increasing fiber addition (as seen when comparing mixtures with

different fiber loads) may be attributed to the introduction of micro-porosity at the fiber-matrix interface, as suggested by Macedo, Carneiro and Perlingeiro (2021). These air-filled voids act as barriers to the pulse, further contributing to the overall acoustic damping of the composite.

4.3.8 Statistical analysis and Response Surface Modeling (RSM)

The average mechanical strength results were modeled using Response Surface Methodology (RSM) to evaluate the interactions between the rubber/total solids (ST) ratio, rubber particle size, and polypropylene fiber content.

The response surfaces and corresponding contour plots for flexural strength are presented in Figure 4-10. The analysis of the rubber/ST ratio versus fiber content (Figure 4-10a) indicates that while fiber addition remains relatively constant in its influence, the resistance is predominantly governed by the rubber/ST ratio. Specifically, the flexural strength decreases from 1.20 MPa to less than 0.75 MPa as the rubber content increases. A similar trend is observed in the interaction between particle size and fiber (Figure 4-10b), where a marginal increase in strength is noted with higher fiber additions. Conversely, Figure 4-10c demonstrates that flexural strength tends to increase as the rubber particle size decreases.

The statistical significance of these factors is confirmed by the Pareto Diagram (Figure 4-11). Using a significance level of a = 0.05 (t-value = 2.23), it is evident that both the rubber/ST ratio and particle size significantly influence flexural strength. This is further corroborated by the Main Effects Plot (Figure 4-12), where the steep slopes for rubber content and particle size contrast with the nearly horizontal line for fiber content, indicating the latter's lower individual sensitivity within the tested range.

These findings align with Ferrández *et al.* (2025), who reported that flexural strength declines as recycled rubber content increases due to poor adhesion between the gypsum paste and rubber particles. Pinto (2017) attributes this reduction to a lack of interfacial bonding, which compromises material cohesion. Furthermore, the higher strength observed in composites with particles smaller than 0.8 mm compared to those with diameters between 2.0 and 4.0 mm is consistent with the results of Ferrández *et al.* (2025).

The response surfaces and contour plots for compressive strength are shown in Figure 4-13. Consistent with the flexural results, the rubber/ST ratio is the primary driver of strength reduction (Figure 4-13a). However, an interesting interaction appears between particle size and fiber content (Figure 4-13b), where compressive strength tends to increase for particle sizes near 0.6 mm when combined with fiber reinforcement.

Figure 4-10 – Response surfaces for average flexural tensile strength between (a) rubber/total solids ratio and fiber; (b) rubber residue particle size and polypropylene fiber; (c) rubber/total solids ratio and rubber residue particle size

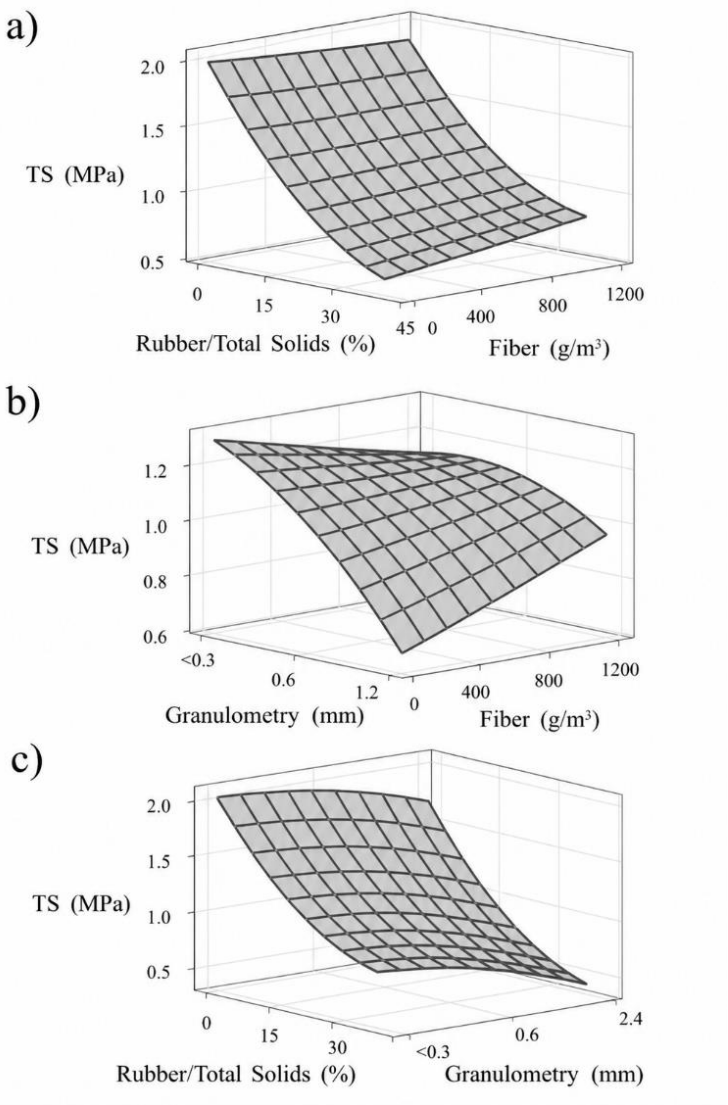

Figure 4-11 – Pareto chart for flexural strength

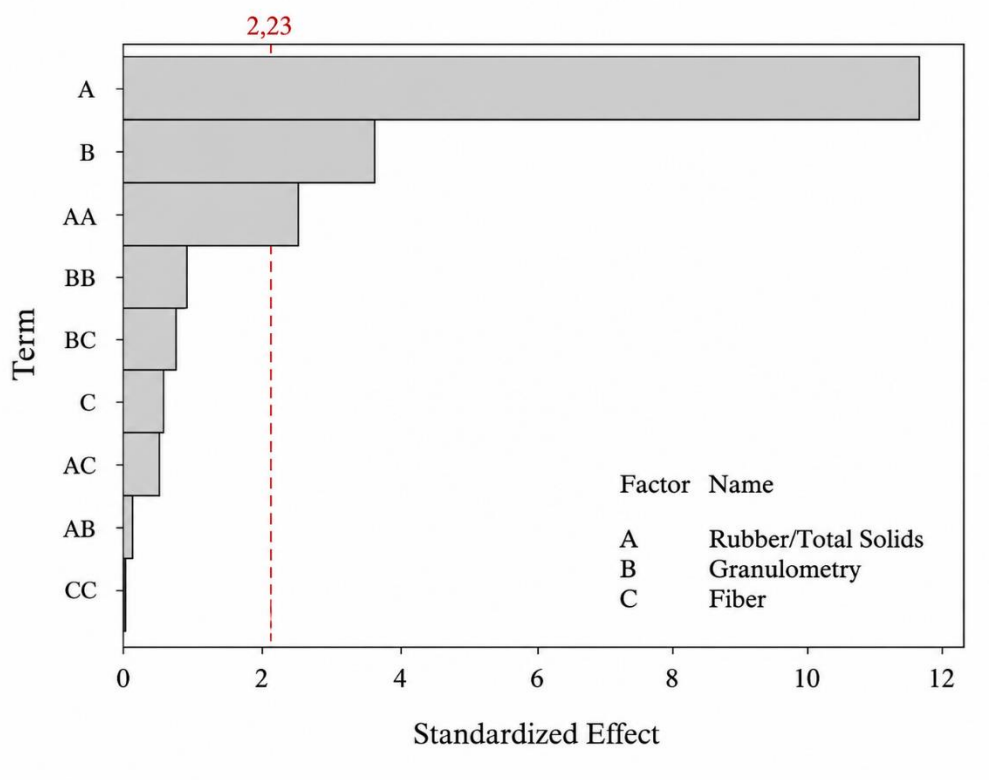

Figure 4-12 – Main effects plot of rubber residue particle size, rubber/total solids ratio, and polypropylene fiber on flexural tensile strength

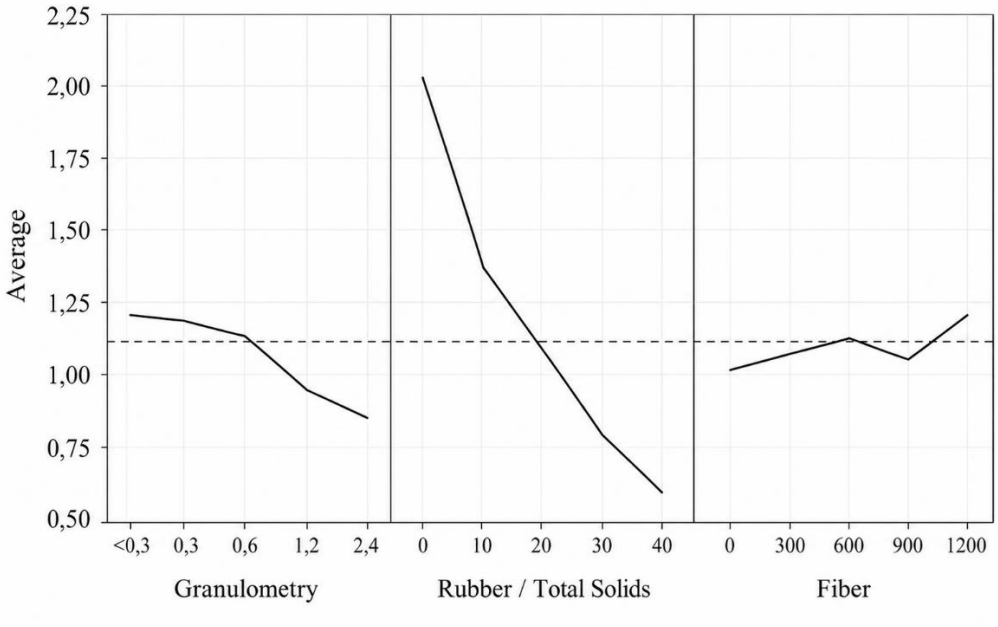

Figure 4-13 – Response surfaces for compressive strength between (a) rubber/total solids ratio and fiber; (b) rubber residue particle size and polypropylene fiber; (c) rubber/total solids ratio and rubber residue particle size

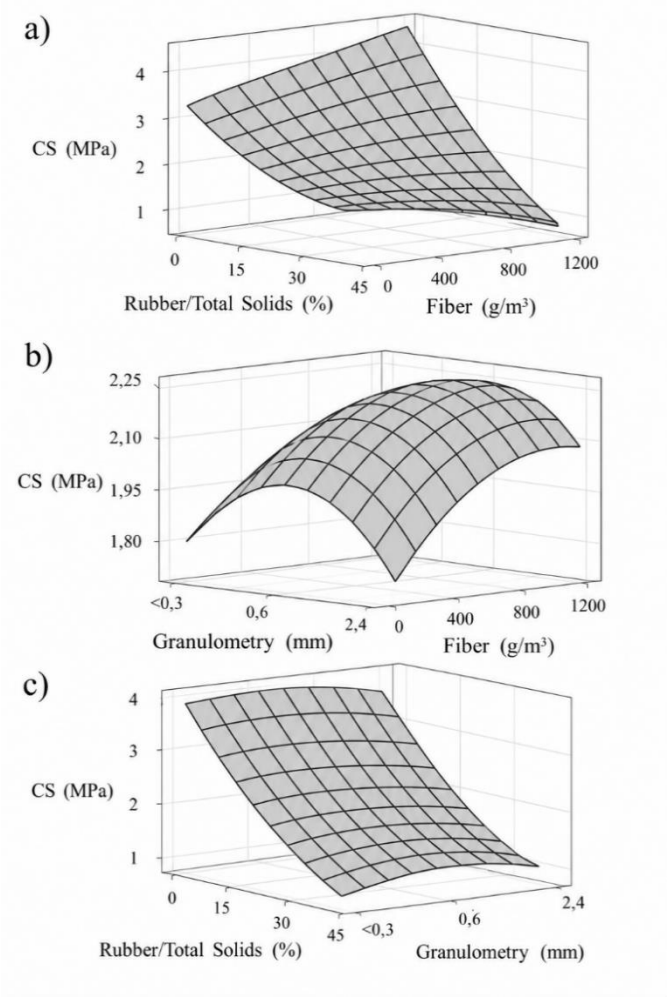

The Pareto Diagram for Compressive Strength (Figure 4-14) identifies the rubber/ST ratio as the only factor with high statistical significance ($t > 2.23$). The Main Effects Plot (Figure 4-15) confirms this, showing a significant slope for rubber content, while the slopes for particle size and fiber remain nearly constant.

The inverse relationship between rubber content and compressive strength is well-documented by Serna *et al.* (2012). Physically, Lozano-Díez *et al.* (2021) explain that although rubber particles bond to the gypsum, they effectively act as voids that interfere with the gypsum's crystalline structure. The presence of micropores around the rubber aggregates, as noted by the same authors, further disrupts the material's cohesion, leading to the observed mechanical decline.

Figure 4-14 – Pareto chart for compressive strength

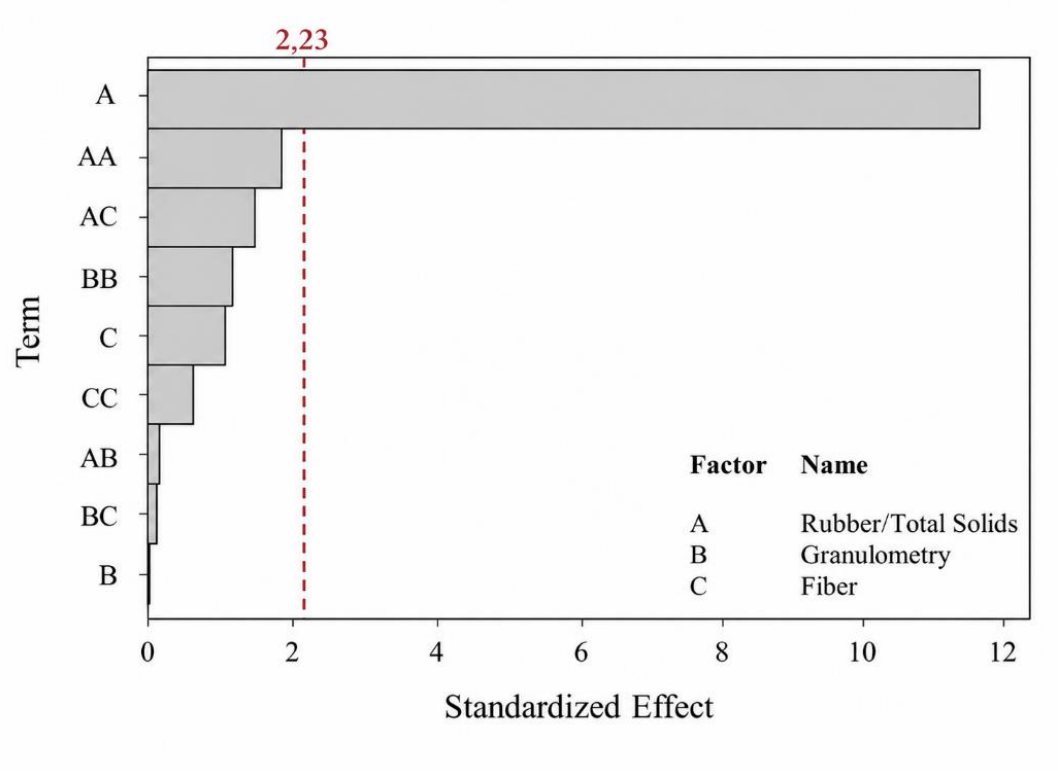

Figure 4-15 – Main effects plot of rubber residue particle size, rubber/total solids ratio, and polypropylene fiber on compressive strength

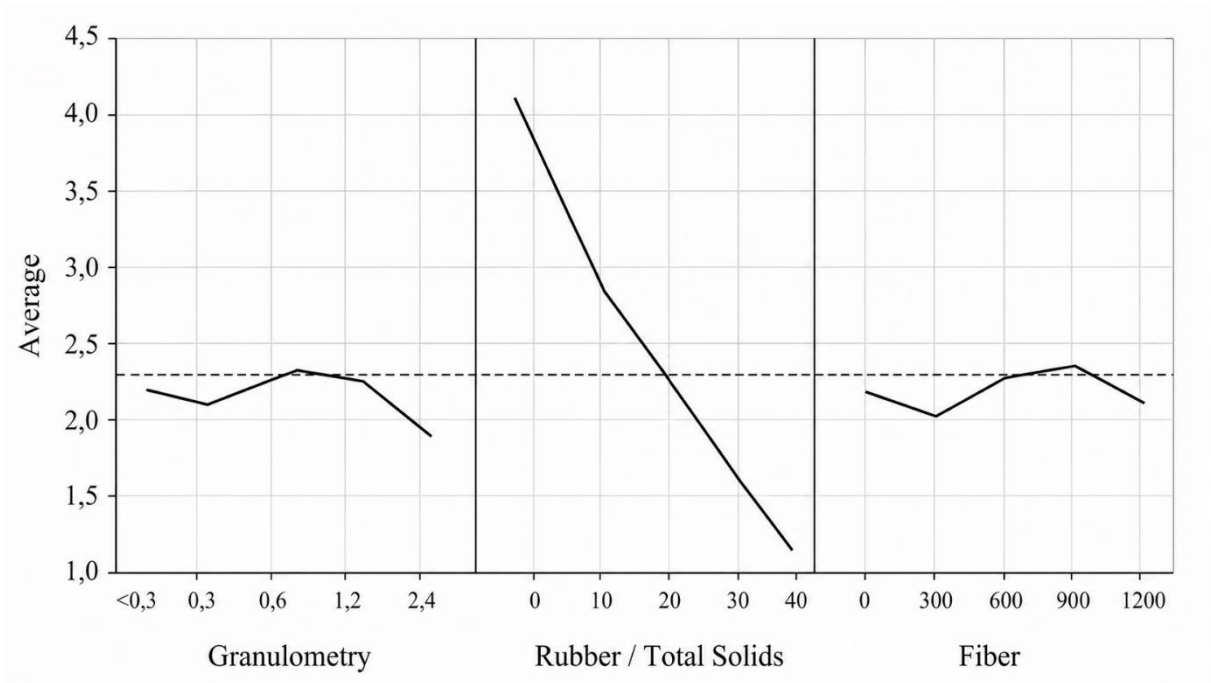

The non-destructive characterization through Ultrasonic Pulse Velocity (UPV) provides a direct correlation with the composite's internal density and acoustic damping potential. The response surfaces (Figure 4-16) indicate that UPV decreases as the rubber/ST ratio increases.

Figure 4-16 – Response surfaces for ultrasonic pulse velocity between (a) rubber/total solids ratio and fiber; (b) rubber residue particle size and polypropylene fiber; (c) rubber/total solids ratio and rubber residue particle size

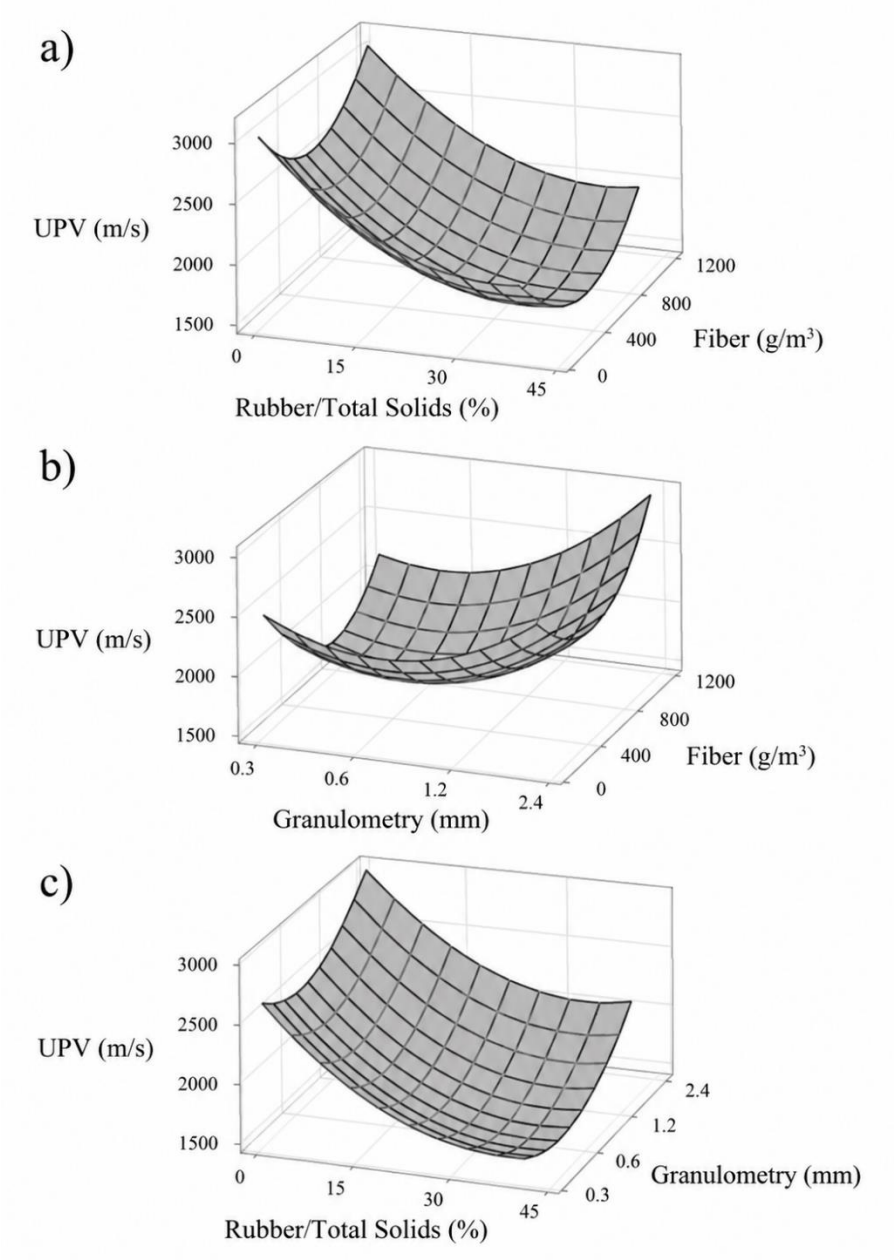

This phenomenon, also observed by Pinto and Akasaki (2016), occurs because rubber acts as a damping agent that delays the propagation of sound waves. In a pure gypsum matrix, sound travels rapidly due to its homogeneous and dense structure; however, the inclusion of

elastomeric particles disrupts this path. Interestingly, the particle size distribution also plays a critical role: finer rubber particles — being more dispersed — cause a more significant delay in sound propagation compared to coarser particles at the same volume fraction.

Regarding the fiber reinforcement, the results show that UPV tends to decrease as the fiber volume increases from 0 to 600 g/m^3. This is consistent with findings by Hedjazi and Castillo (2022) and Macedo, Carneiro and Perlingeiro (2021), who observed that high fiber concentrations can introduce micro-porosity into the matrix. These interfacial voids further scatter the ultrasonic waves, reducing the overall propagation velocity and potentially enhancing the material's sound absorption characteristics.

4.3.9 Sound absorption performance results

The determination of the sound absorption coefficient (a) using an impedance tube involved three measurements for each of the two specimens per sample, using microphone pairs 1-2, 2-3, and 3-4. Consequently, six data sets were generated for each mixture, providing the definitive absorption coefficients for the 1/3 octave bands from 100 Hz to 3150 Hz. The averages of these readings were calculated for each frequency, followed by an analysis of the peak absorption coefficients across the tested spectrum for the 15 mixtures.

The sample exhibiting the best acoustic performance, defined by the highest concentration of coefficients exceeding 0.50, was mixture 2400B20F06 (specifically Specimen 2, measured at Microphone Pair 1-2). This configuration presented the best overall global performance. The highest absorption coefficients occurred at 1000 Hz (a = 0.66) and 1250 Hz (a = 0.73), the latter being the absolute maximum value recorded in this study. Other results for this mixture included a = 0.47 at 1600 Hz, a = 0.41 at 2000 Hz, a = 0.32 at 2500 Hz, and a = 0.29 at 3150 Hz. These figures, illustrated in Figure 4-17, indicate that at higher frequencies, the material tends to be more reflective than absorptive.

Mixture 2400B20F06 concentrates the highest average values in the medium-high frequency range, which is critical for speech intelligibility and acoustic comfort. Its configuration consisted of a 20% rubber/total solids ratio, a 2.4 mm particle size, and 600 g/m3 of polypropylene fiber. Mechanically, it reached a flexural strength of 0.88 MPa and a compressive strength of 1.91 MPa, as detailed in Table 4-3.

Figure 4-17 – Sound absorption coefficient performance of mixture 2400B20F06 (Specimen 12.2)

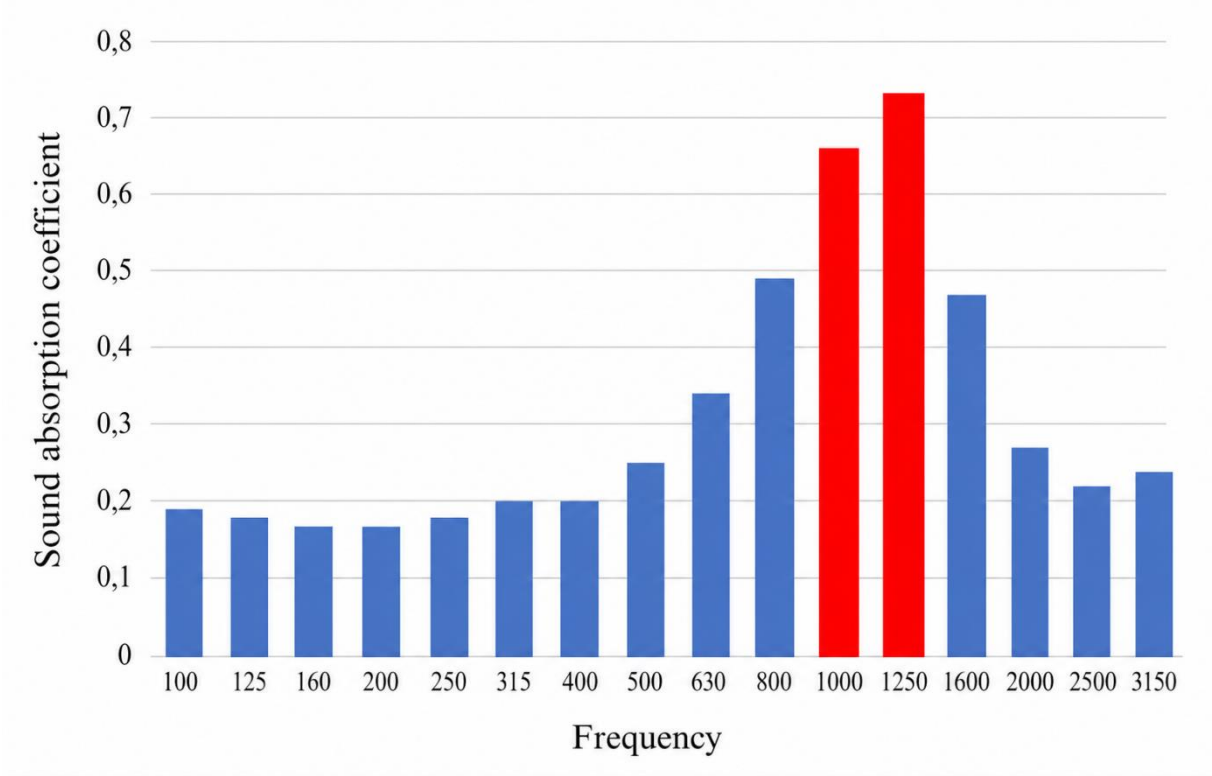

In contrast, mixture 1200B30F03 (specifically Specimen 1, measured at Microphone Pair 3-4) demonstrated the poorest acoustic performance. Its lowest values were recorded in the low-frequency range: 100 Hz (a = 0.13), 125 Hz (a = 0.12), and 160 Hz to 250 Hz (a = 0.13). As shown in Figure 4-18, this mixture maintained consistently low performance across all frequencies. Mixture 1200B30F03 was configured with a 30% rubber ratio, 1.2 mm particle size, and 300 g/m^3 of fiber, resulting in lower mechanical strengths (0.64 MPa flexural and 1.60 MPa compressive).

Comparing the best (2400B20F06) and worst (1200B30F03) performers, it is evident that the optimal sample utilized the largest studied particle size (2.4 mm) and a higher fiber concentration (600 g/m^3). This suggests that larger rubber granulometry and higher fiber density contribute to better mechanical strength and superior sound absorption within the context of this study. The highest absorption values obtained across all 15 mixtures per frequency are compiled in Table 4-5.

Figure 4-18 – Sound absorption coefficient performance of mixture 1200B30F03 (Specimen 4.1)

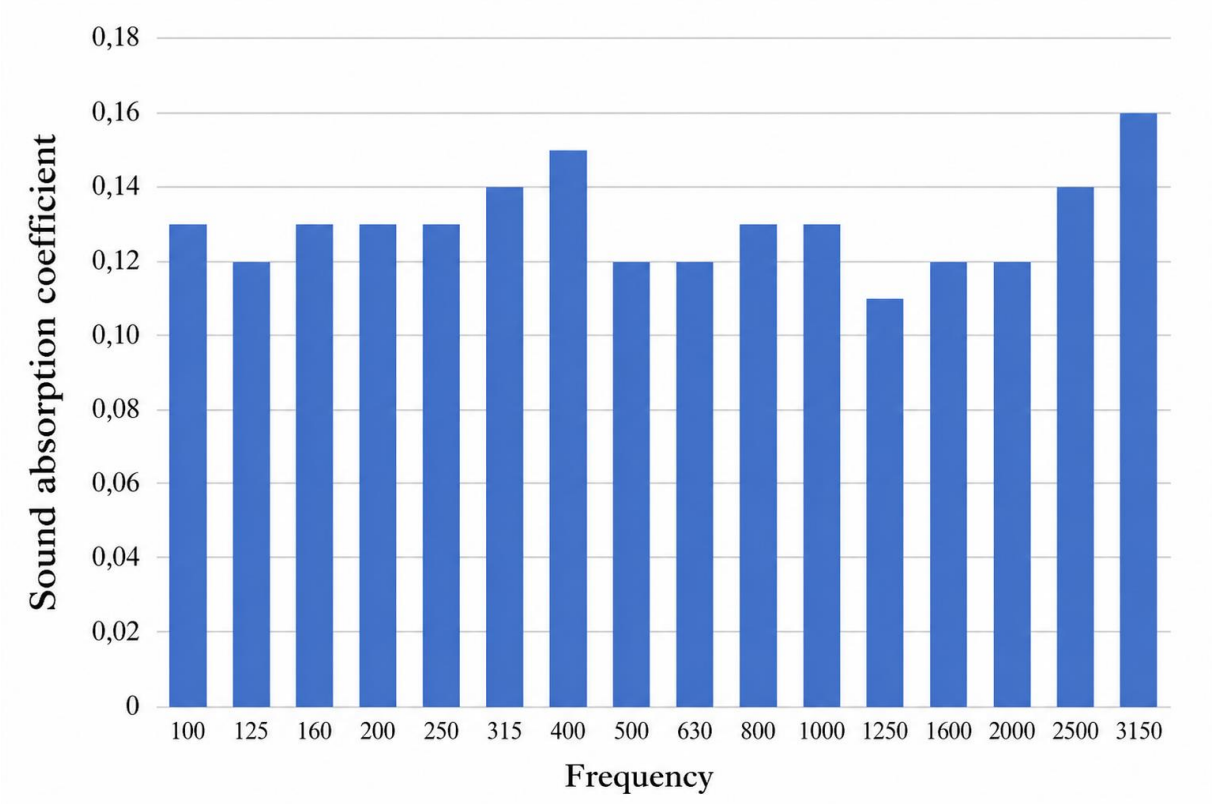

Table 4-5 – Maximum sound absorption coefficients obtained by frequency across all 15 mixtures

Frequency (f) [Hz]	Mixture ID	Specimen.Version	Microphone Pair	α
100	300B10F03	1.2	1-2	0.22
125	600B20F06	15.2	3-4	0.21
160	600B20F06	15.2	3-4	0.20
200	600B20F06	15.2	3-4	0.20
250	600B20F06	15.2	1-2	0.20
315	600B40F06	10.1	2-3	0.22
400	600B40F06	10.1	3-4	0.27
500	600B20F12	14.1	2-3	0.32
630	600B20F12	14.1	2-3	0.48
800	600B20F12	14.1	2-3	0.58
1000	2400B20F06	12.2	1-2	0.66
1250	2400B20F06	12.2	1-2	0.73
1600	2400B20F06	12.2	1-2	0.47
2000	300B10F03	1.2	1-2	0.41
2500	300B10F03	1.2	1-2	0.32
3150	600B20F00	13.1	1-2	0.29

As observed in Table 4-5, below the 500 Hz threshold, no sample achieved a coefficient $a > 0.50$. This indicates that rubber particle insertion does not yield effective absorption at low frequencies, where the composite behaves primarily as a reflective material. Rubber's efficacy in literature is largely tied to vibration damping; however, for airborne sound, the range of maximum efficiency was found between 800 Hz and 1250 Hz.

The conclusion regarding the optimal composition was primarily driven by these acoustic results, as mixture 2400B20F06 was the only one to present significant absorption relevant for technical applications ($a > 0.50$). This emphasizes the effectiveness of the 2.40 mm particle size in modifying the acoustic properties of gypsum-based composites.

The results obtained from the impedance tube tests reveal a significant correlation between the composite's microstructure and its ability to dissipate sound energy. The superior performance of mixture 2400B20F06 ($a = 0.73$ at 1250 Hz) compared to the poor performance of 1200B30F03 can be explained through three fundamental mechanisms: The role of particle size, damping and energy dissipation and fiber reinforcement and micro-porosity.

The peak absorption in the 800 Hz to 1250 Hz range for the 2.4 mm rubber particles suggests that larger aggregates create a more tortuous and interconnected pore network within the gypsum matrix. As sound waves enter these larger interfacial zones, energy is dissipated through viscous friction between the air molecules and the pore walls. This aligns with Ferrández *et al.* (2025), who noted that while smaller particles improve mechanical strength, larger rubber granules can create "acoustic pathways" that facilitate energy absorption in the mid-frequency range. In contrast, the 1.2 mm particles in mixture 1200B30F03 likely resulted in a more "closed" structure, increasing sound reflection ($a < 0.15$) rather than absorption.

The elastomeric nature of rubber contributes to sound attenuation via internal damping. When the gypsum-rubber composite is subjected to incident sound waves, the rubber particles undergo micro-deformations that convert acoustic energy into low-grade heat. This confirms the findings of Pinto and Akasaki (2016), who established that rubber inclusion increases the damping capacity of gypsum. However, the current study clarifies that this effect is frequency-dependent; below 500 Hz, the high stiffness of the gypsum matrix dominates, causing the material to behave as a reflective barrier, regardless of the rubber content.

The higher fiber concentration in the optimal mixture (600 g/m³) likely contributed to the formation of micro-voids at the fiber-matrix interface. According to Macedo, Carneiro and Perlingeiro (2021), these micro-pores are instrumental in reducing the velocity of sound (as seen in the UPV results) and increasing the probability of wave scattering. This "stitching" effect of the fibers not only maintains the 1.21 MPa flexural strength but also serves as an

auxiliary mechanism for acoustic dissipation, explaining why mixture 2400B20F06 outperformed the low-fiber samples.

The efficiency concentration in the 800–1250 Hz band is particularly relevant for architectural applications. This range covers a significant portion of the human speech spectrum. Therefore, the developed composite, especially in the 2400B20F06 configuration, proves to be a viable sustainable alternative for indoor acoustic conditioning, balancing a 1.91 MPa compressive strength with high-performance absorption that far exceeds that of traditional gypsum boards.

4.4 Conclusion

The experimental campaign demonstrated that integrating recycled tire rubber into a gypsum matrix significantly alters its mechanical and acoustic properties. These changes are primarily governed by particle size and the rubber-to-gypsum ratio, resulting in physical inclusions and fragile transition zones that cause a progressive decline in mechanical strength as rubber content increases.

Specifically, the mixture utilizing 2.40 mm particles with 600 g/m³ of fiber (Mixture 2400B20F06) achieved the optimal technical balance, reaching a compressive strength of 1.91 MPa, which exceeds the requirements for non-structural architectural components. Acoustically, this configuration yielded a maximum absorption coefficient of 0.73 at 1250 Hz, a performance range critical for speech intelligibility and indoor comfort.

However, the findings reveal that the acoustic efficiency of internal rubber inclusions is severely limited by the "encapsulation effect". The cementitious gypsum paste effectively seals the rubber's surface pores, obstructing the viscous friction mechanisms necessary for sound dissipation in the low-frequency range (below 500 Hz). Consequently, while the composite acts as an effective damping agent for vibrations, it behaves primarily as a reflective barrier for airborne sound at lower frequencies.

To overcome these limitations, future developments should prioritize a dual-layer design where the rubber aggregates are positioned on the external face of the boards. This structural transition would prevent pore sealing by the matrix, maximizing the tortuosity and pore accessibility of the rubber waste. This study establishes clear technical guidelines for the industrial production of sustainable, acoustically efficient gypsum systems, contributing to the valorization of tire waste in the circular economy.

4.5 Acknowledgements

The authors express their gratitude to the National Council for Scientific and Technological Development (CNPq), the Coordination for the Improvement of Higher Education Personnel (CAPES), and the Minas Gerais Research Funding Foundation (FAPEMIG) for their ongoing support through research fellowships and institutional programs. Special thanks are also extended to the Research Group SICon-CNPq/UFV and the partner groups within the Minas Gerais Research, Scientific, Technological, and Innovation Network (*Rede Mineira de Desenvolvimento Cinentífico, Tecnológico e de Inovação*) for providing the infrastructure, technical assistance, and academic environment essential to the development of this work.

4.6 Declaration of generative AI and AI-assisted technologies in the writing process

During the preparation of this work, the authors utilized generative AI and AI-assisted technologies to improve grammar, stylistic flow, and overall readability. Following this process, the authors critically reviewed and edited the generated content to ensure technical accuracy and assume full responsibility for the final integrity and originality of the publication.

4.7 References

ADVANCING STANDARDS TRANSFORMING MARKETS. **ASTM E1050-19**: standard test method for impedance and absorption of acoustical materials using a tube, two microphones and a digital frequency analysis system. West Conshohocken, PA: ASTM, 2019. Available in: https://webstore.ansi.org/standards/astm/astme105019. Access in: 15 jun. 2024.

ADVANCING STANDARDS TRANSFORMING MARKETS. **ASTM C597-22**: standard test method for pulse velocity through concrete. West Conshohocken, PA: ASTM, 2022. Available in: https://store.astm.org/c0597-22.html. Access in: 20 jun. 2024.

ASSOCIAÇÃO BRASILEIRA DE NORMAS TÉCNICAS. **NBR NM 248/2003**: Agregados – Determinação da composição granulométrica. Rio de Janeiro: ABNT, 2003. Available in: https://www.target.com.br/produtos/normas-tecnicas/36135/nbrnm248-agregados-determinacao-da-composicao-granulometrica. Access in: 8 abr. 2025.

ASSOCIAÇÃO BRASILEIRA DE NORMAS TÉCNICAS. **NBR NM 45/2006** – Agregados – Determinação da massa unitária e do volume de vazios. Rio de Janeiro: ABNT, 2006. Available in: https://www.normas.com.br/autorizar/visualizacao-nbr/10053/identificar/visitante. Access in: 3 mai. 2024.

ASSOCIAÇÃO MERCOSUL DE NORMALIZAÇÃO. **NM ISO 3310-1/2010**: Peneiras de ensaio – Requisitos técnicos e verificação. Parte 1: Peneiras de ensaio com tela de tecido metálico. 2.ed. Rio de Janeiro: ABNT, 2010. Available in: https://www.normas.com.br/autorizar/visualizacao-nbr/10201/identificar/visitante. Access in: 10 fev. 2025.

ASSOCIAÇÃO BRASILEIRA DE NORMAS TÉCNICAS. **NBR 7222/2011**: Concreto e argamassa – Determinação da resistência à tração por compressão diametral de corpos de prova cilíndricos. Rio de Janeiro: ABNT, 2011. Available in: https://www.target.com.br/produtos/normas-tecnicas/36322/nbr7222-concreto-e-argamassa-determinacao-da-resistencia-a-tracao-por-compressao-diametral-de-corpos-de-prova-cilindricos. Access in: 22 fev. 2025.

ASSOCIAÇÃO BRASILEIRA DE NORMAS TÉCNICAS. **NBR 13207/2017**: Gesso para construção civil – Requisitos. Rio de Janeiro: ABNT, 2017a. Available in: https://www.normas.com.br/autorizar/visualizacao-nbr/1907/identificar/visitante. Access in: 7 set. 2023.

ASSOCIAÇÃO BRASILEIRA DE NORMAS TÉCNICAS. **NBR 16605/2017**: Cimento Portland e outros materiais em pó – Determinação da massa específica. Rio de Janeiro: ABNT, 2017b. Available in: https://www.normas.com.br/autorizar/visualizacao-nbr/11971/identificar/visitante. Access in: 17 set. 2025.

ASSOCIAÇÃO BRASILEIRA DE NORMAS TÉCNICAS. **NBR 5739/1994**: Concreto – Ensaio de compressão de corpos-de prova cilíndricos. Rio de Janeiro: ABNT, 2018. Available in: https://www.ipaam.am.gov.br/wp-content/uploads/2021/01/NBR-05739-94-Ensaio-de-Compress%C3%A3o-de-Corpos-de-Prova-Cil%C3%ADndricos-de-Concreto.pdf. Access in: 3 set. 2025.

ASSOCIAÇÃO BRASILEIRA DE NORMAS TÉCNICAS. **NBR 12128/2019**: Gesso para construção civil – Determinação das propriedades físicas da pasta de gesso. 3.ed. Rio de Janeiro: ABNT, 2019. Available in: https://www.normas.com.br/autorizar/visualizacao-nbr/4862/identificar/visitante. Access in: 26 ago. 2024.

CHEN, B.; ZHENG, D.; XU, R.; LENG, S.; HAN, L.; ZHANG, Q.; ... ; CHENG, J. Disposal methods for used passenger car tires: One of the fastest growing solid wastes in China. **Green Energy and Environment**, v. 7, n. 6, p. 1298-1309, 2021. https://doi.org/10.1016/j.gee.2021.02.003

FERRÁNDEZ, D.; ZARAGOZA-BENZAL, A.; ATANES-SÁNCHEZ, E.; MERILLAS, B.; MATEUS, R.; SANTOS, P. Study of different recycling approaches for gypsum-based composites with recycled rubber aggregates. **Buildings**, v. 15, n. 4, 577, 2025. https://doi.org/10.3390/buildings15040577

GYPSUM S/A. **Tudo sobre as placas drywall (ou gesso acartonado)**. 26 abr. 2021. Available in: https://www.gypsum.com.br/pt-br/centro-de-apoio/blog/141783/tudo-sobre-placa-drywall/. Access in: 24 fev. 2025.

HEDJAZI, S.; CASTILLO, D. Utilizing polypropylene fiber in sustainable structural concrete mixtures. **CivilEng**, v. 3, n. 3, p. 562-572, 2022. https://doi.org/10.3390/civileng3030033

INTERNATIONAL ORGANIZATION FOR STANDARDIZATION. **ISO 247-1/2018**: Rubber – Determination of ash. Part 1: Combustion method. Genebra, Suíça: ISO, 2018. Available in: https://www.iso.org/standard/66372.html. Access in: 2 jul. 2023.

INTERNATIONAL ORGANIZATION FOR STANDARDIZATION. **ISO 10534-2:2023**: Acoustics – Determination of acoustic properties in impedance in tubes. Part 2: Two-microphone technique for normal sound absorption coefficient and normal surface impedance. 2.ed. Genebra, Suíça: ISO, 2023. Available in: https://www.iso.org/standard/81294.html. Access in: 20 abr. 2025.

JENA, B. P.; NAYAK, B. B.; SATAPATHY, S. Physical & mechanical characterization of composites from waste tire rubber crumb. **Materials Today: Proceedings**, v. 26, n. 2, p. 1752-1756, 2020. https://doi.org/10.1016/j.matpr.2020.02.368

LOZANO-DÍEZ, R. V.; LÓPEZ-ZALDÍVAR, O.; HERRERO-DEL-CURA, S.; MAYOR-LOBO, P. L.; HERNÁNDEZ-OLIVARES, F. Mechanical behavior of plaster composites based on rubber particles from end-of-life tires reinforced with carbon fibers. **Materials**, v. 14, n. 14, 3979, 2021. https://doi.org/10.3390/ma14143979

MACEDO, W. W.; CARNEIRO, L.; PERLINGEIRO, M. Velocidade de propagação de onda ultrassônica em concretos com fibras. In: Congresso Internacional sobre Patologia e Reabilitação das Construções, 17, 2021, Fortaleza. Anais... Fortaleza, 2021. https://doi.org/10.4322/CINPAR.2021.144

MASUERO, A. B. Desafio da construção civil: crescimento com sustentabilidade ambiental. **Matéria (Rio de Janeiro)**, v. 26, n. 4, 2021. https://doi.org/10.1590/S1517-707620210004.13123

MEDDAH, A.; LAOUBI, H.; BEDERINA, M. Effectiveness of using rubber waste as aggregates for improving thermal performance of plaster-based composites. **Innovative Infrastructure Solutions**, v. 5, 61, 2020. https://doi.org/10.1007/s41062-020-00311-0

PARRES, F.; CRESPO-AMORÓS, J. E.; NADAL-GISBERT, A. Mechanical properties analysis of plaster reinforced with fiber and microfiber obtained from shredded tires. **Construction and Building Materials**, v. 23, n. 10, p. 3182-3188, 2009. https://doi.org/10.1016/j.conbuildmat.2009.06.040

PINTO, N. A. Compósitos à base de gesso incorporados com resíduos de borracha proveniente do processo de recauchutagem de pneus. 2017. 135f. Dissertação (Mestrado em Engenharia Civil) – Universidade Estadual Paulista "Júlio de Mesquita Filho", Ilha Solteira, 2017. http://hdl.handle.net/11449/151166

PINTO, N. A.; AKASAKI, J. L. Incorporação de resíduos de borracha de pneus em matriz de gesso para utilização na construção civil. **Revista de Engenharia Civil (UM)**, n. 53, p. 43-56, 2016. Available in: https://www.civil.uminho.pt/revista/artigos/n53/Pag.43-56.pdf. Access in: 6 mai. 2024.

RASHAD, A. M. A comprehensive overview about recycling rubber as fine aggregate replacement in traditional cementitious materials. **International Journal of Sustainable Built Environment**, v. 5, n. 1, p. 46-82, 2016. https://doi.org/10.1016/j.ijsbe.2015.11.003

SERNA, A.; DEL RÍO, M.; PALOMO, J. G.; GONZÁLEZ, M. Improvement of gypsum plaster strain capacity by the addition of rubber particles from recycled tyres. **Construction and Building Materials**, v. 35, p. 633-641, 2012. https://doi.org/10.1016/j.conbuildmat.2012.04.093

SERVIÇO SOCIAL DO TRANSPORTE/SERVIÇO NACIONAL DE APRENDIZAGEM DO TRANSPORTE. **Cerca de 450 mil toneladas de pneus são descartados por ano no Brasil**. 8 fev. 2017. Available in: https://www.sestsenat.org.br/noticia/cerca-de-450-mil-toneladas-de-pneus-sao-descartados-por-ano-no-brasil. Access in: 21 fev. 2025.

VELOSO, M. C. R. A.; VILLELA, L. S.; MESQUITA JÚNIOR, L.; VALLE, M. L. A.; MENDES, L. M.; GUIMARÃES JÚNIOR, J. B. Produção e caracterização de compósitos à base de gesso reforçado com partículas de resíduo da agroindústria do cacau. **Matéria (Rio de Janeiro)**, v. 26, n. 1, 2021. https://doi.org/10.1590/S1517-707620210001.1245

ZHANG, S. L.; XIN, Z. X.; ZHANG, Z.X.; KIM, J. K. Characterization of the properties of thermoplastic elastomers containing waste rubber tire powder. **Waste Management**, v. 29, n. 5, p. 1480-1485, 2009. https://doi.org/10.1016/j.wasman.2008.10.004

5 PROPOSITION AND CHARACTERIZATION OF A GYPSUM BOARD COATED WITH RUBBER WASTE UNDER REAL CONDITIONS OF USE FOR ACOUSTIC CONDITIONING PURPOSES

Abstract: This chapter investigates the performance and characterization of a gypsum-based composite coated with shredded tire rubber waste, focusing on acoustic absorption under real application conditions as an alternative and sustainable solution for the acoustic conditioning of educational environments. The study is based on the assumption that the sound absorption performance of the board under real conditions of use differs significantly from the results obtained in controlled laboratory tests. This occurs due to the dimensions of the environment and the angle of incidence of the sound wave, which justifies the adoption of comparative in situ measurements. The main objective was to evaluate the acoustic performance of this material in the sound conditioning of rooms intended for speech, especially regarding reverberation time control, as well as to verify the sound absorption performance of the rubber-coated boards at low frequencies. The experimental methodology consisted of installing 16 boards in classrooms and in a laboratory at the Federal University of Viçosa, with measurements conducted according to ABNT NBR ISO 3382-2. Comparative measurements were performed before and after the installation of the boards, using different sound excitation signals (white noise, pink noise, and sweep signal), with analysis of the EDT10, T20, and T30 descriptors in octave bands ranging from 63 Hz to 8000 Hz. The evaluated environments had distinct volumes, also allowing the observation of the influence of room volumetry on the material's performance. The results demonstrated that, although there was a reduction in reverberation time in some low-frequency bands for certain descriptors, the predominant behavior of the boards was reflective at medium and high frequencies, especially in the 500 Hz band, considered critical for speech intelligibility. In several cases, the installation of the boards resulted in an increase in reverberation time, compromising the acoustic performance of the analyzed environments. It was concluded that, under the tested conditions and with the applied coverage area, the boards were not sufficient to adjust the reverberation time of the environments to the recommended values for classrooms, indicating the need for a larger number of boards to achieve a more significant effect in reducing reverberation time in the frequency bands where the material showed better performance.
Keywords: Boards, Reverberation Time, Sound Absorption, Waste, Rubber.

5.1 Introduction

The purpose of this experimental study was to install prototype gypsum boards coated with shredded tire rubber waste on the walls of classrooms. This procedure practically simulates a real condition of use for the boards by promoting a diffuse incidence of sound waves on their surfaces, similarly to what occurs in reverberation chambers. According to the methodology described in ABNT NBR ISO 3382-2, the reverberation time of the environment was measured in order to verify how much the boards would influence the acoustic conditioning of the space. Thus, the acoustic performance of a composite made of gypsum, nylon fiber, and rubber was

evaluated for sound absorption purposes in the control of reverberation time within an environment.

It is important to emphasize that there are different ways to measure the reverberation time of an environment. One of these procedures is the statistical method, which is based on the theory that, within a diffuse and uniformly distributed sound field inside a closed environment, the decay of sound energy follows a linear statistical law on a logarithmic scale. A common methodology is the use of Sabine's equation to calculate reverberation time, while another approach involves measuring the reverberation time of a room with and without the presence of absorbing material. As defined by Bistafa (2018), reverberation time is the period elapsed from the moment a sound wave is emitted by the source until it loses 60 dB of its sound level, corresponding to a decrease in the order of 10^6 W/m² in sound intensity. The reverberation time of an environment is calculated using the simple Sabine formula. This equation considers the volume of the environment and the amount of absorbing material present in the space. The formula is given by: TR=0.161.V/A where TR is the reverberation time, V is the room volume in cubic meters, and A is the sum of the total absorption of the absorbing surfaces in square sabins. There are different approaches for calculating reverberation time, such as the Eyring formula and the Millington and Sette formula (Ginn, 1978). However, according to ABNT NBR ISO 3382-2, there are two methods for measuring the reverberation time of an environment: the interrupted noise method and the integrated impulse response method. The interrupted noise method involves interrupting the sound in the environment and measuring the time required for the sound energy to decay by 60 dB after the sound emission stops. This method allows a frequency range that may vary depending on the purpose of the measurement, covering at least from 250 Hz to 2,000 Hz for the survey method and from 125 Hz to 4,000 Hz in octave bands or from 100 Hz to 5,000 Hz in one-third octave bands for engineering and precision methods. The other measurement approach is the integrated impulse response method, in which short-duration sounds are used, such as gunshots from blank cartridges or balloon bursts for precise approximations, or deterministic signals with flat spectra that are transformed into the room's impulse response. These methods are applied to evaluate and measure reverberation time in different environments such as residential rooms, theaters, offices, classrooms, among others.

In environments where sound expression requires acoustic quality, it is important to highlight some factors that affect this performance, including space geometry, reverberation time, speech intelligibility, and background noise (Procel Edifica, 2011). The materials present in an environment are important for acoustics because every surface in a room and every object within it absorbs sound to some extent (Ginn, 1978). The absorption capacity of construction

materials varies according to their physical characteristics, such as porosity, rigidity, installation method, and sound frequency (Procel Edifica, 2011). When a sound wave interacts with an absorbing surface, the air within its pores begins to vibrate; however, this vibration depends on the resistance to airflow passage, where part of the sound energy is dissipated in the form of thermal energy. Thus, the vibration amplitude of air particles is progressively damped by interaction or friction against the pore walls, acting as an acoustic resistance (Ginn, 1978). Therefore, the careful selection of materials used in the construction and decoration of an environment can have a significant impact on reverberation time and on the overall acoustics of the space (Patrício, 2018). An adequate reverberation time is essential to ensure speech intelligibility and thereby provide clarity to the transmitted message (Procel Edifica, 2011).

However, the absorption coefficient of materials varies according to the angle of incidence of the sound wave upon them and generally differs from one frequency to another. When a sample is evaluated inside an impedance tube, according to ISO 10534-2, the coefficient is determined considering a plane wave incident normally on the composite surface. Nevertheless, under real conditions of use, sound reaches a material diffusely, as in a reverberation chamber, that is, from various directions or angles. This occurs due to successive reflections from the surfaces within the environment, in addition to the direct sound coming from the sound source. These surfaces include the materials present in the environment, whether ceiling, walls, floor, or even furniture. It is important to emphasize that reflected sound may reach the boards already at a somewhat lower sound level because of its interaction with several surfaces, where part of its energy has already been absorbed. To verify the performance of these boards within the acoustic conditioning of the environment through absorption, the reverberation time was compared before and after their installation. Due to this condition, the methodology established by ABNT NBR ISO 3382-2 was adopted for measuring the reverberation time of the environment.

5.2 Materials and methods

The materials used in the manufacture of the acoustic board were: gypsum boards for drywall walls, granulated shredded tire rubber, and white glue for fixing the rubber granules to the external surface of the board.

5.2.1 Measurement equipment

To perform the measurement of Reverberation Time (RT) in the rooms, equipment such as a sound pressure level meter and/or sound analyzer, together with an external calibrator, were used in accordance with the specifications of ABNT NBR 10151 and ABNT NBR 10152. Following ABNT NBR ISO 3382-2, the equipment used for the measurements included a sound excitation source to generate interrupted noise in the room, which was an omnidirectional source shown in Figure 5-1. A set of microphones was used to capture the sound within the environment, a sound pressure measurement system, known as a sound level meter, was used to record the data, and a spectrum analyzer was employed to analyze the measurements performed. To ensure measurement accuracy, it was important to calibrate all the equipment used. The equipment utilized to determine the reverberation time of the classrooms included the FUSION Analyzer FSN3031000 Class 1 sound level meter from 01dB, CAL 3014000 calibrator, FUSION Option – Building Acoustics, dBINSIDE software, LS04 omnidirectional sound source, and dBTRAIT Viewer software.

Figure 5-1 – Fonte ominidirecional, sonômetro 01dB, calibrador 01dB e case de transporte

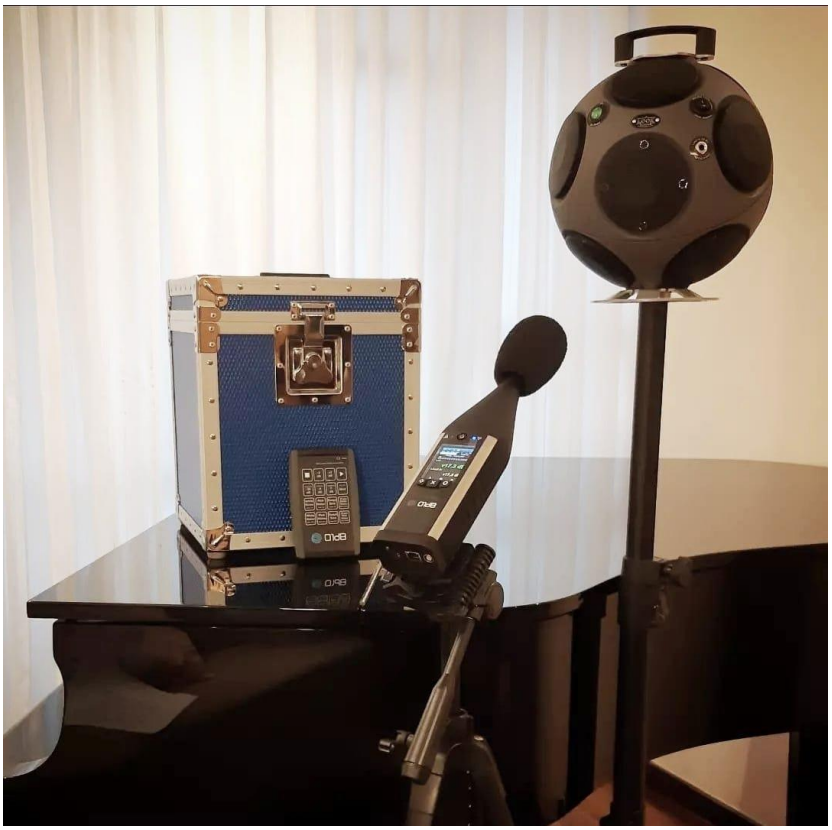

Photo: Rodrigo Spinelli – Empresa Spinelli Acústica

The sound level meter was connected to a notebook computer with software for data analysis and subsequent report generation, providing information such as background noise and reverberation time.

The instrumentation used to perform the measurements included a Class 1 sound level meter (integrating sound level meter or sound pressure level measurement system), Fusion model, serial number PSN3031000, manufactured by 01dB, in accordance with the criteria established by IEC 61672 (all parts), with 1/1 octave and 1/3 octave filters compliant with IEC 61260 (all parts), for random incidence applications. The sound level meter is equipped with a ½-inch pre-polarized condenser microphone, type 1, GRAS 40 CE model, integrated in accordance with IEC 61672-1.

The sound level meter was calibrated by Total Safety – Laboratório de Calibração e Ensaios (CALILAB), a member of the Rede Brasileira de Calibração (RBC), accredited by Cgcre-Inmetro under accreditation CAL-0307. Calibration was performed according to the edition of the IEC standard declared by the manufacturer, resulting in Calibration Certificate RBC3-12474-379. The most recent calibration of the instrument was carried out on February 6, 2024. ABNT NBR 10151 establishes in item 6 that the period between two consecutive calibrations must not exceed 24 months; therefore, the latest calibration performed on the equipment used for the preparation of this report remains valid.

The high-precision condenser measurement microphone used was the Behringer ECM8000 model, designed for integrated use with real-time analyzers that provide an instantaneous acoustic image of the room. The microphone has an extremely flat frequency response from 15 Hz to 20 kHz and an omnidirectional pickup pattern. The USB Audio Interface used was the Focusrite Scarlett Solo (3rd Generation), featuring microphone preamplifier, P10 inputs and outputs, AIR mode, sampling and conversion rates up to 192 kHz/ 24 bits, and gain up to 56 dB. The interface was connected to a Samsung Galaxy Tab S7 FE LTE (Wi-Fi) 128 GB tablet.

The sound source used was the omnidirectional source LS04 from 01dB, which complies with the reference standards ISO 140-1 / ISO 717-1; ISO 10052 / ISO 3382-3; and DIN 52210-6, and is CE compliant with IEC 60065 + A1; immunity standard EN 55024 (09/1998) + A1 (10/2001) + A2 (01/2003) + S1 (03/2008); and emission standard EN 55022 (01/2009).

The omnidirectional source operated by producing a sound pressure level sufficient to provide decay curves with the minimum required dynamic range, without contamination by residual sound. The standard procedure for impulse responses obtained with white noise and

pink noise was performed as follows: the room was excited with a broadband signal at a sound intensity 40 dB above the measured background noise for approximately 20 seconds, sufficient for the room to reach steady-state conditions. From that moment onward, the sound source was interrupted and the decay signal captured by the condenser microphone coupled to the audio interface, powered by the tablet, which remained recording the signal through the WavePad Audio Editing software installed on the device. After the measurement set, the WAV file generated during this stage was processed using the Audacity Audio Editor software so that only the representative decay excerpt would be used in the subsequent processing and analysis stage. Data analysis was performed using the REW (Room EQ Wizard) software.

For impulse responses obtained with sine sweep excitation, the room was excited with a sine sweep signal at a sound intensity 40 dB above the measured background noise. The sound level meter remained capturing the signal in real time. This equipment has integrated processing software capable of generating instantaneous results.

5.2.2 The gypsum board

Sixteen drywall gypsum boards measuring 0.60 m × 0.90 m were used and subsequently coated with shredded tire rubber waste with a particle size of 1.20 mm. The rubber waste particles were bonded to the surface of the boards using white school glue.

Figure 5-2 – Photos of the drywall gypsum boards with tire rubber waste bonded to the surface

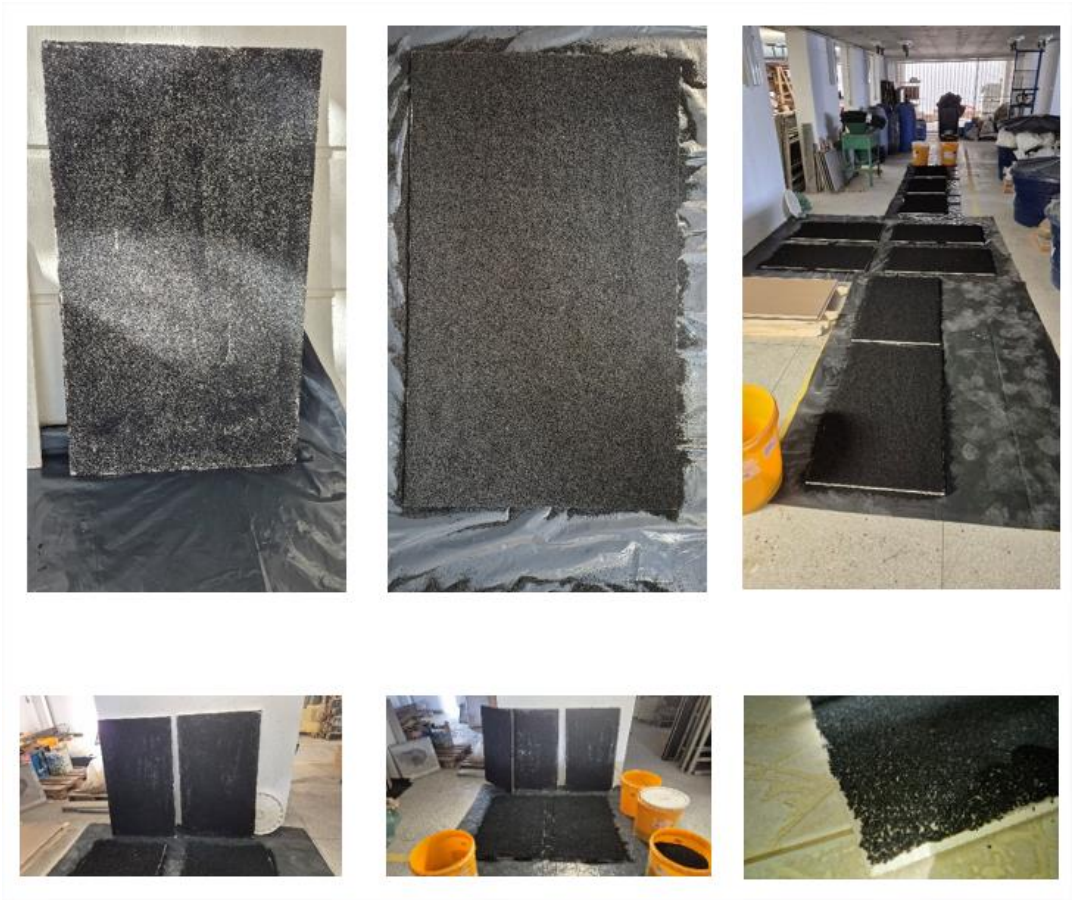

Source: Author (2025).

5.2.3 Locations for evaluating the performance of the boards under real conditions of use

The locations used for the evaluation of the boards and the measurement of reverberation time were the classrooms of the Department of Architecture and Urbanism (Figure 5-3 and Figure 5-4) and the laboratory of the Department of Civil Engineering (Figure 5-5), both at the Federal University of Viçosa.

Figure 5-3 – Schematic floor plan of the Architecture Classroom with its dimensions

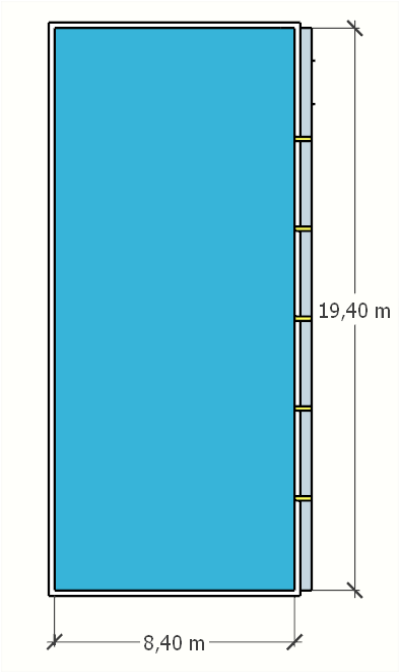

Source: Author (2025).

Figure 5-4 – Perspective view of the Architecture Classroom with its dimensions

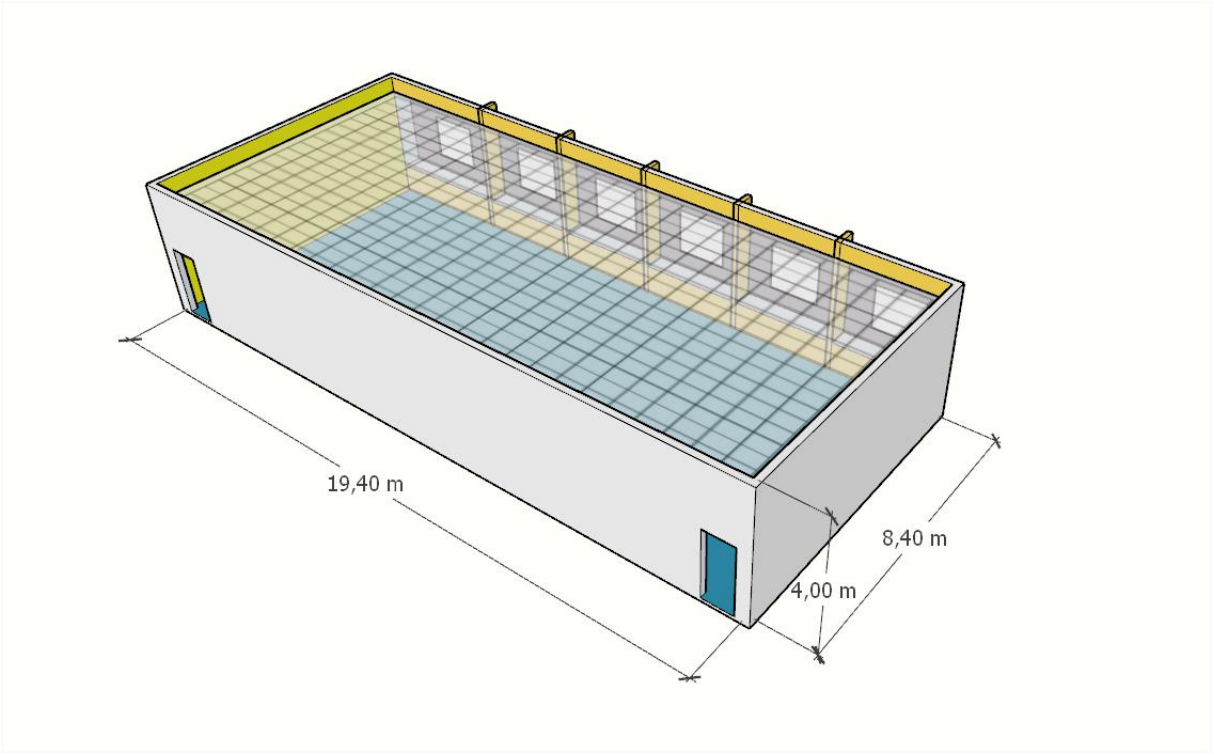

Source: Author (2025).

The materials in the Architecture classroom include vinyl flooring, painted masonry walls, acoustic mineral ceiling panels, aluminum windows, vinyl curtains, wooden doors, plywood and laminate tables, plastic chairs, a vinyl projection screen, and a wooden board. In the Engineering Classroom, the differences in materials include terrazzo flooring, plastic blinds covered with fabric, and a granite countertop.

Figure 5-5 – Perspective view of the Engineering Classroom with its dimensions

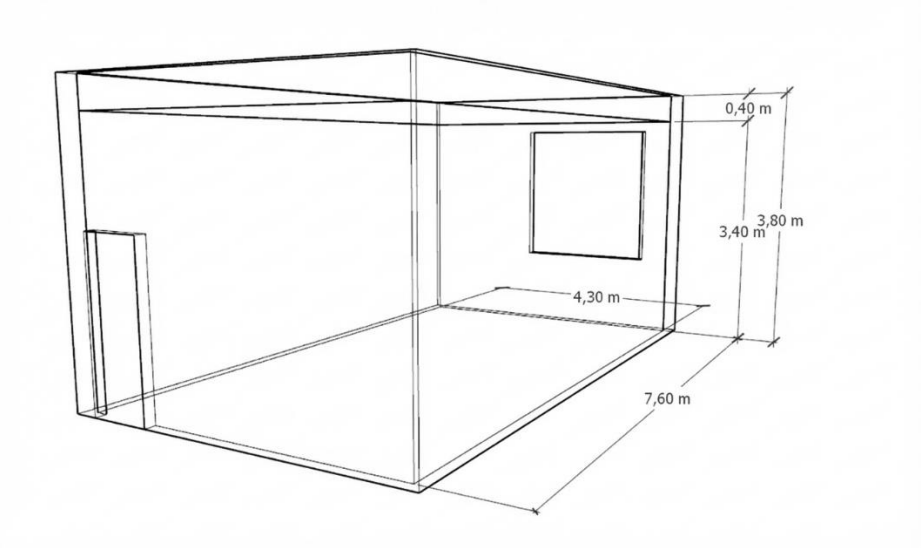

Source: Author (2025).

5.2.4 Acoustic tests of the boards

After measuring the reverberation time of the rooms according to ABNT NBR ISO 3382-2, it was possible to evaluate the results by comparing the two rooms with and without the boards using three different signals. The objective was to compare and evaluate the ability of the boards to reduce the reverberation time of the environment within the frequency bands from 63 Hz to 8000 Hz. Consequently, the performance of the boards in low-frequency sound absorption was also verified through their effectiveness in reducing reverberation time at bass and sub-bass frequencies.

Through these practical tests, it was also possible to identify the frequency ranges in which the material exhibited better absorption performance, thereby justifying its application.

For rooms intended for human speech, the primary objective is speech intelligibility, which requires reverberation times (RT) significantly shorter than those recommended for music (Kleiner; Tichy, 2014). If the reverberation time is excessively long, syllables and consonants, which have short duration and low energy, become masked by the residual sound

of preceding vowels, resulting in a “muddy” or unclear sound (Kuttruff, 2016). For classrooms with volumes between 150 and 250 m³, technical standards such as DIN 18041 recommend a reverberation time range between 0.5 s and 0.7 s (Mommertz, 2009).

In the case of the Architecture classroom at the Federal University of Viçosa, where the measurements were conducted and which has a volume of 570 m³, fitting within the range of 200 m³ ≤ Volume < 10,000 m³, the applicable formula is:$T=0.75\times\log(V)-1.00$ where T is expressed in seconds. The resulting value of approximately 0.8 s, when adjusted to the classroom context focused on speech, corresponds to around 0.6–0.7 s, prioritizing speech intelligibility. Recommended values for low-volume rooms (< 200 m³) are below 0.6 s. For intermediate volumes, such as 600 m³, the recommended reverberation time is close to 0.6 s in order to optimize speech comprehension. At the upper limit, the reverberation time should not exceed 0.7–0.8 s within the mid-frequency range (500–2000 Hz).

These values are specifically recommended for octave frequency bands between 250 Hz and 2000 Hz, referred to as critical frequencies, which directly include the range from 500 Hz to 1000 Hz (Mommertz, 2009). The desired frequency behavior differs from that of music rooms, where an increase in reverberation time at low frequencies is desirable to provide “warmth” to the sound. In classrooms intended for speech or spoken communication, however, the reverberation time should remain as constant as possible throughout the entire audible spectrum (Mommertz, 2009). This recommendation is based on recognized technical guidelines, such as DIN 18041, which addresses acoustic quality in small and medium-sized rooms. Additionally, other international standards, such as ANSI S12.60, suggest even stricter limits to ensure communication clarity, establishing that reverberation time should not exceed 0.6 seconds for room volumes up to approximately 283 m³ (Long, 2006).

An analogy can be made in which the reverberation time in a classroom function like the focus of a camera lens: if it is excessively long, it resembles a blurred photograph where the edges of the letters (the consonants) merge together, making reading impossible. A short reverberation time “cleans” the sound field, allowing each syllable to stand out clearly before the next one reaches the listener’s ears.

The descriptors D50, which refers to the balance of early reflections and is associated with speech clarity, requiring values greater than 0.3 at frequencies below 2000 Hz, and C80, which refers to musical clarity within the environment and should present values greater than 4 dB to indicate adequate musical clarity, were also measured in both rooms under the same conditions, with and without the boards. However, these descriptors are more applicable to rooms with volumes significantly larger than those of the two rooms used for the evaluation of

the boards. Therefore, their values were discarded, and the descriptors were not considered in the analysis.

Regarding the sound signal generated by the omnidirectional source used for room excitation and, consequently, for measuring sound decay, three types of sound signals were employed: white noise, pink noise, and sweep signal. White noise has a constant spectral density across all frequencies (equal energy per cycle) and is mainly used for electrical measurements or constant bandwidth analyses (Everest; Pohlmann, 2021). Pink noise is the preferred signal for acoustic measurements when compared to white noise because its energy distribution more closely resembles the way the human ear subjectively perceives sound (Everest; Pohlmann, 2021).

The sweep signal is another type of signal used to measure the reverberation time of an environment. It consists of a sinusoidal frequency that continuously increases over time, often exponentially (Kuttruff, 2016). This signal is highly efficient because it provides a better signal-to-noise ratio (SNR) and is immune to harmonic distortions (Rindel, 2017). The signal is widely used in modern techniques for measuring the Room Impulse Response (RIR) (Rindel, 2017).

According to ABNT NBR ISO 3382-2, which addresses the measurement of reverberation time in ordinary rooms, there are two main methods for room excitation, each using specific types of signals. The first is known as the Interrupted Noise Method. This is the traditional method that uses noise signals emitted by a loudspeaker and abruptly interrupted in order to measure sound decay. The recommended signals are Pink Noise, which is often preferred because it has equal energy per octave, aligning with human auditory perception and facilitating frequency-band analysis, and White Noise, which has equal energy per frequency (hertz) and is also described in the standard as an acceptable option. These signals may be emitted either as broadband noise or as filtered noise in frequency bands, such as octave bands or one-third octave bands, before being transmitted to the loudspeaker.

The other approach is the Integrated Impulse Response Method. This modern method uses deterministic signals to obtain the Room Impulse Response (RIR), which is subsequently squared and integrated. The types of signals commonly used are the Sine Sweep (sine-sweep or swept-sine), which consists of a signal whose frequency continuously varies over time (Rindel, 2017). It is considered highly advantageous because it is immune to harmonic distortions and allows for a high signal-to-noise ratio (Rindel, 2017). Another signal that may be used is the MLS (Maximum Length Sequence), which is a periodic pseudo-random signal that enables recovery of the impulse response through correlation (Rindel, 2017).

Regarding signal requirements, regardless of the type of noise or signal selected, the standard and acoustic practice establish several conditions. First, the sound source must be omnidirectional, radiating sound uniformly in all directions to ensure a diffuse sound field (Rindel, 2017). Second, the excitation level must be sufficiently high so that the sound decay remains at least 35 dB to 45 dB above the room background noise in each frequency band of interest (Aletta; Kang, 2020). Finally, the analysis should typically be performed in octave bands or one-third octave bands, covering at least the frequency range from 100 Hz to 5000 Hz (Rindel, 2017). For small rooms, such as classrooms, the measurements should focus on the frequency bands where speech energy is predominant, ensuring that reverberation time is accurately measured in the 500 Hz to 2000 Hz range (Mehta; Johnson; Rocafort, 1998).

The results were processed into tables and graphs used to compare the behavior of reverberation time in the Architecture classrooms and the Civil Engineering laboratory at the Federal University of Viçosa. Both rooms were excited using the omnidirectional source under two conditions. The first condition was without the boards, in order to determine the existing reverberation time of the empty room. The second condition involved the installation of the 16 boards at an initial height ranging from 0.90 m to 1.80 m, covering the height range corresponding to a seated or standing student.

In the Architecture classroom, eight boards were installed on each of the two parallel and longer walls of the room, as shown in the photographs (to be numbered subsequently). In the Engineering laboratory, due to the smaller room dimensions, the boards were distributed across three walls, namely the two longer walls and the rear wall opposite the professor's board. The gypsum board coated with tire rubber waste measured 0.60 m × 0.90 m and was installed with its 0.60 m side parallel to the floor and its 0.90 m dimension positioned vertically.

Figure 5-6 – Architecture Classroom at the Federal University of Viçosa: (a) without the boards and (b) with the boards

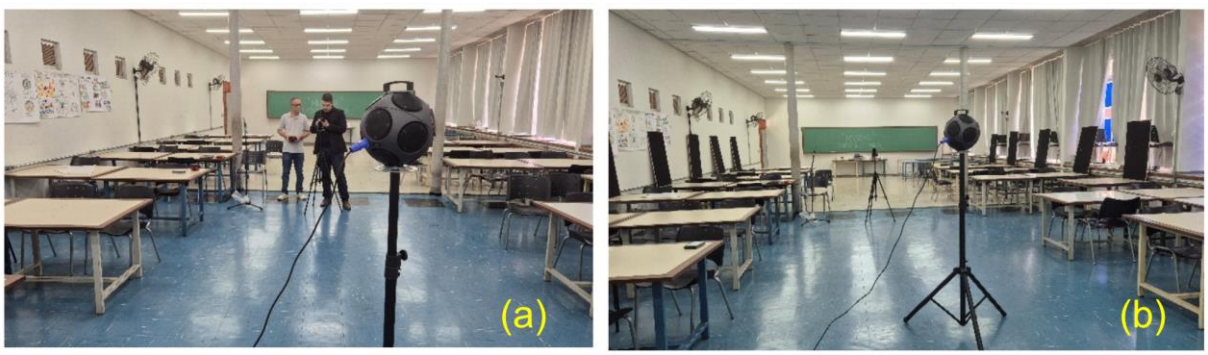

Source: Author (2025).

Figure 5-7 – Civil Engineering Laboratory/Classroom at the Federal University of Viçosa: (a) without the boards and (b) with the boards

Source: Author (2025).

5.3 Analysis of results

5.3.1 Analysis of the measurement results in the Civil Engineering Laboratory/ Classroom at the Federal University of Viçosa

It is important to emphasize, before analyzing the values presented in the tables, that they were generated using the REW software. The REW (Room EQ Wizard) software is primarily used for acoustic measurements in environments, assisting in the analysis and correction of room frequency response. The software also enables the measurement of the acoustic behavior of a room or sound setup using a measurement microphone. It generates test signals such as pink noise and calculates frequency, time, and distortion responses in order to identify issues such as peaks, dips, and reverberation.

In some fields of the tables, the term “NA” (“Not Available”) appeared in the T20 or T30 results. This indicates that it was not possible to reliably calculate the reverberation time in that frequency band due to erratic values. This may have occurred because of several possible factors. One possibility would be a high background noise level, which was not the case in this measurement, since the source was calibrated to excite the room at 40 dB above the environmental background noise, in accordance with ABNT NBR ISO 3382-2. If this had been the reason, the sound decay curve would not have reached –20 dB or –30 dB relative to the initial level because the background noise would have interrupted the decay curve. Consequently, the REW software would not have had sufficient dynamic range to accurately calculate T20 or T30.

Another more plausible possibility, and one that provides a more logical explanation, is that the decay time was extremely short. This may occur in rooms with volumes smaller than 500 m³ or in highly absorptive spaces. Under such conditions, the sound may decay so rapidly that the software cannot detect a sufficiently linear interval of –20 dB or –30 dB to perform logarithmic regression. For this reason, the EDT10 (Early Decay Time) descriptor values, which use only the first 10 dB of decay and were in fact successfully recorded, became more relevant in comparison to the absence of values for the T20 and T30 descriptors in some procedures.

Finally, another possibility more consistent with the experiment is an error in detecting the initial decay point. This is related to the configuration of the test, which was conducted in a non-acoustically controlled environment rather than in a reverberation chamber, for example. In some cases, the REW software may incorrectly identify the point where the impulse begins to decay, largely because of highly energetic reflections near the measurement point caused by the proximity of furniture and other objects within the environment.

The interpretation of the tables followed the following order. First, the room with the smaller volume was analyzed, namely the Civil Engineering laboratory classroom, with a volume of 111.12 m³. Subsequently, the room with the larger volume, the Architecture Classroom, with a volume of 570.36 m³, was analyzed. In both rooms, volumetry was calculated considering the height from the floor to the suspended acoustic mineral ceiling. Regarding room conditions, the measurements were first conducted without the boards and subsequently with the boards installed; this same sequence was followed in the interpretation of the results.

For the sound source excitation signals, the interpretation sequence of the tables was as follows: first white noise, followed by pink noise, and finally the sweep signal, thereby following the order of efficiency in determining reverberation time.

5.3.2 Analysis of the acoustic measurement results in the Civil Engineering Laboratory using white noise

According to Table 5-1, it can be observed that at the central frequency of 500 Hz, the reverberation time measured through the T20 descriptor presented an adequate value within the recommended interval of $0.5 \leq \text{value} \leq 0.7$, with an RT of 0.67 s. At both high and low frequencies, however, the reverberation time exceeded the values considered appropriate for the acoustic function of the environment.

It can also be verified from the T20 results that, within the mid-frequency range from 500 Hz to 1000 Hz, the room without the boards exhibited acoustic conditions close to the ideal for a classroom environment. Furthermore, the EDT10 results indicate that the low frequencies recorded values above 1 s, with the exception of the 500 Hz and 8000 Hz bands.

Table 5-1 – Reverberation Time (RT) results in seconds from the acoustic test conducted in the Civil Engineering Laboratory without the boards using the white noise signal

Laboratory without boards White noise								
EDT10	**63**	**125**	**250**	**500**	**1000**	**2000**	**4000**	**8000**
	4,03	3,53	1,31	0,79	0,94	1,28	1,16	0,86
T20	**63**	**125**	**250**	**500**	**1000**	**2000**	**4000**	**8000**
	3,28	NA	1,32	0,67	0,71	1,23	1,38	0,78
T30	**63**	**125**	**250**	**500**	**1000**	**2000**	**4000**	**8000**
	3,11	NA	NA	NA	NA	1,17	1,48	0,82

Source: Author (2025).

According to Table 5-2, only the T30 descriptor at the frequency of 1000 Hz presented an adequate value within the interval of $0.5 \leq$ value ≤ 0.7, with an RT of 0.65 s. In the EDT10 and T20 descriptors, the central and most relevant frequency of 500 Hz showed values above 0.7 s. All the other frequencies in all descriptors also presented values above 0.7 s and, when compared to the condition of the laboratory without the boards measured using the same white noise signal, demonstrated a deterioration in the acoustic conditioning of the environment.

As the reverberation time increased with the use of the boards at medium frequencies, this indicates that the material behaved predominantly in a reflective manner, resulting in an increase in reverberation time within these frequency bands. However, it is noteworthy that at the low frequency of 63 Hz, in the T20 and T30 descriptors, the RT decreased to values less than half of those measured in the laboratory condition with the boards, indicating improved performance. Nevertheless, caution is required when interpreting measurements carried out in environments with very small volumes, since low frequencies are dominated by normal vibration modes. White noise, being a random signal, excites these modes inconsistently. Because less energy is available per octave band at low frequencies, the decay of these few modes may be masked by background noise or by electrical noise from the measurement system, making the decay curve irregular and difficult to analyze (Everest; Pohlmann, 2021).

The use of a signal with lower energy density, such as white noise in these bands, increases statistical uncertainty, requiring multiple measurements and averaging procedures to obtain minimally reliable reverberation time values (Everest; Pohlmann, 2021). For this reason, pink noise is generally preferred over white noise for acoustic measurements. Its energy is distributed equally per octave (–3 dB per hertz), which compensates for the bandwidth width and provides a more uniform signal-to-noise ratio (SNR) throughout the audible spectrum, facilitating the measurement of decay times at low frequencies (Everest; Pohlmann, 2021). Both pink noise and the sweep signal are considered more suitable for measurements because they are more closely aligned with the subjective perception of sound.

Table 5-2 – Reverberation Time (RT) results in seconds from the acoustic test conducted in the Civil Engineering Laboratory with the boards using the white noise signal

Laboratory with boards White noise								
EDT10	**63**	**125**	**250**	**500**	**1000**	**2000**	**4000**	**8000**
	9,36	2,89	2,65	1,40	1,22	1,68	1,87	1,44
T20	**63**	**125**	**250**	**500**	**1000**	**2000**	**4000**	**8000**
	0,88	NA	1,31	0,81	0,74	0,82	0,83	0,79
T30	**63**	**125**	**250**	**500**	**1000**	**2000**	**4000**	**8000**
	0,74	NA	1,37	0,86	0,65	0,78	0,80	0,73

Source: Author (2025).

As previously discussed, the tables corresponding to the laboratory with and without the boards were analyzed using white noise, considering the EDT10, T20, and T30 descriptors for the frequencies of 63, 125, 250, 500, 1000, 2000, 4000, and 8000 Hz, and adopting the interval $0.5 \leq \text{value} \leq 0.7$ as the ideal reverberation time range.

In the case of the laboratory with the boards, the EDT10 value at the central frequency of 500 Hz increased from 0.79 s to 1.40 s, while at the frequency of 1000 Hz the value increased from 0.94 s to 1.22 s, according to Table 5-2. The use of the boards therefore caused an increase in the reverberation of the environment, compromising speech intelligibility. This increase was also observed for the T20 descriptor at both frequencies.

It was also found that, in the laboratory with the boards, the T30 descriptor at the frequency of 1000 Hz presented a value of 0.65 s, which falls within the desired reverberation

time interval. However, the equipment did not register T30 values in the laboratory without the boards at the 500 Hz and 1000 Hz bands, which could also have been within the range of 0.6 s to 0.7 s and possibly even lower than 0.65 s. This would indicate a potential reduction in reverberation; however, there are no available data to confirm this assumption. It was also observed that the T30 value at the principal and central frequency of 500 Hz, in the laboratory with the boards, reached 0.86 s, which is above 0.7 s, indicating that the reverberation time remained above the ideal value.

Due to this uncertainty, or the absence of T30 values for the laboratory without the boards, the T30 descriptor was discarded for comparative performance evaluation purposes.

It can therefore be concluded that the reverberation time values obtained using white noise in the laboratory with the boards demonstrated a decrease in acoustic performance, based on the EDT10 and T20 values, which increased and indicated a reflective behavior of the boards at medium frequencies. However, at high and low frequencies, the boards showed improved absorption compared to the environment without the boards in the T20 and T30 descriptors, where comparative values were available. Therefore, according to the white noise signal analysis, the laboratory without the boards exhibited better acoustic conditions at medium frequencies for spoken communication.

5.3.3 Analysis of the acoustic measurement results in the Civil Engineering Laboratory using pink noise

Analyzing the frequencies of 500 Hz and 1000 Hz for the EDT10, T20, and T30 descriptors, it was observed that all values for the 500 Hz frequency in T20 and T30, according to Table 5-3, which had previously been within the desirable limit, except for the EDT10 descriptor that presented RT = 0.82 s, showed an increase in reverberation time in Table 5-4. However, at the frequency of 1000 Hz, the values that had previously been above the acceptable range for EDT10, T20, and T30 became acceptable in T20 and T30 with the use of the boards.

At the frequencies of 2000 Hz and 4000 Hz, the T20 and T30 descriptors presented a slight reduction in reverberation time, although still outside the interval of $0.5 \leq \text{value} \leq 0.7$. In the EDT10 descriptor of the laboratory with the boards, at the low frequencies of 63 Hz, 125 Hz, and 250 Hz, according to Table 5-4, the reverberation time values increased by at least 1 s.

Table 5-3 – Reverberation Time (RT) results in seconds from the acoustic test conducted in the Civil Engineering Laboratory without the boards using the pink noise signal

Laboratory without boards Pink noise								
EDT10	**63**	**125**	**250**	**500**	**1000**	**2000**	**4000**	**8000**
	1,86	3,21	1,43	0,82	0,97	1,34	1,32	1,05
T20	**63**	**125**	**250**	**500**	**1000**	**2000**	**4000**	**8000**
	NA	2,18	1,14	0,65	0,83	1,10	1,21	0,78
T30	**63**	**125**	**250**	**500**	**1000**	**2000**	**4000**	**8000**
	NA	1,93	1,2	0,70	0,80	1,13	1,38	0,78

Source: Author (2025).

Table 5-4 – Reverberation Time (RT) results in seconds from the acoustic test conducted in the Civil Engineering Laboratory with the boards using the pink noise signal

Laboratory with boards Pink noise								
EDT10	**63**	**125**	**250**	**500**	**1000**	**2000**	**4000**	**8000**
	2,97	4,39	2,46	1,43	1,25	1,55	1,60	1,39
T20	**63**	**125**	**250**	**500**	**1000**	**2000**	**4000**	**8000**
	NA	2,06	1,24	0,82	0,69	0,84	0,93	0,79
T30	**63**	**125**	**250**	**500**	**1000**	**2000**	**4000**	**8000**
	NA	1,94	1,47	0,80	0,67	0,79	0,86	0,75

Source: Author (2025).

When comparing the acoustic behavior of the environment after the installation of the boards, a considerable deterioration in reverberation time was observed. Prior to the installation of the boards, the environment had already presented reverberation times within the desirable interval of $0.5 \leq \text{value} \leq 0.7$ for speech intelligibility, specifically in the T20 and T30 descriptors at the central frequency of 500 Hz, with RT values of 0.65 s and 0.70 s, respectively. Although the EDT10, T20, and T30 values at the frequency of 1000 Hz were already outside the recommended interval according to Table 5-3, Table 5-4 demonstrates that the central

frequency of 500 Hz exhibited a worsening in performance with the use of the boards for the EDT10, T20, and T30 descriptors.

Nevertheless, at frequencies above 1000 Hz, the reverberation time decreased, indicating improved absorption performance at high frequencies with the use of the boards, as shown in Table 5-4 for the T20 and T30 descriptors.

5.3.4 Analysis of the acoustic measurement results in the Civil Engineering Laboratory using the sweep signal

In the analysis of the values at the frequencies of 500 Hz and 1000 Hz, it was observed that the environment, both before and after the installation of the boards, presented measured values outside the desirable reverberation time interval, according to Table 5-5 and Table 5-6. This occurred despite a slight reduction in the 1000 Hz frequency value for the T20 descriptor after the installation of the boards, as shown in Table 5-6.

Table 5-5 – Reverberation Time (RT) results in seconds from the acoustic test conducted in the Civil Engineering Laboratory without the boards using the sine sweep signal

	Laboratory without boards Sine sweep							
T20	**63**	**125**	**250**	**500**	**1000**	**2000**	**4000**	**8000**
	1,40	1,35	1,10	1,25	0,95	0,95	1,40	NA
T30	**63**	**125**	**250**	**500**	**1000**	**2000**	**4000**	**8000**
	1,51	1,52	1,25	1,20	1,20	1,20	1,35	NA

Source: Author (2025).

Table 5-6 – Reverberation Time (RT) results in seconds from the acoustic test conducted in the Civil Engineering Laboratory with the boards using the sine sweep signal

	Laboratory with boards Sine sweep							
T20	**63**	**125**	**250**	**500**	**1000**	**2000**	**4000**	**8000**
	1,45	1,35	2,10	1,35	0,80	0,95	1,40	NA
T30	**63**	**125**	**250**	**500**	**1000**	**2000**	**4000**	**8000**
	1,51	1,50	1,70	1,25	1,00	1,00	1,30	NA

Source: Author (2025).

Even with the small increase in the T20 reverberation time value at the 500 Hz frequency in the laboratory with the boards, according to Table 5-6, the interval remained outside the ideal range, and the use of the boards did not demonstrate efficiency in reducing reverberation within this band. At high frequencies, such as 2000 Hz, the T30 descriptor presented a slight reduction. However, the boards proved ineffective at frequencies below 500 Hz, presenting equal or slightly higher values, as observed at 250 Hz in the T20 descriptor in Table 5-6.

This performance characteristic indicates that the boards behaved more as reflective surfaces than as absorptive materials at low frequencies. This behavior became evident through the increase in room reverberation observed in Table 5-6. At high frequencies, in the T20 descriptor, the reverberation time remained unchanged under both conditions, with and without the boards. For T30, there was a reduction in reverberation time with the use of the boards; however, the values still remained well above the recommended interval.

5.3.5 Analysis of the average results of the acoustic measurements in the Civil Engineering Laboratory

When analyzing all the values for all frequencies across the three descriptors, it can be observed that the Civil Engineering room does not present adequate reverberation time values at any frequency according to the calculated averages. However, at the central frequency of 500 Hz, the EDT10 and T20 descriptors presented values close to 0.7 s, specifically 0.81 s and 0.86 s, respectively, as shown in Table 5-7.

Table 5-7 – Average Reverberation Time (RT) results in seconds from the acoustic tests conducted in the Civil Engineering Laboratory without the boards

Average empty laboratory								
EDT10	**63**	**125**	**250**	**500**	**1000**	**2000**	**4000**	**8000**
	2,95	3,37	1,37	0,81	0,96	1,31	1,24	0,96
T20	**63**	**125**	**250**	**500**	**1000**	**2000**	**4000**	**8000**
	2,34	1,77	1,19	0,86	0,83	1,09	1,33	0,78
T30	**63**	**125**	**250**	**500**	**1000**	**2000**	**4000**	**8000**
	2,31	1,73	1,23	0,95	1,00	1,17	1,40	0,80

Source: Author (2025).

When comparing the reverberation times at high and low frequencies, it can also be observed that the environment is more reverberant at low frequencies, with reverberation times reaching two to three times the maximum ideal limit of 0.7 s.

Once again, a discrepancy can be observed in the behavior of the EDT10 descriptor when compared to the T20 and T30 results, according to the values presented in Table 5-8. At high frequencies, reverberation increased in EDT10, whereas T20 and T30 showed a reduction, indicating that the boards exhibited a slightly more absorptive behavior compared to the room walls. The same behavior can be observed for the T20 and T30 descriptors at the frequencies of 63 Hz and 125 Hz.

Table 5-8 – Average Reverberation Time (RT) results in seconds from the acoustic tests conducted in the Civil Engineering Laboratory with the boards

	Average laboratory with boards							
EDT10	**63**	**125**	**250**	**500**	**1000**	**2000**	**4000**	**8000**
	6,17	3,64	2,56	1,42	1,24	1,62	1,74	1,42
T20	**63**	**125**	**250**	**500**	**1000**	**2000**	**4000**	**8000**
	1,17	1,71	1,55	0,99	0,74	0,87	1,05	0,79
T30	**63**	**125**	**250**	**500**	**1000**	**2000**	**4000**	**8000**
	1,13	1,72	1,51	0,97	0,77	0,86	0,99	0,74

Source: Author (2025).

However, at the frequency of 250 Hz, all three descriptors showed an increase in reverberation. At the central frequency of 500 Hz, reverberation also increased with the use of the boards in all three descriptors. Nevertheless, from 1000 Hz onward, the T20 and T30 descriptors exhibited a slight reduction in reverberation time, almost reaching the desired interval.

From Figures 5-8, 5-9, and 5-10, which graphically present the average values obtained for the white noise, pink noise, and sweep signals in the EDT10, T20, and T30 descriptors for the Civil Engineering laboratory room, it can be observed that, in the EDT10 descriptor, after the installation of the boards, all reverberation times showed a slight increase at high frequencies, a greater increase at the low-mid frequencies, and a considerable variation at the frequency of 63 Hz.

Nevertheless, it is evident that the use of the boards worsened the acoustic performance of the environment regarding reverberation reduction according to the EDT10 descriptor.

Figure 5-8 – Comparison of the Average Reverberation Time (RT) results in seconds for the EDT10 descriptor obtained from the white noise, pink noise, and sweep signal measurements in the Civil Engineering Laboratory room with and without the boards

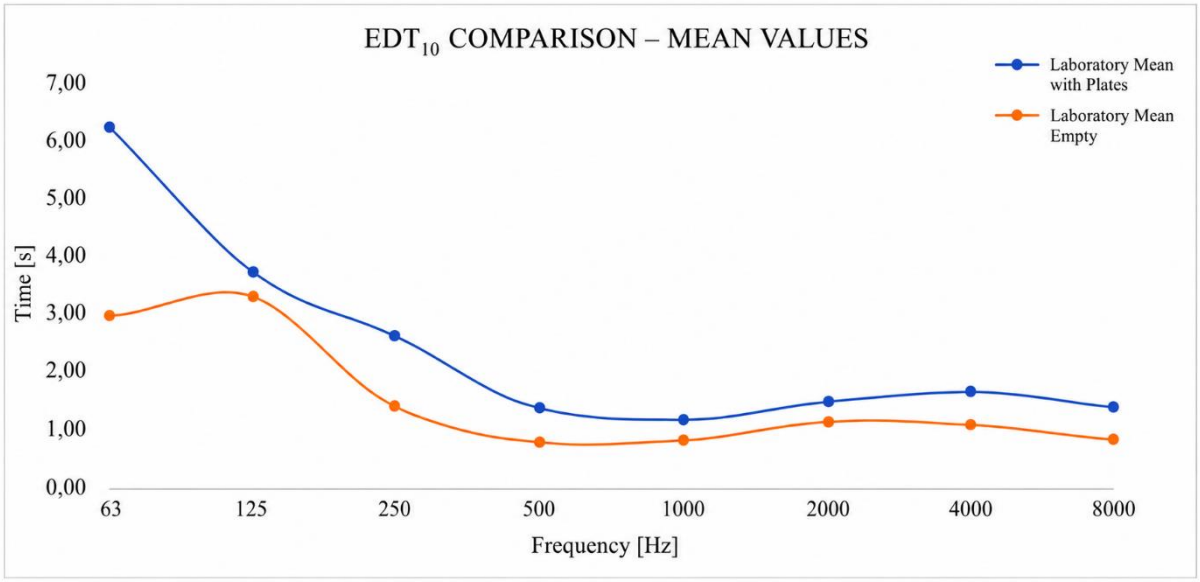

Source: Author (2025).

For the T20 descriptor shown in Figure 5-9, the averages of the signals with and without the boards indicate an improvement at medium and high frequencies starting from 1000 Hz. However, at frequencies below 1000 Hz, the performance decreased, corroborating the increase in reverberation. It can also be observed that only at the frequency of 63 Hz was there a reduction of approximately 2 s in reverberation time.

At the central frequency of 500 Hz, the absorption performance was poor, beginning to show slight improvement only from 1000 Hz onward. In no frequency band did the reverberation time remain within the ideal interval for spoken communication when using the 16 boards.

The same behavior can also be observed for the T30 descriptor in the average values presented in Figure 5-10. The boards exhibited notable absorption performance below 125 Hz, with evidence of good performance at the frequency of 63 Hz, as well as at frequencies above 500 Hz.

Figure 5-9 – Comparison of the Average Reverberation Time (RT) results in seconds for the T20 descriptor obtained from the white noise, pink noise, and sweep signal measurements in the Civil Engineering Laboratory room with and without the boards

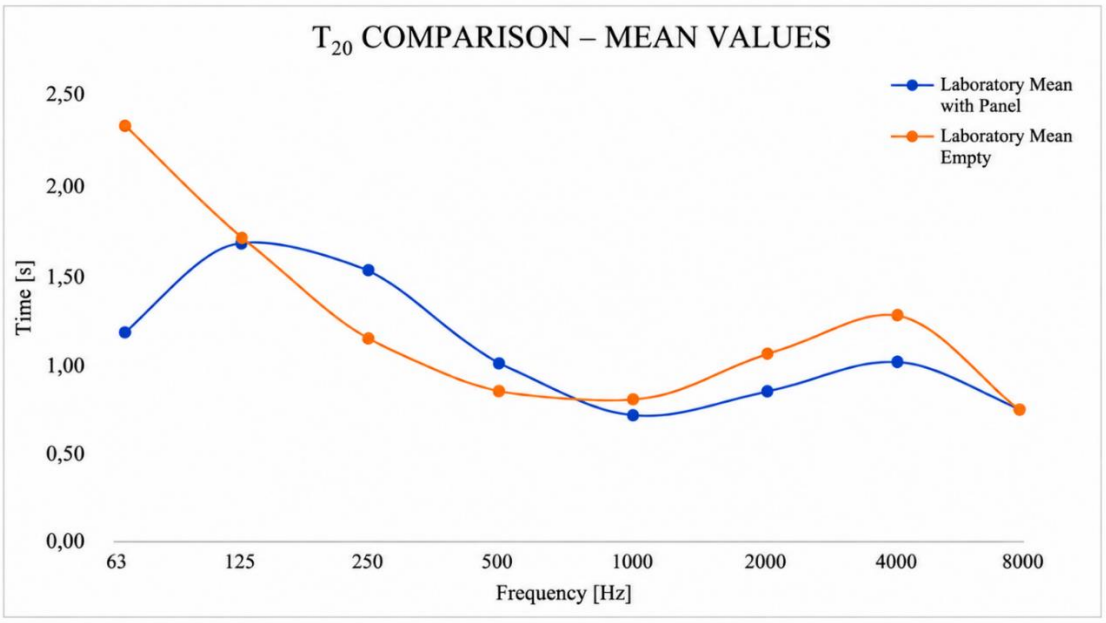

Source: Author (2025).

Figure 5-10– Comparison of the Average Reverberation Time (RT) results in seconds for the T30 descriptor obtained from the white noise, pink noise, and sweep signal measurements in the Civil Engineering Laboratory room with and without the boards

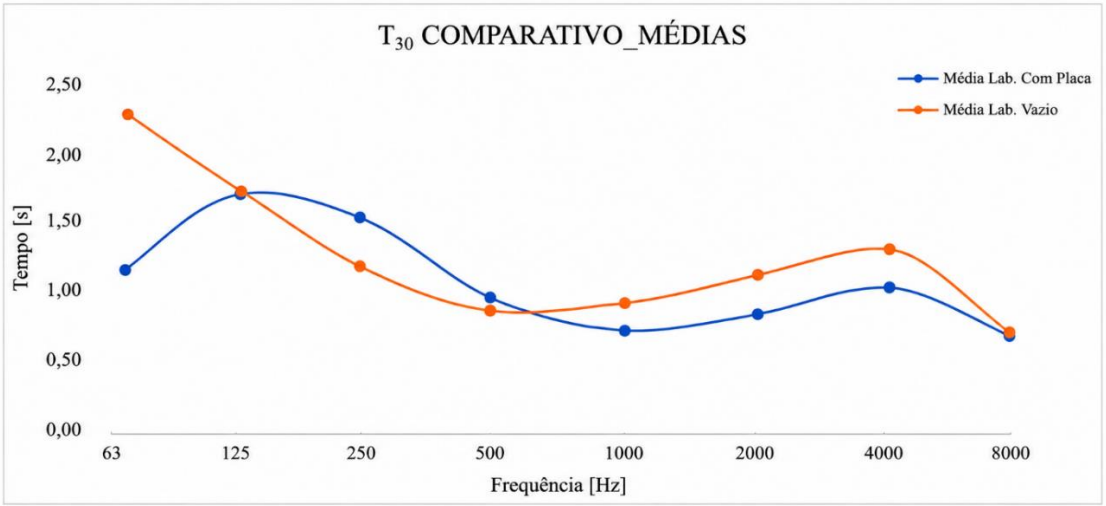

Source: Author (2025).

In this environment with smaller dimensions and volumetry, a better performance can be observed at the mid-to-high frequencies. However, at the central frequency of 500 Hz, its behavior was identical to that of the environment without the boards.

5.3.6 Analysis of the measurement results in the Architecture Classroom at the Federal

The Architecture Classroom at the Federal University of Viçosa, where the second verification of the boards' performance was carried out, has a volume of 570 m^3 and falls within the range of 200 $m^3 \leq$ Volume $<$ 10,000 m^3. For this environment, also intended for spoken communication, the desired reverberation time falls within the same recommended interval of $0.5 \leq$ value ≤ 0.7 s to ensure good speech intelligibility.

The same procedures performed in the Civil Engineering laboratory classroom at the Federal University of Viçosa were also applied in this environment. The room was excited using white noise, pink noise, and sweep signals under conditions both with and without the boards installed.

5.3.7 Analysis of the acoustic measurement results in the Architecture Classroom using white noise

According to Table 5-9, the central frequency of 500 Hz, measured only for the EDT10 descriptor, presented a reverberation time of 1.44 s, which is considerably outside the desirable range, as was also observed for the 1000 Hz frequency. No other frequency presented an RT value within the ideal interval. For the T20 and T30 descriptors, the readings were registered as NA, as previously explained for the white noise measurements conducted in the Civil Engineering Classroom.

After the installation of the boards and the new measurement procedure using white noise, it was observed that, in the EDT10 descriptor, all frequencies presented a slight reduction in their values. However, at low frequencies, these reductions were more significant, approaching a difference of 2 s, as observed at the frequencies of 63 Hz and 125 Hz in Figure 5-10.

For the T20 descriptor, the frequencies of 63 Hz and 125 Hz exhibited an even greater reduction, decreasing from 3.68 s and 4.62 s to 0.89 s and 1.99 s, respectively. This larger reduction interval occurs because the characteristics of white noise emphasize low frequencies more strongly.

Table 5-9 – Reverberation Time (RT) results in seconds from the acoustic test conducted in the Architecture Classroom at the Federal University of Viçosa without the boards using white noise

Architecture Classroom without boards White noise								
EDT10	63	125	250	500	1000	2000	4000	8000
	7,63	7,00	1,94	1,44	1,16	1,43	1,54	1,16
T20	63	125	250	500	1000	2000	4000	8000
	3,68	4,62	NA	NA	0,92	0,96	1,01	0,81
T30	63	125	250	500	1000	2000	4000	8000
	3,63	4,24	NA	NA	NA	NA	1,04	0,82

Source: Author (2025).

For EDT10, the frequencies above 1000 Hz presented a slight reduction in reverberation time after the installation of the boards. In contrast, for the T20 and T30 descriptors at frequencies above 1000 Hz, a slight increase in reverberation time was observed. This demonstrates how white noise is more effective at emphasizing low frequencies due to its spectral density characteristics.

The divergence in behavior between the T20 and T30 descriptors in relation to EDT10 (Early Decay Time) occurs because they measure different portions of the sound decay process and are influenced differently by room geometry and the distribution of absorption (Kuttruff, 2016). According to Kleiner and Tichy (2014), another probable reason may be that the ceilings of the rooms consist of acoustic mineral ceiling panels, which present absorption coefficients different from those of the room walls. This causes sound waves traveling horizontally to persist much longer than vertical waves within the environment. Consequently, the late decay represented by T30 may be significantly longer than the initial impression of “liveliness” in the room captured by EDT10.

Table 5-10 – Reverberation Time (RT) results in seconds from the acoustic test conducted in the Architecture Classroom at the Federal University of Viçosa with the boards using white noise

Architecture Classroom with boards White noise								
EDT10	63	125	250	500	1000	2000	4000	8000
	5,73	4,72	2,35	1,17	1,13	1,22	1,14	0,99
T20	63	125	250	500	1000	2000	4000	8000
	0,89	1,99	NA	1,06	0,99	0,98	1,08	0,81
T30	63	125	250	500	1000	2000	4000	8000
	0,83	1,47	NA	NA	NA	MA	1,13	0,84

Source: Author (2025).

If the values at the frequencies of 63 Hz and 125 Hz are examined again after the installation of the boards, it can be observed that all three descriptors presented a considerable reduction within these frequency bands, classified as sub-bass frequencies. However, this reduction was still insufficient to lower the reverberation time to within the ideal interval. This may have occurred because the total surface area of the boards was not large enough to provide greater absorption. Nevertheless, it is important to consider the influence of white noise at low frequencies, whose behavior does not necessarily reflect the subjective perception of the human auditory system.

5.3.8 Analysis of the acoustic measurement results in the Architecture Classroom using pink noise

Analyzing the values obtained at the central frequencies of 500 Hz and 1000 Hz, which were 1.42 s and 1.09 s respectively for the EDT10 descriptor, and for the T20 descriptor at the frequency of 1000 Hz, whose value was 1.04 s according to Table 5-11, it can be concluded that the room presents acoustically unfavorable conditions, since the values exceed the ideal reverberation time interval of $0.5\ s \leq RT \leq 0.7\ s$ recommended for environments intended for spoken communication.

Table 5-11 – Reverberation Time (RT) results in seconds from the acoustic test conducted in the Architecture Classroom at the Federal University of Viçosa without the boards using pink noise

Architecture Classroom without boards								
Pink noise								
EDT10	63	125	250	500	1000	2000	4000	8000
	7,66	5,29	1,52	1,42	1,09	1,16	1,20	0,94
T20	63	125	250	500	1000	2000	4000	8000
	3,59	NA	NA	NA	1,04	1,01	1,02	0,94
T30	63	125	250	500	1000	2000	4000	8000
	2,16	NA	NA	NA	NA	NA	NA	NA

Source: Author (2025).

The room exhibited high-frequency values that were closer to the ideal range, although still numerically above the recommended interval. However, when analyzing the low frequencies, the environment proved to be highly unfavorable because the reverberation time was extremely high, reaching values of 7.66 s at the frequency of 63 Hz and 5.29 s at 125 Hz for the EDT10 descriptor, while similarly elevated values were also observed in T20 at 63 Hz.

After the installation of the boards, the EDT10 descriptor for the frequencies of 500 Hz and 1000 Hz presented values of 2.77 s and 1.43 s, respectively, resulting in extremely high values for environments intended for spoken communication, as shown in Table 5-12. The boards behaved more as reflective materials than as absorptive ones, since they caused a greater persistence of sound within the environment. This was confirmed by the increase in reverberation time and was particularly evident at the central frequency of 500 Hz, where the value almost doubled, increasing from 1.42 s to 2.77 s.

It was also observed that, at the high frequencies of 2000 Hz, 4000 Hz, and 8000 Hz, the EDT10 and T20 descriptors showed an increase in reverberation time, confirming the more reflective behavior of the boards compared to the absorption characteristics of the room walls. At the low frequencies of 63 Hz and 250 Hz, the EDT10 descriptor also exhibited an increase in reverberation, demonstrating reflective behavior at low frequencies as well.

Table 5-12 – Reverberation Time (RT) results in seconds from the acoustic test conducted in the Architecture Classroom at the Federal University of Viçosa with the boards using pink noise

Architecture Classroom with boards Pink noise								
EDT10	63	125	250	500	1000	2000	4000	8000
	7,80	3,77	2,58	2,77	1,43	1,47	1,48	0,99
T20	63	125	250	500	1000	2000	4000	8000
	0,76	1,93	NA	NA	NA	1,26	1,06	0,95
T30	63	125	250	500	1000	2000	4000	8000
	0,63	1,87	NA	NA	NA	NA	1,12	0,93

Source: Author (2025).

However, at the low frequency of 63 Hz, the T20 and T30 descriptors presented values considerably lower than those observed at the other frequencies, falling within the ideal reverberation time range for spoken communication. The values for 125 Hz and 250 Hz were not determined in the room without the boards; therefore, it was not possible to compare the same frequencies after the installation of the boards with the subsequently obtained values. These values might have continued the tendency of reverberation time reduction observed in the T20 and T30 descriptors.

At high frequencies above 1000 Hz, all frequency bands presented an increase in reverberation time, indicating a more reflective behavior at high frequencies, as evidenced by the EDT10 and T20 descriptors. Only the frequency of 63 Hz, in the T20 and T30 descriptors, demonstrated good absorption performance at low frequencies. Nevertheless, due to the lack of available information, the frequencies of 125 Hz and 250 Hz could not be compared because of the NA values.

5.3.9 Analysis of the acoustic measurement results in the Architecture Classroom using the sweep signal

Using the sweep signal in the evaluation of the room without the boards, it was observed that, for both the T20 and T30 descriptors, the values at the central frequencies of 500 Hz and 1000 Hz were 1.90 s and 1.35 s of reverberation time, respectively, according to Table 5-13. These values are excessively high and remain outside the acceptable limits for the acoustic

function intended for a classroom environment. Furthermore, for all the other frequencies and descriptors, the reverberation time values were also above 1s.

Table 5-13 – Reverberation Time (RT) results in seconds from the acoustic test conducted in the Architecture Classroom at the Federal University of Viçosa without the boards using the sine sweep signal

Architecture Classroom without boards Sine sweep								
T20	63	125	250	500	1000	2000	4000	8000
	1,75	1,70	1,35	**1,90**	**1,35**	1,40	1,35	NA
T30	63	125	250	500	1000	2000	4000	8000
	1,80	1,75	1,35	**1,60**	**1,30**	1,30	1,30	NA

Source: Author (2025).

After the installation of the boards, a new measurement was performed using the sweep signal, and the values at the frequencies of 500 Hz and 1000 Hz still remained above the ideal values for a classroom environment. Even though the T20 descriptor showed a slight decrease at 500 Hz, varying from 1.90 s in the room without the boards to 1.75 s in the room with the boards, according to Table 5-14, the reverberation times remained excessively high.

Table 5-14 – Reverberation Time (RT) results in seconds from the acoustic test conducted in the Architecture Classroom at the Federal University of Viçosa with the boards using the sine sweep signal

Architecture Classroom with boards Sine sweep								
T20	63	125	250	500	1000	2000	4000	8000
	1,65	1,50	1,21	1,75	1,35	1,40	1,38	NA
T30	63	125	250	500	1000	2000	4000	8000
	1,70	1,65	1,30	1,50	1,18	1,18	1,23	NA

Source: Author (2025).

All T20 and T30 reverberation time values for all frequencies were unsuitable for spoken communication and instead more characteristic of a musical environment, since they indicate greater sound persistence within the room. The behavior of the 16 boards was

insufficient to promote a substantial reduction in reverberation capable of bringing the environment within the recommended limits, despite the slight reduction in values observed at nearly all frequencies in both descriptors.

5.3.10 Analysis of the average results of the acoustic measurements in the Architecture Classroom

When analyzing the average values of the three descriptors for the environment without the boards, it can be concluded that all frequencies presented values above 1 s, therefore remaining outside the ideal reverberation time interval. At low frequencies, the room exhibited extremely high values in the 63 Hz and 125 Hz bands, indicating a reflective behavior of the materials composing the environment, as shown in Table 5-15. At high frequencies, the environment proved to be less reflective.

Table 5-15 – Average Reverberation Time (RT) results in seconds from the acoustic tests conducted in the Architecture Classroom at the Federal University of Viçosa without the boards using the sine sweep signal

Architecture Classroom **Average classroom without boards**								
EDT10	63	125	250	500	1000	2000	4000	8000
	7,65	6,15	1,73	1,43	1,13	1,30	1,37	1,05
T20	63	125	250	500	1000	2000	4000	8000
	3,01	3,16	1,35	1,90	1,10	1,12	1,13	0,88
T30	63	125	250	500	1000	2000	4000	8000
	2,53	3,00	1,35	1,60	1,30	1,30	1,17	0,82

Source: Author (2025).

However, despite these differences, the room was not found to provide adequate acoustic conditions for spoken communication in any of the descriptors or at any of the analyzed frequencies.

Based on the average measurements performed in the environment after the installation of the boards, it can be concluded that, for all three descriptors, the frequencies of 63 Hz and 125 Hz presented a reduction in reverberation time, with the exception of the 250 Hz frequency in the EDT10 descriptor, whose value increased from 1.73 s to 2.47 s. However, the values still

remained above 1 s despite reductions of nearly 2 s at some frequencies, such as 63 Hz in T20, and approximately 1.5 s at 125 Hz for T20 and T30.

This performance could potentially be enhanced by increasing the absorptive area of the environment through the installation of a greater number of boards. At the high frequencies of 2000 Hz, 4000 Hz, and 8000 Hz, the values fluctuated slightly upward or downward within a maximum interval of 0.12 s, indicating that the boards exhibited essentially the same reflective behavior as the original walls of the environment, making them unnecessary for absorption purposes at high frequencies.

Table 5-16 – Average Reverberation Time (RT) results in seconds from the acoustic tests conducted in the Architecture Classroom at the Federal University of Viçosa with the boards using the sine sweep signal

Architecture Classroom **Average classroom with boards**								
EDT10	63	125	250	500	1000	2000	4000	8000
	6,77	4,25	2,47	1,97	1,28	1,35	1,31	0,99
T20	63	125	250	500	1000	2000	4000	8000
	1,10	1,81	1,21	1,41	1,17	1,21	1,17	0,88
T30	63	125	250	500	1000	2000	4000	8000
	1,05	1,66	1,30	1,50	1,18	1,18	1,16	0,89

Source: Author (2025).

From Figures 5-11, 5-12, and 5-13, which present the average values obtained for the white noise, pink noise, and sweep signals in the EDT10, T20, and T30 descriptors for the Architecture Classroom with and without the installation of the boards, it is possible to infer the acoustic absorption performance behavior of these boards.

For the EDT10 descriptor, after the installation of the boards, an increase in acoustic absorption was observed at low frequencies only in the 63 Hz and 125 Hz bands. In the frequency range between 250 Hz and 1000 Hz, a slight deterioration in performance was verified in comparison to the condition without the boards. This frequency range is considered critical for speech intelligibility, indicating that the application of the boards did not provide significant improvement in reverberation time within these bands.

Figure 5-11 – Comparison of the average Reverberation Time (RT) results in seconds for the EDT10 descriptor obtained from the white noise, pink noise, and sweep signal measurements in the Architecture Classroom with and without the boards

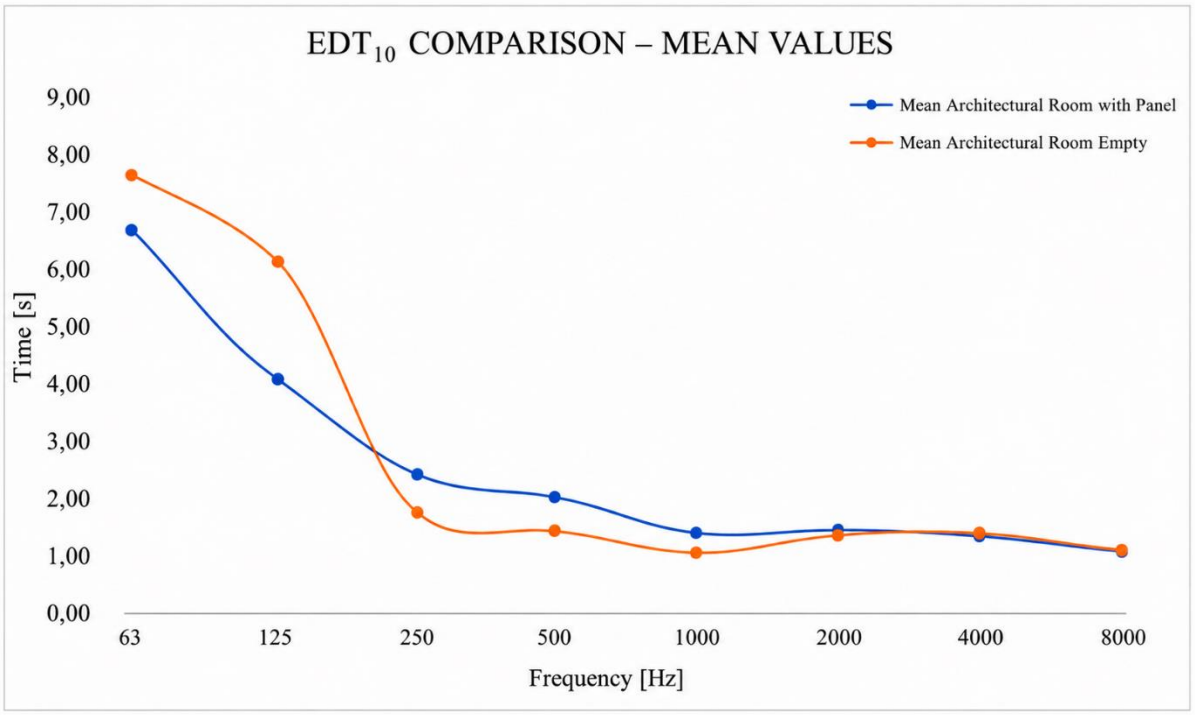

Source: Author (2025).

Figure 5-12 – Comparison of the average Reverberation Time (RT) results in seconds for the t20 descriptor obtained from the white noise, pink noise, and sweep signal measurements in the Architecture Classroom with and without the boards

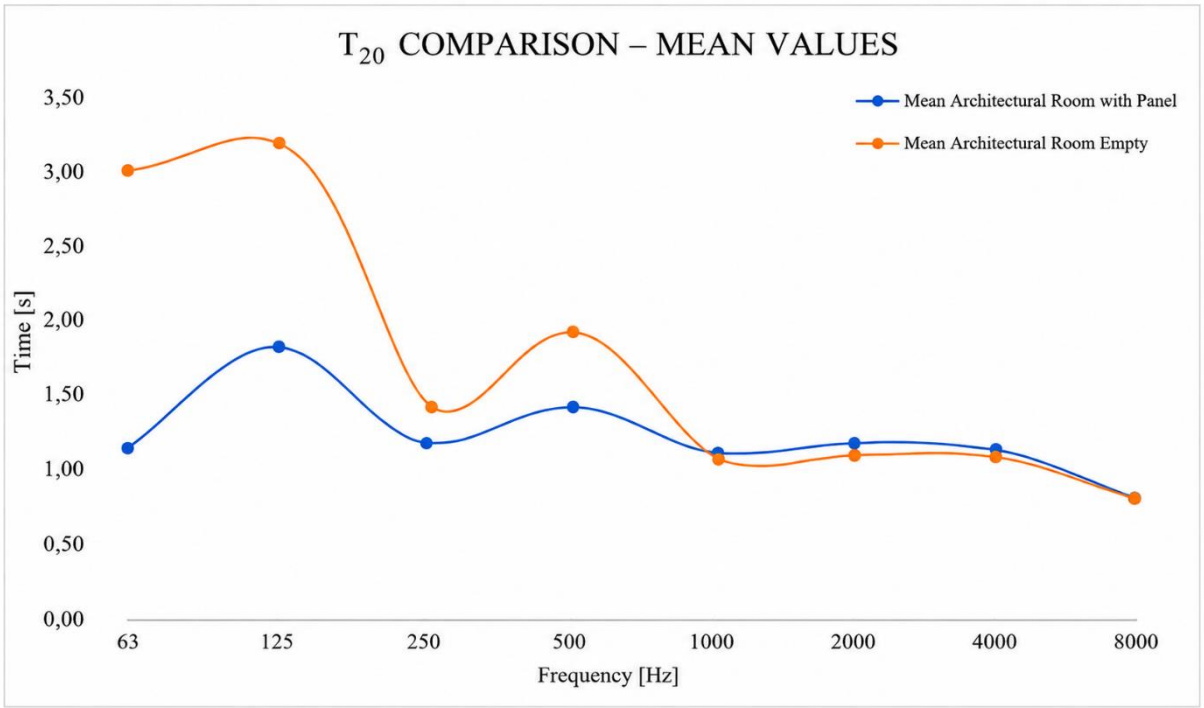

Source: Author (2025).

Figure 5-13 – Comparison of the average Reverberation Time (RT) results in seconds for the t30 descriptor obtained from the white noise, pink noise, and sweep signal measurements in the Architecture Classroom with and without the boards

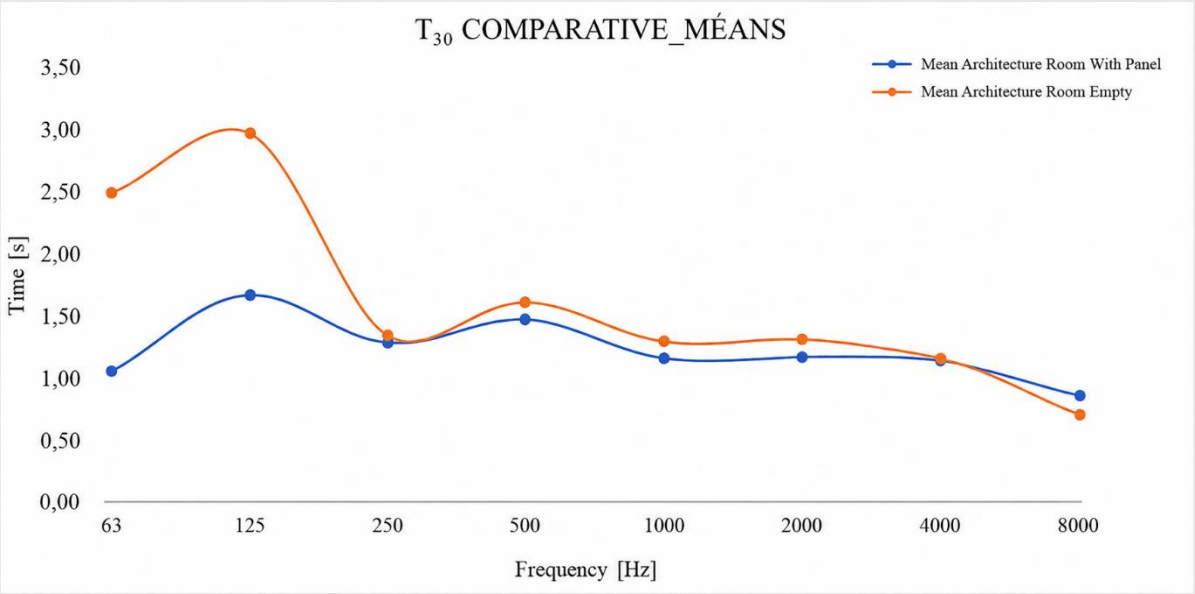

Source: Author (2025).

Furthermore, at high frequencies, the acoustic absorption behavior was similar to that observed for the room walls without the boards, suggesting that, at these frequencies, the boards present an acoustic absorption coefficient equivalent to that of the wall surface for this descriptor.

For the T20 descriptor, it can be observed that, at frequencies below 1000 Hz, according to Table 5-12, the installation of the boards resulted in a reduction in the room reverberation time. In the 63 Hz and 125 Hz bands, this reduction was approximately 2 s, demonstrating a significant improvement in reverberation control attributed to the acoustic absorption behavior of the boards at sub-bass frequencies.

However, for frequencies above 1000 Hz, the observed performance was inferior to that presented by the room wall surfaces themselves. This result indicates that, at high frequencies, the boards exhibit a more reflective behavior when compared to the room walls. Therefore, the acoustic absorption coefficient of the boards within these bands is lower than that of the walls, making them unsuitable or only minimally effective for controlling reverberation time at high frequencies.

For the T30 descriptor, it was observed that below 4000 Hz the boards presented a subtle improvement in reverberation time. However, their best performance was also perceived at the

frequencies of 63 Hz and 125 Hz, where they achieved a reduction of approximately 1 s to 1.5 s in the room reverberation time.

5.5 Conclusion

Fundamentally, it is well established that the critical frequencies for communication, ensuring that speech is perfectly understood within an environment (good speech intelligibility), are those between 2000 Hz and 4000 Hz. From the perspective of information concentration, the three octave bands of 1000 Hz, 2000 Hz, and 4000 Hz are the most important because they provide approximately 75% of the intelligibility content of human speech.

Regarding auditory sensitivity, the human ear evolved to be more sensitive precisely within the range between 2000 Hz and 4000 Hz, where consonants and vocal tract resonances (formants) are more prominent. Based on this information, it was found that the reverberation time at these frequencies in the Architecture Classroom, with the use of the boards, remained practically with the same acoustic behavior, or even worse, than when the boards were absent. Therefore, for high frequencies, the boards became unnecessary, since they behaved as though they possessed the same absorption coefficient as the uncovered walls.

In this research, one of the specific objectives was to determine whether the rubber contributed to reducing reverberation times at low frequencies, and the results demonstrated that it did. The reverberation times obtained through the use of the boards in the Architecture Classroom contributed to an almost 50% reduction in RT at the so-called sub-bass frequencies of 63 Hz and 125 Hz. The reverberation time within the environment at these frequencies, for the T20 and T30 descriptors, was reduced to nearly half with the installation of the boards, as shown in Figure 5-12 and Figure 5-13.

However, for the descriptor that most closely resembles the subjective behavior of human hearing, EDT10, the reduction at 63 Hz and 125 Hz was approximately 1 s. In contrast, within the principal speech frequency bands, the boards exhibited worse performance, increasing reverberation more than the uncovered walls.

Nevertheless, the 16 boards were unable to reduce the low-frequency reverberation times to within the ideal interval, despite these frequencies not being critical for speech communication. This likely occurred due to the insufficient amount of absorptive material in the environment, indicating that the total surface area of the boards was insufficient or that their absorption coefficient was low.

In the Civil Engineering laboratory classroom at the Federal University of Viçosa, which has a smaller volume and a smaller wall area relative to the board area, a deterioration was observed across all frequency bands in the EDT10 descriptor. This indicates that the boards are more reflective than the walls, or at least less absorptive than them. The boards slightly reduced the RT values at high frequencies from 500 Hz to 8000 Hz in the T20 and T30 descriptors, indicating an absorption coefficient slightly better than that of the walls. They also produced a 50% reduction in RT at the frequency of 63 Hz for the same descriptors.

However, at the central and most important frequency of 500 Hz, the values remained very close, making the use of the boards practically unnecessary for environments intended for spoken communication and with small volumes. It can therefore be concluded from these comparisons that the boards present good performance at sub-bass frequencies; however, at medium and high frequencies, their use, according to the EDT10 descriptor, is not necessary.

5.6 References

ALETTA, F.; KANG, J. Historical acoustics: relationships between people and sound over time. **Acoustics**, v. 2, n. 1, p. 128-130, 2020. https://doi.org/10.3390/acoustics2010009

BISTAFA, S. R. **Acústica aplicada ao controle do ruído**. 2.ed. São Paulo: Blucher, 2018.

EVEREST, F. A.; POHLMANN, K. C. **Master handbook of acoustics**. 7.ed. New York: McGraw Hill, 2021.

GINN, K. B. **Architectural acoustics**. São Paulo: Brüel & Kjær, 1978.

KLEINER, M.; TICHY, J. **Acoustics of small rooms**. London: CRC Press, 2014. https://doi.org/10.1201/b16866

KUTTRUFF, H. **Room acoustics**. 6.ed. Boca Raton: CRC Press, 2016. https://doi.org/10.1201/9781315372150

LONG, M. **Architectural a coustics**. Burlington, MA: Elsevier Academic Press, 2006.

MEHTA, M. L.; JOHNSON, J.; ROCAFORT, J. **Architectural acoustics**: principles and design. London, UK: Pearson, 1998.

MOMMERTZ, E. **Acoustics and sound insulation**: principles, planning, examples. Basel, Suíça: Birkhäuser, 2009.

PATRÍCIO, J. **Acústica nos edifícios**. Porto, Espanha: Publindústria Edições Técnicas, 2018.

PROCEL EDIFICA. **Acústica arquitetônica**. Rio de Janeiro: PROCEL, 2011. Available in: https://toaz.info/doc-view-4. Access in: 4 nov. 2025.

RINDEL, J. H. **Sound insulation in buildings**. Boca Raton, FL: CRC Press, 2017. https://doi.org/10.1201/9781351228206

6 CONCLUDING REMARKS

The present research consistently demonstrated the importance of the sustainable nature of the work by incorporating shredded tire rubber waste into gypsum matrices. The study promotes the valorization of a waste material that has difficult environmental disposal. In this way, it contributes to reducing the consumption of virgin raw materials in the construction industry. The reuse of this waste is aligned with sustainability guidelines, the circular economy, and the reduction of environmental impacts, while also presenting technical feasibility for acoustic applications in buildings, respecting its structural and acoustic limitations.

Regarding the specific objectives, all were achieved throughout the development of the research. The study defined the limits of rubber incorporation that did not compromise the mechanical performance of the panels, ensuring compressive and flexural strength compatible with the proposed non-structural use. Subsequently, different particle sizes and rubber contents were evaluated, identifying those that provided the best overall acoustic performance and, especially, better behavior at low frequencies, which was the central focus of the research.

The literature review highlighted the relevance of rubber as a material with a high damping capacity in various applications due to its viscoelastic behavior, an essential characteristic for the dissipation of sound energy, especially at low frequencies. National and international studies indicated that rubber waste, when incorporated into composites used in various civil construction applications, presents significant potential for sound absorption and vibration reduction. This addresses an important gap in the acoustic control of built environments, especially where conventional materials show limited insulation performance.

The results of the experimental tests, obtained through mechanical strength tests and impedance tube measurements, confirmed that the controlled incorporation of rubber waste did not make the structural performance of the panels unfeasible and, at the same time, improved their acoustic behavior.

In the impedance tube tests, the obtained absorption coefficient values demonstrated that, for airborne noise absorption, rubber particles should be applied on the surface of the panel, leaving their pores in direct contact with the sound energy for airborne noise absorption purposes. This would contribute to subsequent reverberation control in environments intended for speech. In this way, the role of rubber as an acoustic energy dissipation element would be further enhanced.

Finally, when verifying the sound absorption results under real conditions of use, with the application of the panels in classrooms, it was observed that they achieved good

performance in the so-called sub-bass frequencies, located in frequency bands below 125 Hz. However, for the purpose of reverberation time control within the critical range for speech intelligibility, the performance was not satisfactory, making their application unnecessary for this purpose.

Although this result was not relevant for the human voice frequency range, in which intelligibility is more associated with medium and high frequencies, the control of low frequencies contributes to reducing acoustic discomfort, sound masking, and the sensation of residual noise within the environment.

As a suggestion for future research, it is recommended to further investigate the incorporation of rubber into gypsum panels mainly intended for sound insulation, due to its vibration damping capacity, as demonstrated in the literature review and in the low absorption coefficient values obtained in the impedance tube tests and in the real application tests conducted in classrooms. Exploring mass-spring-mass systems, which are typical of gypsum partitions, indicates an approach with strong potential to improve sound insulation between environments, especially at low frequencies, consolidating its use as a sustainable, efficient, and technically feasible solution for acoustic comfort in civil construction.

GLOSSARY

Acoustic Comfort: The condition of an environment in which sound pressure levels and acoustic parameters (reverberation time, speech intelligibility, and background noise) are appropriate to the function of the space and the needs of its users. In Brazil, it is regulated by ABNT NBR 10152:2017, which establishes reference sound pressure level values for indoor building environments according to their intended use.

Acoustic Conditioning: A set of acoustic interventions applied to an environment with the aim of creating a pleasant acoustic quality by controlling undesirable echoes and reverberation without necessarily preventing sound transmission between spaces. It differs from sound insulation: in acoustic conditioning, the incident sound energy should be absorbed or transmitted rather than reflected back into the environment.

Acoustic Impedance: A quantity expressing the resistance that a medium or material offers to the propagation of sound waves. It is defined as the product of the medium density and the speed of sound propagation ($Z = \rho \cdot c$). Differences in impedance between media cause partial reflection of waves at the interface. Impedance matching is a fundamental principle in the design of sound-absorbing materials.

Acoustic Insulation: A set of techniques and materials intended to prevent or reduce the transmission of sound energy (airborne noise) from one environment to another adjacent space through walls, floors, roofs, and partitions. In a system with good acoustic insulation, the incident sound energy is reflected back into the source environment. It is quantified by Sound Transmission Loss (STL) and regulated in Brazil by ABNT NBR 15575.

Airborne Noise: Noise that propagates through the air and enters an environment through open paths (such as gaps in doors and windows) or through direct transmission across walls and partitions. Airborne noise insulation is quantified by Sound Transmission Loss (STL), regulated in Brazil by ABNT NBR 15575.

Airflow Resistivity: A property that quantifies the resistance of a material to airflow through its porous structure, measured in $Pa \cdot s/m^2$ ($N \cdot s/m^4$). It constitutes one of the three fundamental parameters for the acoustic characterization of sound-absorbing materials, together with porosity and tortuosity. Materials with appropriate airflow resistivity exhibit greater absorption efficiency.

α (alpha) – Sound Absorption Coefficient: A dimensionless quantity that expresses the ratio between the non-reflected sound energy (absorbed and transmitted) and the incident sound energy on a material. Its value ranges from 0 (total reflection) to 1 (total absorption). It is defined by the equation: $\alpha = 1 - (Er / Ei)$, where Er is the reflected energy and Ei is the incident energy. It may be measured in a reverberation chamber (Sabine absorption coefficient, ãS) according to ISO 354:2003, or in an impedance tube according to ISO 10534:2001 and ASTM E1050-12.

ãS – Sabine Absorption Coefficient: A sound absorption coefficient determined in a reverberation chamber according to ISO 354:2003. It represents the average absorption of a surface or material under diffuse sound field conditions within the chamber. It is mainly used for the calculation and control of room reverberation time.

Background Noise: The sound pressure level present in an environment in the absence of the specific sound sources being evaluated. Background noise must be controlled so that it does not compromise speech intelligibility or acoustic measurements. In reverberation time measurements, the excitation signal must exceed the background noise by at least 35 dB (for T20) or 45 dB (for T30), according to ABNT NBR ISO 3382-2.

Band Center Frequency: The frequency representing the geometric center of an octave band or one-third octave band. The standardized center frequencies of octave bands are: 31.5, 63, 125, 250, 500, 1000, 2000, 4000, 8000, and 16,000 Hz. Each center frequency is twice the value of the preceding one in the octave series.

Bel (B): A logarithmic unit used to measure power level relative to a reference power, named after Alexander Graham Bell. It may assume positive values (power greater than the reference) or negative values (power lower than the reference). In practice, its submultiple, the decibel (dB), is commonly used, such that 1 B = 10 dB.

Bulk Viscosity: A fluid property that encompasses the energy loss effects associated with hydrostatic compression of the fluid, distinct from shear viscosity. It contributes to sound dissipation in compressible fluids.

C80 – Clarity Index: An objective acoustic descriptor used to evaluate the clarity and transparency of music in enclosed spaces. It is defined as the logarithmic ratio (in dB) between the sound energy arriving within the first 80 ms after the direct sound and the total sound energy arriving after this 80 ms interval. It is calculated by: $C80 = 10 \cdot \log_{10} [\int_0^{80} p^2(t)\, dt / \int_{80}^{\infty} p^2(t)\, dt]$, where p represents sound pressure and t represents time. Typical values in concert halls range from −4 dB to +1 dB. Positive values indicate high clarity, whereas negative values indicate predominance of late reverberant energy.

Cocktail Party Effect: A psychoacoustic phenomenon describing the human ability to focus auditory attention on a single sound stimulus while simultaneously filtering out other stimuli and background noise present in the environment. It is relevant in the assessment of acoustic comfort in collective-use environments, such as restaurants and dining spaces.

Coincidence Effect: An acoustic phenomenon that occurs when the wavelength of the wall's bending wave component coincides with the wavelength of the incident sound at a given angle, resulting in a significant reduction in sound insulation at that frequency. The coincidence frequency depends on the mass and bending stiffness of the wall material.

Coincidence Frequency – see Coincidence Effect: See entry: Coincidence Effect.

D50 – Definition (Definition 50): An acoustic descriptor used to evaluate speech clarity in an environment. It represents the ratio between useful sound energy (direct sound and reflections arriving within 50 ms) and the total sound energy. It is calculated by: $D50 = \int_0^{50} g^2(t)\, dt / \int_0^{\infty} g^2(t)\, dt$, where g(t) is the impulse response of the room. D50 values above 0.5 (50%) indicate good speech clarity, whereas values below 0.3 (30%) denote poor clarity, especially in frequency bands up to 2 kHz. It is the speech equivalent of the C80 parameter used for music.

dB (decibel): A submultiple of the bel, equal to one tenth of a bel (1 B = 10 dB). It is a logarithmic unit widely used to express sound levels, power, and derived quantities in

acoustics. A doubling of sound energy corresponds to an increase of 3 dB, whereas a tenfold increase corresponds to an increase of 10 dB.

Dry Construction (Drywall): A vertical partition construction system that uses galvanized steel profiles and gypsum plasterboards (drywall) without the use of mortar. It offers advantages such as rapid installation, reduced weight, and the possibility of incorporating acoustic materials. In this thesis, it is the target construction system for the application of the developed gypsum–rubber boards.

Early Decay Time – see EDT10: See entry: EDT10 – Early Decay Time.

Early Reflections (Primary Reflections): Sound reflections that occur within an enclosed environment before the sound field becomes diffuse. They are generated by reflective surfaces located near the sound source and reach the listener with short delays relative to the direct sound. Depending on the delay time and room geometry, they may cause sound cancellations, echoes, and reduced speech intelligibility.

EDT10 – Early Decay Time: An acoustic descriptor that measures the time required for the sound pressure level to decay by 10 dB from its initial steady-state value, with this time multiplied by 6 to extrapolate the equivalent 60 dB decay. It is calculated from the initial portion of the room decay curve. EDT10 is the descriptor most strongly correlated with the subjective perception of reverberation by the human ear, since the auditory system is more sensitive to the initial decay. It is measured over the range from 0 to −10 dB.

Elastomer: A class of polymers with pronounced elastic properties, capable of undergoing large deformations and returning to their original shape after load removal. Natural rubber (polyisoprene) and synthetic SBR rubber (styrene-butadiene rubber) are examples of elastomers used in tire manufacturing and investigated in this thesis due to their vibroacoustic properties.

f – Frequency: The number of complete oscillation cycles of a sound wave per unit time, measured in hertz (Hz). It is defined as the inverse of the period (T): $f = 1/T$. Frequency is one of the most important characteristics of sound, determining the perception of pitch (low or high). The human hearing range extends from 20 Hz to 20,000 Hz (20 kHz).

FFT – Fast Fourier Transform: An efficient computational algorithm for calculating the Discrete Fourier Transform. It is used in the processing of sweep signals (sine sweep signals) to obtain the Room Impulse Response (RIR) in room acoustics measurements. It enables the decomposition of a time-domain signal into its frequency components.

Fibrous Materials: A class of sound-absorbing materials composed of fibers (natural or synthetic) forming a porous network. Examples include rock wool, glass wool, and cellulose fiber. The absorption mechanism is primarily based on the viscous effect of air converting acoustic energy into thermal energy. These materials exhibit good absorption at medium and high frequencies (above 2,000 Hz).

Fourier Transform: A mathematical operation that decomposes a signal in the time domain into its frequency components (spectrum), and vice versa. It is fundamental in acoustic analysis, being used to obtain the sound spectrum from the waveform and to process the sweep signal in the determination of the Room Impulse Response (RIR).

FTIR – Fourier Transform Infrared Spectroscopy: An analytical technique for chemical characterization that uses the absorption of infrared radiation to identify the functional groups and chemical bonds present in a material. In this thesis, it was used for the chemical characterization of shredded tire rubber particles, identifying groups such as C–H, C=C, S–S, and aromatic rings present in the composition of SBR rubber.

fu and fL – Frequency Band Limits: fu designates the upper frequency limit of a band, while fL designates the lower frequency limit. In an octave band, the ratio fu/fL = 2:1. In a one-third octave band, the ratio is 2^(1/3) ≈ 1.26.

g(t) – Room Impulse Response: A function describing the acoustic response of an enclosure in the time domain to excitation by an ideal acoustic impulse (Dirac impulse). It represents the "acoustic signature" of the space. It is used in the calculation of acoustic descriptors such as D50 and C80 and is obtained through measurements using sweep signals and FFT processing, according to the Schroeder Method.

Gypsum (Calcium Sulfate Hemihydrate): A mineral binder obtained through the partial calcination of calcium sulfate dihydrate (gypsum rock). Chemical formula: $CaSO_4 \cdot \frac{1}{2}H_2O$. It is the principal component of gypsum plasterboards (drywall). In this thesis, it constitutes the matrix of the investigated composites, into which shredded tire rubber particles are incorporated.

Gypsum–Rubber Composite: A material produced by incorporating shredded tire rubber particles into a gypsum matrix (calcium sulfate hemihydrate). The composite combines acoustic properties (particularly low-frequency sound absorption) with mechanical feasibility and environmental sustainability. It is the subject of investigation in this thesis for application in boards and vertical partition panels in drywall construction systems.

Haas Effect: A psychoacoustic phenomenon in which the human auditory system integrates the direct sound and the first reflections (with delays of up to 35 ms) as if they were a single sound event, merging them in the perception of direction and intensity. It is relevant for understanding the EDT and D50 metrics.

Helmholtz Resonator: A resonant acoustic device consisting of a rigid cavity connected to the surrounding space through a neck (narrow opening). It selectively absorbs sound energy at a resonance frequency determined by the cavity volume and the dimensions of the neck. Energy is dissipated through viscous friction of the air within the neck. It is commonly used as a low-frequency absorber.

Human Hearing Range: The interval of frequencies detectable by the human auditory system, extending approximately from 20 Hz to 20,000 Hz (20 kHz). Sounds below 20 Hz are called infrasound, while sounds above 20 kHz are referred to as ultrasound. In architectural acoustics, the most relevant frequency bands are typically between 63 Hz and 8000 Hz.

Hz (hertz): The International System (SI) unit of frequency, equivalent to one cycle per second (1 Hz = 1 cycle/s). In acoustics, it is used to express the frequency of sound waves and the center frequency of spectral analysis bands.

Impact Noise: Noise generated by the direct mechanical excitation of structures (floors, slabs) due to impacts (footsteps, falling objects). It propagates predominantly through structural transmission (solid vibration). The control of impact noise is referred to as sound isolation.

Impedance Tube (Kundt Tube): A laboratory device used to measure the sound absorption coefficient (α) and the acoustic impedance of materials under normal incidence, according to ISO 10534:2001 and ASTM E1050-12. It consists of a rigid tube with a sound source at one end and the sample material at the other, with two microphones positioned along the tube for transfer function analysis. In this thesis, it was used to measure the α of gypsum–rubber composites in cylindrical samples with diameters of 29 mm or 100 mm.

Infrasound: Sounds with frequencies below 20 Hz, beneath the threshold of human hearing. Although inaudible, prolonged exposure to high levels may produce adverse physical and psychological effects. Infrasound is relevant in the context of low-frequency noise control in buildings.

Internal Damping (Hysteresis): A mechanism of energy dissipation occurring in solids and elastomeric materials, such as rubber, in which mechanical energy is dissipated through internal friction between molecules during cycles of deformation and elastic recovery. This phenomenon is particularly relevant to the vibroacoustic behavior of rubber-based composites.

λ (lambda) – Wavelength: The distance traveled by a sound wave during one complete cycle of pressure variation. It is defined as the distance between two consecutive points in the same phase. It is calculated by the equation: $\lambda = c / f$, where c is the speed of sound in the medium (approximately 343 m/s in air at 20 °C) and f is the frequency in Hz.

LAeq – A-Weighted Equivalent Sound Pressure Level: The average sound pressure level over a given period of time, calculated using the A-weighting filter (which simulates human auditory sensitivity). It is the most widely used index for assessing noise exposure because it shows strong correlation with the psychophysiological effects of noise. Expressed in dB(A).

LCA – Life Cycle Assessment: An environmental assessment methodology that considers all impacts associated with a product throughout its life cycle, from raw material extraction to final disposal. In this thesis, it is referenced in the context of End-of-Life Tires (ELT), whose use phase generates approximately 550 to 840 kg CO_2 equivalent per tire.

Leq – Equivalent Sound Pressure Level: The average sound pressure level that, if continuously present during the same period, would correspond to the same total sound energy as a signal varying over time. When calculated using the A-weighting filter, it is designated LAeq. Expressed in dB.

Lmax: The maximum sound pressure level recorded during a given measurement period. Expressed in dB or dB(A). It is used as a complementary parameter in the assessment of acoustic comfort in indoor environments, according to ABNT NBR 10152:2017.

LOI – Loss on Ignition: A thermogravimetric test that determines the percentage of mass lost by a sample when subjected to high temperatures (generally between 500 °C and 1000 °C). In this thesis, it was used for the thermal characterization of tire rubber particles, indicating the content of volatile organic materials and the thermal stability of the material.

Lombard Effect: A phenomenon describing the involuntary tendency of speakers to increase their vocal level as background noise increases, in order to maintain speech intelligibility. The relationship between speech level and background noise is known as the “Lombard Slope”:

after the onset of the effect (around 45 dB of background noise), the speech level increases by approximately 0.5 dB for every 1 dB increase in ambient noise.

Lombard Slope – see Lombard Effect: See entry: Lombard Effect.

Mass Law: A principle establishing a direct proportionality between the mass per unit area (kg/m^2) of a partition and its acoustic insulation index, particularly for airborne noise. According to the mass law, sound insulation increases with increasing frequency and increasing surface mass of the wall. Low-frequency sounds are more difficult to insulate than high-frequency sounds with the same material mass.

Mass–Spring–Mass Effect: A phenomenon describing the behavior of construction systems composed of two masses (panels) separated by an air layer or absorbing material (spring). Increasing the distance between the panels improves sound insulation at low frequencies. The greater the separation and the mass of the panels, the greater the acoustic insulation of the system. This is a fundamental principle of dry construction systems with air cavities.

MLS – Maximum Length Sequence: A type of deterministic pseudo-random signal used in acoustic measurements to determine the Room Impulse Response (RIR). It is an alternative to the sweep signal in room acoustics measurement systems.

Molecular Absorption (Molecular Relaxation): A sound dissipation mechanism in polyatomic gases (such as air) in which the energy of the acoustic wave is transferred from the translational motion of molecules to internal rotational and vibrational modes. Dissipation occurs when the molecular relaxation time is compatible with the period of the sound wave.

NC / RC – Noise Criteria / Room Criteria: Standardized curves and methods used to specify the maximum permissible levels of continuous background noise in indoor environments, especially noise originating from HVAC systems. They are used as acoustic comfort parameters to ensure that background noise does not mask speech or cause distraction.

NPS – Sound Pressure Level (SPL): See entry: SPL – Sound Pressure Level.

NRC – Noise Reduction Coefficient: A single-number value summarizing the sound absorption capability of a material, calculated as the arithmetic mean of the sound absorption coefficients at the octave band frequencies of 250, 500, 1000, and 2000 Hz. Formula: $NRC = (\alpha_{250} + \alpha_{500} + \alpha_{1000} + \alpha_{2000}) / 4$. It is used for rapid comparison of the performance of sound-absorbing materials. However, it does not reflect the material's behavior across the entire audible frequency range.

Octave Bands: Frequency interval groupings used in acoustics to simplify the measurement and analysis of sound spectra. An octave is defined as an interval in which the upper frequency (fu) is twice the lower frequency (fL), corresponding to a 2:1 ratio. The audible spectrum is standardized (ISO/ANSI) into 10 octave bands with the following center frequencies: 31.5, 63, 125, 250, 500, 1000, 2000, 4000, 8000, and 16,000 Hz. In architectural acoustics, the bands from 63 Hz to 8000 Hz are the most commonly used.

One-Third Octave Bands: A subdivision of octave bands into three smaller frequency ranges, each covering one third of an octave interval. This allows for a more detailed spectral analysis of the acoustic behavior of materials and environments. They are frequently used in sound absorption tests conducted with impedance tubes.

Optimal Reverberation Time (OT): The T60 value considered ideal for a specific enclosure and activity, according to ABNT NBR 12179:1992. The OT depends on the room volume and its intended function (speech, music, cinema, etc.). For speech-oriented environments (classrooms, auditoriums), the OT should be short to ensure speech intelligibility; for musical environments, it should be longer to provide sound richness.

Particle Size Distribution (Granulometry): The distribution of particle sizes within a granular material, determined through granulometric analysis (sieving or laser diffraction). In this thesis, it constitutes an independent experimental variable: the investigated rubber particle sizes correspond to the fractions retained on 0.15 mm, 0.30 mm, and 0.60 mm sieves, with direct influence on the sound absorption coefficient, especially at low frequencies.

Period (T): The time interval required for one complete oscillation cycle of a sound wave. Measured in seconds (s). It is related to frequency (f) by the equation: $T = 1/f$.

Pink Noise: An aperiodic signal whose power spectral density is inversely proportional to frequency ($\propto 1/f$), resulting in equal energy per octave band (or one-third octave band). The spectral level decreases at a rate of −3 dB/octave. It is preferred in room acoustics measurements (according to ABNT NBR ISO 3382-2) because it resembles human auditory perception and ensures adequate energy distribution across all analysis bands.

Porosity: The ratio between the volume of voids (pores) and the total volume of a material. It is one of the three fundamental parameters for the characterization of sound-absorbing materials, together with airflow resistivity and tortuosity. Materials with higher porosity tend to exhibit greater sound absorption, especially at high frequencies.

Porous Materials: A class of sound-absorbing materials containing interconnected pores that allow the penetration of sound waves. Dissipation occurs through frictional heating between vibrating air molecules and the pore surfaces. These materials generally exhibit good absorption at medium and high frequencies. Materials with absorption coefficients above 0.50 are generally classified as absorbers, whereas those below 0.20 are classified as reflectors.

PT – Sound Transmission Loss – see Sound Transmission Loss: See entry: Sound Transmission Loss (STL).

RASTI – Rapid Speech Transmission Index: A simplified version of the Speech Transmission Index (STI) that uses only two frequency bands (500 Hz and 2000 Hz) to rapidly estimate speech intelligibility within an environment. Low RASTI values are associated with reduced listener performance in noisy environments.

Reference Pressure (p_0): The sound pressure value adopted as a reference for calculating the Sound Pressure Level (SPL/NPS) in air. It corresponds to 20 μPa (2×10^{-5} Pa), representing the threshold of human hearing at a frequency of 1000 Hz.

Reverberation: The persistence of sound in an enclosed or semi-enclosed environment after the sound source has ceased, resulting from multiple reflections of sound waves on the surfaces of the enclosure. It is measured by the Reverberation Time (RT or T60). Reverberation control is one of the primary objectives of acoustic conditioning.

Reverberation Time – see T60: See entry: T60 – Reverberation Time.

RIR – see Room Impulse Response: See entry: Room Impulse Response (RIR).

Room Impulse Response (RIR): A time-domain function describing the complete acoustic response of an enclosure to an ideal sound impulse. It represents the "acoustic signature" of the space and contains all the information necessary to calculate room acoustics parameters such as T60, EDT, T20, T30, C80, D50, and STI. It is obtained through measurements using sweep signals and processing according to the Schroeder Method.

RT – Reverberation Time – see T60: See entry: T60 – Reverberation Time.

SBR – Styrene-Butadiene Rubber: A widely used synthetic elastomer, particularly in tire manufacturing. It is the principal polymer constituent of automobile tires. It exhibits high elasticity, resistance to swelling in organic solvents, and the ability to retard crack propagation. In this thesis, it constitutes the base material of the shredded rubber particles incorporated into gypsum.

Schroeder Method: A method for calculating reverberation time from the integrated impulse response, proposed by Schroeder (1965). It consists of the backward integration over time of the squared impulse response, generating a decay curve with high statistical accuracy from a single measurement. It is widely used in conjunction with sweep signals.

SEM – Scanning Electron Microscopy: A morphological and microstructural analysis technique that uses an electron beam to obtain high-resolution images of material surfaces. In this thesis, it was used for characterizing the surface morphology of shredded tire rubber particles, revealing surface porosity and texture across different particle size fractions.

Signal-to-Noise Ratio (S/N): The ratio between the sound pressure level of the useful signal (speech or music) and the background noise level in the receiving environment, expressed in dB. For good speech intelligibility, the speaker's signal should exceed the background noise by at least +10 to +15 dB. The signal-to-noise ratio is a fundamental parameter in the acoustic evaluation of classrooms and environments intended for oral communication.

Sine Sweep Signal – see Sweep Signal: See entry: Sweep Signal.

Sound: A variation in pressure within an environment (physical disturbance) that propagates through an elastic medium (air, solid, or liquid) and can be detected by the human auditory system. In the physical sense, sound is a longitudinal pressure wave; in the psychophysiological sense, it is the sensation produced in the auditory system by these pressure variations.

Sound Absorption: The property of a material or surface to convert incident sound energy into heat, thereby reducing the amount of energy reflected back into the environment. It is quantified by the sound absorption coefficient (α). Porous and fibrous materials generally exhibit high absorption, especially at medium and high frequencies.

Sound Absorption Coefficient – see α (alpha): See entry: α (alpha) – Sound Absorption Coefficient.

Sound Decay: The progressive reduction of sound energy level within an enclosure after the sound source has ceased. The decay rate is measured in dB/s and forms the basis for calculating reverberation time parameters (T60, T20, T30, EDT). The decay curve is obtained through backward integration of the squared impulse response over time (Schroeder Method).

Sound Diffusion: The homogeneous distribution of sound energy within an enclosure such that sound intensity is practically equal at all points and in all directions. A perfectly diffuse sound field is assumed in reverberation time calculations using the Sabine and Eyring formulas.

Sound Dissipation: The fundamental process by which the organized mechanical energy of a sound wave is converted into thermal energy (heat) or removed from an acoustic system. It occurs through multiple mechanisms, including viscosity, thermal conduction, molecular relaxation, friction in porous materials, hysteresis in elastomers, and dissipation in resonators.

Sound Isolation: A measure of the performance of a construction system in preventing the transmission of impact noise or vibration between environments. It differs from acoustic insulation, which refers to the reduction of airborne noise. It is quantified by Sound Transmission Loss (STL).

Sound Level Meter: An instrument used to measure Sound Pressure Level (SPL/NPS) in dB. It incorporates weighting filters (A, B, C) to simulate the sensitivity of human hearing.

Sound Masking: A phenomenon in which the presence of one sound makes the perception of another sound more difficult or impossible. In educational environments, masking of the teacher's voice by background noise or excessive reverberation compromises speech intelligibility and student learning.

Sound Spectrum: A representation of the distribution of effective sound pressure (or sound energy) as a function of frequency, obtained through the application of the Fourier Transform to the sound waveform. It enables the identification of the spectral components of a sound or noise and is fundamental for analyzing acoustic performance as a function of frequency.

Sound Transmission Coefficient – see τ (tau): See entry: τ (tau) – Sound Transmission Coefficient.

Sound Transmission Loss (STL): A quantity characterizing the sound isolation performance of a wall or partition, derived from the sound transmission coefficient (τ). Expressed in decibels (dB), it represents the amount of sound energy attenuated while passing through a material. Formula: $STL = -10 \cdot \log_{10}(\tau)$. The greater the STL, the greater the acoustic insulation. It may be measured using an impedance tube according to ASTM E1050-12 and ISO 10534:2001.

Spectral Density: The distribution of sound energy across frequencies. In white noise, the spectral density is constant (uniform energy per frequency). In pink noise, the spectral density is inversely proportional to frequency ($\propto 1/f$), resulting in uniform energy per octave band.

Speech Intelligibility: The ability of listeners to understand speech within an environment, expressed as the percentage of phonemes or words correctly understood. It is the fundamental acoustic characteristic of spaces intended for oral communication. It is influenced by reverberation time (RT), background noise level, and room geometry. It is objectively quantified using the Speech Transmission Index (STI).

SPL – Sound Pressure Level (NPS): A logarithmic measure of effective sound pressure relative to the reference pressure in air ($p_0 = 20$ μPa). Expressed in decibels (dB): $SPL = 20 \cdot \log_{10}(p/p_0)$. It is the fundamental parameter for quantifying sound levels in environmental and architectural acoustics and is regulated in Brazil by ABNT NBR 10152:2017.

STI – Speech Transmission Index: An objective method for measuring speech intelligibility within an environment, standardized by IEC 60268-16:2020. Values range from 0 to 1: below 0.30 = poor; 0.30–0.45 = bad; 0.45–0.60 = fair; 0.60–0.75 = good; above 0.75 = excellent. It is one of the most important acoustic descriptors for classrooms, together with T60 and D50.

Sweep Signal (Swept-Sine / Chirp Signal): A deterministic signal used in acoustic measurements, consisting of a sinusoidal wave with frequency varying over time, covering the entire frequency range of interest in a single sweep. Its advantages over interrupted noise include high signal-to-noise ratio (SNR), immunity to harmonic distortion, low crest factor, and robustness against temporal variations. From the sweep signal, the Room Impulse Response (RIR) is obtained through deconvolution, according to ABNT NBR ISO 3382-2.

τ (tau) – Sound Transmission Coefficient: A parameter that characterizes the ability of a wall or partition to transmit sound energy. The lower the value of τ, the lower the transmitted sound intensity and the greater the acoustic insulation provided by the wall. It is the fundamental quantity used for calculating Sound Transmission Loss (STL).

T – Period – see Period: See entry: Period (T).

T20: An estimate of the T60 reverberation time calculated from a 20 dB decay in sound pressure level. The evaluation range extends from −5 dB to −25 dB relative to the average steady-state level. The measured value is multiplied by 3 to extrapolate T60. Regulated by ABNT NBR ISO 3382-2:2017. It is less susceptible to nonlinearities than T30, but less robust against background noise.

T30: An estimate of the T60 reverberation time calculated from a 30 dB decay in sound pressure level. The evaluation range extends from −5 dB to −35 dB relative to the average steady-state level. The measured value is multiplied by 2 to extrapolate T60. It is more robust than T20 because it uses a larger decay range and is the method recommended by ABNT NBR ISO 3382-2:2017 for precision measurements.

T60 – Reverberation Time: A fundamental acoustic descriptor of an enclosure, defined as the time required for sound energy to decay to one millionth of its original value after the sound source has ceased, corresponding to a 60 dB reduction in sound pressure level. Measured in seconds (s). It depends primarily on the room volume and the total sound absorption of its surfaces. For classrooms, the recommended mid-frequency T60 is ≤ 0.8 s (up to 0.4 s for maximum speech intelligibility). In acoustics, the convention is to specify T60 at 500 Hz.

Thermal Conduction (Dissipation Mechanism): A mechanism of sound energy dissipation in which the compressions and rarefactions of an acoustic wave create local temperature variations. Heat flows from compressed regions (hotter) to rarefied regions (cooler) in an irreversible process that dissipates part of the acoustic energy into the medium.

Thermoviscous Boundary Layer: A transition region formed near a rigid surface during the propagation of sound waves, composed of two sublayers: the viscous boundary layer (where air velocity decreases to zero, generating friction) and the thermal boundary layer (where temperature fluctuations of the wave are dissipated through heat conduction). It constitutes a relevant mechanism of sound dissipation in porous materials.

Tortuosity: A parameter describing the complexity of the path traveled by air through the pores of a material relative to a straight-line path. It is one of the three fundamental parameters for the acoustic characterization of porous materials, together with porosity and airflow resistivity. Greater tortuosity implies greater sound energy dissipation.

Ultrasound: Sounds with frequencies above 20,000 Hz (20 kHz), exceeding the threshold of human hearing. Ultrasound is used in non-destructive testing methods, such as Ultrasonic Pulse Velocity (UPV), for evaluating the integrity and homogeneity of solid materials.

UPV – Ultrasonic Pulse Velocity: A non-destructive test that determines the propagation velocity of ultrasonic pulses (typically at 54 kHz) within a solid material. The velocity is inversely proportional to porosity and directly proportional to the stiffness and homogeneity of the material. In this thesis, it was used to evaluate the quality and microstructural integrity of gypsum–rubber specimens using a Proceq Pundit Lab device.

Vibrating Membrane (Vibrating Panel): A type of acoustic absorber consisting of a flexible panel or membrane mounted at a certain distance from a wall, thereby forming an air cavity. It absorbs sound energy through the mechanical vibration of the panel and is more efficient at low frequencies, complementing the action of porous and fibrous materials.

Viscoelasticity: A property of materials that simultaneously exhibit viscous and elastic behavior when subjected to deformation. Viscoelastic materials (such as rubber and polymers) dissipate mechanical energy through internal damping (hysteresis) during deformation cycles. This property is fundamental to the vibration damping and sound absorption behavior of rubber-based composites.

Viscosity (Dissipation Mechanism): A sound dissipation mechanism in fluids in which differences in velocity between neighboring particles during the propagation of a sound wave generate internal friction ("viscous drag"). This promotes the diffusion of particle linear momentum, resulting in the conversion of kinetic energy into heat.

Vocal Effort: Classification of the sound pressure level produced by the human voice during speech, according to ISO 9921:2003. The levels are: relaxed speech (54 dB), normal speech (60 dB), raised speech (66 dB), loud speech (72 dB), and very loud speech (78 dB), measured in dB re 20 μPa at 1 m in front of the mouth of a male speaker, using A-weighting.

Vulcanization: A thermochemical treatment process for rubber that promotes the formation of cross-links between polymer chains through sulfur, providing the material with greater mechanical strength, elasticity, durability, and resilience. It was discovered by Charles Goodyear in 1839. Natural rubber is vulcanized between 120 °C and 145 °C; above 150 °C, material decomposition occurs.

Wavelength – see λ (lambda): See entry: λ (lambda) – Wavelength.

White Noise: An aperiodic signal with a flat power spectrum (constant spectral density), containing equal amounts of energy at all frequencies within a frequency band of interest. By analogy with white light, it exhibits a uniform energy distribution per unit frequency (Hz). It is used in electrical and acoustic measurements as an excitation signal.

XRD – X-ray Diffraction: A mineralogical characterization technique that identifies crystalline phases present in a material through the analysis of X-ray diffraction patterns. In

this thesis, it was used for the mineralogical characterization of shredded tire rubber particles, confirming the predominantly amorphous nature of the material.